Integration of Genetics, Environment, and Time (G x E x T) for Neurodevelopmental Toxicology and Risk Assessment

Julie Juyoung Park

A dissertation
submitted in partial fulfillment of the
requirements for the degree of

Doctor of Philosophy

University of Washington
2017

Reading Committee:
Elaine M. Faustman, Chair
Lucio G. Costa
William C. Griffith

Program Authorized to Offer Degree:
Environmental and Occupational Health Sciences
School of Public Health

University of Washington

ABSTRACT

Integration of genetics, environment, and time (G x E x T)
for neurodevelopmental toxicology and risk assessment

Julie Juyoung Park

Chair of Supervisory Committee:
Professor Elaine M. Faustman
Department of Environmental and Occupational Health Sciences

Processes of neurodevelopment are complex and highly orchestrated, making the brain development one of the most sensitive time frames for perturbations. Because of this complexity and sophistication, *in vivo* studies have been conducted traditionally for neurodevelopmental toxicity. With a movement to save the number of experimental animals used, neurodevelopmental toxicology is an area where there is a pressing need for *in vitro* alternative methods development. In this research, two *in vitro* neurodevelopmental models were evaluated: a primary fetal mouse midbrain micromass system and a human neural progenitor cell culture. Dynamics of C57BL/6 and A/J micromass cultures over 22 days *in vitro* (DIV) were characterized. Changes in morphology, protein content, the extent of differentiation, and stage-specific proteins were assessed over time, which revealed similar dynamics to *in vivo*. The second *in vitro* model used differentiating human neural progenitor cells (hNPCs). Without any additional external morphogens, hNPCs are thought to differentiate towards forebrain identity over 21 days in culture. When gene ontology (GO) processes and relative gene expression intensity of genes associated with GO terms of interest were compared using gene expressions obtained from microarray, our hNPCs showed high concordance with *in vivo* human neocortical brain tissue. Together, these observations defined the potential of two *in vitro* neurodevelopmental models as a screening tool for prioritizing compounds.

Using characterized *in vitro* neurodevelopmental models, factors that may contribute to susceptibility were evaluated. Exposures to silver nanoparticles (AgNPs) with different sizes and coating on C57BL/6 or A/J micromass cultures at three different developmental stages illustrated differential yet significant

adverse effects of particle coatings, sizes, and time of exposures on cytotoxicity. Genetic backgrounds also contributed to differential responses to AgNPs. Exposures to chlorpyrifos, arsenic, and cadmium on proliferating and differentiating hNPCs *in vitro* revealed compound- and stage-specific impacts on cell viability and epigenetics. AgNPs-exposed hNPCs showed that particle coatings and sizes significantly contributed to cell viability. We found that fetal mouse midbrain cells and hNPCs were generally most sensitive to various types of compounds during early differentiation when differentiation is initiated, but proliferation signaling was still active. Moreover, *in vitro* hNPCs were differentially sensitive to AgNPs from embryonic mouse midbrain cells, suggesting potential regional-specific responses to AgNPs. Altogether, the results suggest that factors including developmental stages, genetics, and region of the brain contribute to susceptibility; therefore, the impacts of genetics/epigenetics and time of exposures on neurodevelopment also need to be assessed to better define response-disease pathway that can later be applied in risk assessments and regulatory decisions.

TABLE OF CONTENTS

LIST OF FIGURES

CHAPTER 2

CHAPTER 3

CHAPTER 4

CHAPTER 5

CHAPTER 6

CHAPTER 7

CHAPTER 8

LIST OF TABLES

CHAPTER 2

CHAPTER 4

CHAPTER 5

CHAPTER 7

CHAPTER 8

ACKNOWLEDGEMENTS

I would like to express my appreciation to my advisor Dr. Elaine M. Faustman. Thank you for patience and guidance throughout my undergraduate and graduate school education. I am grateful to the rest of my dissertation committee members, Dr. Danny Shen, Dr. Lucio G. Costa, Dr. Thomas M. Burbacher, Dr. William C. Griffith, and Jim Wallace for their encouragement and insightful comments.

I am grateful to my fellow graduate students in the lab, especially Brittany Weldon, Susanna H. Wegner, Sean Harris, and Hee Yeon Kim who supported me with cell cultures, running assays, and data analysis as well as encouraged me. Ian B. Stanaway provided an excellent insight on transcriptomic data analysis, and Sungwoo Hong along with many undergraduate students provided invaluable support in the lab, helping with cell cultures and assays. Collin White in the cytometry core and Wai Pang Chan in the biology imaging facility taught me how to use fluorescent microscope, laser scanning cytometry (iCys), and confocal microscope with their technical expertise and patience. I also want to acknowledge our collaborator Russell Dills and Rosie Schaffer for dosimetry analysis.

Everyone in the Institute for Risk Analysis and Risk Communication including Kethanh Duong, Tomomi Workman, Marissa Smith, Sanne A.B. Hermsen, Carly Strecker, Alison Liang, Sara Pacheco, and Jihyun Lee also has been supportive and helpful throughout my graduate school education. I especially thank Tomomi for running last minute data analysis and for replying back to my texts after work.

My fellow graduate students and staffs in the Department, especially Hao Wang, Rachael Yu-Chi Chang, Shih-Yu Chang, Yanfei Cindy Li, Hyoung-Gon Frank Yu, Boris Reiss, Khoi Dao, and Dianne Botta have been my moral support. Lastly but not least, I cannot find words to express my sincere gratitude to my family and friends for their continuous love and support.

This work would not have been possible without funding from EPA Predictive Toxicology Center grants, NIEHS Centers for Nanotechnology Health Implications Research Consortium, and the Child Health Center grants.

CHAPTER 1: Introduction and background

The brain plays a vital role in our everyday life from motor control and perception to homeostasis, learning, and memory. Thus, proper brain development is critical. Neurogenesis is a precisely orchestrated process where different regions develop at specific times with specific dynamics. These processes represent a developmental trajectory with increasing complexity and requiring more complex interactions.

Exposures to toxicants during the neurodevelopmental period may alter developmental processes and result in lifelong neuropathologies (Grandjean and Landrigan, 2006, 2014; Landrigan, 2010; Rice and Barone, 2000a; Rodier, 1995a; Wegner et al., 2014). Exposures to environmental toxicants during development can also lead to subtle functional impairments in a brain. As a result, life-long behavioral changes such as shortened attention span, increased aggressiveness, impaired memory and language skills, and decreased IQ in children will be produced (Grandjean and Landrigan, 2014, 2006; Needleman et al., 2002). For instance, *in utero* exposures to chlorpyrifos in humans has been associated with developmental delays in learning, impairments in mental and motor development, and changes in brain structure and function including attention disorders (Engel et al., 2011; Eskenazi et al., 2014; Eskenazi et al., 2010; Eskenazi et al., 2008; Horton et al., 2012; Rauh et al., 2012; Rauh et al., 2006). Moreover, exposures to methylmercury and alcohol have been demonstrated to result in minimal long-lasting effects on maternal health while *in utero* exposures to these toxicants produced neurodevelopmental disorders and delays (de Sanctis et al., 2011; Grandjean and Herz, 2011).

Even though the changes in function may be small, the consequences of these alterations can be tremendous. There will be increased need for specialized health, education, and social services (Boyle et al., 2011; Grandjean and Landrigan, 2014, 2006), leading to increased burden on society as they are on a population-based increase in the number of children. Families and caregivers will also need to be considered in addition to diminished economic productivity (Bellinger, 2012; Grandjean and Landrigan, 2006). To prevent these consequences and burden on society and to protect children from environmental toxicant-induced neurodevelopmental disorders, it is important to understand the key “window of susceptibility” and factors that may contribute to adverse health outcomes upon exposures.

Challenges to developmental neurotoxicology testing.

Despite the sensitivity of developmental processes to perturbation by chemicals, less than 1% of US Environmental Protection Agency (EPA) registered chemicals are known to affect neurodevelopment in humans (Judson et al., 2009; Miodovnik, 2011). According to Organization for Economic Co-operation and Development (OECD) Testing Guidelines 414, 415, 416, 421, and 422 (OECD, 1983, 2001a, b, 2016a, b), developmental toxicity testing requires *in vivo* studies. However, traditional developmental toxicity tests are complicated, time-consuming, and resource-intensive, requiring a larger number of animals (Bailey et al., 2005; Piersma, 2004; Pratten et al., 2012; Smirnova et al., 2014). Given the large number of chemicals that still remain to be tested, there is a need to develop alternative methods to screen and identify potential developmental neurotoxicants (Bal-Price et al., 2012; Crofton et al., 2014; Crofton et al., 2011; Crofton et al., 2012; Krewski et al., 2010; Lein et al., 2007; Smirnova et al., 2014).

Special challenges are encountered when creating robust *in vitro* models for developmental toxicology due to dynamic and complex processes of brain development (Knudsen et al., 2011). We need to develop *in vitro* alternative methods that can capture dynamic stages and processes. Because dynamic stages and processes in the brain are driven and regulated by different biological pathways, the neurodevelopmental period will be sensitive to perturbation in a time- and pathway-specific manner. *In vitro* alternative models also need to capture the complexity of brain development, critical windows of susceptibility, and toxicokinetics and dynamics in order to predict better neurodevelopmental toxicity that is reflective of humans. Once developed and validated, *in vitro* alternative tests will allow us to screen many untested compounds and prioritize potential neurotoxicants as well as to inform regulatory decision makers (Bal-Price et al., 2012; Krewski et al., 2010; Lein et al., 2007).

Emerging approaches for in vitro developmental neurotoxicology models.

The US National Research Council (NRC) enunciated that there is an urgent need for rapid screening and prioritization of chemicals and shifting towards a systems biology-based approach to evaluate toxicity in *in vitro* models, requiring *in vitro* developmental toxicity models that can capture key processes (Gibb, 2008; The National Academy of Sciences, 2007; NRC, 2007). Substantial progress in developing high content *in vitro* models have been made so far (Bal-Price et al., 2010; Buzanska et al., 2010; Fritsche et al., 2011; Park et al., 2017; Roque et al., 2014; Theunissen et al., 2012). However, sensitivity and specificity of *in vitro* alternative methods still need to be evaluated (Bal-Price et al., 2012; Crofton et al., 2011; Lein et

al., 2007; Smirnova et al., 2014). The European Centre for the Validation of Alternative Methods (ECVAM) coordinated pre-validation and validation study on *in vitro* embryotoxicity tests from 1996 to 2000 (Genschow et al., 2002). The ECVAM included three *in vitro* models for embryotoxicity, and two of them were embryonic stem cell lines and the micromass test. These two *in vitro* models are ones that our lab also works with to investigate and screen developmental neurotoxicants.

High-density micromass cultures of limb bud or neuronal cells isolated midway through organogenesis have been proposed as one of the in vitro developmental toxicity screening tool by ECVAM in addition to embryonic stem cell test and whole embryo cultures (Balls and Hellsten, 2002; Genschow et al., 2002; Spielmann et al., 2006). Our previously established *in vitro* rat embryonic cell micromass culture system was first characterized by Flint (1983). This organotypic 3D micromass system was found provide a model of cellular differentiation *in vitro* (Flint et al., 1984; Flint, 1983; Gregotti et al., 1994; Whittaker and Faustman, 1992) and to mimic certain, complex *in vivo* like niches including the inside-out development of a brain (Whittaker and Faustman, 1992). *In vitro* micromass cultures have several advantages. First, a large number of primary culture cells can be prepared from a small number of embryonic midbrains (Flint, 1993). This reduces the number of whole animals required for assessing neurodevelopmental toxicity. The differentiation process is purely driven by the cell density, without any addition of exogenous factors. Also, mechanistic studies can be done using this culture system. Lastly, studies have confirmed the accuracy of prediction and specificity of *in vitro* fetal rat embryo limb bud and midbrain micromass system, concluding that the micromass culture is a robust model for evaluating potential teratogens (Flint, 1993; Flint and Orton, 1984; Genschow et al., 2002; Piersma, 2004; Reinhardt, 1993; Uphill et al., 1990).

The Embryonic Stem Cell Test (EST) is another *in vitro* model of cellular differentiation (Cho and Li, 2007; Robinson et al., 2010; Stummann and Bremer, 2008; van Dartel and Piersma, 2011). For this test, mouse or human stem cells are used to capture early stages of embryonic development and differentiation into a range of specific cell types (Pal et al., 2011; Seiler et al., 2004; zur Nieden et al., 2004). Human neural progenitor cells (hNPCs) have become a valuable tool for neurodevelopmental toxicology as they can be directed to undergo differentiation and can provide an opportunity to study early stages of neuronal differentiation processes (Breier et al., 2008; Radio and Mundy, 2008; Shin et al., 2006). It also closely represents processes of human brain development and provides opportunities to study the effects of neurotoxicants at various neurodevelopmental stages. Our recent papers with hNPCs have focused on

detailed transcriptomics of their proliferating and differentiating dynamics (Wegner et al., 2014). Specifically, an untargeted analysis of gene ontology processes enriched among genes significantly changed over time in both *in vitro* hNPC system and *in vivo* human neocortex (publicly available dataset by Kang et al. (2011)) revealed that several fundamental neurodevelopmental processes concorded (Wegner et al., 2014). Wegner et al. (2014) also found that highly expressed genes in both *in vitro* and *in vivo* were involved with key brain developmental processes including proliferation, differentiation, migration, synapse formation, and neurotransmission. This work clarified which fundamental processes of brain development are captured in our hNPC model by relating *in vitro* dynamics to *in vivo* reference points.

Incorporating emerging *in vitro* developmental neurotoxicology models in testing paradigms requires a clear understanding of the extent to which they reflect the processes that are important to *in vivo* brain development. Thus, there is a need for validating the optimized developmental neurotoxicity testing models including micromass and ETS.

Factors that affect susceptibility during neurodevelopment.

In the US, one in every six children has a developmental disability including learning impairment and developmental delays (Boyle et al., 1994; Boyle et al., 2011; Grandjean and Landrigan, 2006). National Research Council (NRC) in 2000 estimated that 3% of developmental disabilities are from environmental exposures and 25% are from interactions between environmental factors and individual genetic susceptibility (National Research Council Committee on Developmental Toxicology, 2000). Because these percentages are drawn from limited information about neurotoxicity, the actual prevalence may be underestimated (Boyle et al., 2011).

Many factors contribute to sensitivity in response to developmental neurotoxicants. Factors such as the developmental timing of exposures, species, gender, and genetic background contribute to adverse effects of neurotoxic exposures on brain development and function (Barry et al., 2017; Faustman et al., 2000; Rice and Barone, 2000b; Rodier, 1995b). For example, genetic variability in paraoxanase-1 (PON1) is known to be associated with differences in metabolism of organophosphate (OP) pesticide oxons. With PON1R192 isoform, mice were able to catalyze the oxons of CP two to ten times greater than PON1Q192 isoform, leading to lesser acetylcholine esterase inhibition (Cole et al., 2005; Li et al., 2000). However, the PON1

enzymes in offspring do not reach adult levels until approximated age of seven; thus, both genetics and temporal components are involved defining susceptibility. Because genetics contribute significantly to an individual's susceptibility to xenobiotics, the US NRC envisioned that investigating changes in gene, protein, and metabolite profiles from toxicant exposures will also allow us to identify target pathways and understand consequences of perturbed pathways (Gatzidou et al., 2007; Ge and He, 2009; Harrill and Rusyn, 2008; Krewski et al., 2011). This is especially important in developmental neurotoxicity because different regions of the brain develop at different times, and it will be sensitive to perturbation in a time-, pathway-, cell type-, and tissue-specific manner. Therefore, it is important to consider genetics as a contributor to vulnerability and integrate genetics, environment, and time when investigating developmental neurotoxicity.

A systems-based approach for translation of in vitro data for risk assessment.

The impacts of a particular perturbed signaling pathway after exposures to environmental toxicants will depend on the role of the pathway and time in development. Moreover, the complex dynamics these pathways orchestrate during development are highly context dependent. Therefore, it is critical to have dynamic models of these sensitive phases of development, especially ones that are organotypic and that can capture some of these context-specific responses as well as the more general developmental responses (The National Academy of Sciences, 2007). And as we develop more confidence in these models, we can begin to use an adverse outcome pathway (AOP) framework to link chemical exposures with adverse health outcome. With the AOP framework, more in-depth normal versus perturbed pathways during brain development after exposures to toxicants will be captured. This can be done by defining molecular initiating events and using defined events in a response-disease pathway to link adverse human or environmental health risk that can later be used for risk assessments and regulatory decisions.

Here, I propose characterizing two different, dynamic *in vitro* models of brain and using these models to assess factors that affect susceptibility during neurodevelopment and their implications in neurodevelopmental toxicity. To supplement this goal, I will characterize two *in vitro* neurodevelopment models, embryonic mouse midbrain micromass and hNPCs, by identifying dynamics of key neurodevelopmental processes. Using gene x environment x time (G x E x T) approach, I will also focus on defining the sensitive time windows for susceptibility in neurodevelopmental period, using various environmental toxicants including pesticide, metal, and nanomaterial in this study. This study will add new

information to current literature by validating two *in vitro* developmental neurotoxicity models and by evaluating adverse effects of neurotoxicants with different contributing factors using characterized *in vitro* alternative methods.

DISSERTATION OUTLINE

The overarching goal of current dissertation is to characterize *in vitro* alternative methods for brain development and to assess the impacts of environmental agents, time of exposures, and genetics/epigenetics on brain development using characterized *in vitro* neurodevelopment models. Regarding the effects of exposure timing, I hypothesized that the impacts of environmental agents on neurodevelopment would be greater during early neurodevelopment when differentiation is initiated, but proliferation signaling pathways are still active.

In Chapter 2, I have modified previous *in vitro* fetal rat midbrain micromass culture system using embryonic mouse midbrain cells. The 3D organotypic mouse midbrain micromass model is characterized to define dynamics of the model over 22 days *in vitro*. This characterization work will be the baseline for normal development of the mouse micromass system, providing a framework for evaluating perturbations in midbrain development.

Chapter 3 discusses effects of silver nanoparticles with different coatings and sizes, exposure timing, and genetics on midbrain development using in vitro three-dimensional organotypic mouse midbrain micromass model. This work illustrates the potential of *in vitro* 3D organotypic mouse midbrain micromass model as a medium-throughput, high-content screening tool as well as the potential impacts of particle coatings and sizes, time of exposures, and genetics on midbrain development.

Another *in vitro* model is characterized in Chapter 4 using commercially available human neural progenitor cells in differentiation condition. Gene expression dynamics between *in vitro* and *in vivo* are compared to define the relevance of our *in vitro* human neural progenitor cell model to early human neurodevelopment *in vivo*. This chapter will be the baseline for normal differentiation of the human neural progenitor cell system, providing a framework for assessing perturbations in forebrain development.

Proliferating and differentiating human neural progenitor cells *in vitro* are used to examine effects of chlorpyrifos and arsenic on neurotoxicity and epigenetics in Chapter 5. This work presents the potential of *in vitro* human neural progenitor cell model as a medium-throughput, high-content screening tool in addition to the potential impacts of environmental toxicants and developmental stages on forebrain development and epigenetics.

In Chapter 6, I reveal the impacts of silver nanoparticles with various coatings and sizes and of exposure timing on forebrain development using *in vitro* human neural progenitor cells in proliferating and differentiation conditions. Like Chapter 5, this work also demonstrates the potential of *in vitro* human neural progenitor cell model as a screening tool to prioritize compounds and the effect of various silver nanoparticles on forebrain development.

Chapter 7 demonstrates adverse effects of acute cadmium exposures on proliferating and differentiating hNPCs *in vitro*. Similar to Chapter 5 and 6, this chapter not only captures the potential of *in vitro* hNPC model as a developmental neurotoxicity screening tool, but also examines changes in cell viability, in neuronal markers of proliferation and differentiation, and in epigenetics after acute cadmium exposures.

Key findings and future directions that arose from this research are summarized in Chapter 8.

SPECIFIC AIMS AND HYPOTHESES

CHAPTER 2

SPECIFIC AIM: Characterize an *in vitro* 3D organotypic embryonic mouse midbrain micromass model in its capability to capture early neurodevelopmental processes that are sensitive to perturbation.

HYPOTHESIS: The *in vitro* 3D organotypic embryonic mouse midbrain micromass culture will capture dynamics of *in vivo* midbrain development.

CHAPTER 3

SPECIFIC AIM: Determine effects of silver nanoparticle coatings and sizes, time of exposures, and genetics on midbrain development by exposing *in vitro* 3D embryonic C57BL/6 or A/J mouse midbrain cells with silver nanoparticles at three different stages of the culture period.

HYPOTHESIS: *In vitro* 3D organotypic embryonic mouse midbrain cells will be sensitive to silver nanoparticles with different coatings and sizes during early midbrain development, and that genetics also play a critical role in susceptibility to silver nanoparticle exposures.

CHAPTER 4

SPECIFIC AIM: Characterize an *in vitro* human neural progenitor cell model in its ability to capture early neurodevelopmental processes that are sensitive to perturbation.

HYPOTHESIS: The *in vitro* human neural progenitor cell model will capture specific pathways that are critical for *in vivo* forebrain development.

CHAPTER 5

SPECIFIC AIM: Investigate impacts of chlorpyrifos, arsenic, and time of exposures on forebrain development and epigenetics by exposing *in vitro* proliferating and differentiating human neural progenitor cells with chlorpyrifos and arsenic.

HYPOTHESIS: *In vitro* human neural progenitor cells will be sensitive to chlorpyrifos and arsenic during early forebrain differentiation, and epigenetics of proliferating and differentiating human neural progenitor cells *in vitro* are also impacted by chlorpyrifos and arsenic exposures.

CHAPTER 6

SPECIFIC AIM: Determine effects of silver nanoparticle coatings and sizes and time of exposures on forebrain development by exposing *in vitro* proliferating and differentiating human neural progenitor cells with silver nanoparticles.

HYPOTHESIS: *In vitro* human neural progenitor cells will be sensitive to silver nanoparticles with various coatings and sizes during early differentiation.

CHAPTER 7

SPECIFIC AIM: Examine effects of acute exposures to cadmium on forebrain development using proliferating and differentiating human neural progenitor cells *in vitro*.

HYPOTHESIS: *In vitro* human neural progenitor cells will be sensitive to cadmium during early differentiation.

CHAPTER 1 REFERENCES

Bailey, J., Knight, A. and Balcombe, J. (2005). The future of teratology research is in vitro. *Biogenic Amines 19*, 97-145.

Bal-Price, A. K., Hogberg, H. T., Buzanska, L. et al. (2010). In vitro developmental neurotoxicity (DNT) testing: relevant models and endpoints. *Neurotoxicology 31*, 545-554. http://dx.doi.org/10.1016/j.neuro.2009.11.006

Bal-Price, A. K., Coecke, S., Costa, L. et al. (2012). Advancing the science of developmental neurotoxicity (DNT): testing for better safety evaluation. *ALTEX 29*, 202-215.

Balls, M. and Hellsten, E. (2002). Statement on the scientific validity of the mircromass test -- an in Vitro for embryotoxicity. *Altern Lab Anim 30*, 268-270.

Barry, C., Schmitz, M. T., Jiang, P. et al. (2017). Species-specific developmental timing is maintained by pluripotent stem cells ex utero. *Dev Biol 423*, 101-110. http://dx.doi.org/10.1016/j.ydbio.2017.02.002

Bellinger, D. C. (2012). A strategy for comparing the contributions of environmental chemicals and other risk factors to neurodevelopment of children. *Environ Health Perspect 120*, 501-507. http://dx.doi.org/10.1289/ehp.1104170

Boyle, C. A., Decoufle, P. and Yeargin-Allsopp, M. (1994). Prevalence and health impact of developmental disabilities in US children. *Pediatrics 93*, 399-403.

Boyle, C. A., Boulet, S., Schieve, L. A. et al. (2011). Trends in the prevalence of developmental disabilities in US children, 1997-2008. *Pediatrics 127*, 1034-1042. http://dx.doi.org/10.1542/peds.2010-2989

Breier, J. M., Radio, N. M., Mundy, W. R. et al. (2008). Development of a high-throughput screening assay for chemical effects on proliferation and viability of immortalized human neural progenitor cells. *Toxicol Sci 105*, 119-133. http://dx.doi.org/10.1093/toxsci/kfn115

Buzanska, L., Zychowicz, M., Ruiz, A. et al. (2010). Neural stem cells from human cord blood on bioengineered surfaces--novel approach to multiparameter bio-tests. *Toxicology 270*, 35-42. http://dx.doi.org/10.1016/j.tox.2009.06.005

Cho, E. and Li, W. J. (2007). Human stem cells, chromatin, and tissue engineering: boosting relevancy in developmental toxicity testing. *Birth Defects Res C Embryo Today 81*, 20-40. http://dx.doi.org/10.1002/bdrc.20088

Cole, T. B., Walter, B. J., Shih, D. M. et al. (2005). Toxicity of chlorpyrifos and chlorpyrifos oxon in a transgenic mouse model of the human paraoxonase (PON1) Q192R polymorphism. *Pharmacogenet Genomics 15*, 589-598.

Crofton, K., Fritsche, E., Ylikomi, T. et al. (2014). International STakeholder NETwork (ISTNET) for creating a developmental neurotoxicity testing (DNT) roadmap for regulatory purposes. *ALTEX 31*, 223-224. http://dx.doi.org/http://dx.doi.org/10.14573/altex.1402121

Crofton, K. M., Mundy, W. R., Lein, P. J. et al. (2011). Developmental neurotoxicity testing: recommendations for developing alternative methods for the screening and prioritization of chemicals. *ALTEX 28*, 9-15.

Crofton, K. M., Mundy, W. R. and Shafer, T. J. (2012). Developmental neurotoxicity testing: a path forward. *Congenit Anom (Kyoto) 52*, 140-146. http://dx.doi.org/10.1111/j.1741-4520.2012.00377.x

de Sanctis, L., Memo, L., Pichini, S. et al. (2011). Fetal alcohol syndrome: new perspectives for an ancient and underestimated problem. *J Matern Fetal Neonatal Med 24 Suppl 1*, 34-37. http://dx.doi.org/10.3109/14767058.2011.607576

Engel, S. M., Wetmur, J., Chen, J. et al. (2011). Prenatal exposure to organophosphates, paraoxonase 1, and cognitive development in childhood. *Environ Health Perspect 119*, 1182-1188. http://dx.doi.org/10.1289/ehp.1003183

Eskenazi, B., Rosas, L. G., Marks, A. R. et al. (2008). Pesticide toxicity and the developing brain. *Basic Clin Pharmacol Toxicol 102*, 228-236. http://dx.doi.org/10.1111/j.1742-7843.2007.00171.x

Eskenazi, B., Huen, K., Marks, A. et al. (2010). PON1 and neurodevelopment in children from the CHAMACOS study exposed to organophosphate pesticides in utero. *Environ Health Perspect 118*, 1775-1781. http://dx.doi.org/10.1289/ehp.1002234

Eskenazi, B., Kogut, K., Huen, K. et al. (2014). Organophosphate pesticide exposure, PON1, and neurodevelopment in school-age children from the CHAMACOS study. *Environ Res 134*, 149-157. http://dx.doi.org/10.1016/j.envres.2014.07.001

Faustman, E. M., Silbernagel, S. M., Fenske, R. A. et al. (2000). Mechanisms underlying Children's susceptibility to environmental toxicants. *Environ Health Perspect 108 Suppl 1*, 13-21.

Flint, O. P. (1983). A micromass culture method for rat embryonic neural cells. *J Cell Sci 61*, 247-262.

Flint, O. P. and Orton, T. C. (1984). An in vitro assay for teratogens with cultures of rat embryo midbrain and limb bud cells. *Toxicol Appl Pharmacol 76*, 383-395.

Flint, O. P., Orton, T. C. and Ferguson, R. A. (1984). Differentiation of rat embyo cells in culture: Response following acute maternal exposure to teratogens and non-teratogens. *J Appl Toxicol 4*, 109-116.

Flint, O. P. (1993). In vitro tests for teratogens: desirable endpoints, test batteries and current status of the micromass teratogen test. *Reprod Toxicol 7 Suppl 1*, 103-111.

Fritsche, E., Gassmann, K. and Schreiber, T. (2011). Neurospheres as a model for developmental neurotoxicity testing. *Methods Mol Biol 758*, 99-114. http://dx.doi.org/10.1007/978-1-61779-170-3_7

Gatzidou, E. T., Zira, A. N. and Theocharis, S. E. (2007). Toxicogenomics: a pivotal piece in the puzzle of toxicological research. *Journal of Applied Toxicology 27*, 302-309. http://dx.doi.org/10.1002/jat.1248

Ge, F. and He, Q. Y. (2009). Genomic and proteomic approaches for predicting toxicity and adverse drug reactions. *Expert Opin Drug Metab Toxicol 5*, 29-37. http://dx.doi.org/10.1517/17425250802661895

Genschow, E., Spielmann, H., Scholz, G. et al. (2002). The ECVAM international validation study on in vitro embryotoxicity tests: results of the definitive phase and evaluation of prediction models. European Centre for the Validation of Alternative Methods. *Altern Lab Anim 30*, 151-176.

Gibb, S. (2008). Toxicity testing in the 21st century: a vision and a strategy. *Reprod Toxicol 25*, 136-138. http://dx.doi.org/10.1016/j.reprotox.2007.10.013

Grandjean, P. and Landrigan, P. J. (2006). Developmental neurotoxicity of industrial chemicals. *Lancet 368*, 2167-2178. http://dx.doi.org/10.1016/S0140-6736(06)69665-7

Grandjean, P. and Herz, K. T. (2011). Methylmercury and brain development: imprecision and underestimation of developmental neurotoxicity in humans. *Mt Sinai J Med 78*, 107-118. http://dx.doi.org/10.1002/msj.20228

Grandjean, P. and Landrigan, P. J. (2014). Neurobehavioural effects of developmental toxicity. *Lancet Neurol 13*, 330-338. http://dx.doi.org/10.1016/S1474-4422(13)70278-3

Gregotti, C. F., Kirby, Z., Manzo, L. et al. (1994). Effects of styrene oxide on differentiation and viability of rodent embryo cultures. *Toxicol Appl Pharmacol 128*, 25-35. http://dx.doi.org/10.1006/taap.1994.1176

Harrill, A. H. and Rusyn, I. (2008). Systems biology and functional genomics approaches for the identification of cellular responses to drug toxicity. *Expert Opin Drug Metab Toxicol 4*, 1379-1389. http://dx.doi.org/10.1517/17425255.4.11.1379

Horton, M. K., Kahn, L. G., Perera, F. et al. (2012). Does the home environment and the sex of the child modify the adverse effects of prenatal exposure to chlorpyrifos on child working memory? *Neurotoxicol Teratol 34*, 534-541. http://dx.doi.org/10.1016/j.ntt.2012.07.004

Judson, R., Richard, A., Dix, D. J. et al. (2009). The toxicity data landscape for environmental chemicals. *Environ Health Perspect 117*, 685-695. http://dx.doi.org/10.1289/ehp.0800168

Kang, H. J., Kawasawa, Y. I., Cheng, F. et al. (2011). Spatio-temporal transcriptome of the human brain. *Nature 478*, 483-489. http://dx.doi.org/10.1038/nature10523

Knudsen, T. B., Kavlock, R. J., Daston, G. P. et al. (2011). Developmental toxicity testing for safety assessment: new approaches and technologies. *Birth Defects Research Part B: Developmental and Reproductive Toxicology 92*, 413-420. http://dx.doi.org/10.1002/bdrb.20315

Krewski, D., Acosta, D., Jr., Andersen, M. et al. (2010). Toxicity testing in the 21st century: a vision and a strategy. *J Toxicol Environ Health B Crit Rev 13*, 51-138. http://dx.doi.org/10.1080/10937404.2010.483176

Krewski, D., Westphal, M., Al-Zoughool, M. et al. (2011). New directions in toxicity testing. *Annu Rev Public Health 32*, 161-178. http://dx.doi.org/10.1146/annurev-publhealth-031210-101153

Landrigan, P. J. (2010). What causes autism? Exploring the environmental contribution. *Curr Opin Pediatr 22*, 219-225.

Lein, P., Locke, P. and Goldberg, A. (2007). Meeting report: alternatives for developmental neurotoxicity testing. *Environ Health Perspect 115*, 764-768. http://dx.doi.org/10.1289/ehp.9841

Li, W. F., Costa, L. G., Richter, R. J. et al. (2000). Catalytic efficiency determines the in-vivo efficacy of PON1 for detoxifying organophosphorus compounds. *Pharmacogenetics 10*, 767-779.

Miodovnik, A. (2011). Environmental neurotoxicants and developing brain. *Mt Sinai J Med 78*, 58-77. http://dx.doi.org/10.1002/msj.20237

National Research Council Committee on Developmental Toxicology (2000). In (eds.), *Scientific Frontiers in Developmental Toxicology and Risk Assessment*. Washington (DC): National Academies Press (US)
Copyright 2000 by the National Academy of Sciences. All rights reserved.
http://dx.doi.org/10.17226/9871

Needleman, H. L., McFarland, C., Ness, R. B. et al. (2002). Bone lead levels in adjudicated delinquents. A case control study. *Neurotoxicol Teratol 24*, 711-717.

NRC (2007). *Toxicity Testing in the 21st Century: A Vision and a Strategy*. Vol. The National Academies Press. http://www.nap.edu/openbook.php?record_id=11970

OECD (1983). *Test No. 415: One-Generation Reproduction Toxicity Study*. Vol. OECD Publishing. /content/book/9789264070844-en
http://dx.doi.org/10.1787/9789264070844-en

OECD (2001a). *Test No. 414: Prenatal Development Toxicity Study*. Vol. OECD Publishing. /content/book/9789264070820-en
http://dx.doi.org/10.1787/9789264070820-en

OECD (2001b). *Test No. 416: Two-Generation Reproduction Toxicity*. Vol. OECD Publishing. /content/book/9789264070868-en
http://dx.doi.org/10.1787/9789264070868-en

OECD (2016a). *Test No. 421: Reproduction/Developmental Toxicity Screening Test*. Vol. OECD Publishing. /content/book/9789264264380-en
http://dx.doi.org/10.1787/9789264264380-en

OECD (2016b). *Test No. 422: Combined Repeated Dose Toxicity Study with the Reproduction/Developmental Toxicity Screening Test*. Vol. OECD Publishing. /content/book/9789264264403-en
http://dx.doi.org/10.1787/9789264264403-en

Pal, R., Mamidi, M. K., Das, A. K. et al. (2011). Human embryonic stem cell proliferation and differentiation as parameters to evaluate developmental toxicity. *J Cell Physiol 226*, 1583-1595. http://dx.doi.org/10.1002/jcp.22484

Park, J. J., Weldon, B. A., Park, J. H. et al. (2017). Characterization of *in vitro* organotypic 3D embryonic mouse midbrain micromass cultures using C57BL/6 and A/J mice. *ALTEX* ***In submission***

Piersma, A. H. (2004). Validation of alternative methods for developmental toxicity testing. *Toxicol Lett 149*, 147-153. http://dx.doi.org/10.1016/j.toxlet.2003.12.029

Pratten, M., Ahir, B. K., Smith-Hurst, H. et al. (2012). Primary cell and micromass culture in assessing developmental toxicity. *Methods Mol Biol 889*, 115-146. http://dx.doi.org/10.1007/978-1-61779-867-2_9

Radio, N. M. and Mundy, W. R. (2008). Developmental neurotoxicity testing in vitro: models for assessing chemical effects on neurite outgrowth. *Neurotoxicology 29*, 361-376. http://dx.doi.org/10.1016/j.neuro.2008.02.011

Rauh, V. A., Garfinkel, R., Perera, F. P. et al. (2006). Impact of prenatal chlorpyrifos exposure on neurodevelopment in the first 3 years of life among inner-city children. *Pediatrics 118*, e1845-1859. http://dx.doi.org/10.1542/peds.2006-0338

Rauh, V. A., Perera, F. P., Horton, M. K. et al. (2012). Brain anomalies in children exposed prenatally to a common organophosphate pesticide. *Proc Natl Acad Sci U S A 109*, 7871-7876. http://dx.doi.org/10.1073/pnas.1203396109

Reinhardt, C. A. (1993). Neurodevelopmental toxicity in vitro: primary cell culture models for screening and risk assessment. *Reprod Toxicol 7 Suppl 1*, 165-170.

Rice, D. and Barone, S. (2000a). Critical periods of vulnerability for the developing nervous system: Evidence from humans and animal models. *Environmental Health Perspectives 108*, 511-533. http://dx.doi.org/Doi 10.2307/3454543

Rice, D. and Barone, S., Jr. (2000b). Critical periods of vulnerability for the developing nervous system: evidence from humans and animal models. *Environ Health Perspect 108 Suppl 3*, 511-533.

Robinson, J. F., Guerrette, Z., Yu, X. et al. (2010). A systems-based approach to investigate dose- and time-dependent methylmercury-induced gene expression response in C57BL/6 mouse embryos undergoing neurulation. *Birth Defects Res B Dev Reprod Toxicol 89*, 188-200. http://dx.doi.org/10.1002/bdrb.20241

Rodier, P. M. (1995a). Developing Brain as a Target of Toxicity. *Environmental Health Perspectives 103*, 73-76. http://dx.doi.org/Doi 10.2307/3432351

Rodier, P. M. (1995b). Developing brain as a target of toxicity. *Environ Health Perspect 103 Suppl 6*, 73-76.

Roque, P. J., Guizzetti, M. and Costa, L. G. (2014). Synaptic structure quantification in cultured neurons. *Curr Protoc Toxicol 60*, 12 22 11-12 22 32. http://dx.doi.org/10.1002/0471140856.tx1222s60

Seiler, A., Visan, A., Buesen, R. et al. (2004). Improvement of an in vitro stem cell assay for developmental toxicity: the use of molecular endpoints in the embryonic stem cell test. *Reprod Toxicol 18*, 231-240. http://dx.doi.org/10.1016/j.reprotox.2003.10.015

Shin, S., Mitalipova, M., Noggle, S. et al. (2006). Long-term proliferation of human embryonic stem cell-derived neuroepithelial cells using defined adherent culture conditions. *Stem Cells 24*, 125-138. http://dx.doi.org/10.1634/stemcells.2004-0150

Smirnova, L., Hogberg, H. T., Leist, M. et al. (2014). Developmental neurotoxicity - challenges in the 21st century and in vitro opportunities. *ALTEX 31*, 129-156. http://dx.doi.org/http://dx.doi.org/10.14573/altex.1403271

Spielmann, H., Seiler, A., Bremer, S. et al. (2006). The practical application of three validated in vitro embryotoxicity tests. The report and recommendations of an ECVAM/ZEBET workshop (ECVAM workshop 57). *Altern Lab Anim 34*, 527-538.

Stummann, T. C. and Bremer, S. (2008). The possible impact of human embryonic stem cells on safety pharmacological and toxicological assessments in drug discovery and drug development. *Curr Stem Cell Res Ther 3*, 118-131.

The National Academy of Sciences (2007). Toxicity Testing in the 21st Century: A Vision and a Strategy. *The National Academies Press.*

Theunissen, P. T., Robinson, J. F., Pennings, J. L. et al. (2012). Compound-specific effects of diverse neurodevelopmental toxicants on global gene expression in the neural embryonic stem cell test (ESTn). *Toxicology and applied pharmacology 262*, 330-340. http://dx.doi.org/10.1016/j.taap.2012.05.011

Uphill, P. F., Wilkins, S. R. and Allen, J. A. (1990). In vitro micromass teratogen test: Results from a blind trial of 25 compounds. *Toxicol In Vitro 4*, 623-626.

van Dartel, D. A. and Piersma, A. H. (2011). The embryonic stem cell test combined with toxicogenomics as an alternative testing model for the assessment of developmental toxicity. *Reprod Toxicol 32*, 235-244. http://dx.doi.org/10.1016/j.reprotox.2011.04.008

Wegner, S. H., Stanaway, I. B., Kim, H. Y. et al. (2014). Anchoring a dynamic *in vitro* model of human neuronal differentiation to key processes of early brain development *in vivo*. Ph.D., University of Washington,

Whittaker, S. G. and Faustman, E. M. (1992). Effects of benzimidazole analogs on cultures of differentiating rodent embryonic cells. *Toxicol Appl Pharmacol 113*, 144-151.

zur Nieden, N. I., Kempka, G. and Ahr, H. J. (2004). Molecular multiple endpoint embryonic stem cell test--a possible approach to test for the teratogenic potential of compounds. *Toxicol Appl Pharmacol 194*, 257-269. http://dx.doi.org/10.1016/j.taap.2003.09.019

CHAPTER 2: Characterization of *in vitro* organotypic 3D embryonic mouse midbrain micromass cultures using C57BL/6 and A/J mice

This Chapter is in preparation for submission. The authors of the manuscript are:

Julie Juyoung Park[1, 2], Brittany A. Weldon[1, 2], Julie H. Park[2], Sungwoo Hong[1, 2], Elaine M. Faustman[1, 2]*

[1] Institute for Risk Analysis and Risk Communication, University of Washington, Seattle, WA, USA

[2] Department of Environmental and Occupational Health Sciences, University of Washington, Seattle, WA, USA

* Corresponding author: Elaine M. Faustman

Institute for Risk Analysis and Risk Communication, Department of Environmental and Occupational Health Sciences, University of Washington, Seattle, WA, USA.

Email: faustman@uw.edu

ABSTRACT

In vivo developmental toxicity tests not only are complex and laborious but also require a large number of animals. To reduce such number but still maintain a three-dimensional concept, an *in vitro* rat micromass system has been proposed and validated as one of the alternative methods for developmental toxicity assessment by the European Centre for the Validation of Alternative Methods (Balls and Hellsten, 2002; Flint, 1993; Flint and Orton, 1984; Genschow et al., 2002; Piersma, 2004; Reinhardt, 1993; Spielmann et al., 2006; Uphill et al., 1990). For this study, a modified method of *in vitro* rat embryonic midbrain cells is described, which uses mouse cells and which can be used with mouse strains to investigate. Gestational day (GD) 11 C57BL/6 or GD 12 A/J fetal mouse midbrain cells were isolated and plated in high-density micromass format. The culture was grown for 22 days *in vitro* (DIV), and its morphology as well as the extent of neuronal differentiation were followed. Proliferation, migration, and differentiation similar to *in vivo* were observed *in vitro* during the culture period as verified by morphology, hematoxylin staining, protein content, Western blotting, and immunohistochemistry. The intensities of hematoxylin and protein content revealed that neuronal differentiation increase linearly over time in both C57BL/6 and A/J cultures, and that proliferation slowed after DIV 6. Protein expressions via Western blotting demonstrated time-dependency—proliferation markers such as PCNA showed a significant increase in protein expressions between DIV 4-6 when compared to DIV 1 while early differentiation markers (e.g. β-tubulin III and NeuN) and late differentiation markers (e.g. GluR-1 and NMDAε1) were detected between DIV 6-8 and DIV 8-15, respectively. Immunohistochemistry results for both proliferation and differentiation markers were consistent with Western blotting findings. Protein expression patterns for *in vitro* C57BL/6 and A/J micromass systems were similar. These studies characterize another set of assay options for evaluating early neurogenesis in mouse strains and extend test systems for gene and environment interaction studies.

INTRODUCTION

The brain has important functions from motor control, perception, and homeostasis to learning and memory. Thus, a proper development of the brain is critical for everyday life. Processes of brain development are highly orchestrated, making the neurodevelopmental period one of the most sensitive time frame for responses to toxicants. Because of its vulnerability, identifying windows of susceptibility in addition to dose and duration of potential exposure is critical. Exposures to various toxicants during this period may alter developmental processes and lead to functional impairments. For example, *in utero* exposures to organophosphate pesticides have been linked with neurodevelopmental effects including delays in learning and changes in brain structure (Engel et al., 2011; Rauh et al., 2006; Rauh et al., 2012). Heavy metals such as arsenic, methylmercury, and cadmium have also been well studied as developmental neurotoxicants (Burbacher and Grant, 2012; Flora et al., 2011; Kim et al., 2016; Robinson et al., 2010; Tolins et al., 2014). Less than 0.01% of chemicals registered at the U. S. Environmental Protection Agency is known to be toxic to human neurodevelopment (Miodovnik, 2011). Many of the registered compounds are yet to be examined for human developmental neurotoxicity.

International guidelines for developmental toxicity testing requires the use of *in vivo* studies as stated in Organization for Economic Co-operation and Development (OECD) Testing Guidelines 414, 415, 416, 421, and 422 (OECD, 1983, 2001b, a, 2016b, a). The traditional animal models are not only complex and laborious but also resource intensive, requiring a large number of experimental animals (Bailey et al., 2005; Piersma, 2004; Pratten et al., 2012). This has led to a recognition of developmental neurotoxicity testing as an area in need of *in vitro* alternative methods (Bal-Price et al., 2012; Crofton et al., 2014; Crofton et al., 2011; Crofton et al., 2012; Krewski et al., 2010; Lein et al., 2007; Smirnova et al., 2014). Developed *in vitro* alternative tests that can capture key neurodevelopmental processes would allow us to screen and prioritize potential neurotoxicants and to inform regulatory decision makers (Bal-Price et al., 2012; Krewski et al., 2010; Lein et al., 2007). To better predict neurodevelopmental toxicity that is reflective of humans, specificity and sensitivity of *in vitro* alternative methods need to be assessed (Bal-Price et al., 2012; Crofton et al., 2011; Lein et al., 2007; Smirnova et al., 2014). The European Centre for the Validation of Alternative Methods (ECVAM) also proposed validation project on *in vitro* embryotoxicity tests as a movement to reduce the number of experimental animals used for developmental toxicity evaluations (Genschow et al., 2002).

The micromass model has been proposed as one of the *in vitro* developmental toxicity testing tool by ECVAM in addition to whole embryo cultures and embryonic stem cell test (Balls and Hellsten, 2002; Genschow et al., 2002; Spielmann et al., 2006). An organotypic three-dimensional micromass system was initially developed using the embryonic rat limb bud and midbrain cells and was characterized by Flint (Flint, 1983; Flint and Ede, 1982; Flint et al., 1984). The fetal rat micromass cultures have several advantages. Micromass cultures use primary cells, but it can reduce the number of whole animals used for evaluating neurodevelopmental toxicity since large numbers of culture cells can be prepared from a few embryonic midbrains (Flint, 1993). The model is a medium-throughput *in vitro* assay that may be used to investigate mechanistic studies. The most important advantage is that the cell density drives the differentiation process without any addition of exogenous factors. Flint and Orton in 1984 validated the predictability of *in vitro* rat embryo limb bud and midbrain micromass cells. They reported that specificity of the *in vitro* micromass model was similar to those of *in vivo* after a blind trial for teratogenicity (Flint and Orton, 1984). Multiple other studies confirmed accuracy of prediction, concluding that the fetal rat limb bud micromass culture system is highly reproducible (Genschow et al., 2002; Piersma, 2004; Uphill et al., 1990). These studies concluded that the micromass is a robust *in vitro* model for testing potential teratogens (Flint, 1993; Flint and Orton, 1984; Genschow et al., 2002; Piersma, 2004; Reinhardt, 1993; Uphill et al., 1990).

For the current study, we have newly revised and have established a system for the organotypic three-dimensional fetal rat micromass midbrain system for mice with C57BL/6 and A/J mouse embryonic midbrain cells. We have optimized the cultures using C57BL/6 mouse strain because it is the most commonly used strain of mouse. A/J mouse strain was also characterized by comparing similarities and differences at the baseline as this strain is one of “classical laboratory strains” (Morgan and Welsh, 2015) and by genetic differences in response to a variety of developmental neurotoxicants *in vivo* (Scoville et al., 2015; Silbergeld et al., 2005). The *in vitro* alternative method optimized in this paper further characterize the neurodynamics of a mouse micromass culture system. This model may also be a useful tool for assessing cellular/molecular changes after exposures to various compounds and may be utilized as a medium-throughput screening tool for prioritizing potential neurotoxicants in risk assessment. With these establishments, differences in susceptibility due to genetic variability may be studied by using embryonic midbrain cells from C57BL/6 and A/J as well as from various other mouse strains.

METHODS

Midbrain cell isolation and culture conditions.

Previously optimized micromass culture methods in rats were modified and adapted for mouse embryonic midbrain micromass cultures (Flint, 1983; Ribeiro and Faustman, 1990). All experimental procedures included in this study were approved by University of Washington's Institutional Animal Care and Use Committee. Gravid uteri were obtained from the time-mated gestational day (GD) 11 C57BL/6 mice (Jackson Laboratory, Bar Harbor, ME, USA) or GD 12 A/J mice (Jackson Laboratory, Bar Harbor, ME, USA). To match the developmental maturity of the *in vitro* rat cultures, we used somite count across the species and strains. Embryonic midbrains were excised, pooled, and washed three times in 1X CMF-EBSS (Gibco, Life Technologies, Grand Island, NY, USA). During the final wash, harvested midbrains were immersed in 1X CMF-EBSS and incubated at 37°C for 20 minutes. Washed midbrains were then digested 20 minutes with 0.25% trypsin (Gibco, Life Technologies, Grand Island, NY, USA) in 37°C. Once digestion was completed, midbrain cells were dissociated in complete media (Dulbecco's Modified Eagle's Medium Nutrient Mixture F-12 (DMEM/F-12; Gibco, Life Technologies, Grand Island, NY, USA) with 10% fetal bovine serum (FBS, Gibco, Life Technologies, Grand Island, NY, USA)). Cells were then passed through a Swinney filter and brought into a single cell suspension. Cells were then seeded in a single 10 µL three-dimensional micromass island per well at a density of 5 x 10^6 cells/mL on 24-well matrigel-coated (BD Biosciences, Bedford, MA, USA) tissue culture plates (Corning Primaria, Corning, NY, USA). Micromass islands were then incubated for 1.5 hours at 37°C in a 5% CO_2 to allow for attachment and adhesion of cells to the culture plate. Following incubation, 500 µL of complete media was added to each well. For 22 days *in vitro*, the cultures were maintained with half of the medium refreshed every two days.

Morphology.

Imaging provides a useful insight in evaluating morphological changes of embryonic midbrain cells and in monitoring differentiation process of cultures over time. For 22 days *in vitro*, morphological images of mouse embryonic midbrain micromass cell cultures were acquired using an Olympus IMT-2 inverted microscope with phase-contrast optics (Olympus Inc., Tokyo, Japan). Morphological images were captured at 400x magnification and then digitized using a Coolsnap Camera (Roper Scientific, Inc., Duluth, GA, USA).

Hematoxylin staining.

The hematoxylin protocol was modified from Flint and Orton (Flint and Orton, 1984). At days *in vitro* (DIV) 1, 2, 4, 6, 8, 15, and 22, mouse midbrain micromass cultures were fixed with 10% formaldehyde for 20 minutes after aspirating medium. Fixed plates were stored in 1X Dulbecco's phosphate buffered saline (DPBS; Gibco, Life Technologies, Grand Island, NY, USA) at 4°C until use. Plates were rinsed with tap water and incubated with FluKa hematoxylin (Sigma-Aldrich, St. Louis, MO, USA) for 2-3 minutes. This basophilic stain was used to indicate the presence of neuronal nuclei. Plates were then de-stained by immersing them in tap water for 15 minutes for color development. Water was aspirated from the wells, and plates were air-dried overnight. The intensity of hematoxylin staining was measured and quantified the following day using Bio-Rad Gel Doc 2000 (an automated image analyzer; Bio-Rad Laboratories, Hercules, CA, USA) and Quantity One Software (Bio-Rad Laboratories, Hercules, CA, USA). The intensity of hematoxylin staining at DIV 1, 2, 4, 6, 8, 15, and 22 was adjusted DIV 1 hematoxylin staining density.

Immunohistochemistry.

At DIV 1, 2, 4, 6, 8, 15, and 22, cultures were fixed with 4% paraformaldehyde (Alfa Aesar, Ward Hill, MA, USA) for 30 minutes. Plates were stored at 4°C in 1X DPBS (Gibco, Life Technologies, Grand Island, NY, USA) until the time of analysis. For immunohistochemistry, culture plates were washed twice with 1X DPBS and incubated with blocking buffer (5% v/v goat serum dissolved in 1X DPBS with Tween) for an hour. A cocktail of primary antibodies in antibody dilution buffer (1% v/v bovine serum albumin dissolved in 1X DPBS with Tween) was added to plates and incubated overnight at 4°C. Plates were washed three times in 1X DPBS the following day, and then incubated 2 hours in dark with a cocktail of Alexa-fluor® fluorochromes (ThermoFisher, Grand Island, NY, USA) secondary antibodies diluted in antibody dilution buffer. Plates were washed three times with 1X DPBS after secondary antibody incubation. Hoechst 33342 (Sigma-Aldrich, St. Louis, MO, USA) was diluted in 1X DPBS to counterstain nuclei. Fluorescence-labeled cells were visualized under Leica TCS SP5 II laser scanning confocal microscope using HC Plan Apo CS 10x, NA 0.4 lens (Leica Microsystems, Wetzlar, Germany). Fiji software (Schindelin et al., 2012) was utilized to process images.

Western blotting.

Changes in protein expression throughout time in our embryonic mouse midbrain micromass culture system were analyzed using Western blotting. Total protein samples were harvested at DIV 1, 2, 4, 6, 8, 15, and 22 using 1X cell lysis buffer (Cell Signaling Technology, Danvers, MA, USA). Cell lysates were frozen and

thawed three times, centrifuged at 13,000rpm for 5 minutes, and quantified using Bio-Rad protein assay kit (Bio-Rad Laboratories, Hercules, CA, USA). Protein samples were diluted with sample buffer (Life Technologies, Carlsbad, CA, USA) and reducing agent (Life Technologies, Carlsbad, CA, USA) to ensure equal protein concentration between samples. Protein samples were run on 4-12% bis-tris SDS-PAGE gels (Life Technologies, Carlsbad, CA, USA) and transferred to poly-vinyl difluoride membrane (Merck Millipore, Billerica, MA, USA) in cold transfer buffer (Bio-Rad Laboratories, Hercules, CA, USA). Membranes were then washed in 1X Tris-buffered saline (TBS) for 10 minutes and blocked with 5% milk in 1X TBS with Tween (TTBS) for an hour to prevent non-specific protein bindings. Following blocking, membranes were then washed in 1X TTBS three times and incubated overnight at 4°C in primary antibody (1:1000 – 1:5000). Membranes were washed the next day with 1X TTBS three times and then incubated for 2 hours in 5% milk in 1X TTBS with the secondary antibody diluted. The membranes were then washed three times with 1X TTBS, and Amersham ECL buffer (GE Healthcare Life Sciences, Little Chalfont, United Kingdom) was used to detect the immunocomplex. The ECL-reactive membranes were exposed to X-ray films and developed. Image J software (National Institute of Health, Bethesda, Maryland, USA) was used to assess the intensity of bands. Data were normalized to corresponding β-actin values. The results were presented as average fold change to concurrent gel β-actin ± 95% confidence interval.

Primary antibodies used to characterize the dynamics of cell culture are summarized in Table 2.1 and include (sex determining region Y)-box 2 (SOX-2; Proteintech, Rosemont, IL, USA), nestin (Proteintech, Rosemont, IL, USA), proliferating cell nuclear antigen (PCNA; Merck Millipore, Billerica, MA, USA), β-tubulin III (Merck Millipore, Billerica, MA, USA), microtubule-associated protein 2 (MAP-2; Proteintech, Rosemont, IL, USA), neuronal nuclei (NeuN; Merck Millipore, Billerica, MA, USA), glutamate receptor 1 (GluR-1; Epitomics, Burlingame, CA, USA), N-methyl-D-aspartic acid ε1 (NMDAε1; Santa Cruz Biotechnology, Dallas, TX, USA), α-synuclein (BD Biosciences, Franklin Lakes, NJ, USA), engrailed 1 (EN1; Epitomics, Burlingame, CA, USA); glial fibrillary acidic protein (GFAP; Stemcell Technologies, Vancouver, BC, Canada), and cleaved caspase-3 (Cell Signaling Technology, Danvers, MA, USA). As a loading control, β-actin (Sigma-Aldrich, St. Louis, MO, USA) was used. Goat anti-mouse (BD Biosciences, San Jose, CA, USA) and goat anti-rabbit (BD Biosciences, San Jose, CA, USA) were used as secondary antibodies.

Statistical analysis.

A linear mixed effects model was used to analyze significant differences over days *in vitro* (DIV) in differentiating mouse embryonic midbrain cell culture systems. For protein and Western blot analysis, statistical significance was determined by mixed effects analysis of variance with fixed effects of DIV, and random effects of experimental dates. We used mixed effects model of the change from DIV 1, Y,

$$Y_{ij} = A + B_jX_i + R_i + E_i,$$

$$R_i \sim N(0, r) \text{ and } E_i \sim N(0, s) \text{ for } i = 1 \ldots i \text{ samples}$$

where X_i is the DIV, A is the intercept, and B_j is the effect on the j^{th} DIV, R_i is the random effect for preparation date of the i^{th} sample, r is the variance for the random effects, and s is the residual variance after accounting for the fixed effect of DIV.

For hematoxylin analysis, a linear mixed effect model was used in which DIV was used as a continuous fixed effect variable and experimental dates as a random effect. We used a linear model of Y,

$$Y_i = A + BX_i + R_i + E_i,$$

$$R_i \sim N(0, r) \text{ and } E_i \sim N(0, s) \text{ for } i = 1 \ldots i \text{ samples}$$

where X_i is the DIV, A is the intercept, and B is the slope of change over time (DIV), R_i is the random effect for preparation date of the i^{th} sample, the random effects, r, is the variance for the random effects, and s is the residual variance after accounting for the fixed effect of DIV.

R statistical software (https://www.R-project.org) was utilized for statistical analyses, and "lme4" package was used for modeling mixed effects (Bates et al., 2014). P-values less than 0.05 ($p\text{-value} < 0.05$) were considered statistically significant.

RESULTS

Description of mouse midbrain micromass culture development.

Cell cultures were observed and analyzed on the basis of cell proliferation and differentiation over 22 days *in vitro*. After 24 hours of plating, midbrain cells from C57BL/6 or A/J exhibited characteristics of cell aggregation (Flint, 1983). Within each micromass island, these discrete groups of mouse midbrain cells formed tightly packed, irregular foci. The size of foci increased over time, and bigger foci were observed towards the center of the island. Over 22 days of culture, increasing characteristics of differentiating neural

networks, including the formation of dense neuronal foci and extension of neurite outgrowths, were observed (Figure 2.1). Cross-sectional images captured using a confocal microscope revealed that neuronal foci in C57BL/6 and A/J midbrain cells were also growing three-dimensionally over culture days (data not shown).

Growth and differentiation of in vitro micromass islands.

Hematoxylin staining was utilized to demonstrate the extent of neuronal differentiation in our culture system at seven different time points (DIV 1, 2, 4, 6, 8, 15, and 22). Microscopic examination of darkly stained embryonic mouse midbrain micromass illustrated increased radius of each micromass island over time, suggesting that the micromass islands had spread within a well as described in Flint (1983). Microscopic examination indicated sparsely stained midbrain cells at DIV 1, but the density of stained neuronal foci enlarged through DIV 22 (data not shown).

When the intensity of hematoxylin staining was quantitated and then compared to DIV 1, our culture system showed a linear increase in the presence of neuronal differentiation (Figure 2.2), indicating that the presence of differentiated midbrain cells increases linearly during 22-days of the culture period. The extent of differentiation in C57BL/6 and A/J micromass cultures were examined using slopes of a linear mixed-effect regression line (Figure 2.2A). The slopes of C57BL/6 and A/J were 0.11 ± 0.004 and 0.26 ± 0.024, respectively. When effects of mouse strain on the extent of neuronal differentiation via hematoxylin staining were calculated, the slope between the two systems was not significantly different.

The amount of protein content in both C57BL/6 and A/J culture systems were evaluated across DIV and were compared across both strains. An increase of total protein concentration was observed between days 1 and 6 (Figure 2.3), suggested that not only differentiation but also proliferation is occurring in our mouse midbrain cells during early days in cultures. This linear increase in total protein was also observed between days 1 and 5 of rat micromass system as described by Flint (1983). After DIV 6, protein content seemed to be stabilized, indicating that there may be a limited growth as midbrain cells differentiate further.

Dynamics of in vitro mouse embryonic midbrain micromass.

Changes in developmental and neuronal stage-specific protein expression over time illustrated the progression of neuronal differentiation in our C57BL/6 and A/J mouse micromass culture systems. Western

blots identified three unique groups of protein markers. The first group includes proteins involved with stem cells or proliferating cells such as SOX-2, Nestin, and PCNA (Figure 2.4A and Figure 2.4B). These antibodies were used to examine the extent of proliferation in our C57BL/6 and A/J midbrain cells and to provide clues about the dynamics of cell proliferation versus differentiation during early stages *in vitro*. No significant increase in the embryonic stem cell marker, SOX-2, and the neural progenitor cell marker, nestin, were observed in both C57BL/6 and A/J micromass cultures (Figure 2.4A and 2.4B), but the expressions of SOX-2 and nestin were present in both systems. This finding indicated that a subpopulation of mouse embryonic midbrain cells maintained pluripotency as differentiation advanced (Chambers and Tomlinson, 2009; Kim et al., 2016; Kuegler et al., 2010; Wilson and Stice, 2006). A proliferating cell marker, PCNA, showed a significant increase in expression at DIV 4 and 6 (p-value < 0.001 for both DIV) for C57BL/6 mouse and at DIV 4 (p-value < 0.01) for A/J mouse micromass systems (Figure 2.4A and 2.4B). PCNA expression then decreased after DIV 4 in both, suggesting that cells are predominantly proliferating during early days of the micromass culture. Similar patterns were observed via immunofluorescence (Figure 2.5A, 2.5B, 2.5C, and 2.5F). Immunofluorescence images of nestin and PCNA demonstrated that both of these markers were expressed the most at early days of the culture period.

The second cluster of protein markers included early neuronal differentiation markers: β-tubulin III, MAP-2, and NeuN. Cytoskeleton proteins, β-tubulin III and MAP-2, were chosen because we expected these to be expressed as the cells differentiate and develop neurite outgrowths (Boer et al., 2010). Neuronal nuclei-specific protein, NeuN, was examined because it first appears upon withdrawal from the cell cycle and/or initiation of terminal differentiation (Lavezzi et al., 2013; Mullen et al., 1992). The expressions of structural-specific and neuronal nuclei-specific proteins were at their highest levels between 4 and 15 days in culture (Figure 2.4C and 2.4D), demonstrating that differentiation was initiated, and yet proliferation was still active during early days of culture. As shown in Figure 2.4C, Western blots illustrated a significant increase in expression of MAP-2 at DIV 4 and 6 (p-value < 0.001 for both DIV) and of NeuN at DIV 6 and 8 (p-value < 0.001 at both time points) in the C57BL/6 micromass system. Similar trends were observed for A/J mouse strain. MAP-2 expressions were significantly increased during DIV 4 to 15 (Figure 2.4D; p-value for DIV 4, 6, 8, and 15 are < 0.01, < 0.05, < 0.01, and < 0.05, respectively). NeuN in A/J cultures showed significant increase in its expression between DIV6 and 15 (Figure 2.4D; DIV 6 p-value < 0.05 and p-value < 0.001 for both DIV 8 and 15). NeuN is first detected during development when neuronal cells are withdrawn from the cell cycle and/or are at the initiation of neuronal terminal differentiation (Mullen et al., 1992),

suggesting that our midbrain cells may be withdrawn from the cell cycle and/or starting neuronal terminal differentiation at days 6 *in vitro*. Figure 2.4C and 2.4D demonstrated a significant increase in β-tubulin III expressions from DIV 6 through 15 in both C57BL/6 (p-value < 0.01 for DIV 6 and 8 and p-value < 0.05) and A/J mouse strains (p-value < 0.001 for DIV 6, 8, and 15). This result confirmed that our cultured fetal mouse midbrain cells further differentiate into neuronal cells. Protein expressions of early differentiation markers shown by Western blotting highly concorded with immunofluorescence images (Figure 2.5A – 2.5E). As these protein levels decreased, expressions of another protein group surged as discussed next.

The last group of proteins that was comprised of late neuronal differentiation markers (GluR-1, NMDAε1, α-synuclein, and EN1). GluR-1 and NMDAε1 are subtypes of glutamate receptors in the CNS and are expressed in glutamatergic neurons, which starts to appear during late gestation and neonatal life. During 22 days of the C57BL/6 micromass culture period, a significant increase in expressions of two glutamate subtype receptors, GluR-1 and NMDAε1, were observed at DIV8 and DIV 15 (Figure 2.4E). The expression of GluR-1 was more significant at DIV 15 (p-value < 0.001) compared to DIV 8 (p-value < 0.05). Immunohistochemistry also revealed that GluR-1 was expressed highly between DIV 8 and 15 (Figure 2.5E and 2.5F), which aligned with Western blotting data. Similar to GluR-1, NMDAε1 showed more significantly increased expressions at DIV 15 (p-value < 0.001) compared to DIV8 (p-value < 0.01). Both of these suggest that our midbrain cells initiated to form glutamate receptors. In A/J micromass culture system, only NMDAε1 expression significantly increased at DIV15 (p-value < 0.05) as illustrated in Figure 2.4F. We examined a presynaptic terminal specific protein marker, α-synuclein, to investigate the maturity of our differentiating midbrain cells over 22 days of the culture period. Expression of α-synuclein demonstrated significantly increased expression only at DIV 15 in both C57BL/6 (p-value < 0.05) and A/J (p-value < 0.001). EN1 was also examined to confirm midbrain development. Midbrain specific marker, EN1, continued to be expressed throughout the culture period, with a significant increase at DIV 15 (p-value < 0.05) in C57BL/6 (Figure 2.4E). An increasing trend in EN1 expression was observed from DIV 1 to 15 in A/J over 22 days of the culture period (Figure 2.4F), but no significant increase was found. This result confirmed that both of our embryonic mouse midbrain cultures were differentiating further into neuronal cells with midbrain characteristics.

Cleaved caspase-3 is used as a marker of oxidative stress, which plays a significant role in neurodevelopment as well as in apoptosis (D'Amelio et al., 2010). During the time when proliferation

signals are decreasing, and differentiation signals are most active, the expression of cleaved caspase-3 also increased in C57BL/6 micromass cultures, reaching its peak at DIV 8 (Figure 2.4G; p-value < 0.01). An increasing trend of cleaved caspase-3 expression was illustrated in A/J, but no significance was found (Figure 2.4H). This finding suggested that natural apoptosis and/or oxidative stress may be occurring as our culture develops over time as casepase-3 is also recognized to be involved in neural stem cell differentiation *in vitro* (D'Amelio et al., 2010; Fernando et al., 2005). However, what portion of our observed cleaved caspase-3 expression is contributing to natural apoptosis versus neurogenesis is unclear.

GFAP antibody was also examined via Western blotting to determine the presence of various central nervous system cell types, including astrocytes; however, GFAP expression was not detected even in day-22 C57BL/6 and A/J mouse midbrain micromass cultures (data not shown). This result is consistent with previously reported observations in Flint (1983) and Whittaker et al. (1993). Our fetal mouse midbrain micromass cultures may not be differentiated far enough to have astrocytes present in the system.

DISCUSSION

The true uniqueness of the embryonic mouse midbrain micromass cultures lies in the fact that differentiation was solely driven by the cell density, as our media only included 10% serum and did not include any additional external stimulants. In addition, previous CNS micromass models were cultured only up to 5 days while current midbrain micromass culture lasted 3 weeks. Throughout the 22 days of culture, the dynamics of neurodevelopment were observed, ranging from proliferation to migration and differentiation. As noted in Flint (1983) and Ribeiro and Faustman (1990), active aggregation of midbrain cells formed small, distinct foci, which spread into larger but still distinct foci. Further differentiation of cells occurred within the foci, and neurite outgrowths developed and connected among foci. Small islands of cells at DIV1 became larger over 22 days *in vitro*.

In both C57BL/6 and A/J midbrain cell cultures, the growth of each embryonic mouse midbrain micromass island in terms of protein content was linear between DIV 1 through 6; however, very limited proliferation was observed between DIV 6 to 22. Hematoxylin, which is acidic, stains neuronal nuclei by binding to basic proteins such as histones and deoxyribonucleic acid (DNA) (Flint, 1983; Flint et al., 1984; Myers; Ribeiro and Faustman, 1990). We have used this method to determine the level of neuronal differentiation, by

measuring the intensity of darkly stained foci. This provided evidence that the foci comprised differentiated neuronal cells. When the intensity of hematoxylin staining was quantitated and adjusted to DIV 1, our culture system indicated that the presence of differentiated midbrain cells increases linearly. This result agreed with cell cycle analysis performed by Ribeiro and Faustman (1990) that a gradual increase in the CNS micromass cell percentages at the G0/G1 phase of the cell cycle was observed. The cells withdrawn from the cell cycle irreversibly lose a proliferation activity followed by the terminally differentiated phenotype expressions, and this temporal coupling plays a critical role in normal development and growth and continues to be vital for homeostasis and cell replacement throughout life. An increased number of fetal mouse midbrain cells may also be slowly withdrawn from the cell cycle until DIV 6 and lose their proliferation capacity and begin differentiating as shown in terms of protein content and hematoxylin staining. Results from Western blot and immunofluorescence is consistent with this conclusion. By DIV 6, expressions of proteins involved in proliferation have peaked and decreased in both C57BL/6 and A/J micromass cultures (Figure 2.4 and Figure 2.5). A linear increase was observed in both systems with greater extent of differentiation in A/J compared to C57BL/6 cultures, suggesting that the differentiation rate between the two systems may be different.

Neural markers serve as good indicators that allow detection and identification of specific cell types. They are expressed at different times of neurogenesis and help us characterize developing neuronal cells. Both Western blotting and immunohistochemistry analysis confirmed our observations with the differentiation trajectory. First, protein levels via Western blotting demonstrated a great concordance with immunofluorescence images for both C57BL/6 and A/J midbrain cells. The profiles of protein markers examined for this study were also consistent with those described in the previous literature (Flint, 1983; Mamber et al., 2012; Whittaker et al., 1993). The expressions of proliferation markers (e.g. nestin and PCNA) were seen at DIV 4 to 6 while those of early differentiation markers (e.g. β-tubulin III, MAP2, and NeuN) appeared during DIV 4 to 15. Significant late differentiation marker (e.g. GluR-1) expressions were observed after DIV 8, which is after the proliferation signals had decreased. Altogether, results suggested that both proliferation and differentiation signals may be present during early days of culture, but when significant proliferation signals decrease after DIV6, and the cells were primarily committed to differentiation. The absence of GFAP markers in fetal mouse midbrain micromass cultures is consistent with previous publications by Mamber et al. (2012). They reported that expression of GFAPd, one isoform that is expressed in proliferating radial glial cells during neurodevelopment, was observed starting from

embryonic day 18 of C57BL/6 mice via immunohistochemistry. Similar protein expression patterns found between C57BL/6 and A/J micromass cultures confirmed that neurodevelopmental stages are comparable even though the differentiation rate between the two systems may be different.

Embryonic C57BL/6 and A/J mouse midbrain micromass culture systems are *in vitro* methods that closely resemble *in vivo* neurodevelopment without additional exogenous growth factors (Flint, 1983; Flint and Ede, 1982; Flint and Orton, 1984; Flint et al., 1984; Walum and Flint, 1990). When imaged with confocal microscope at DIV 1, 2, 4, 6, 8, 15, and 22, neuronal cells in micromass islands move outwards (data not shown). Twenty-two days of the culture period in C57BL/6 and A/J micromass may represent mouse *in vivo* GD 11 and 18 as cultures with GFAP yet to be expressed in our culture system (Mamber et al., 2012). This period (mouse GD 11 to 18) is reflective of human gestational days of 32 to 60 (O'Rahilly et al., 1987; Otis and Brent, 1954; Theiler, 1989). Therefore, adverse neurodevelopmental effects of various chemicals during the first trimester of human gestational days could be examined using this mouse midbrain micromass system.

Currently, *in vitro* neurodevelopmental test batteries cannot completely replace *in vivo* studies even though they could be useful tools as a means to reduce the number of animals used and to refine the priority of toxicants to be tested *in vivo* (Lein et al., 2007; Piersma, 2004; Pratten et al., 2012). In addition to the micromass systems, *in vitro* embryonic stem cell test was suggested as neurodevelopmental toxicity screening tools. We previously have characterized *in vitro* human neural progenitor cell (hNPC) cultures derived from human ESCs and were also able to capture neuronal proliferation, migration, and differentiation over 3 weeks of the culture period (Wegner et al., 2014). Increases in β-tubulin III, nestin, and α-synuclein expressions was observed over time in our *in vitro* hNPCs while PCNA expression spiked at day 10 of culture then decreased (Wegner et al., 2014), reflecting DIV 4 of our *in vitro* mouse midbrain micromass. MAP-2 expression peaked at day 14 after PCNA levels have decreased (Wegner et al., 2014), indicating the similar neurodevelopmental maturity of DIV 6 – 8 in mouse midbrain micromass. A similar pattern was observed between mouse midbrain micromass and hNPC cultures—early differentiation markers, β-tubulin III and MAP-2, increased after the decrease in proliferation marker. GFAP was not expressed in hNPC cultures even at 21 days of the culture period. These suggested that the mouse micromass system and hNPCs may share similar neurodevelopmental stages; however, hNPCs, in contrast to the midbrain micromass system, ultimately would give rise to neurons with forebrain characteristics

without any morphogenic signals as with our hNPCs system (Gaspard and Vanderhaeghen, 2010; Wegner et al., 2014). Another alternative method for neurodevelopment is human 3D neurospheres. In this system, the decrease in nestin and increase in β-tubulin III expressions were observed after 7 days in culture (Moors et al., 2009). GFAP was detected from day 1 using neurosphere method (Moors et al., 2009), suggesting that this system is differentiated further than *in vitro* mouse micromass and hNPCs cultures. Moors et al. (2009) also reported that $O4^+$ oligodendrocytes were emerging in this culture system. With the inclusion of our *in vitro* mouse midbrain micromass, we may be able to capture both regional- and stage-specific effects of potential neurotoxicants during neurodevelopment.

Moreover, genetic factors can also be studied using mouse midbrain cells using various mouse strains as differential susceptibility is observed. For example, A/J mouse was most sensitive to quantum dot exposures compared to other Collaborative Cross founder mouse strains Scoville et al. (2015). Robinson et al. (2010) also observed differing susceptibility to MeHg on neural tube closure of C57BL/6 and SWV mouse strains after single intraperitoneal injection at GD 8. With *in vitro* 3D mouse midbrain cell cultures, differential responses to potential neurotoxicants can be screened with less animal, time, and labor-intensive procedures.

Unlike cell lines, the micromass system requires primary cells, needing a fresh cell suspension for every new experiment. Midbrain cells isolated from the fetal C57BL/6 and A/J mice would consist of a mixture of cell types, instead of a single cell type, as the cells are directly collected from mouse embryos and reflect an organotypic context. Organ-organ interactions or other regulatory mechanisms that are necessary for neurodevelopment and embryogenesis also lack in primary cell cultures (Piersma, 2004). Upon further validation, however, the fetal mouse midbrain micromass culture may be a promising *in vitro* alternative model for studying normal *in vivo* neurodevelopment as well as for testing chemically-induced developmental neurotoxicity. Examinations of cellular as well as molecular processes governing neurodevelopment may also be further investigated in addition to neurodevelopmental pathways perturbed by various toxicants. Differences in response due to genetic variability may also be studied with this model using different mouse strains. Further studies examining reproducibility, predictability, and metabolic capability of fetal mouse midbrain micromass model would be critical. Future studies should include a comparison between *in vitro* and *in vivo* pharmacokinetics as *in vitro* may have limited metabolomic activity (Flint, 1993). As neurodevelopment is complex, and its cellular signals are tightly

regulated, comparing genetic profiles between *in vitro* embryo mouse midbrain cultures and *in vivo* across time will also enhance our knowledge on time-course (Piersma, 2004).

We conclude that embryonic mouse midbrain micromass cultures offer a useful *in vitro* alternative method for neurodevelopmental toxicity testing. The system captures dynamics of *in vivo* development including proliferation, migration, and differentiation phases as described in this paper. Because this system has now been established *in vitro* and developmental dynamics compared across *in vivo* time points, across applications, and across genetically diverse mouse model, it opens up new potential applications. Upon further validation, mouse micromass may be applied to risk assessment in screening and prioritizing potential neurotoxicants in addition to investigating differences in response to various toxicants by performing Collaborative Cross studies.

Table 2.1. Neuronal markers used for *in vitro* mouse embryonic midbrain micromass cultures (Table was modified from Kim et al. (2016))

Antibody	Biological Function	Cells Detected	References
Sex determining region Y box 2 (SOX-2)	Transcription factor essential for maintaining self-renewal and regulating pluripotency	Embryonic stem cells	Chambers and Tomlinson (2009); Kim et al. (2016) Kuegler et al. (2010); Okumura-Nakanishi et al. (2005)
Nestin	Intermediate filament protein involved in radial axon growth	Neural progenitor cells	Kim et al. (2016); Kuegler et al. (2010); Wilson and Stice (2006)
Proliferating cell nuclear antigen (PCNA)	Proliferation	Proliferating cells	Kim et al. (2016); Nguyen et al. (2014)
β-tubulin III	Component of microtubules found in cytoskeleton and axons	Structural neuron specific marker	Kuegler et al. (2010); von Bohlen Und Halbach (2007)
Microtubule-associated protein 2 (MAP-2)	Microtubule associated protein located primarily in dendrites	Structural neuron specific marker	Kuegler et al. (2010); Palaga et al. (2013)
Neuronal nuclei (NeuN)	Neuronal nuclei	CNS and PNS neuronal cells	Mullen et al. (1992); Palaga et al. (2013); Lavezzi et al. (2013)
Glutamate receptor 1 (GluR-1)	Glutamate receptor	Glutamatergic neurons	Boer et al. (2010)
N-methyl-D-aspartic acid ε1 (NMDAε1)	Ionotropic glutamate receptor	Glutamatergic neurons	Chakraborty et al. (2017)
α-synuclein	Neuronal vesicle trafficking in presynaptic terminals	Presynaptic terminals of neurons	Ettle et al. (2014)
Engrailed 1 (EN1)	Regulates development of midbrain in humans	Midbrain	Kuegler et al. (2010); Kirkeby et al. (2012)
Glial fibrillary acidic protein (GFAP)	Intermediate filament expressed in astrocytes during central nervous system development	Astrocytes	Ghandour et al. (1979); Kuegler et al. (2010); Rodnight et al. (1997)
Cleaved Caspase-3	Activated form of Caspase-3, which as a role in apoptosis in natural brain development	Ubiquitous	Ceccatelli et al. (2004)

A

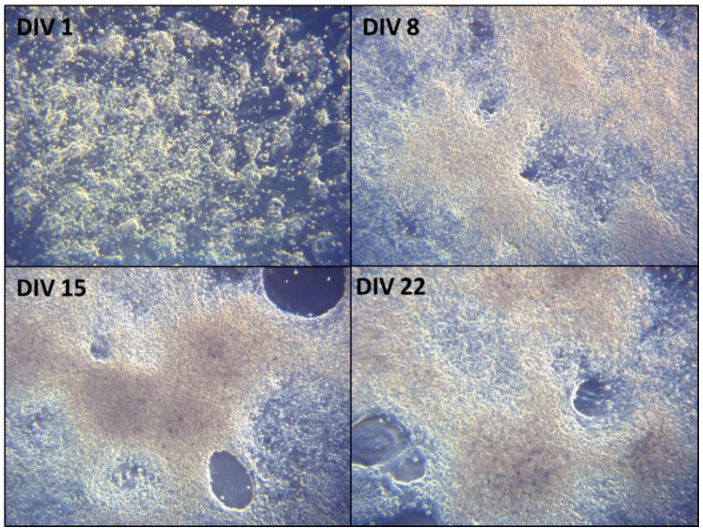

B

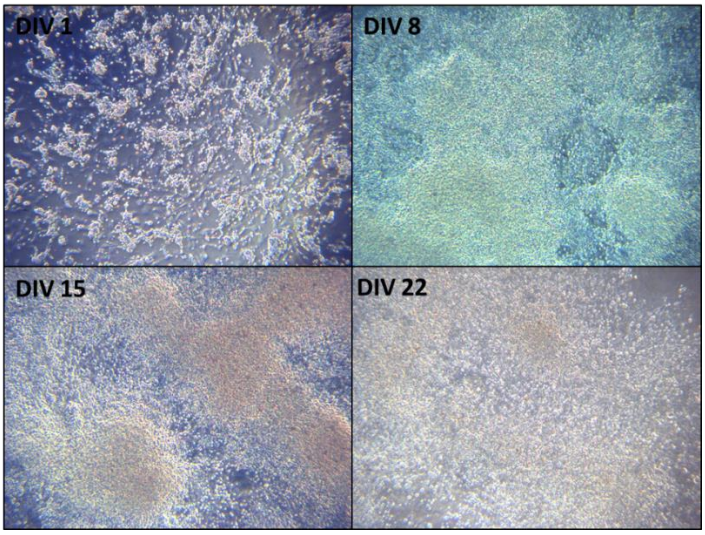

Figure 2.1. 400x magnification phase-contrast microscope images of (A) C57BL/6 and (B) A/J mouse embryonic midbrain cell micromass over 22 days in culture. Migration and differentiation including dense neuronal foci formation of C57BL/6 and A/J mouse midbrain cells and neurite outgrowths were observed over time. Foci and neurite outgrowths in A/J micromass cultures were not as distinguishable as in C57BL/6.

A

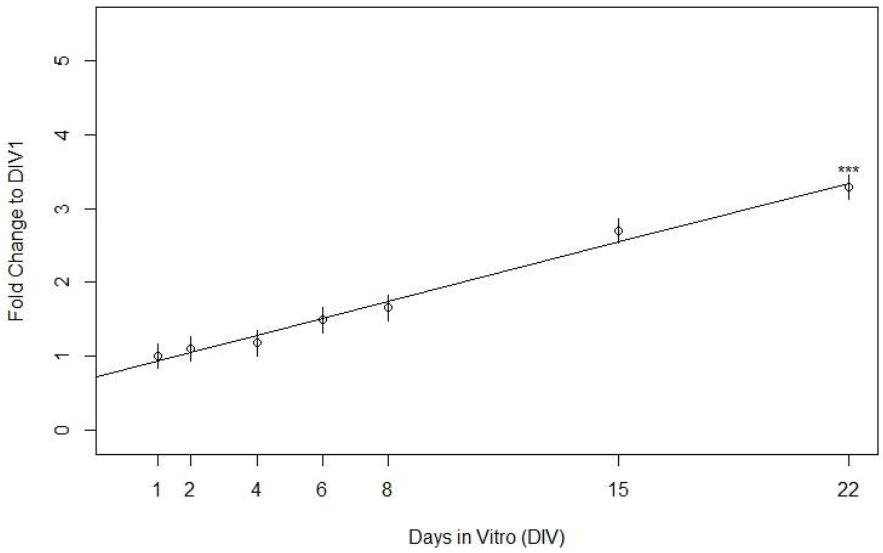

B

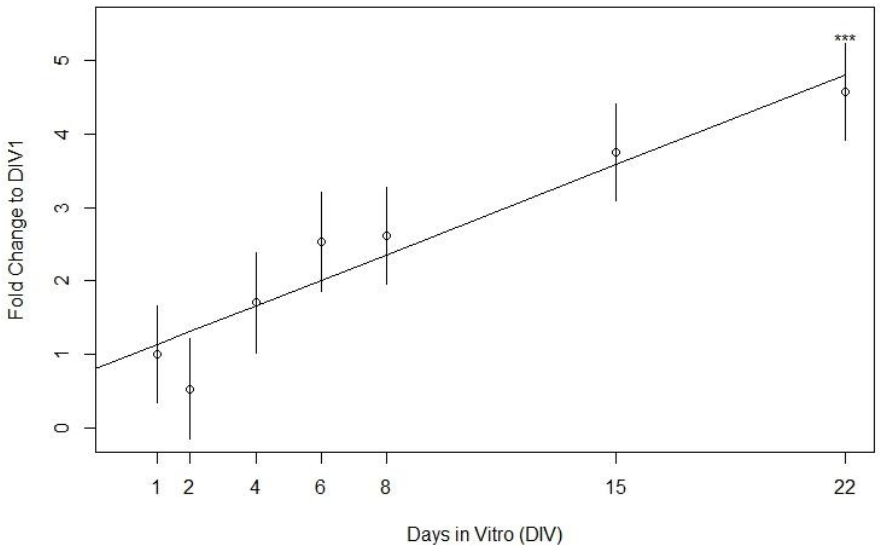

Figure 2.2. Hematoxylin staining of mouse embryonic midbrain cell micromass cultures during 22-day of the culture period. A plot of fold change in staining intensity against culture days 1 *in vitro* in (A) C57BL/6 and (B) A/J micromss systems demonstrated a linear increase in the presence of neuronal differentiation over time. Data points and 95% confidence intervals (Mean ± 95% CI) were drawn based on the mixed effects model. N = 3 - 5; ***: p-value < 0.001 for the slopes

A

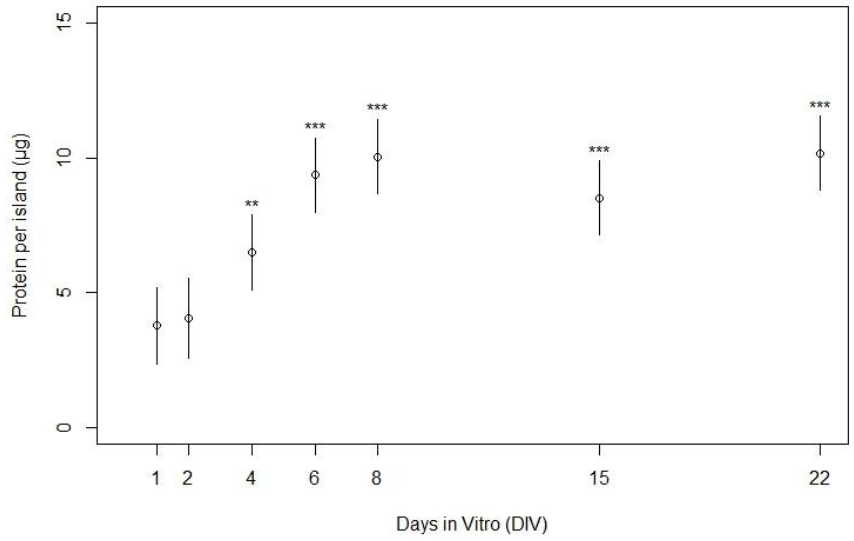

B

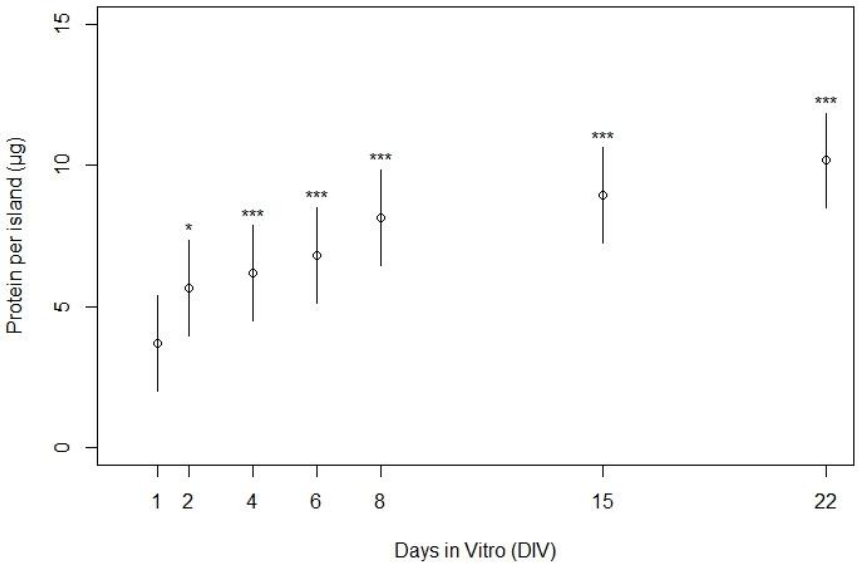

Figure 2.3. The amount of protein per mouse embryonic midbrain cell islands over 22-day of the culture period. (A) C57BL/6 and (B) A/J cultures demonstrated a similar trend in protein content over time. An increase in protein content per micromass island was observed during first 6 days of the culture period. Stabilized protein concentration was observed after DIV 6. The data points and 95% confidence intervals (Mean ± 95% CI) were drawn based on the mixed effects model. N = 3 - 7; *: p-value < 0.05; **: p-value < 0.01; ***: p-value < 0.001

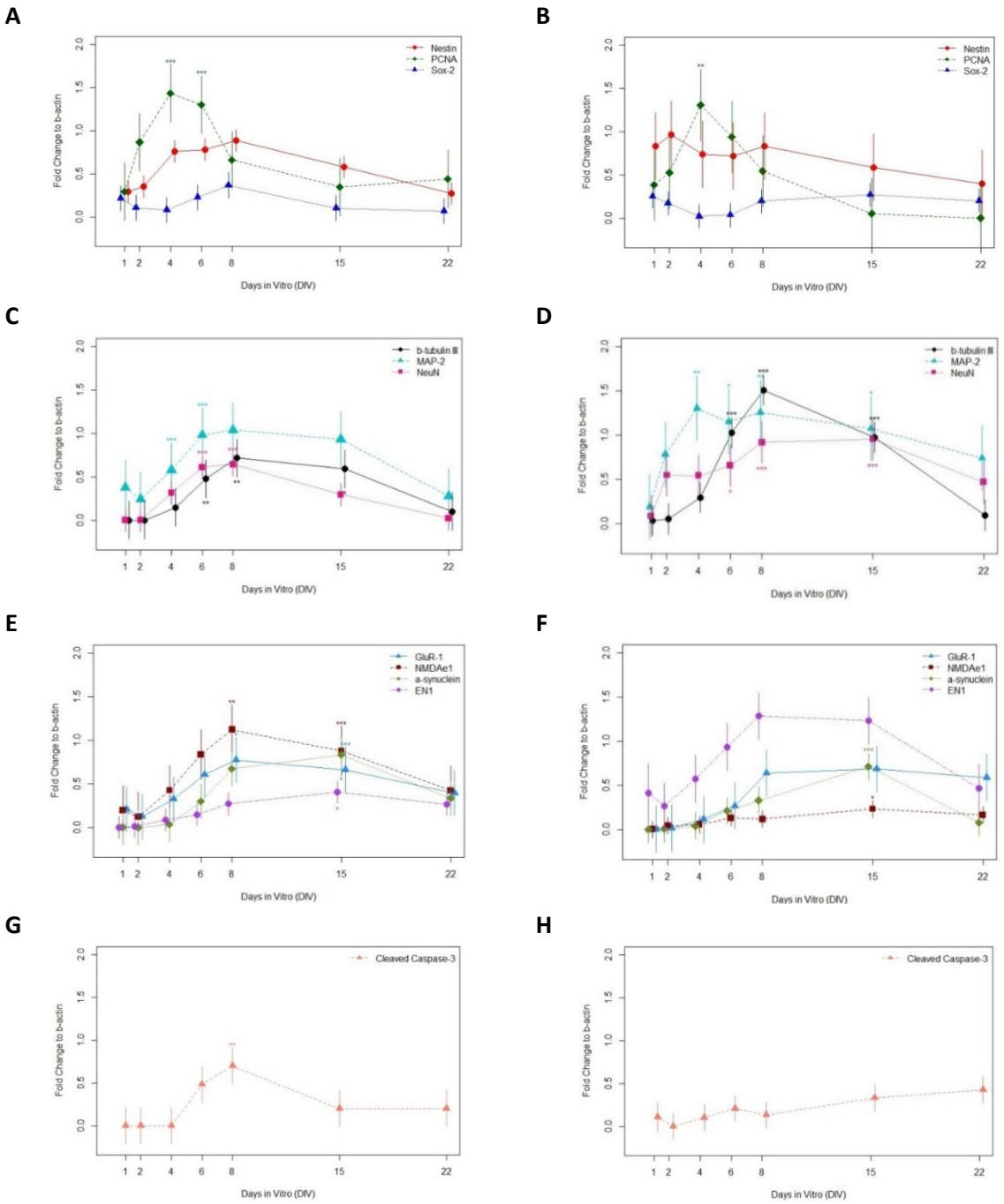

Figure 2.4. Dynamics of various proteins over time in mouse embryonic midbrain cell micromass cultures via western blotting. Similar trends among protein markers of (A - B) proliferation, (C - D) early differentiation, (E - F) late differentiation, and (G - H) apoptosis in C57BL/6 (A, C, E, and G) and A/J (B, D, F, and H) mouse micromass systems were found. Data points and 95% confidence intervals (Mean ± 95% CI) were estimated from the mixed-effect model, and lines connect those estimated data points. N = 3 - 5; *: p-value < 0.05; **: p-value < 0.01; ***: p-value < 0.001 compared to β-actin.

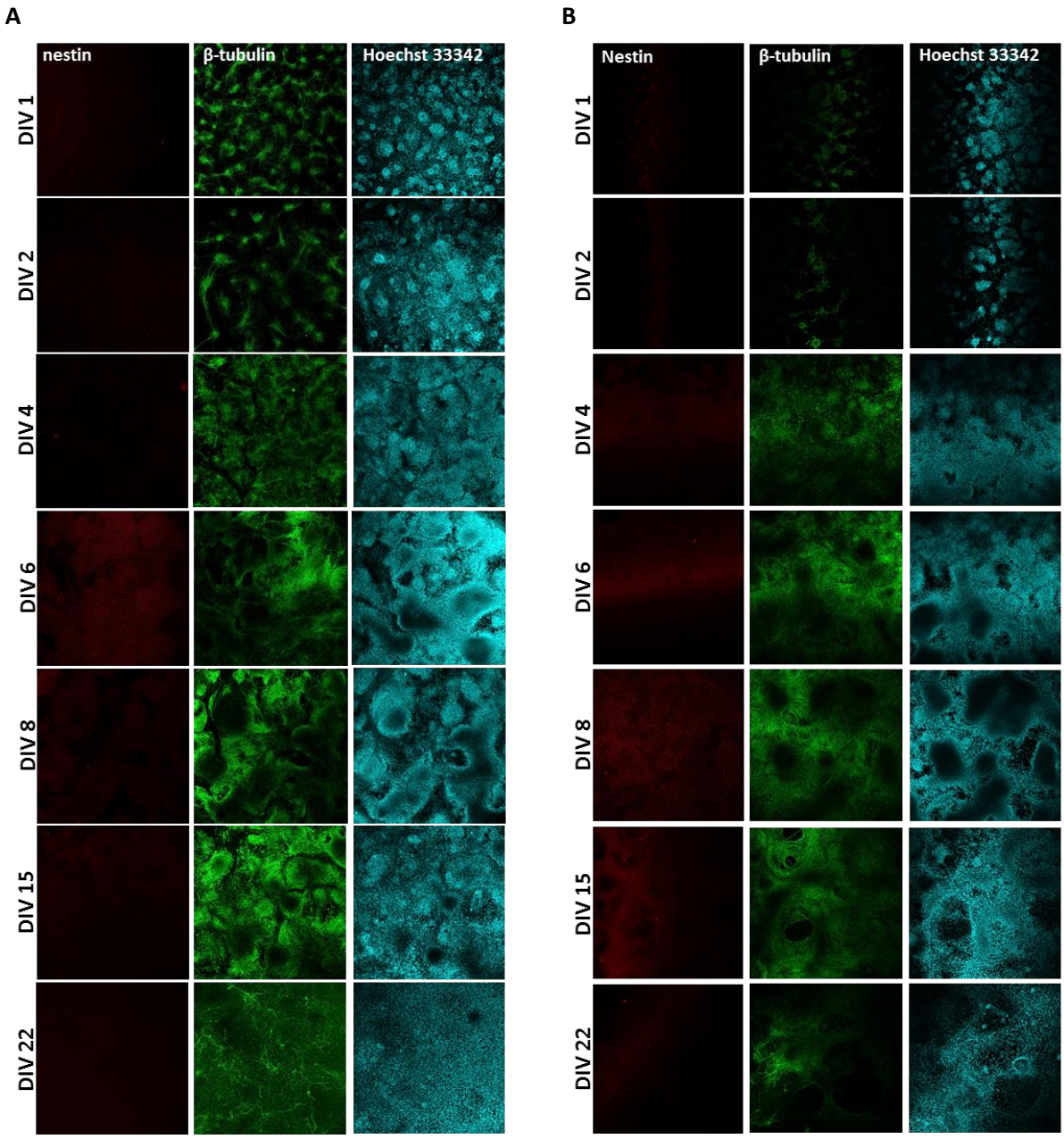
A
nestin
β-tubulin
Hoechst 33342
DIV 1
DIV 2
DIV 4
DIV 6
DIV 8
DIV 15
DIV 22
B
Nestin
β-tubulin
Hoechst 33342
DIV 1
DIV 2
DIV 4
DIV 6
DIV 8
DIV 15
DIV 22

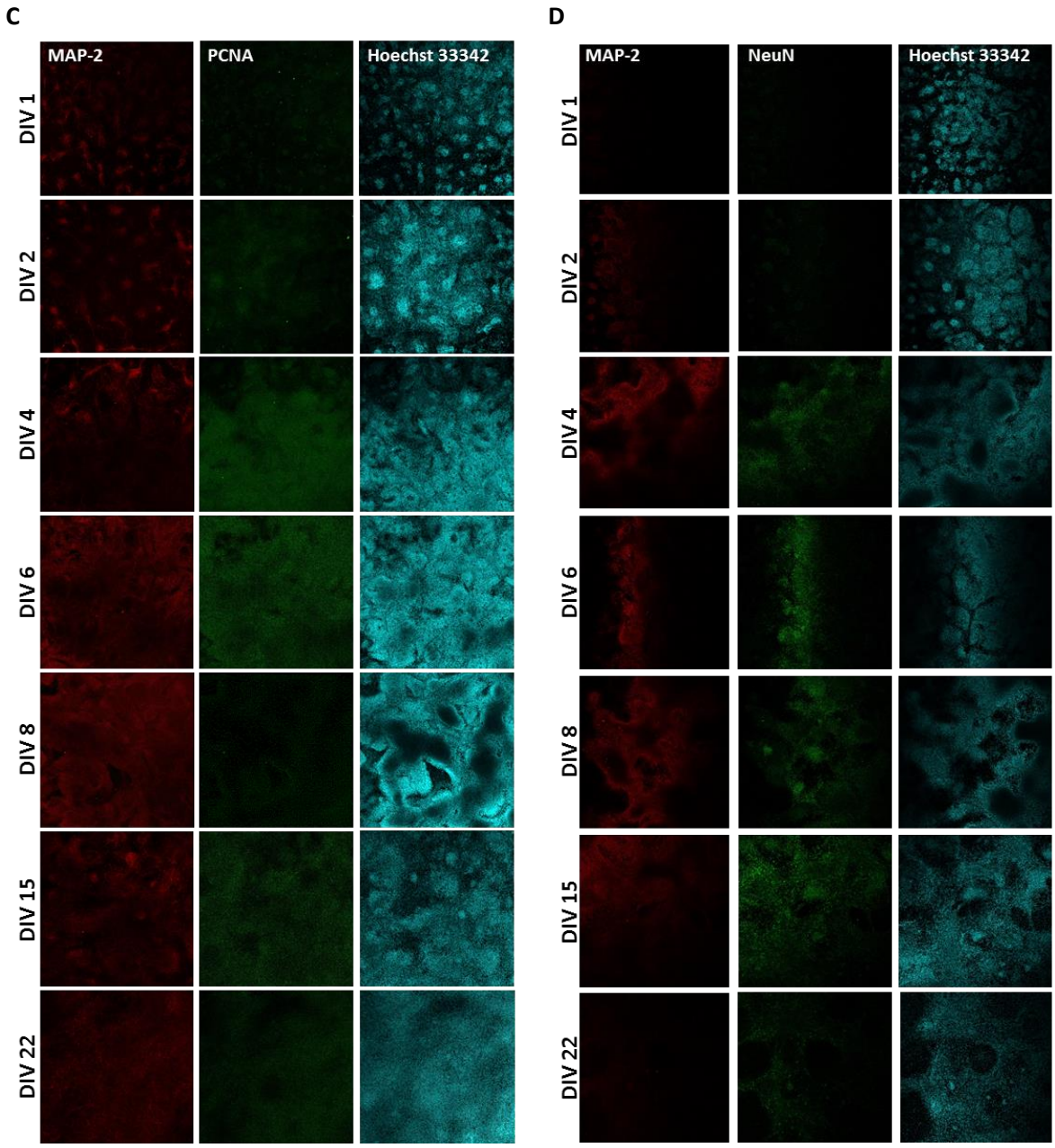
C
MAP-2
PCNA
Hoechst 33342
DIV 1
DIV 2
DIV 4
DIV 6
DIV 8
DIV 15
DIV 22
D
MAP-2
NeuN
Hoechst 33342
DIV 1
DIV 2
DIV 4
DIV 6
DIV 8
DIV 15
DIV 22

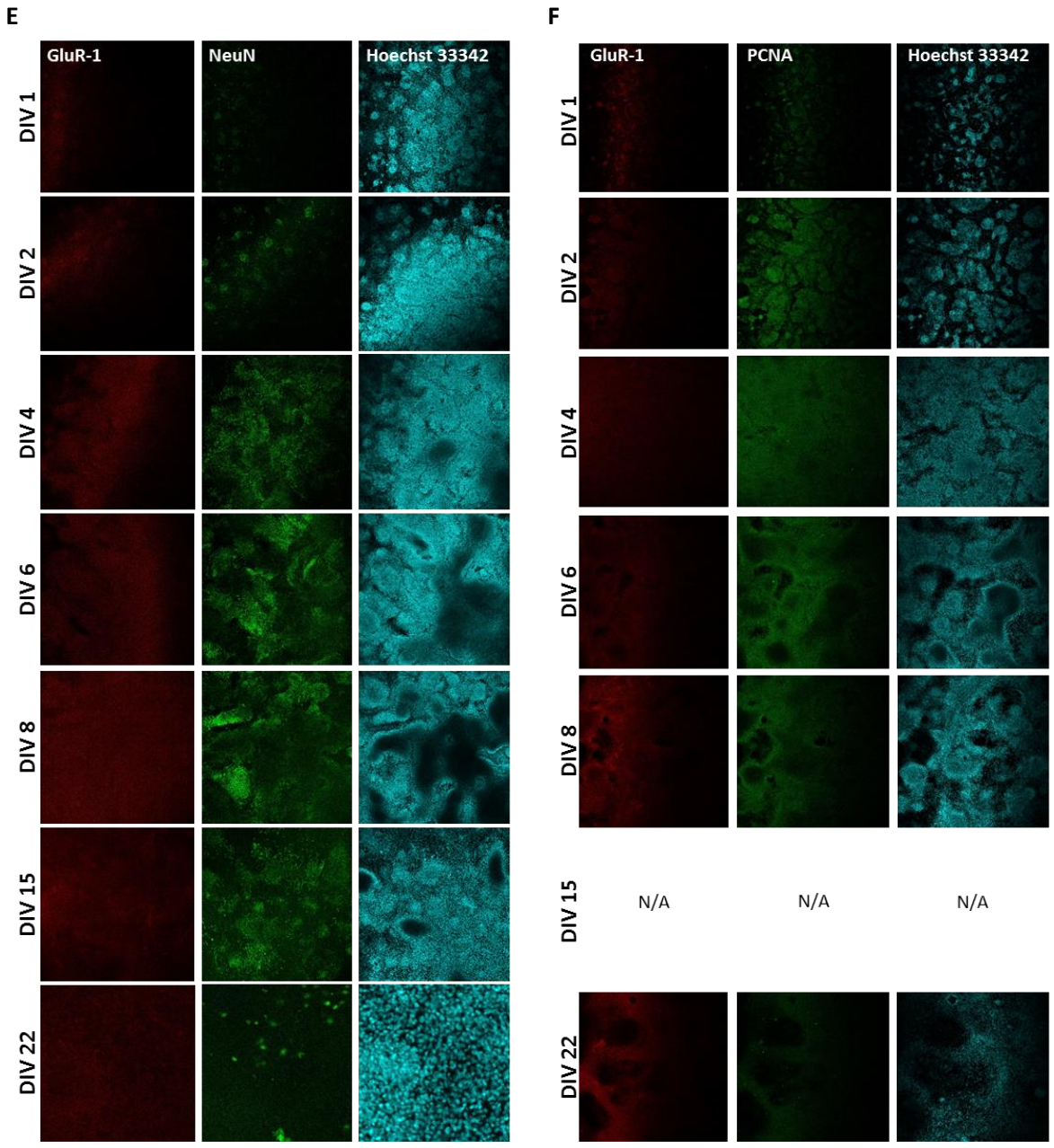

Figure 2.5. Confocal microscope images of mouse embryonic midbrain cell micromass over 22 days *in vitro*. Dynamic expressions of various proteins were captured over culture period. Nestin (red) and β-tubulin III (green) in (A) C57BL/6 and (B) A/J cultures, (C) MAP-2 (red) and PCNA (green) in C57BL/6, (D) MAP-2 (red) and NeuN (green) in A/J, (E) GluR-1 (red) and NeuN (green) in C57BL/6 and (F) GluR-1 (red) and PCNA (green) in A/J. Nucleus (cyan) was stained with Hoechst 33342.

CHAPTER 2 REFERENCES

Bailey, J., Knight, A. and Balcombe, J. (2005). The future of teratology research is in vitro. *Biogenic Amines 19*, 97-145.

Bal-Price, A. K., Coecke, S., Costa, L. et al. (2012). Advancing the science of developmental neurotoxicity (DNT): testing for better safety evaluation. *ALTEX 29*, 202-215.

Balls, M. and Hellsten, E. (2002). Statement on the scientific validity of the mircromass test -- an in Vitro for embryotoxicity. *Altern Lab Anim 30*, 268-270.

Bates, D., Machler, M., Bolker, B. M. et al. (2014). Fitting linear mixed-effects models using lme4. *Journal of Statistical Software 67*, 1-48.

Boer, K., Encha-Razavi, F., Sinico, M. et al. (2010). Differential distribution of group I metabotropic glutamate receptors in developing human cortex. *Brain Res 1324*, 24-33. http://dx.doi.org/10.1016/j.brainres.2010.02.005

Burbacher, T. M. and Grant, K. S. (2012). Measuring infant memory: Utility of the visual paired-comparison test paradigm for studies in developmental neurotoxicology. *Neurotoxicol Teratol 34*, 473-480. http://dx.doi.org/10.1016/j.ntt.2012.06.003

Ceccatelli, S., Tamm, C., Sleeper, E. et al. (2004). Neural stem cells and cell death. *Toxicol Lett 149*, 59-66. http://dx.doi.org/10.1016/j.toxlet.2003.12.060

Chakraborty, A., Murphy, S. and Coleman, N. (2017). The role of NMDA receptors in neural stem cell proliferation and differentiation. *Stem Cells Dev* http://dx.doi.org/10.1089/scd.2016.0325

Chambers, I. and Tomlinson, S. R. (2009). The transcriptional foundation of pluripotency. *Development 136*, 2311-2322. http://dx.doi.org/10.1242/dev.024398

Crofton, K., Fritsche, E., Ylikomi, T. et al. (2014). International STakeholder NETwork (ISTNET) for creating a developmental neurotoxicity testing (DNT) roadmap for regulatory purposes. *ALTEX 31*, 223-224. http://dx.doi.org/http://dx.doi.org/10.14573/altex.1402121

Crofton, K. M., Mundy, W. R., Lein, P. J. et al. (2011). Developmental neurotoxicity testing: recommendations for developing alternative methods for the screening and prioritization of chemicals. *ALTEX 28*, 9-15.

Crofton, K. M., Mundy, W. R. and Shafer, T. J. (2012). Developmental neurotoxicity testing: a path forward. *Congenit Anom (Kyoto) 52*, 140-146. http://dx.doi.org/10.1111/j.1741-4520.2012.00377.x

D'Amelio, M., Cavallucci, V. and Cecconi, F. (2010). Neuronal caspase-3 signaling: not only cell death. *Cell death and differentiation 17*, 1104-1114.

Engel, S. M., Wetmur, J., Chen, J. et al. (2011). Prenatal exposure to organophosphates, paraoxonase 1, and cognitive development in childhood. *Environ Health Perspect 119*, 1182-1188. http://dx.doi.org/10.1289/ehp.1003183

Ettle, B., Reiprich, S., Deusser, J. et al. (2014). Intracellular alpha-synuclein affects early maturation of primary oligodendrocyte progenitor cells. *Mol Cell Neurosci 62*, 68-78. http://dx.doi.org/10.1016/j.mcn.2014.06.012

Fernando, P., Brunette, S. and Megeney, L. A. (2005). Neural stem cell differentiation is dependent upon endogenous caspase 3 activity. *FASEB J 19*, 1671-1673. http://dx.doi.org/10.1096/fj.04-2981fje

Flint, O. P. and Ede, D. A. (1982). Cell interactions in the developing somite: in vitro comparisons between amputated (am/am) and normal mouse embryos. *J Embryol Exp Morphol 67*, 113-125.

Flint, O. P. (1983). A micromass culture method for rat embryonic neural cells. *J Cell Sci 61*, 247-262.

Flint, O. P. and Orton, T. C. (1984). An in vitro assay for teratogens with cultures of rat embryo midbrain and limb bud cells. *Toxicol Appl Pharmacol 76*, 383-395.

Flint, O. P., Orton, T. C. and Ferguson, R. A. (1984). Differentiation of rat embyo cells in culture: Response following acute maternal exposure to teratogens and non-teratogens. *J Appl Toxicol 4*, 109-116.

Flint, O. P. (1993). In vitro tests for teratogens: desirable endpoints, test batteries and current status of the micromass teratogen test. *Reprod Toxicol 7 Suppl 1*, 103-111.

Flora, S. J. S., Pachauri, V. and Saxena, G. (2011). Arsenic, cadmium, and lead. In R. C. Gupta (eds.), *Reproductive and developmental toxicology*. Oxford, UK: Elsevier Inc.

Gaspard, N. and Vanderhaeghen, P. (2010). Mechanisms of neural specification from embryonic stem cells. *Curr Opin Neurobiol 20*, 37-43. http://dx.doi.org/10.1016/j.conb.2009.12.001

Genschow, E., Spielmann, H., Scholz, G. et al. (2002). The ECVAM international validation study on in vitro embryotoxicity tests: results of the definitive phase and evaluation of prediction models. European Centre for the Validation of Alternative Methods. *Altern Lab Anim 30*, 151-176.

Ghandour, M. S., Langley, O. K., Vincendon, G. et al. (1979). Double labeling immunohistochemical technique provides evidence of the specificity of glial cell markers. *J Histochem Cytochem 27*, 1634-1637. http://dx.doi.org/10.1177/27.12.118210

Kim, H. Y., Wegner, S. H., Van Ness, K. P. et al. (2016). Differential epigenetic effects of chlorpyrifos and arsenic in proliferating and differentiating human neural progenitor cells. *Reprod Toxicol 65*, 212-223. http://dx.doi.org/10.1016/j.reprotox.2016.08.005

Kirkeby, A., Grealish, S., Wolf, D. A. et al. (2012). Generation of regionally specified neural progenitors and functional neurons from human embryonic stem cells under defined conditions. *Cell Rep 1*, 703-714. http://dx.doi.org/10.1016/j.celrep.2012.04.009

Krewski, D., Acosta, D., Jr., Andersen, M. et al. (2010). Toxicity testing in the 21st century: a vision and a strategy. *J Toxicol Environ Health B Crit Rev 13*, 51-138. http://dx.doi.org/10.1080/10937404.2010.483176

Kuegler, P. B., Zimmer, B., Waldmann, T. et al. (2010). Markers of murine embryonic and neural stem cells, neurons and astrocytes: reference points for developmental neurotoxicity testing. *ALTEX 27*, 17-42.

Lavezzi, A. M., Corna, M. F. and Matturri, L. (2013). Neuronal nuclear antigen (NeuN): a useful marker of neuronal immaturity in sudden unexplained perinatal death. *J Neurol Sci 329*, 45-50. http://dx.doi.org/10.1016/j.jns.2013.03.012

Lein, P., Locke, P. and Goldberg, A. (2007). Meeting report: alternatives for developmental neurotoxicity testing. *Environ Health Perspect 115*, 764-768. http://dx.doi.org/10.1289/ehp.9841

Mamber, C., Kamphuis, W., Haring, N. L. et al. (2012). GFAPdelta expression in glia of the developmental and adolescent mouse brain. *PLoS One 7*, e52659. http://dx.doi.org/10.1371/journal.pone.0052659

Miodovnik, A. (2011). Environmental neurotoxicants and developing brain. *Mt Sinai J Med 78*, 58-77. http://dx.doi.org/10.1002/msj.20237

Moors, M., Rockel, T. D., Abel, J. et al. (2009). Human neurospheres as three-dimensional cellular systems for developmental neurotoxicity testing. *Environ Health Perspect 117*, 1131-1138. http://dx.doi.org/10.1289/ehp.0800207

Morgan, A. P. and Welsh, C. E. (2015). Informatics resources for the Collaborative Cross and related mouse populations. *Mamm Genome 26*, 521-539. http://dx.doi.org/10.1007/s00335-015-9581-z

Mullen, R. J., Buck, C. R. and Smith, A. M. (1992). NeuN, a neuronal specific nuclear protein in vertebrates. *Development 116*, 201-211.

Nguyen, H. X., Nekanti, U., Haus, D. L. et al. (2014). Induction of early neural precursors and derivation of tripotent neural stem cells from human pluripotent stem cells under xeno-free conditions. *J Comp Neurol 522*, 2767-2783. http://dx.doi.org/10.1002/cne.23604

O'Rahilly, R., Muller, F., Hutchins, G. M. et al. (1987). Computer ranking of the sequence of appearance of 73 features of the brain and related structures in staged human embryos during the sixth week of development. *Am J Anat 180*, 69-86. http://dx.doi.org/10.1002/aja.1001800106

OECD (1983). *Test No. 415: One-Generation Reproduction Toxicity Study*. Vol. OECD Publishing. /content/book/9789264070844-en
http://dx.doi.org/10.1787/9789264070844-en

OECD (2001a). *Test No. 416: Two-Generation Reproduction Toxicity*. Vol. OECD Publishing. /content/book/9789264070868-en
http://dx.doi.org/10.1787/9789264070868-en

OECD (2001b). *Test No. 414: Prenatal Development Toxicity Study*. Vol. OECD Publishing. /content/book/9789264070820-en
http://dx.doi.org/10.1787/9789264070820-en

OECD (2016a). *Test No. 422: Combined Repeated Dose Toxicity Study with the Reproduction/Developmental Toxicity Screening Test*. Vol. OECD Publishing. /content/book/9789264264403-en
http://dx.doi.org/10.1787/9789264264403-en

OECD (2016b). *Test No. 421: Reproduction/Developmental Toxicity Screening Test*. Vol. OECD Publishing. /content/book/9789264264380-en
http://dx.doi.org/10.1787/9789264264380-en

Okumura-Nakanishi, S., Saito, M., Niwa, H. et al. (2005). Oct-3/4 and Sox2 regulate Oct-3/4 gene in embryonic stem cells. *J Biol Chem 280*, 5307-5317. http://dx.doi.org/10.1074/jbc.M410015200

Otis, E. M. and Brent, R. (1954). Equivalent ages in mouse and human embryos. *Anat Rec 120*, 33-63.

Palaga, T., Ratanabunyong, S., Pattarakankul, T. et al. (2013). Notch signaling regulates expression of Mcl-1 and apoptosis in PPD-treated macrophages. *Cell Mol Immunol 10*, 444-452. http://dx.doi.org/10.1038/cmi.2013.22

Piersma, A. H. (2004). Validation of alternative methods for developmental toxicity testing. *Toxicol Lett 149*, 147-153. http://dx.doi.org/10.1016/j.toxlet.2003.12.029

Pratten, M., Ahir, B. K., Smith-Hurst, H. et al. (2012). Primary cell and micromass culture in assessing developmental toxicity. *Methods Mol Biol 889*, 115-146. http://dx.doi.org/10.1007/978-1-61779-867-2_9

Rauh, V. A., Garfinkel, R., Perera, F. P. et al. (2006). Impact of prenatal chlorpyrifos exposure on neurodevelopment in the first 3 years of life among inner-city children. *Pediatrics 118*, e1845-1859. http://dx.doi.org/10.1542/peds.2006-0338

Rauh, V. A., Perera, F. P., Horton, M. K. et al. (2012). Brain anomalies in children exposed prenatally to a common organophosphate pesticide. *Proc Natl Acad Sci U S A 109*, 7871-7876. http://dx.doi.org/10.1073/pnas.1203396109

Reinhardt, C. A. (1993). Neurodevelopmental toxicity in vitro: primary cell culture models for screening and risk assessment. *Reprod Toxicol 7 Suppl 1*, 165-170.

Ribeiro, P. L. and Faustman, E. M. (1990). Embryonic micromass limb bud and midbrain cultures: Different cell cycle kinetics during differentiation in vitro. *Toxicol In Vitro 4*, 603-608.

Robinson, J. F., Griffith, W. C., Yu, X. et al. (2010). Methylmercury induced toxicogenomic response in C57 and SWV mouse embryos undergoing neural tube closure. *Reprod Toxicol 30*, 284-291. http://dx.doi.org/10.1016/j.reprotox.2010.05.009

Rodnight, R., Goncalves, C. A., Wofchuk, S. T. et al. (1997). Control of the phosphorylation of the astrocyte marker glial fibrillary acidic protein (GFAP) in the immature rat hippocampus by glutamate and calcium ions: possible key factor in astrocytic plasticity. *Braz J Med Biol Res 30*, 325-338.

Schindelin, J., Arganda-Carreras, I., Frise, E. et al. (2012). Fiji: an open-source platform for biological-image analysis. *Nat Methods 9*, 676-682. http://dx.doi.org/10.1038/nmeth.2019

Scoville, D. K., White, C. C., Botta, D. et al. (2015). Susceptibility to quantum dot induced lung inflammation differs widely among the Collaborative Cross founder mouse strains. *Toxicology and Applied Pharmacology 289*, 240-250. http://dx.doi.org/10.1016/j.taap.2015.09.019

Silbergeld, E. K., Silva, I. A. and Nyland, J. F. (2005). Mercury and autoimmunity: implications for occupational and environmental health. *Toxicol Appl Pharmacol 207*, 282-292. http://dx.doi.org/10.1016/j.taap.2004.11.035

Smirnova, L., Hogberg, H. T., Leist, M. et al. (2014). Developmental neurotoxicity - challenges in the 21st century and in vitro opportunities. *ALTEX 31*, 129-156. http://dx.doi.org/http://dx.doi.org/10.14573/altex.1403271

Spielmann, H., Seiler, A., Bremer, S. et al. (2006). The practical application of three validated in vitro embryotoxicity tests. The report and recommendations of an ECVAM/ZEBET workshop (ECVAM workshop 57). *Altern Lab Anim 34*, 527-538.

Theiler, K. (1989). The house mouse: atlas of mouse development. 1-178.

Tolins, M., Ruchirawat, M. and Landrigan, P. (2014). The developmental neurotoxicity of arsenic: cognitive and behavioral consequences of early life exposure. *Ann Glob Health 80*, 303-314. http://dx.doi.org/10.1016/j.aogh.2014.09.005

Uphill, P. F., Wilkins, S. R. and Allen, J. A. (1990). In vitro micromass teratogen test: Results from a blind trial of 25 compounds. *Toxicol In Vitro 4*, 623-626.

von Bohlen Und Halbach, O. (2007). Immunohistological markers for staging neurogenesis in adult hippocampus. *Cell Tissue Res 329*, 409-420. http://dx.doi.org/10.1007/s00441-007-0432-4

Walum, E. and Flint, O. P. (1990). Midbrain micromass cultures: a model for studies of teratogenic and sub-teratogenic effects on CNS development. *Acta Physiol Scand Suppl 592*, 61-72.

Wegner, S. H., Stanaway, I. B., Kim, H. Y. et al. (2014). Anchoring a dynamic *in vitro* model of human neuronal differentiation to key processes of early brain development *in vivo*. Ph.D., University of Washington,

Whittaker, S. G., Wroble, J. T., Silbernagel, S. M. et al. (1993). Characterization of cytoskeletal and neuronal markers in micromass cultures of rat embryonic midbrain cells. *Cell Biol Toxicol 9*, 359-375.

Wilson, P. G. and Stice, S. S. (2006). Development and differentiation of neural rosettes derived from human embryonic stem cells. *Stem Cell Rev 2*, 67-77. http://dx.doi.org/10.1007/s12015-006-0011-1

CHAPTER 3: Effects of developmental stage, particle size and coating on dosimetry and toxicity of silver nanoparticles in developing primary organotypic C57BL/6 and A/J mouse midbrain cultures

This Chapter is in preparation for submission. The authors of the manuscript are:

Brittany A. Weldon[1, 2]†, Julie Juyoung Park[1, 2]†, Sungwoo Hong[2], Tomomi Workman[1], Russell Dills[2], William C. Griffith[1], Terrance J. Kavanagh[2], Elaine M. Faustman[1, 2]*

[1] Institute for Risk Analysis and Risk Communication, University of Washington, Seattle, WA, USA

[2] Department of Environmental and Occupational Health Sciences, University of Washington, Seattle, WA, USA

† These authors contributed equally to this manuscript

* Corresponding author: Elaine M. Faustman

Institute for Risk Analysis and Risk Communication, Department of Environmental and Occupational Health Sciences, University of Washington, Seattle, WA, USA.

Email: faustman@uw.edu

ABSTRACT

Silver nanoparticles (AgNPs) are increasingly used in consumer, commercial, and medical products for their antimicrobial properties. Human exposures to AgNPs and potential adverse effects from exposure are likely increasing with these developments. Observations of Ag in adult and fetal brain following exposures to AgNPs has led to concerns about the potential for AgNPs to elicit adverse effects on neurodevelopment and neurological function. In this study, we investigated the effects of gold-cored AgNPs of differing sizes and coatings on developing embryonic C57BL/6 or A/J midbrain cells grown in three-dimensional organotypic cultures. Effects were evaluated at three time points of *in vitro* development corresponding to proliferation and differentiation stages of development by both nominal dose and dosimetric dose. Dosimetry was assessed in cultures using ICP-MS and utilized the gold core component of the AgNPs for determination of uptake of AgNPs and silver dissolution from particles. Results by both nominal and dosimetric dose for both C57BL/6 and A/J mouse midbrain cells showed a significant dose-dependent increase in cell death at later time points that coincide with differentiation stages of development. When assessed by dosimetric dose, we found that the fetal effects of AgNPs on neuronal growth, proliferation, and differentiation in both C57BL/6 and A/J mice micromass cells. Midbrain cells from C57BL/6 and A/J mouse were not affected by particle coatings, but were more sensitive to 20 nm particles compared to 110 nm at all developmental times, despite less uptake of Ag in smaller particles. Of three time points evaluated *in vitro* with dosimetry, C57BL/6 were most susceptible to AgNPs at DIV 8 while A/J were most vulnerable at DIV 15. Despite the slight difference in the time frame, both of these time points were associated with similar adverse impacts on early differentiation, suggesting that this period is a “window of susceptibility” for AgNPs. These mouse models offer approaches to assess both environmental and genetic factors affecting neurodevelopmental susceptibility.

Introduction

The proper function of the central nervous system (CNS) is essential for the survival and prosperity of humans and many other species. The CNS can be damaged by many environmental and pharmacological toxicants and has been identified as a sensitive target of toxicity in a variety of exposures. The developing nervous system has been shown to be even more susceptible to perturbations than a mature nervous system (Rice and Barone, 2000). Disruption of the development of the CNS can result in lifelong neuropathologies including autism, attention deficit disorder, cerebral palsy, and mental retardation (Grandjean and Landrigan, 2006). These disorders can put immense strain on individuals, families, the healthcare system, and society. Yet, less than 0.01% of the U. S. Environmental Protection Agency registered chemicals are have been tested for potential developmental neurotoxicity (Miodovnik, 2011), suggesting there is a pressing need to develop *in vitro* alternative methods that captures key processes of neurodevelopment in order to screen and prioritize potential neurotoxicants (Genschow et al., 2002; Krewski et al., 2010).

Because traditional neurodevelopmental studies can require a large number of animals and intensive labor and time (Bailey et al., 2005; Piersma, 2004; Pratten et al., 2012), our *in vitro* 3D organotypic embryonic mouse midbrain micromass system was used in these evaluations to not only evaluate the effects of nanoparticles on neuronal processes but also to optimize procedures for dosing and dosimetry. This culture is capable of capturing key early neurodevelopmental processes similar to *in vivo*, from proliferation, migration, to differentiation in three dimensions (Park et al., 2017). Without adding any external stimulation, the high-density micromass format drives differentiation in this culture. Micromass techniques have enhanced our understanding of neurodevelopmental systems by serving as a model for progression of *in vivo* neurodevelopment without the use of time intensive, costly *in vivo* studies (Park et al., 2017; Sidhu et al., 2006; Whittaker and Faustman, 1991; Whittaker et al., 1993).

Recent technological developments have employed the use of a wide array of nano-scale materials, referred to generally as Engineered Nanomaterials (ENMs), which often have at least one dimension ranging from 1 to 100 nm (Yokel and Macphail, 2011). Characteristics of ENMs include having a small size with large surface area and being light weight. Due to these unique properties of ENMs, their uses have been increasing exponentially. Silver nanoparticles (AgNPs), in particular, are widely used in food storage, textile coatings, health industry, and consumer products for their antimicrobial property (El-Nour et al.,

2010; Woodrow Wilson International Center for Scholars, 2016). One particular interest for these studies is their increased uses in children's products (Quadros et al., 2013; Tulve et al., 2015). Despite its increasing uses and potential impact on human and environmental health, much is still unknown about their potential for toxicity in many organ systems, including the developing CNS. And, only a limited number of available studies have focused on the effects of AgNPs during neurodevelopment. For example, Tang et al. (2009; 2010) found that AgNPs can cross the blood brain barrier *in vivo* and *in vitro*. Other animal studies also have demonstrated that AgNPs translocate throughout the main organs in the body including the brain after oral or inhalation exposures, leading to inflammatory responses and reduced spatial cognition (Loeschner et al., 2011; Patchin et al., 2016; Tang et al., 2009; Wu et al., 2015; Yang et al., 2010). Fennell et al. (2017) recently discovered that the silver crossed placenta regardless of its form and that the amount of silver in fetuses increased after oral or intravenous exposures to dams. AgNPs, in addition, have been shown to act as antimicrobials by disrupting structural proteins, enzymes, and DNA (Reidy et al., 2013). Moreover, silver was found to escape from nanoparticle-functionalized materials and can enter water systems, air, dust, and soil (Levard et al., 2012), suggesting increased potential for human and environmental exposures.

Because of the unique characteristics of particles in liquid media, assessments in terms of concentration (by mass, surface area, or particle number) does not allow for direct comparison of different particles. We have conducted a dosimetry assessment of AgNPs via inductively coupled plasma mass spectrometry (ICP-MS) as a common denominator to estimate potential cytotoxic responses of AgNPs in our *in vitro* 3D micromass systems as different AgNPs have their unique physicochemical properties in media (Weldon et al., 2017). This analysis would also allow us to compare effects of AgNPs across different particle coatings and sizes, cell types, *in vitro,* and *in vivo* systems (Weldon et al., 2017; Wildt et al., 2016). Therefore, we assessed cytotoxicity on our cultures *in vitro* by both nominal doses (µg AgNP/mL medium) and by dosimetric dose (µg AgNP/mg protein) using ICP-MS. Also, we utilized gold (Au)-cored AgNPs, with Au serving as a tracer. Detection of Au would represent a number of whole nanoparticles associated with the cells where that of Ag would represent Ag ion dissolution from the whole particles.

In addition to the new particles themselves producing cytotoxic effects, we also recognized that many factors other than exposures could contribute to susceptibility during neurodevelopment. The United States National Research Council in 2000 estimated that one in every six children have the developmental

disability, and of these developmental disabilities in children, 3% are from environmental exposures and 25% are from interactions between environmental factors and individual genetic susceptibility (National Research Council Committee on Developmental Toxicology, 2000). With such broad reaching and powerful implications, it is critical to understand whether exposures to AgNPs can disrupt the developing nervous system. It is our goal to characterize the potential of AgNPs to interact with and disrupt the development of the CNS using a 3D organotypic *in vitro* model. We aim to determine potential impacts of AgNPs of varied sizes and coatings, time of exposure, and genetics on adverse responses in addition to interactions between dosimetry and each factor in this chapter by exposing *in vitro* 3D embryonic C57BL/6 or A/J mouse midbrain cells with AgNPs at three different stages of the culture period.

METHODS

Embryonic mouse midbrain cell isolation and culture conditions.

The micromass culture method was used to study effects of silver nanoparticles (AgNPs) on neurodevelopment. Time-mated gestational day (GD) 11 C57BL/6 and GD 12 A/J mouse midbrains were isolated, digested, and dissociated into single cell suspension. Cells were then plated on Matrigel-coated 24-well Corning™ Primaria™ cell culture plates (Corning Primaria, Corning, NY, USA) using micromass format (10 μL 3D island with 5 x 10^6 cells/mL density). 500 μL of DMEM/F-12 media with 10 % fetal bovine serum, 1 % penicillin/streptomycin, and 1 % L-glutamate was added to each well after incubating plated cells for 1.5-hour at 37°C in a 5% CO2. Half of culture media was changed every two days until treatment. All experimental procedures and methods in this study were approved by University of Washington's Institutional Animal Care and Use Committee.

Silver nanoparticle treatment.

Both 20 nm and 110 nm silver nanoparticles (AgNPs) with Citrate coating and 110 nm Polyvinylpyrrolidone (PVP)-stabilized AgNPs were obtained from NanoComposix (San Diego, CA, USA). All nanoparticles contained a 7nm gold core and were selected by the National Institute of Environmental Health Sciences (NIEHS) Centers for Nanotechnology and Health Implications Research (NCNHIR) Consortium laboratories. Physiochemical properties of selected AgNPs (20 nm AgCitrate, 110 nm AgCitrate, and 110 nm AgPVP) were provided by the manufacturer and are described in Fennell et al. (2017). AgNPs stock solutions (1 mg/mL) were stored at 4°C in the dark until use.

For AgNP treatment, 20 nm AgCitrate, 110 nm AgCitrate, or 110 nm AgPVP stock solution (1 mg/mL) was diluted in cell culture medium to prepare exposure medium with 0, 6.25, 12.5, 25, and 50 μg/mL concentrations. ZnO and TiO_2 at 50 μg/mL were used as a positive and negative control, respectively. Stabilizer coating controls sodium citrate (NaCitrate) at 100 μM, and 40kD-sized PVP at 50 μg/mL served as coating controls for citrate- or PVP-coated particles, respectively. Embryonic C57BL/6 and A/J mouse midbrains cells at DIV 7, 14, or 21 were treated with AgNPs for 24 hours by replacing cell culture medium with 500 μL of exposure medium and continuing incubation at 37°C with 5% CO_2. Cytotoxicity and dosimetry were evaluated by collecting cells 24 hours after the exposures, at DIV 8, 15, or 22 as shown in Figure 3.1.

Assessing cytotoxicity using lactate dehydrogenase (LDH) cytotoxicity assay.

Lactate dehydrogenase (LDH) assay is used to quantitatively measure the amount of LDH released into the media as a marker of damaged cells. Cytotoxicity of embryonic C57BL/6 and A/J mouse micromass cultures were measured by following the manufacturer's protocol. After 24hours of AgNP exposures, 50 μL of media was transferred to a 96-well plate. To each sample aliquot, 50 μL of CytoTox 96® Reagent (CytoTox 96® Non-Radioactive Cytotoxicity Kit; Promega, Madison, WI, USA) was added and incubated in the dark at room temperature for 30 minutes. The Stop Solution (50 μL) was then added, and the absorbance was measured at 490 nm using SpectraMax 190 plate reader (Molecular Devices, Sunnyvale, CA, USA).

Obtained cytotoxicity data were first normalized by subtracting the average absorbance of culture media background. The corrected values were then divided by percent maximum LDH release (cells lysed with 10% TritoxnX provided by Promega CytoTox 96® Non-Radioactive Cytotoxicity Kit) to calculate percent cytotoxicity using following formula:

$$\%\ \text{LDH Max} = \frac{\text{Absorbance}_{\text{treatment}} - \text{Absorbance}_{\text{media background}}}{\text{Absorbance}_{\text{LDHmax}} - \text{Absorbance}_{\text{media background}}} \text{ x } 100\ \%$$

Dosimetry analysis using inductively coupled plasma mass spectrometer (ICP-MS).

Inductively coupled plasma mass spectrometer (ICP-MS) was used to quantify silver (Ag) and gold (Au) metals taken up by or associated with embryonic mouse midbrain cells. Samples were washed with 450 μL of fresh culture media three times to remove free and loosely associated AgNPs without disrupting pH or other culture conditions. After the final wash, 450 μL of fresh media was added to each well, and cells

were scraped from the plate. Collected cells were in 15 mL polystyrene tubes (Corning Life Science, Corning, NY, USA) and were stored at 4°C until use.

In order to determine whether toxicity observed following AgNP exposure resulted from uptake of dissolved Ag ions (dissolution in media) or from uptake and association of whole AgNPs, we utilized AgNPs that contained a small Au core (7 nm diameter core in all particles). The ICP-MS analyses of Ag and Au metals were done for cell fractions without any treatments, with exposures to coating controls (NaCitrate and 40kD-sized PVP), and with exposures to 25 and 50 μg/mL of 20 nm AgCitrate, 110 nm AgCitrate, or 110 nm of AgPVP.

Collected cell fraction samples were mixed with nitric acid (TraceMetal Grade; Fisher Scientific, Hampton, NH, USA) and hydrochloric acid (TraceMetal Grade; Fisher Scientific, Hampton, NH, USA) and digested with an open-vessel microwave for inductively coupled plasma mass spectrometer (ICP-MS) analysis. The MARS Xpress microwave (CEM Corporation, Mathews, NC, USA) temperature was increased to 90°C in 10 minutes with a 20-minute hold at final temperature. The power of the microwave as kept at 800 W. Deionized water (≥ 18 Mohm) was added so that the final concentrations of a digestate included 7% nitric acid, 2% hydrochloric acid, and 10 ng/mL Tb. Terbium (Tb) was used to assess internal standard recovery (EPA, 2007).

An Agilent 7900 ICP-MS with ISIS sample valve (Agilent Technologies, Santa Clara, CA, USA) was used for detection. Acquisition was done with a carrier gas flow rate of 1.03 L/min and a helium flow rate of 4.3 mL/min. The temperature of a spray chamber was held at 2°C. Helium gas was used to remove isobaric polyatomic interferences. Isotopes ^{197}Au and ^{107}Ag along with internal standards ^{193}Ir, ^{89}Y, and Tb were quantified. Calibration standards were made from BDH® ARISTAR® Mulit-Element ICP and ICP-MS Certified Reference Standards (VWR International, Radnor, PA, USA) with independent check standard from second vendor, Ultra Scientific (North Kingstown, RI, USA). Calibration was done approximately every 30 samples. Data obtained from ICP-MS were adjusted with process blanks.

Amount of Ag or Au in each cell fractions determined by ICP-MS were reported relative to mg of protein by dividing the Ag or Au mass with amount of total protein from respective samples. For example, mass of Ag and Au found in a well with NaCitrate treatment was divided by total protein measured in a well with

NaCitrate treatment. Bradford protein assay (Bio-Rad Laboratories, Hercules, California, USA) was utilized to measure total protein in a well.

Statistical analysis.

A linear mixed effects dose-response model was used to analyze significant differences among nominal treatment doses of 20 nm AgCitrate, 110 nm AgCitrate, or 110 nm AgPVP at a specific time point (DIV 8, 15, or 22). Fixed effects were concentrations of AgNPs, and random effects included experimental dates to account for any variability between different preps. The significance of dose-response curves, exposure timing, and particle sizes and coatings on cytotoxicity were investigated using analysis of variance (ANOVA). A post-hoc analysis was followed to compare between time points and particles for multi parameter conditions.

Cytotoxicity as a function of Ag dosimetry in cultures after 24 hours of exposure to each particle type at doses of 25 µg/mL and 50 µg/mL at a specific time point (DIV 8, 15, or 22) were also modeled using a linear mixed effects model in order to determine Ag mass at each exposure concentration. Fixed and random effects were the amount of AgNPs taken up by cells (dosimetry) and experimental dates, respectively. An ANOVA analysis was followed by a post-hoc analysis.

To assess the relative ratios of Ag to Au in exposure media and cell fractions, we performed a regression analysis of Ag and Au for each particle type. Differences in slope between exposure media (prior to exposure) and cell fraction (24hr after exposure) for each particle were compared for each particle by ANOVA.

All statistical analyses (dose-response and dosimetry adjusted cytotoxicity) were performed with “lme4” package (Bates et al., 2014) in R statistical software (https://www.R-project.org).

RESULTS

Dose-response effects of 20 nm AgCitrate, 110 nm AgCitrate, and 110 nm AgPVP on C57BL/6 micromass.

An *in vitro* 3D organotypic C57BL/6 micromass culture system was utilized to examine dose-response effects of AgNPs with different coatings and sizes. Cytotoxicity was observed 24 hours after AgNP

exposures at three different time points—DIV 8, 15, and 22. Effects of dose, particle coatings and sizes, and time of exposures on cytotoxicity were investigated. A significant dose-response relationship for 20 nm AgCitrate was observed at DIV 15 and 22 (Figure 3.2A). 110 nm AgCitrate and 110 nm AgPVP demonstrated a significant dose-response relationship at all time points (Figure 3.2A; p-value < 0.001).

Differences in cytotoxic response due to coatings of AgNPs were assessed. When responses to 110 nm AgCitrate (Figure 3.2A black) and 110 nm AgPVP (Figure 3.2A purple) were compared, no significant effects of coating on C57BL/6 midbrain cells were observed at all time points (Figure 3.2A). A significant dose and coating interaction was observed at DIV15 (p-value < 0.05), but not at DIV 8 or 22, suggesting that the effect of coating on cytotoxicity may differ depending on the dose at DIV15.

Effects of particle sizes on cytotoxicity were also examined by comparing 20 nm AgCitrate (Figure 3.2A red) with 110 nm AgCitrate (Figure 3.2A black). For the C57BL/6 mouse midbrain micromass system, differential effects of particle sizes were observed at DIV 8, 15, and 22. A post-hoc test revealed a significant effect of size on cytotoxicity at DIV 15 (p-value < 0.001), but not at DIV 8 or 22, suggesting that size is the unique effect on cytotoxicity. At DIV 8 and 22, dose and size interactions were observed (p-value < 0.01 and p-value < 0.05, respectively), but not at DIV 15. This result suggested that the effect of size on cytotoxic response varied depending on the exposure concentrations at DIV 8 and 22.

Time of exposure also affected cytotoxic response to AgNPs on embryonic C57BL/6 mouse micromass systems. The C57BL/6 midbrain cells were sensitive to 20nm AgCitrate at DIV 15 and 22 than DIV 8 (Figure 3.3A; p-value < 0.001 and p-value < 0.01, respectively). Of all time points, C57BL/6 culture was most sensitive to 110 nm AgCitrate and 110 nm AgPVP at DIV 15 than at DIV 8 (p-value < 0.001 for both particles) and 22 (p-value < 0.001 for both particles) as shown in Figure 3.3A. C57BL/6 midbrain cells exposed to 110nm AgPVP also demonstrated a significant difference between DIV 8 and 22 with DIV 22 being more sensitive than DIV 8 (Figure 3.3A; p-value < 0.05). A significant dose and time interactions were observed for all particles, suggesting that the exposure timing on cytotoxic responses may differ depending on the dose.

Dose-response effects of AgNPs on embryonic A/J midbrain micromass.

Cytotoxicity was measured at DIV 8, 15 and 22 after exposures to 20 nm AgCitrate, 110 nm AgCitrate, or 110 nm AgPVP for 24 hours on *in vitro* embryonic A/J mouse midbrain micromass. Effects of dose, particle coatings and sizes, and developmental stages on cytotoxicity were also investigated on A/J micromass. All AgNPs showed significant dose-response relationship at all time points. For 20 nm AgCitrate, the most significant dose-response was observed at DIV 15 (p-value < 0.001) followed by DIV 22 (p-value < 0.01) and 8 (p-value < 0.05) as illustrated in Figure 3.2B. 110 nm AgCitrate and 110 nm AgPVP illustrated a significant dose-response relationship at all time (Figure 3.2B; p-value < 0.001 for both particles at all time points).

A difference in response due to particle coating was demonstrated in Figure 3.2B. A significant effect of coating on cytotoxicity at DIV 22 was revealed by comparing 110 nm AgCitrate (Figure 3.2B black) and 110 nm AgPVP (Figure 3.2B purple; p-value < 0.01). Cytotoxicity of fetal A/J midbrain cells were not affected by particle coating at earlier time points (DIV 8 and 15). Dose and coating interaction was found at all time points (p-value < 0.05, p-value < 001, and p-value < 0.05 for DIV 8, 15, and 22, respectively). This result demonstrated that the effect of AgNP particle coating on cytotoxic response varied depending on the exposure concentration at all time points; however, particle coating itself was also the unique effect on cytotoxicity at DIV 22.

The A/J mouse midbrain micromass system revealed effects of particle sizes on cytotoxicity at all time points. At DIV 8, 110 nm AgCitrate (Figure 3.2B black) induced greater cytotoxicity compared to 20 nm AgCitrate (Figure 3.2B red; p-value < 0.05) with a significant dose and size interaction (p-value < 0.001). Reversed effects were found at DIV 15 and 22—20 nm AgCitrate (Figure 3.2 red) showed greater cytotoxicity than 110 nm AgCitrate (Figure 3.2 black; p-value < 0.001 for both DIV). No dose and size interactions were observed at later time points (DIV 15 and 22). The difference in cytotoxicity between two particle sizes was at the greatest at DIV 15 (Figure 3.2B). Altogether, we observed that size was the main effect of cytotoxicity of AgNPs on fetal A/J mouse midbrain cells at all time points, and the effect of particle size on cytotoxic response were different depending on the dose at DIV 8 only.

The embryonic A/J mouse micromass system illustrated that time of exposure affected cytotoxic responses to AgNPs. A steeper cytotoxicity response was observed at DIV 15 and 22 than DIV 8 after

exposures to 20 nm AgCitrate (Figure 3.3B; p-value < 0.001 between DIV 8 and 15 and p-value < 0.05 between DIV 8 and 22). No significant differences among three time points were observed for 110 nm AgCitrate. For 110 nm AgPVP, time of exposure contributed to silver nanoparticle susceptibility. The cytotoxicity response at DIV 15 or 22 was significantly different from one at DIV 8 (Figure 3.3B; p-value < 0.001 for both DIV). For all particles, a significant dose and time interactions were observed, suggesting that the time of exposure on cytotoxicity may differ depending on exposure concentrations.

Effects of genetic backgrounds on cytotoxicity.

The potential contribution of genetics in response to AgNP exposures were examined by comparing fetal C57BL/6 and A/J mouse midbrain cells. No significant strain differences were observed for all particles at all times, but interactions between dose and mouse strain were found. For 20 nm AgCitrate, an interaction between dose and mouse strain were found only at DIV 22 (p-value < 0.05). Dose and mouse strain interactions were observed for 110 nm AgCitrate and 110 nm AgPVP at DIV 15 (p-value < 0.001 for both particles). 110 nm AgPVP also showed dose and mouse strain interaction at DIV 22 (p-value < 0.05). Rather than genetic variability being the unique effects on cytotoxicity to AgNP exposures, its effect on cytotoxic response may be different depending on the dose, especially at later time points (DIV 15 and 22).

Dosimetry.

AgNPs taken up by either C57BL/6 or A/J mouse midbrain cells were measured using ICP-MS analysis. When the amount of Ag and Au was plotted against exposure concentrations, a linear increase in uptake was observed in the two strains of mice at all three time points (Figure 3.4). For all particles, lower uptake levels were observed at DIV 8 compared to DIV 15 and 22 for both C57BL/6 and A/J mouse midbrain cells (Figure 3.4). Fetal C57BL/6 and A/J mouse midbrain cultures demonstrated that the amount of 20 nm AgCitrate taken up by or associated with the cells was less than that of larger particles at all three time points (Figure 3.4). Coatings did not have any effects on the amount of AgNPs taken up by C57BL/6 or A/J midbrain cells.

Dosimetry-response effects of AgNPs on C57BL/6 mouse micromass.

Using dosimetry data, we assessed cytotoxicity focusing on potential effects of dose, time of exposures, particle coatings and sizes, and strain differences. Dosimetry data were first normalized to total protein content, resulting dosimetric dose (μg Ag/mg protein). After adjusting cytotoxicity with dosimetry, a

significant dose response was observed in C57BL/6 for all particles at all three time points except for the 20 nm AgCitrate at DIV 8. Both 110 nm AgCitrate and 110 nm AgPVP demonstrated a significant dosimetry-response relationship (Figure 3.5A; p-value < 0.05 for both particles). At DIV 15, all three particles illustrated significance with p-values less than 0.01, 0.01, and 0.05 for 20 nm AgCitrate, 110 nm AgCitrate, and 110 nm AgPVP, respectively (Figure 3.5A). All particles also demonstrated a significant dosimetry-response relationship at DIV 22 as shown in Figure 3.5A (p-value < 0.05 for 20 nm AgCitrate, p-value < 0.01 for 110 nm AgCitrate, and p-value < 0.05 for 110 nm AgPVP).

No significant effects of particle coatings nor interactions between dose and coatings were observed in C57BL/6 micromass even after adjusting cytotoxicity for AgNPs taken up by cells (Figure 3.5A red and purple).

Effect of particle sizes were investigated after adjusting cytotoxicity by dosimetry. C57BL/6 mouse midbrain cells were significantly more sensitive to 20 nm AgCitrate (black) compared to 110 nm AgCitrate (red) at DIV 15 and 22 as shown in Figure 3.5A (p-values < 0.001 for both DIV). An interaction between dosimetry and size at DIV 15 and 22 were demonstrated by an ANOVA followed by a posthoc test, suggesting that the size affects cytotoxic response depending on the amount of AgNPs taken up by the cells. At DIV 8, no significant effect of particle size nor interactions between dosimetry and size were observed. Particle comparisons between 20 nm AgCitrate and 110 nm AgPVP also revealed a significant difference in response between the two particles at DIV 15 and 22 (Figure 3.5A; p-values < 0.001 for both DIV).

Effect of exposure timing was also examined after adjusting cytotoxicity by dosimetry. DIV 8 was when the midbrain cells were the most sensitive to all particles. 20 nm and 110 nm AgCitrate did not show any significant differential effects of developmental stages on cytotoxicity. A significant effect of exposure timing was observed for 110 nm AgPVP on C57BL/6 mouse strains (Figure 3.6A). C57BL/6 embryonic mouse midbrain cells were more sensitive to 110 nm AgPVP at DIV 15 than 22 (p-value < 0.01) after dosimetry adjustment (Figure 3.6A). Interaction terms between dose and time of exposures were detected for 110 nm AgCitrate and 110 nm AgPVP.

Dosimetry adjusted dose-response effects of AgNPs on A/J mouse micromass.

AgNPs taken up by the embryonic A/J mouse midbrain cells were measured and were used to adjust for cytotoxic responses for all particles at all times. After the adjustments, only 110 nm AgCitrate produced a significant dosimetry-response relationship at DIV 8 (p-value < 0.05) while 110 nm AgCitrate and 110 nm AgPVP showed significance at DIV 15 (Figure 3.5B; p-value < 0.01 for both particles). A significant dosimetry-response was observed for all particles at DIV 22 (Figure 3.5B; p-value < 0.01 for all particles).

Even after adjusting cytotoxicity by dosimetry, particle coating was not a significant contributor on differential responses of AgNPs with Citrate (Figure 3.5B red) and PVP (Figure 3.5B purple) coatings at all time points. A significant dose and coating interaction were observed only at DIV 22 (Figure 3.5B; p-value < 0.05), illustrating that coating affects responses to AgNPs depending on dose at this time.

Effects of size on cytotoxicity were also examined after adjusted by dosimetry. Particle size did not significantly affect responses to 20 nm (Figure 3.5B black) and 110 nm AgCitrate (Figure 3.5B red) exposures on embryonic A/J mouse midbrain cells at DIV 8 and 15. A significant dosimetry-response relationship was only demonstrated at DIV 22 when compared 20 nm AgCitrate and 110 nm AgCitrate (Figure 3.5B; p-value < 0.01). A dose and size interaction was also observed (Figure 3.5B; p-value < 0.001) at DIV 22, suggesting that the particle size may have an effect on toxic responses depending on dose during this time. A significant difference in response between 20 nm AgCitrate and 110 nm AgPVP on fetal A/J mouse midbrain cells at DIV 22 was detected when particle comparison was made (Figure 3.5B; p-value < 0.01).

Developmental stages also significantly affected cytotoxicity even after dosimetry adjustment. Particles were most sensitive to AgNPs at DIV 15. Exposures to 20nm AgCitrate showed a significantly greater dosimetry adjusted cytotoxic response at DIV 15 than at DIV 22 (Figure 3.6B; p-value < 0.05). A similar result was found for 110 nm AgCitrate—cytotoxicity adjusted by dosimetry was significantly greater at DIV 15 when compared to that at DIV 22 (Figure 3.6B; p-value < 0.001). An interaction between dose and time of exposure were observed for 110 nm AgCitrate (p-value < 0.001). Together, this suggested that exposure timing is the main effect on cytotoxicity induced by 20 nm AgCitrate. Our data also suggested that the effects of time on cytotoxicity may depend on the exposure concentrations for 110 nm AgCitrate

in addition to exposure time being the unique factor affecting cytotoxicity. No significant effects of time or an interaction between time and dose were not observed for 110 nm AgPVP.

Effects of genetics on cytotoxicity adjusted by dosimetry analysis.

After adjusting cytotoxicity using dosimetry data, we again examined potential effects of genetics on responses to AgNPs. A significant dose and mouse strain interaction was found for 20 nm AgCitrate at DIV 15 (p-value < 0.01) as well as for 110 nm AgPVP at DIV 22 (p-value < 0.05). Depending on the exposure concentration, the effects of genetics on cytotoxic response may be different, especially for the two types of AgNPs—20 nm AgCitrate and 110 nm AgPVP.

DISCUSSION

There is a need to examine the potential for AgNPs to act as neurodevelopmental toxicants as increasing number of studies reported that AgNPs could be found in a brain (Fennell et al., 2017; Loeschner et al., 2011; Morishita et al., 2016; Patchin et al., 2016; Tang et al., 2009; Tang et al., 2010; Yang et al., 2010); yet, the use of AgNPs in many consumer products including children's toys, clothes, and face and body products is increasing exponentially (Woodrow Wilson International Center for Scholars, 2016). In this study, we utilized a three-dimensional organotypic mouse midbrain model to assess the sensitivity of developing primary mouse neural cultures to AgNPs. We investigated the effect of developmental stage at the time of exposure as well as the contribution of AgNP size, coating, and genetics to toxicity. In addition, we measured the contributions of dissolved Ag and intact AgNPs to observed toxicity.

In vitro models provide several advantages over the use of *in vivo* toxicity assessments as they utilize significantly fewer animals, can assess multiple endpoints simultaneously, allow for rapid, high throughput assessments, and often cost far less than animal toxicity studies. These attractive qualities of assessing toxicity using *in vitro* models become even more powerful and necessary to keep pace with the accelerating rate of scientific and technological advancements in chemical and manufactured materials. We utilized an innovative method for assessing neurodevelopmental effects through our 3D micromass model that has been shown to grow and develop without the addition of growth factors or differentiation-promoting factors (Park et al., 2017). The ability to study neurodevelopment *in vitro* without the use of these factors is critical for neurodevelopmental toxicity studies as these growth factors may mask

sensitivity of effects. In addition, many of these factors may be retinoic acid-based (Maden, 2007), and may sensitize neural cultures to developmental disruption as retinoic acid is a well-characterized teratogen (Lammer et al., 1985). The European Centre for the Evaluation of Alternative Methods (ECVAM) has supported the use of micromass cultures as a standard alternative developmental toxicity method in an effort to reduce the number of animals used in toxicity studies (Balls and Hellsten, 2002).

We have developed and thoroughly characterized a micromass culture system from primary embryonic mouse midbrains (Park et al., 2017). Our *in vitro* mouse culture system allows for higher throughput with development occurring in a shortened period compared to *in vivo* rat and other mammalian models. In addition, the availability of many inbred genetic strains of mice allows for the comparison of results across strains for insights on genetic influences of variability in response. This is especially useful in comparison across the Collaborative Cross mouse strains (Churchill et al., 2004). Neurodevelopmental processes are largely conserved across mammalian species, and as such, a mouse embryonic midbrain cell model may serve as a tool to assess the potential for AgNPs to cause neurodevelopmental toxicity in humans.

Particle coatings such as citrate and polyvinylpyrrolidone(PVP) can stabilize silver nanoparticles by reducing aggregation and agglomeration and controlling ion release from particles. In our study, we found no significant differences between PVP- and citrate-coated particles of the same size for C57BL/6 while a significant effect of coating on cytotoxicity at DIV 22 was revealed in A/J before dosimetry analysis (Figure 3.2B black and purple; p-value < 0.01), but not at DIV 8 and 22. This effect, however, disappeared after dosimetry adjustment, suggesting that coatings do not have a significant effect on both C57BL/6 and A/J mice derived fetal mouse midbrain cells. This is consistent with the conclusion from Recordati et al. (2016) that coating did not have an impact on tissue distribution and hepatobiliary toxicity after single intravenous exposure to male CD-1 mice. Some studies including Wang et al. (2014) and Wu et al. (2015), however, discovered that PVP coating reduced pulmonary cytotoxic effects compared to the equivalent sized AgNPs or reduced spatial cognition compared to uncoated AgNPs, respectively. Because we observed a significant effect of coatings on cytotoxicity depending on the dose/dosimetry at later time points for A/J, it would be important for future studies to examine interactions in order to discriminate true effects of the coating from the interaction terms.

Particle sizes were shown to produce an effect on cytotoxicity for both strains of mice when analyzed with nominal dose. When compared by dosimetry, we found that the smaller particle (20 nm AgCitrate) had greater cytotoxic effects than larger particles (110 nm AgCitrate and 110 nm AgPVP) at DIV 15 and DIV 22 in both strains at all times, except for the embryonic A/J midbrain cells at DIV8 (Figure 3.5B). We cannot draw conclusions for the DIV 8 exposures for A/J mouse midbrain cells because we only had one dosimetry data point for 20 nm AgCitrate in addition to the control. However, our findings are consistent with Patchin et al. (2016) and Recordati et al. (2016) that smaller AgNPs are producing greater toxicological responses by depositing in the rodent brain more.

This effect of smaller sizing inducing higher cytotoxicity was observed despite significantly less Ag in cell cultures after exposure to 20 nm particles. Potentially, significant differences in particle size on toxicity may be explained by dissolution occurring primarily in lysosomes. As nanoparticles are taken up into cells, autophagosomes form around particles and other damaged cellular components. Lysosomes then fuse with autophagosomes, and hydrolytic enzymes degrade its contents. Because lysosomes are more acidic (pH 5-6) than cytosol and other cellular components, the acidic environment may result in enhanced AgNP dissolution. Because smaller particles have greater surface area compared to larger particles, this may result in a heightened level of dissolution. As such, more dissolution may occur with smaller particles, leading to greater lysosomal dysfunction and cell death. Ma et al. (2012) found lysosomes play a large role in cytotoxicity and has been proposed to be a major mechanism of nanoparticle toxicity.

Alternatively, it is possible that the 20 nm AgNPs are undergoing so much dissolution in media that the Au core becomes exposed and also undergoes dissolution and uptake into cells. Munusamy et al. (2015) found 20 nm AgNPs containing an Au core had much more rapid dissolution rate in media (approximately 50% particle mass dissolved after 24 hours) compared to 110 nm AgNPs with an Au core (approx. 20% particle mass dissolved after 24 hours). It is possible that cytotoxicity may be occurring through differing mechanisms of delivery of metals to cells between particle sizes, where 110 nm particles elicit effects by associating with outer layers of cell membranes or are taken up into cells as mostly undissolved particles.

Effects of exposure time on response to AgNPs were also examined using embryonic midbrain cells harvested from C57BL/6 or A/J mouse. Before dosimetry adjustments, we observed significantly greater effects on cytotoxicity when exposures occurred at DIV 15 compared to DIV 8 and 22 in both C57BL/6 and

A/J micromass culture systems (Figure 3.3). After adjusting cytotoxicity response with the amount of AgNPs associated with the cells, C57B/6 was found to be more susceptible to AgNPs at DIV 8 while A/J was more susceptible at DIV 15 (Figure 3.6). Park et al. (2017) found that DIV 8 is when differentiation has initiated yet proliferation signals are still present (Chapter 2 Figure 2.4). And, DIV 15 is when both early and late differentiation signals are present (Chapter 2 Figure 2.4; Park et al., 2017). This suggested that early neural differentiation may be the "critical windows of susceptibility" to AgNPs like many other toxicants (Rodier, 1995, 1994). Our findings of neural culture sensitivity during differentiation have also been observed in other *in vitro* neurodevelopment models. Greater sensitivity to metals has been shown during neural differentiation stages of development after exposure to manganese (Hernandez et al., 2011), lead (Bull et al., 1983; Deng et al., 2001; Silbergeld, 1992), and methylmercury (Barone et al., 1998).

The midbrain contains the greatest amount of dopaminergic neurons in the brain, and they first begin to appear at embryonic day 10.5 (Maxwell and Li, 2005) – roughly the time when our cultures are harvested and plated. Metals have been shown to accumulate in dopaminergic neurons (Robison et al., 2015). Alternatively, increased uptake and cytotoxicity of AgNPs at DIV 15 in both C57BL/6 and A/J systems may be due to differentiation into less specialized neurons; however, the potential for Ag^+ to utilize Na^+ channels may lead to increased uptake of Ag^+ and a disruption of ion flow (Bury and Wood, 1999).

When strain differences were investigated, no significant effects of strains on cytotoxic responses were found for all particles at all times. Interaction terms observed between dosimetry and mouse strain were for 20 nm AgCitrate at DIV 15 and 110 nm AgPVP at DIV 22. We hypothesized that A/J mouse midbrain cells would be more susceptible to C57BL/6 because Scoville et al. (2015) found that A/J mice showed the greatest proinflammatory responses to quantum dots among other Collaborative Cross mouse strains. However, we did not observe the same effects with AgNPs. In fact, C57BL/6 was slightly more sensitive to AgNPs compared to A/J. Although strain difference was not found to be the main effect on cytotoxicity, interaction terms suggested that effects of mouse strains on vulnerability may depend on the dosimetry of particle linked with cells at specific time frames. Further study is required to determine why this differences in response exist between quantum dots and AgNPs.

The present study gives valuable insight into the potential for AgNPs to interact with and disrupt developing neural cultures; however, several limitations of this work have been identified. While our

methods were designed to prevent large amounts of aggregation and agglomeration of particles in media, we did not measure AgNP aggregation or agglomeration in exposure solution prior to exposures. This could potentially result in reduced delivery of AgNPs to cultures and may affect uptake and cytotoxicity. As such, the differences in behavior of different sized particles in liquid media may also affect delivery to cultures and may lead to differences in toxic effects. The translation of particle delivery to tissue *in vivo* may also be quite different. In addition, our methods did not allow for the determination of whether complete dissolution of particles occurred in media, which could also result in the lack of change in the ratio of metals. Visualization of cells after exposure by electron microscopy and measurement of particles associated with cells may better inform whether uptake of whole particles is occurring. Future work may investigate markers for dopaminergic neurons or microglia in these cultures to better inform the role of cell type differentiation and mechanisms of uptake and sensitivity observed in cultures at early differentiation stages. The differential in sensitivity of other mouse strains in the Collaborative Cross study should also be investigated to expand our understanding of the effects of genetics on AgNP-induced adverse effects. Mechanistic studies may also help to elucidate how Ag^{+} ion may exert cytotoxicity as mixed results are present.

In summary, we have shown our *in vitro* 3D developing primary midbrain cultures are sensitive to AgNPs. We found that particle sizes, exposure timing, and genetics may be contributing factors to responses upon AgNP exposures. Both C57BL/6 and A/J micromass cultures were more sensitive to smaller sized AgNPs, despite less overall uptake of Ag compared to larger particles. Cultures were more sensitive to AgNP exposures at early differentiation stages of development, with greater uptake of particles occurring at later time points. Generally, embryonic C57BL/6 midbrain cells were more susceptible to AgNPs compared to A/J for all particles at all times, but no significant differences between two strains were observed. We found potential differences on how AgNPs exert toxicity in embryonic C57BL/6 and A/J midbrains. For C57BL/6, dissolution of AgNPs in media may not contribute to the cytotoxic effects while the opposite was observed for A/J. Together, this study significantly contributes to the current literature by defining potential impact of each factor on cytotoxic responses upon AgNP exposures on *in vitro* micromass systems using two mouse strains. These mouse models offer approaches to assess both environmental and genetic factors affecting neurodevelopmental susceptibility.

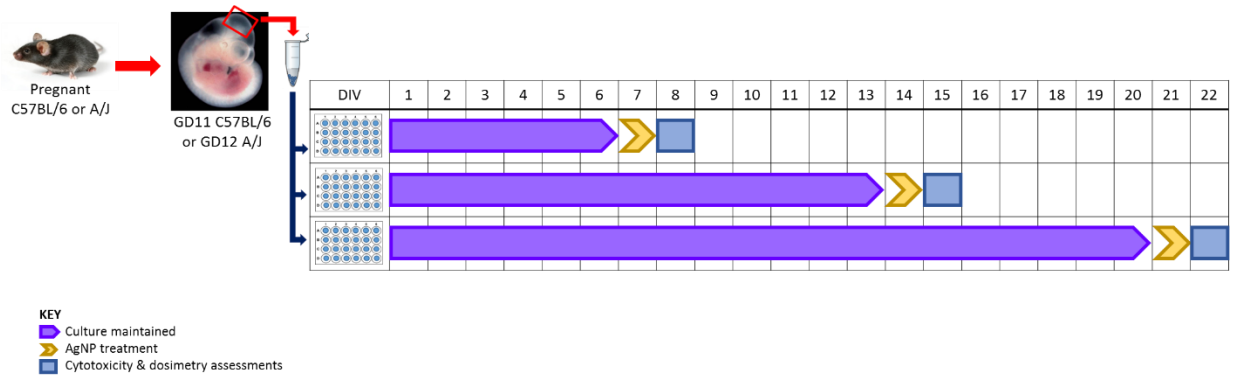

Figure 3.1. Experimental design of silver nanoparticles (AgNPs) using *in vitro* embryonic C57BL/6 and A/J mouse midbrain micromass cultures. The midbrain cells were exposed to 20 nm AgCitrate, 110 nm AgCitrate, or 110 nm AgPVP for 24 hours starting at days *in vitro* (DIV) 7, 14, and 21. Cytotoxicity and dosimetry were assessed 24 hours later, at DIV 8, 15, and 22.

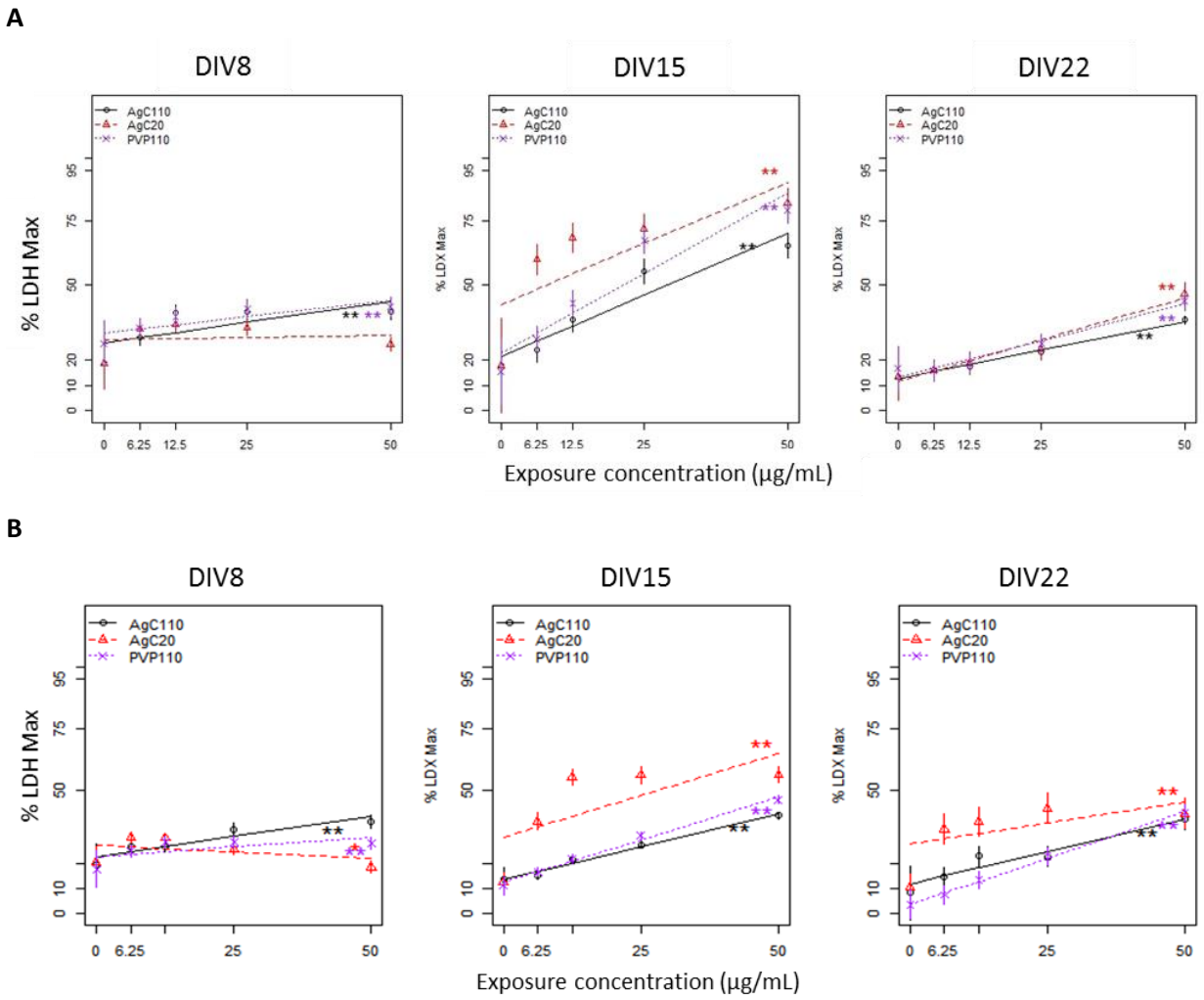

Figure 3.2. Dose-response curves for effects of various silver nanoparticles. Dose-response curves for fetal (A) C57BL/6 and (B) A/J mouse midbrain cells after exposures to AgNPs. Of three different time points we have examined, 20 nm AgCitrate (red) showed the highest cytotoxicity at later time points (DIV 15 and 22) in both strains. At DIV 8, 110 nm particles lead to higher cytotoxicity in both strains. No significant differences between C57BL/6 and AJ were found, but C57BL/6 showed greater cytotoxic responses compared to A/J. Data points and lines were estimated from the mixed-effect model. *: p-value < 0.05; **: p-value < 0.01; ***: p-value < 0.001 compared to controls.

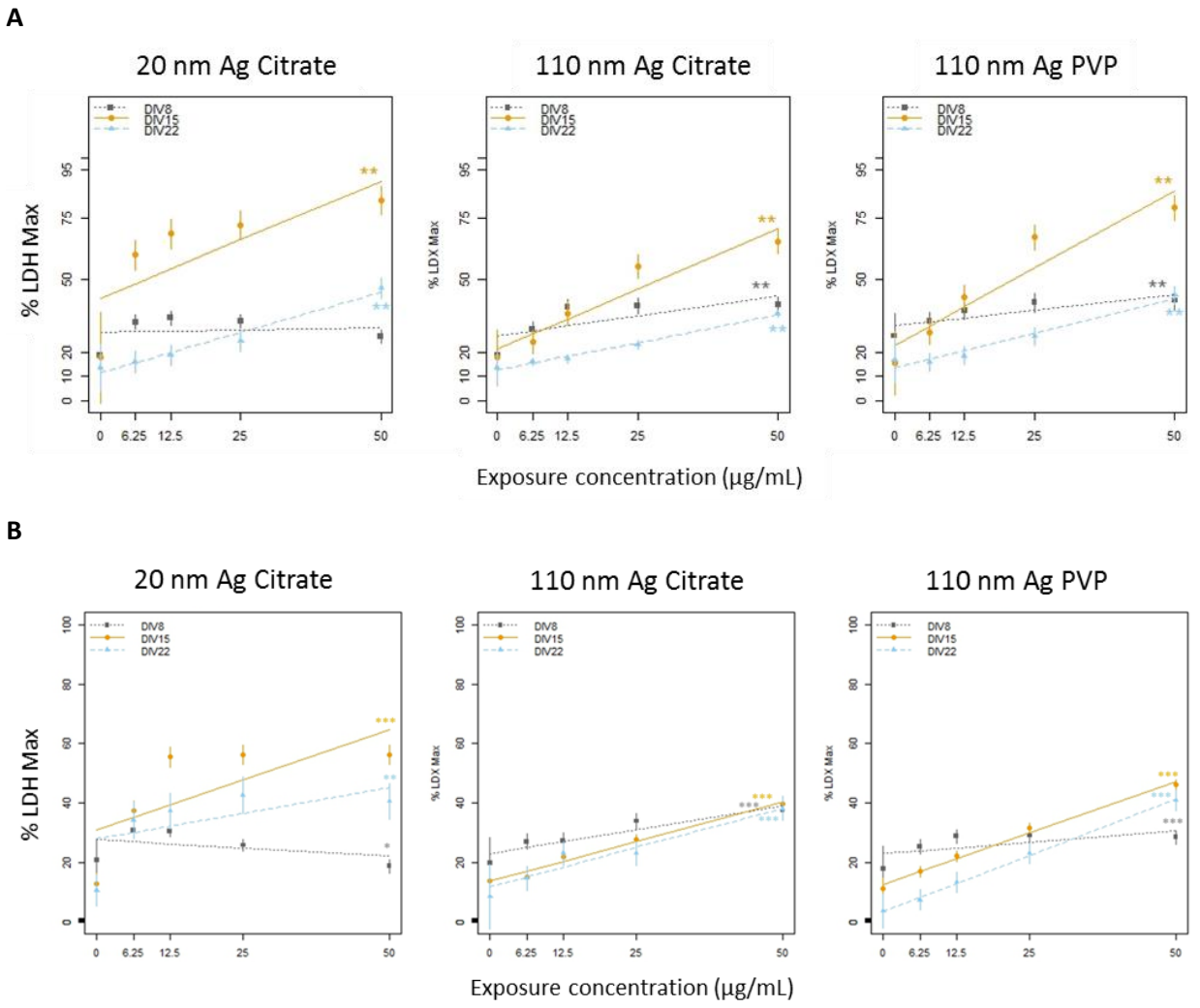

Figure 3.3. Dose-response curves for effects of neurodevelopmental stages. Dose-response curves for fetal (A) C57BL/6 and (B) A/J mouse midbrain cells after exposures at three different time points. Both C57BL/6 and A/J midbrain cells were more susceptible at DIV 15 compared to DIV 8 and 22. C57BL/6 was shown to be more sensitive compared to A/J. Data points and lines were estimated from the mixed-effect model. *: p-value < 0.05; **: p-value < 0.01; ***: p-value < 0.001 compared to controls.

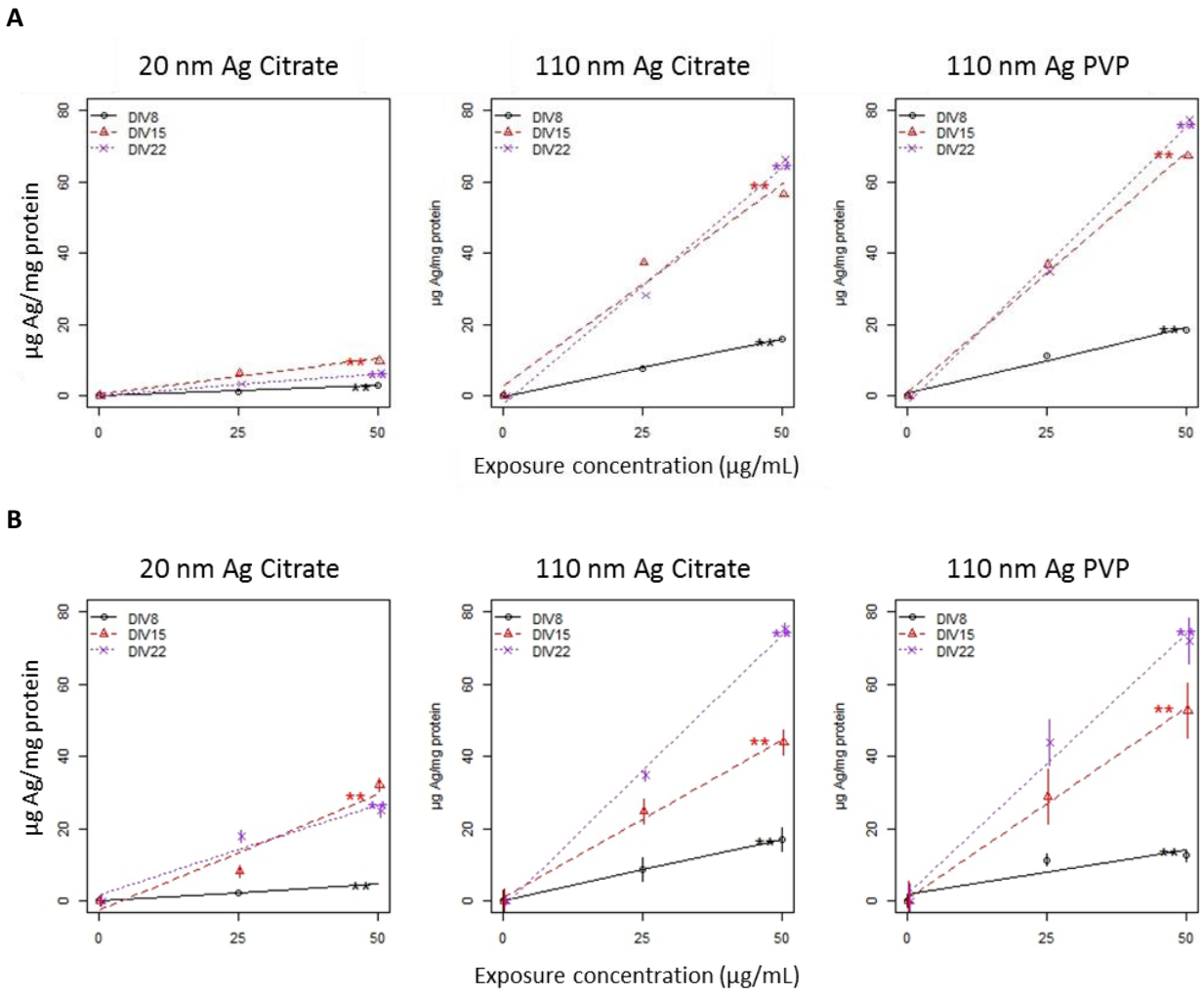

Figure 3.4. AgNPs were taken up by C57BL/6 and A/J mouse midbrain cells. A linear increase in dosimetry was observed with increasing doses. (A) C57BL/6 and (B) A/J midbrain cells demonstrated that greater amount of AgNPs were associated with the cells at DIV 15 and 22 compared to DIV 8 for all particles. Larger particles were associated with midbrain cells more than 20 nm particles in both strains of mouse. Data points and lines were estimated from the mixed-effect model. *: p-value < 0.05; **: p-value < 0.01; ***: p-value < 0.001 compared to controls.

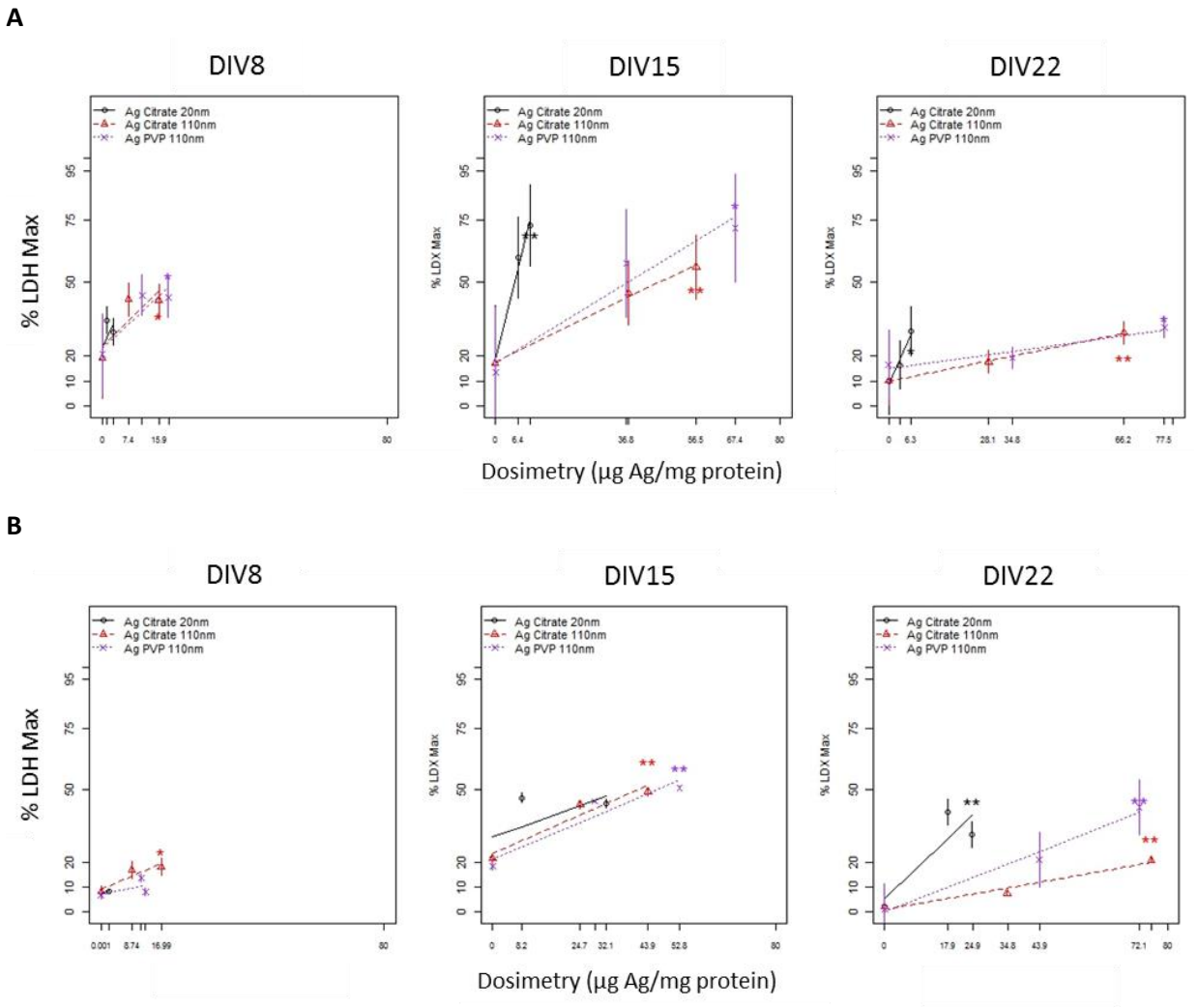

Figure 3.5. Dosimetry adjusted dose-response curves for effects of different AgNPs. Dosimetry-response curves for fetal (A) C57BL/6 and (B) A/J mouse midbrain cells after exposures to three different AgNPs. Even after adjusting for the amount of AgNPs associated with cells, cells were most susceptible to 20 nm particles than 110 nm particles for both strains of mouse. Data points and lines were estimated from the mixed-effect model. *: p-value < 0.05; **: p-value < 0.01; ***: p-value < 0.001 compared to controls.

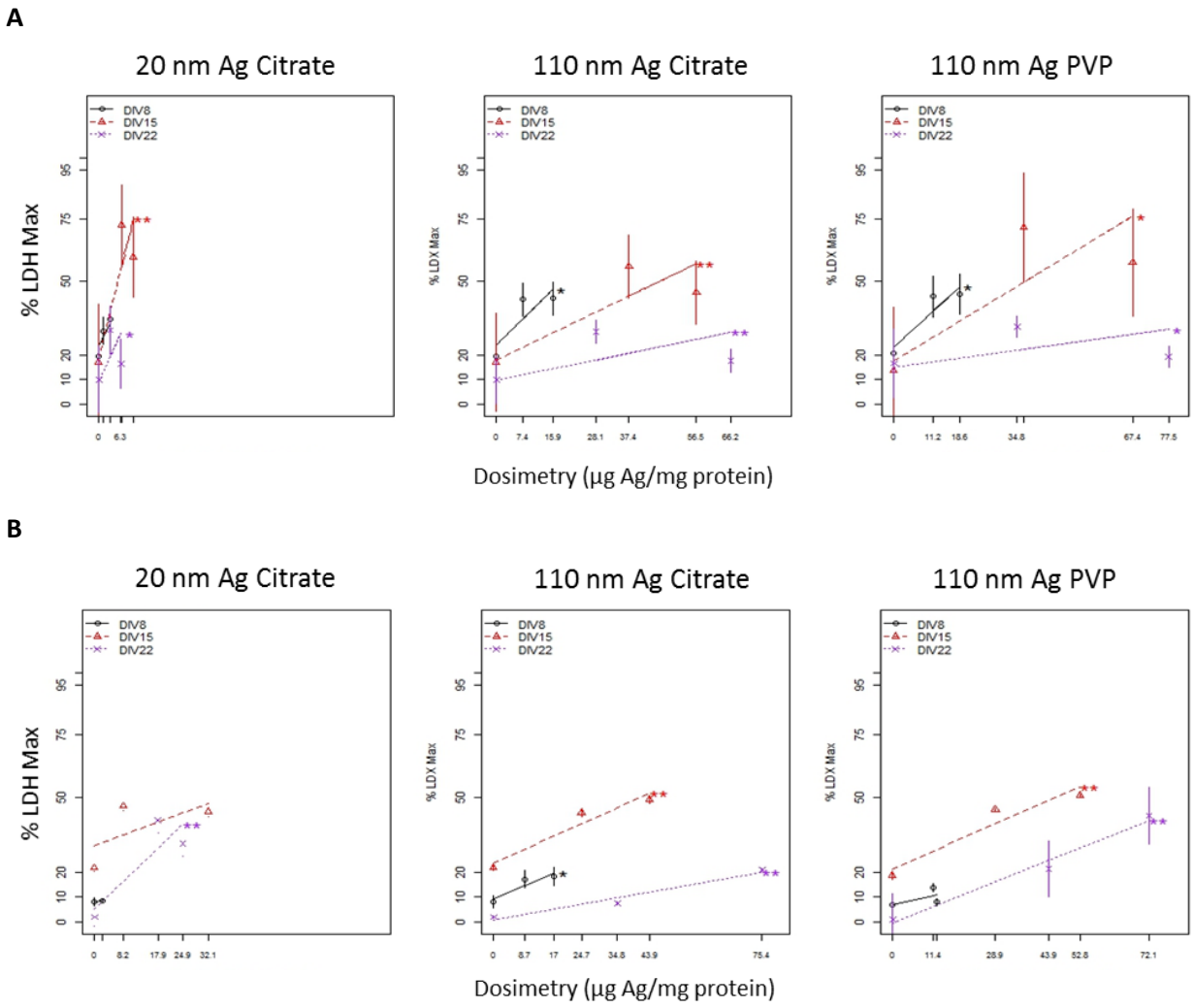

Figure 3.6. Effects of neurodevelopmental stages on dose-response curves adjusted by dosimetry. Dosimetry-response curves for fetal (A) C57BL/6 and (B) A/J mouse midbrain cells after exposures to AgNPs at different time points. After the dosimetry adjustment, embryonic C57BL/6 midbrain cells were most sensitive to all AgNPs at DIV 8 while DIV 15 still showed the highest cytotoxicity for A/J. Data points and lines were estimated from the mixed-effect model. *: p-value < 0.05; **: p-value < 0.01; ***: p-value < 0.001 compared to controls.

CHAPTER 3 REFERENCES

Bailey, J., Knight, A. and Balcombe, J. (2005). The future of teratology research is in vitro. *Biogenic Amines 19*, 97-145.

Balls, M. and Hellsten, E. (2002). Statement on the scientific validity of the mircromass test -- an in Vitro for embryotoxicity. *Altern Lab Anim 30*, 268-270.

Barone, S., Jr., Haykal-Coates, N., Parran, D. K. et al. (1998). Gestational exposure to methylmercury alters the developmental pattern of trk-like immunoreactivity in the rat brain and results in cortical dysmorphology. *Brain Res Dev Brain Res 109*, 13-31.

Bates, D., Machler, M., Bolker, B. M. et al. (2014). Fitting linear mixed-effects models using lme4. *Journal of Statistical Software 67*, 1-48.

Bull, R. J., McCauley, P. T., Taylor, D. H. et al. (1983). The effects of lead on the developing central nervous system of the rat. *Neurotoxicology 4*, 1-17.

Bury, N. R. and Wood, C. M. (1999). Mechanism of branchial apical silver uptake by rainbow trout is via the proton-coupled Na(+) channel. *Am J Physiol 277*, R1385-1391.

Churchill, G. A., Airey, D. C., Allayee, H. et al. (2004). The Collaborative Cross, a community resource for the genetic analysis of complex traits. *Nat Genet 36*, 1133-1137. http://dx.doi.org/ng1104-1133 [pii]
10.1038/ng1104-1133

Deng, W., McKinnon, R. D. and Poretz, R. D. (2001). Lead exposure delays the differentiation of oligodendroglial progenitors in vitro. *Toxicol Appl Pharmacol 174*, 235-244. http://dx.doi.org/10.1006/taap.2001.9219

El-Nour, K. M. M. A., Eftaiha, A., Al-Warthan, A. et al. (2010). Synthesis and applications of silver nanoparticles. *Arabian Journal of Chemistry 3*, 135-140.

EPA (2007). Method 3051A: Microwave Assisted Acid Digestion Of Sediments, Sludges, Soils, and Oils.

Fennell, T. R., Mortensen, N. P., Black, S. R. et al. (2017). Disposition of intravenously or orally administered silver nanoparticles in pregnant rats and the effect on the biochemical profile in urine. *J Appl Toxicol 37*, 530-544. http://dx.doi.org/10.1002/jat.3387

Genschow, E., Spielmann, H., Scholz, G. et al. (2002). The ECVAM international validation study on in vitro embryotoxicity tests: results of the definitive phase and evaluation of prediction models. European Centre for the Validation of Alternative Methods. *Altern Lab Anim 30*, 151-176.

Grandjean, P. and Landrigan, P. J. (2006). Developmental neurotoxicity of industrial chemicals. *Lancet 368*, 2167-2178. http://dx.doi.org/10.1016/S0140-6736(06)69665-7

Hernandez, R. B., Farina, M., Esposito, B. P. et al. (2011). Mechanisms of manganese-induced neurotoxicity in primary neuronal cultures: the role of manganese speciation and cell type. *Toxicol Sci 124*, 414-423. http://dx.doi.org/10.1093/toxsci/kfr234

Krewski, D., Acosta, D., Jr., Andersen, M. et al. (2010). Toxicity testing in the 21st century: a vision and a strategy. *J Toxicol Environ Health B Crit Rev 13*, 51-138. http://dx.doi.org/10.1080/10937404.2010.483176

Lammer, E. J., Chen, D. T., Hoar, R. M. et al. (1985). Retinoic acid embryopathy. *N Engl J Med 313*, 837-841. http://dx.doi.org/10.1056/NEJM198510033131401

Levard, C., Hotze, E. M., Lowry, G. V. et al. (2012). Environmental transformations of silver nanoparticles: impact on stability and toxicity. *Environ Sci Technol 46*, 6900-6914. http://dx.doi.org/10.1021/es2037405

Loeschner, K., Hadrup, N., Qvortrup, K. et al. (2011). Distribution of silver in rats following 28 days of repeated oral exposure to silver nanoparticles or silver acetate. *Part Fibre Toxicol 8*, 18. http://dx.doi.org/10.1186/1743-8977-8-18

Ma, R., Levard, C., Marinakos, S. M. et al. (2012). Size-controlled dissolution of organic-coated silver nanoparticles. *Environ Sci Technol 46*, 752-759. http://dx.doi.org/10.1021/es201686j

Maden, M. (2007). Retinoic acid in the development, regeneration and maintenance of the nervous system. *Nat Rev Neurosci 8*, 755-765. http://dx.doi.org/10.1038/nrn2212

Maxwell, S. L. and Li, M. (2005). Midbrain dopaminergic development in vivo and in vitro from embryonic stem cells. *J Anat 207*, 209-218. http://dx.doi.org/10.1111/j.1469-7580.2005.00453.x

Miodovnik, A. (2011). Environmental neurotoxicants and developing brain. *Mt Sinai J Med 78*, 58-77. http://dx.doi.org/10.1002/msj.20237

Morishita, Y., Yoshioka, Y., Takimura, Y. et al. (2016). Distribution of Silver Nanoparticles to Breast Milk and Their Biological Effects on Breast-Fed Offspring Mice. *ACS Nano 10*, 8180-8191. http://dx.doi.org/10.1021/acsnano.6b01782

Munusamy, P., Wang, C., Engelhard, M. H. et al. (2015). Comparison of 20 nm silver nanoparticles synthesized with and without a gold core: Structure, dissolution in cell culture media, and biological impact on macrophages. *Biointerphases 10*, 031003. http://dx.doi.org/10.1116/1.4926547

National Research Council Committee on Developmental Toxicology (2000). In (eds.), *Scientific Frontiers in Developmental Toxicology and Risk Assessment*. Washington (DC): National Academies Press (US)
Copyright 2000 by the National Academy of Sciences. All rights reserved. http://dx.doi.org/10.17226/9871

Park, J. J., Weldon, B. A., Park, J. H. et al. (2017). Characterization of *in vitro* organotypic 3D embryonic mouse midbrain micromass cultures using C57BL/6 and A/J mice. *ALTEX* ***In submission***

Patchin, E. S., Anderson, D. S., Silva, R. M. et al. (2016). Size-Dependent Deposition, Translocation, and Microglial Activation of Inhaled Silver Nanoparticles in the Rodent Nose and Brain. *Environ Health Perspect 124*, 1870-1875. http://dx.doi.org/10.1289/ehp234

Piersma, A. H. (2004). Validation of alternative methods for developmental toxicity testing. *Toxicol Lett 149*, 147-153. http://dx.doi.org/10.1016/j.toxlet.2003.12.029

Pratten, M., Ahir, B. K., Smith-Hurst, H. et al. (2012). Primary cell and micromass culture in assessing developmental toxicity. *Methods Mol Biol 889*, 115-146. http://dx.doi.org/10.1007/978-1-61779-867-2_9

Quadros, M. E., Pierson, R. t., Tulve, N. S. et al. (2013). Release of silver from nanotechnology-based consumer products for children. *Environ Sci Technol 47*, 8894-8901. http://dx.doi.org/10.1021/es4015844

Recordati, C., De Maglie, M., Bianchessi, S. et al. (2016). Tissue distribution and acute toxicity of silver after single intravenous administration in mice: nano-specific and size-dependent effects. *Part Fibre Toxicol 13*, 12. http://dx.doi.org/10.1186/s12989-016-0124-x

Reidy, B., Haase, A., Luch, A. et al. (2013). Mechanisms of Silver Nanoparticle Release, Transformation and Toxicity: A Critical Review of Current Knowledge and Recommendations for Future Studies and Applications. *Materials 6*, 2295.

Rice, D. and Barone, S. (2000). Critical periods of vulnerability for the developing nervous system: Evidence from humans and animal models. *Environmental Health Perspectives 108*, 511-533. http://dx.doi.org/Doi 10.2307/3454543

Robison, G., Sullivan, B., Cannon, J. R. et al. (2015). Identification of dopaminergic neurons of the substantia nigra pars compacta as a target of manganese accumulation. *Metallomics 7*, 748-755. http://dx.doi.org/10.1039/c5mt00023h

Rodier, P. M. (1994). Vulnerable periods and processes during central nervous system development. *Environ Health Perspect 102 Suppl 2*, 121-124.

Rodier, P. M. (1995). Developing Brain as a Target of Toxicity. *Environmental Health Perspectives 103*, 73-76. http://dx.doi.org/Doi 10.2307/3432351

Scoville, D. K., White, C. C., Botta, D. et al. (2015). Susceptibility to quantum dot induced lung inflammation differs widely among the Collaborative Cross founder mouse strains. *Toxicology and Applied Pharmacology 289*, 240-250. http://dx.doi.org/10.1016/j.taap.2015.09.019

Sidhu, J. S., Ponce, R. A., Vredevoogd, M. A. et al. (2006). Cell cycle inhibition by sodium arsenite in primary embryonic rat midbrain neuroepithelial cells. *Toxicol Sci 89*, 475-484. http://dx.doi.org/10.1093/toxsci/kfj032

Silbergeld, E. K. (1992). Mechanisms of lead neurotoxicity, or looking beyond the lamppost. *FASEB J 6*, 3201-3206.

Tang, J., Xiong, L., Wang, S. et al. (2009). Distribution, translocation and accumulation of silver nanoparticles in rats. *J Nanosci Nanotechnol 9*, 4924-4932.

Tang, J., Xiong, L., Zhou, G. et al. (2010). Silver nanoparticles crossing through and distribution in the blood-brain barrier in vitro. *J Nanosci Nanotechnol 10*, 6313-6317.

Tulve, N. S., Stefaniak, A. B., Vance, M. E. et al. (2015). Characterization of silver nanoparticles in selected consumer products and its relevance for predicting children's potential exposures. *Int J Hyg Environ Health 218*, 345-357. http://dx.doi.org/10.1016/j.ijheh.2015.02.002

Wang, X., Ji, Z., Chang, C. H. et al. (2014). Use of coated silver nanoparticles to understand the relationship of particle dissolution and bioavailability to cell and lung toxicological potential. *Small 10*, 385-398. http://dx.doi.org/10.1002/smll.201301597

Weldon, B. A., Park, J. J., Hong, S. et al. (2017). Effects of developmental stage, particle size, and coating on dosimetry and toxicity of silver nanoparticles in developing primary organotypic mouse midbrain cultures. Ph.D., University of Washington,

Whittaker, S. G. and Faustman, E. M. (1991). Effects of albendazole and albendazole sulfoxide on cultures of differentiating rodent embryonic cells. *Toxicol Appl Pharmacol 109*, 73-84.

Whittaker, S. G., Wroble, J. T., Silbernagel, S. M. et al. (1993). Characterization of cytoskeletal and neuronal markers in micromass cultures of rat embryonic midbrain cells. *Cell Biol Toxicol 9*, 359-375.

Wildt, B. E., Celedon, A., Maurer, E. I. et al. (2016). Intracellular accumulation and dissolution of silver nanoparticles in L-929 fibroblast cells using live cell time-lapse microscopy. *Nanotoxicology 10*, 710-719. http://dx.doi.org/10.3109/17435390.2015.1113321

Woodrow Wilson International Center for Scholars (2016). The project on emerging nanotechnologies.

Wu, J., Yu, C., Tan, Y. et al. (2015). Effects of prenatal exposure to silver nanoparticles on spatial cognition and hippocampal neurodevelopment in rats. *Environ Res 138*, 67-73. http://dx.doi.org/10.1016/j.envres.2015.01.022

Yang, Z., Liu, Z. W., Allaker, R. P. et al. (2010). A review of nanoparticle functionality and toxicity on the central nervous system. *J R Soc Interface 7 Suppl 4*, S411-422. http://dx.doi.org/10.1098/rsif.2010.0158.focus

Yokel, R. A. and Macphail, R. C. (2011). Engineered nanomaterials: exposures, hazards, and risk prevention. *J Occup Med Toxicol 6*, 7. http://dx.doi.org/10.1186/1745-6673-6-7

CHAPTER 4: Concordance of *in vitro* and *in vivo* gene expression dynamics for specific pathways of interest for developmental neurotoxicity

This Chapter is in preparation for submission. The authors of the manuscript are:

Julie Juyoung Park[1, 2], Susanna H. Wegner[1, 2], Tomomi Workman[1], Elaine M. Faustman[1, 2*]

[1] Institute for Risk Analysis and Risk Communication, University of Washington, Seattle, WA, USA

[2] Department of Environmental and Occupational Health Sciences, University of Washington, Seattle, WA, USA

* Corresponding author: Elaine M. Faustman

Institute for Risk Analysis and Risk Communication, Department of Environmental and Occupational Health Sciences, University of Washington, Seattle, WA, USA.

Email: faustman@uw.edu

ABSTRACT

In vitro human neural progenitor cells (hNPCs) offer promising high-throughput and high-content models for developmental neurotoxicity tests. We have previously characterized protein and gene expression dynamics through time in a commercially available differentiating neural progenitor cell model. In this study, we compared gene expression dynamics of genes associated with specific neurodevelopmental processes in differentiating neural progenitor cells *in vitro* and *in vivo* human neocortical brain tissue from 4 individuals during early brain development (gestational weeks 5.7, 6, 8, and 9). Pathways of particular interest for neurodevelopmental toxicity were identified a priori. Gene Ontology (GO) biological processes relevant to each of these pathways were identified in the Gene Ontology database, and lists of human genes associated with each GO term were extracted. Comparisons of relative gene expression intensity of genes associated with GO terms of interest showed substantial concordance between *in vivo* and *in vitro* systems and identified pathways that are more divergent *in vivo* and *in vitro*. This targeted qualitative analysis provided further confirmation that our differentiating *in vitro* hNPC model can capture many fundamental processes of human neurodevelopment and helps to define the appropriate applications of this model. With further validation, this system may be utilized as one of screening tools for neurotoxicants, which then can be applied to the adverse outcome pathway framework.

INTRODUCTION

Disruption of key processes during neurodevelopment can lead to lifelong neuropathologies (Rice and Barone, 2000a; Rodier, 1995b; Wegner et al., 2014). Epidemiological and mechanistic evidence demonstrates that environmental exposures during vulnerable periods of brain development contribute to cognitive deficits and neurodevelopmental disorders (Grandjean and Landrigan, 2006, 2014; Landrigan, 2010). Many factors contribute to sensitivity in response to developmental neurotoxicants. Factors such as the developmental timing of exposures, species, gender, and genetic background contribute to adverse effects of neurotoxic exposures on brain development and function (Barry et al., 2017; Faustman et al., 2000; Rice and Barone, 2000b; Rodier, 1995a). For example, exposures to methylmercury and alcohol have been shown to produce minimal long-lasting effects on maternal health while *in utero* exposures to these developmental neurotoxicants result in neurodevelopmental disorders and delays (de Sanctis et al., 2011; Grandjean and Herz, 2011).

Despite the sensitivity of neurodevelopment to chemical perturbation, only about 200 of 80,000 US Environmental Protection Agency (US EPA) registered chemicals are tested for neurotoxicity (Judson et al., 2009; Crofton et al., 2012). Traditional *in vivo* animal models for developmental toxicity tests are time-consuming, and resource and animal intensive, making them poorly suited to address this immense data gap (Bailey et al., 2005; Piersma, 2004; Pratten et al., 2012; Smirnova et al., 2014). In recognition of the need for more rapid chemical screening and testing, the field of toxicology is increasingly shifting towards the use of high-throughput and high-content *in vitro* methods (Aschner et al., 2010; Bal-Price et al., 2012; Coecke et al., 2007; Crofton et al., 2014; Crofton et al., 2011; Crofton et al., 2012; Lein et al., 2007; NRC, 2000, 2007). Upon validation of these *In vitro* alternative models that can capture key processes in brain development, we would be able to screen and prioritize potential developmental neurotoxicants and to inform policy makers. To accomplish this, emerging *in vitro* neurodevelopmental toxicology models must be well characterized and confirmed for their sensitivity and specificity before they can be incorporated into regulatory contexts (EPA, 2015).

Substantial progress has been made in the development of high-content *in vitro* models that capture dynamic processes and cell-cell interactions (Bal-Price et al., 2010; Buzanska et al., 2010; Fritsche et al., 2011; Park et al., 2017; Roque et al., 2014; Theunissen et al., 2012). For example, embryonic mouse micromass system has also been optimized and characterized, demonstrating the culture system's ability to recapitulate neural proliferation, migration, differentiation, and functional maturation *in vitro* (Park et

al., 2017). Differentiating human neural progenitor cell (hNPC) models capable of differentiating into oligodendrocytes, astrocytes, and neurons (Gaspard and Vanderhaeghen, 2010) are also a promising tool for developmental neurotoxicity screening. A commercially available hNPC line (Shin et al., 2006) derived from a preimplantation blastocyst provides a consistent platform for high throughput or high-content assays (Young et al., 2011; Harrill et al., 2010). hNPCs have advantages of closely representing human brain development processes because the cell line is derived from human. It also provides opportunities to study the impact of various environmental neurotoxicants during different stages of neuronal differentiation processes. For these reasons, hNPC model has been used in development of screening assays in EPA (Harrill et al., 2010)

Using hNPC line, we previously evaluated temporal dynamics of global gene expression in differentiating hNPCs cultures to provide a roadmap of biological processes captured through 21-days of the culture period. To anchor neuronal differentiation observed in the NPC model to *in vivo* development, we characterized analysis of pathways enriched among genes changed during early human brain development *in vivo* (in a publicly available dataset (Kang et al., 2011) and during neuronal differentiation *in vitro* (Wegner et al., 2014). Specifically, we performed an untargeted analysis of gene ontology (GO) terms enriched among genes significantly changed in differentiating hNPCs *in vitro* and during early stages of human neocortical development in four individuals. Gene ontology biological processes enriched among genes highly expressed both *in vivo* and *in vitro* demonstrated that several fundamental processes of brain development that are sensitive to toxicant perturbation are reflected in the *in vitro* hNPC model.

Here, we investigated clusters of gene expression patterns found for each of *in vivo* and *in vitro*, revisited GO terms that were commonly or uniquely enriched *in vitro* and/or *in vivo*, and compared *in vivo* and *in vitro* gene expression for specific pathways of interest for neurodevelopmental toxicology. The analysis employed an unsupervised approach to identify the most highly enriched pathways among highly expressed genes as well as a targeted analysis by identifying a set of pathways of interest a priori for comparison of *in vivo* and *in vitro* gene expression dynamics. By characterizing concordance in gene expression *in vivo* and *in vitro* for processes of particular interest for developmental neurotoxicity, our analysis demonstrated the applicability of this hNPC model for human brain development. The comparisons presented here can facilitate design and interpretation of future studies to maximize the degree to which *in vitro* assays capture biology relevant to *in vivo* conditions. Moreover, we can apply this to adverse outcome pathways (AOPs) framework. AOP is a tool to link perturbation measured *in vitro* to

downstream adverse outcomes (Ankley et al., 2010; Bal-Price and Meek, 2017; EPA, 2013; OECD, 2012). As *in vitro* models are developed, they can be integrated into an AOP framework and be used to anticipate adverse human health outcomes.

METHODS

Human neural progenitor cell (hNPC) culture.

Commercially available hNPCs (ArunA Biomedical, Athens, GA, USA) were expanded for 8 – 10 passages in proliferative conditions using AB2™ Neural Cell Culture media (ArunA Biomedical, Athens, GA, USA). Cells were then plated onto Matrigel®-coated (BD Biosciences, Bedford, MA, USA) dishes with a seeding density of 200,000 cells/mL. Plated hNPCs were then allowed to attach in AB2™ Neural Cell Culture media (ArunA Biomedical, Athens, GA, USA). After 24 hours of plating, differentiation was initiated by replacing media with HyClone™ differentiation media (GE Healthcare Life Science, Chicago, IL, USA). Cells were maintained in differentiating conditions up to 21 days, refreshing half of the media every two days. A diagram of study design is shown in Figure 4.1, and more detailed hNPC cell culture protocol can be found in Wegner et al. (2014).

In vitro hNPCs RNA preparation and microarray processing.

After 0, 1, 3, 7, 14, 21 days of the initiation of differentiation, RNA was harvested in TRIzol (ThermoFisher Scientific, Waltham, MA, USA). Total RNA was isolated using Ambion® RNA Expert (ThermoFisher Scientific, Waltham, MA, USA) and mirVana miRNA Isolation Kit (ThermoFisher Scientific, Waltham, MA, USA). RNA was isolated using the manufacturer's protocol. The extracted samples were further purified with Qiagen's RNeasy MinElute Cleanup Kit (Qiagen, Hilden, Germany) according to kit protocols. The samples were stored in -80°C until use.

Purified RNA from *in vitro* hNPCs was hybridized to Affymetrix GeneChip® Human Gene 1.0 ST Array (Affymetrix, Santa Clara, CA, USA) to measure global gene expression in each sample. Expression data reflects replicate samples from 3 biological replicates. Expression data was normalized and annotated using the Bioconductor Limma package for R software (Ritchie et al., 2015).

***Human in vivo brain microarray data*.**

An *in vivo* dataset from Kang et al. (2011) was used. The data set from Kang et al. (2011) included global gene expressions across brain regions through time based on human brain tissue samples. For our comparison, neocortical brain tissue dataset from 4 individuals at postcoital weeks 5.7, 6, 8, and 9 was selected as shown in Table 4.1 and divided into two periods. Postcoital weeks 5.7 and 6 data were combined into Period 1, and Period 2 included postcoital weeks 8 and 9. Kang et al. (2011) analyzed *in vivo* human brain data with Affymetrix Human Exon 1.0 ST arrays (Affymetrix, Santa Clara, CA, USA). To anchor our *in vitro* hNPCs data to *in vivo*, *in vivo* gene expression was pooled across all neocortical brain regions within each period as demonstrated in Table 4.1.

***In vitro and in vivo gene expression analysis pipeline*.**

Microarray CEL files were normalized and annotated using R (The R Core Team, 2013) with following Bioconductor library packages: limma (Ritchie et al., 2015), oligo (Carvalho and Irizarry, 2010), NbClust (Charrad et al., 2014), annotate (Gentleman, 2017), pd.hugene.1.0.st.v1 (Carvalho, 2015). Probe features were normalized with the rma() function in Affy package (Gautier et al., 2004), followed by annotation with getNetAffx() and Affycore tools (MacDonald, 2008). With the lmFit() function, the gene expression values for biological replicates were fitted. Once *in vitro* hNPCs and *in vivo* human neocortical gene expressions were normalized and annotated, genes significantly changed across time were identified as those with FDR < 0.01. These criteria for significant changes were selected in order to maximize the number of genes with high biological importance included in the analysis. *In vitro* and *in vivo* CEL files were analyzed separately.

K-means clustering for in vitro and in vivo.

For genes that passed the criteria of FDR < 0.01, NbClust() function was utilized to determine the optimal number of cluster for kmeans() function based on expression dynamics of each gene. This procedure is illustrated in Figure 4.2.

Pathway analysis of in vitro and in vivo significantly changed genes.

For each identified cluster from *in vitro* or *in vivo* dataset, Gene Ontology (GO) Elite software was utilized to identify GO biological processes enriched among annotated genes (Zambon et al., 2012). Enrichment analysis was achieved by running 2000 permutations of over-representation analysis (ORA). A p-value cutoff value of less than 0.05 was used for permutation, and at least three genes needed to be significantly

changed for term enrichment. Terms with ID counts greater than 10000 were not included. Enriched GO terms were ranked by Z-score, which represents the proportion of the number of genes predicted to be randomly changed and those actually changed within a given GO term to the standard deviation of the number of genes observed in a hypergeometric distribution. The Z-score calculation as follows:

$$\mathrm{Z-score} = \frac{r-\left(n\times\frac{R}{N}\right)}{\sqrt{\left(n\times\frac{R}{N}\right)\times\left(1-\frac{R}{N}\right)\times\left(1-\frac{n-1}{N-1}\right)}}$$ Zambon et al. (2012)

Where r represents the number of genes that were significantly changed across time within each specific Go term, n is the total number of genes in that specific GO term, R is the total number of significantly changed genes through time, N denotes the total number of genes measured. GO terms with Z-score greater than 1.96 were excluded from further analysis.

Comparison of significantly changed genes between in vitro and in vivo.

To compare significantly changed genes between *in vitro* and *in vivo*, we identified significantly changed genes across time uniquely in *in vitro* or *in vivo* system and commonly in both systems. The same criterion of FDR < 0.01 was applied. Significantly enriched GO terms and GO biological themes in genes significantly changed *in vitro* or *in vivo* system and those changed commonly in both *in vitro* and *in vivo* systems were then identified. For this analysis, Z scores greater than 1.96 were applied. Figure 4.2 illustrates the flow of this analysis.

***Comparing in vitro and in vivo gene expressions in targeted pathways of interest*.**

To investigate significantly changed genes and their expressions through time, GO biological processes relevant to pathways of interest were identified. From the Gene Ontology database (May 2014), a list of human genes associated with each GO term was obtained. Heatmaps were utilized to visualize changes in the relative gene expression across time *in vitro* and *in vivo* for each GO term of interest. Relative gene expression was calculated by each gene expression divided by mean gene expression across all time points within each system. Relative gene expressions *in vitro* and *in vivo* for a specific pathway of interest were mapped rank ordered (y-axis) from highest to lowest mean gene expression through time (x-axis). The color scale scheme depicts gene expression levels where green represents low expression levels and white indicates high expression levels. A flow diagram of gene expression comparison between *in vitro* and *in vivo* for a targeted pathway of interest is demonstrated in Figure 4.2.

RESULTS

K-means clustering for in vitro hNPCs and in vivo human brain gene expression.

Based on the global gene expression, key developmental pathways identified in each of *in vitro* hNPC system and *in vivo* human brain were grouped using K-means clustering. This allowed us to visualize groupings for both systems. *In vitro* hNPCs through 21 days of culture period demonstrated a total of 9482 genes significantly changed (FDR < 0.01) while *in vivo* showed 7354 significantly changed genes (FDR < 0.01). Of 7342 probes identified *in vivo*, only 7264 genes were included for further analysis as 34 of them did not have gene symbols.

For *in vitro* hNPCs, three clusters were identified by K-means clustering (Figure 4.3A). The first cluster included a total of 2922 significantly changed genes with FDR < 0.01 as criteria. Expressions of genes in this cluster reached its maximum expression at day 3 and then decreased over time (Figure 4.3A). Themes that appeared among GO biological processes significantly enriched in this cluster included cell cycle, stem cell proliferation, regulation of gene expression, and differentiation and development. The second cluster consisted of 5000 significantly changed genes and showed decreasing gene expression over time (Figure 4.3A). General themes that emerged among significantly enriched GO biological processes were metabolism and transport, DNA replication, response to stimulus, fate commitment, cell death, and immune response. The third cluster composed of 1560 significantly changed genes showed an opposite trend compared to the second cluster. The expressions in the third cluster increased through the culture time (Figure 4.3A), and themes among significantly enriched GO biological processes included morphological development, axon guidance, synapse formation, migration, and signal transduction.

We identified 2 clusters for *in vivo* human neocortical samples using K-means clustering method. Genes in the first cluster demonstrated a trend of increasing expression over time (week 5.7, 6, 8, and 9) as shown in Figure 4.3B. Unlike cluster 1, a decrease in gene expression over time was illustrated in cluster 2 (Figure 4.3B).

Significantly changed gene expressions commonly in vitro and in vivo and uniquely in vitro or in vivo.

Once genes passed our criteria of FDR < 0.01, gene expressions that significantly changed across time commonly *in vitro* and *in vivo* and uniquely *in vitro* or *in vivo* were evaluated. The number of genes that were uniquely changed through time *in vitro* was 9482 while 7264 genes significantly changed their expressions over time *in vivo* (Figure 4.4).

We discovered that a total of 3792 genes have significantly changed across time in both *in vitro* and *in vivo* as shown in Figure 4.4. GO biological process terms that were enriched in both *in vitro* and *in vivo* included specific processes such as neuronal differentiation, neurotransmission, and brain development. General developmental processes were also found among GO biological process terms enriched among significantly changed genes with our criteria including signal transduction and development and morphogenesis.

In our *in vitro* hNPC system, a total of 5690 genes were uniquely yet significantly changed through time (Figure 4.4). GO biological processes that were unique to *in vitro* involved with cell cycle and stress responses. This result suggested that *in vitro* hNPCs culture may experience increased level of stress such as oxidative stress compared to *in vivo* system. Compared to *in vitro*, expressions of 3472 genes were uniquely changed across time *in vivo* (Figure 4.4). Enriched GO biological process terms from *in vivo* data were related to neurotransmission.

In vitro vs. in vivo gene expression comparison for targeted pathways

The biological processes of interest for developmental neurotoxicology were selected based on the key processes identified in seminal review papers (Rice and Barone, 2000a; Rodier, 1995b), including neural proliferation, differentiation, and subtype specification, synaptic transmission, epigenetic regulation, response to hormones, oxidative stress, and inflammation. We identified GO biological processes relevant to each of these and extracted lists of genes associated with each GO term from the Gene Ontology database (http://geneontology.org/). The heatmaps demonstrates the *in vitro* or *in vivo* temporal dynamics of gene expression associated with a particular GO term of interest through time. Relative gene expression intensity for genes associated with each GO biological process across time is plotted to investigate *in vitro* or *in vivo* dynamics. Figures 4.5 – 4.7 illustrate examples of pathways that are consistent *in vitro* and *in vivo* as well as pathways with divergence.

We compared *in vitro* and *in vivo* expression of genes associated with GO terms related to hNPC proliferation and neuronal differentiation towards specific neuronal subtypes including genes involved in pathways of NPC proliferation, neuronal fate commitment, cortical neuron differentiation, and forebrain neuron differentiation (Figure 4.5). Between *in vitro* and *in vivo*, expression of genes associated with NPC proliferation, neuronal fate commitment, and forebrain neuron differentiation was very similar while that

of genes related to cortical neuron differentiation was more discordant. Genes involved in cortical neuron differentiation (Figure 4.5C) illustrated lower expression levels *in vitro* compared to *in vivo*, suggesting that *in vitro* hNPCs are not as differentiated as *in vivo* neocortex. Evaluation of expression patterns with specific proliferation and differentiation pathways highlighted similarities and differences between *in vivo* and *in vitro* differentiation.

A high degree of concordance between *in vivo* and *in vitro* models over time was found for genes associated with epigenetic changes including histone modification (Figure 4.6A), DNA methylation (Figure 4.6B), and chromatin remodeling (Figure 4.6C). Compared to histone modification and DNA methylation heatmaps (Figure 4.6A and Figure 4.6B), more discordance between *in vivo* and *in vitro* gene expressions over time for genes associated with chromatin remodeling (Figure 4.6C) was observed.

Figure 4.7 illustrated similarities and differences in gene expression patterns over time for oxidative stress between *in vitro* and *in vivo*. Generally, expressions of genes associated with oxidative stress *in vitro* were higher than *in vivo*. Genes associated with inflammatory responses and with cytokine secretion were not significantly changed over time in both culture systems, suggesting that inflammatory responses were not present. This result was expected as *in vitro* hNPCs and *in vivo* human neocortical brain samples were not exposed to a toxicant.

Other targeted pathways involved in cell proliferation and differentiation, different brain regions, synaptic transmission, response to hormones, transporters, and microglia were investigated (Supplementary Figures 4.1 – 4.6). For example, genes associated with forebrain development (Supplementary Figures 4.2C) had highly concordant expression *in vivo* and *in vitro* while genes associated with midbrain (Supplementary Figures 4.2E) and hindbrain development (Supplementary Figures 4.2F) were more discordantly expressed across systems. This finding suggested that our hNPCs may differentiate with forebrain characteristics over 21-days of the culture period. Another example is gene expression patterns for synaptic transmission associated with specific neuronal subtypes (Supplementary Figure 4.3). Less concordance in the expression of genes associated with GABA (Supplementary Figure 4.3A) and choline (Supplementary Figure 4.3B) transmission was revealed. Expression of genes associated with glutamate varied in consistency between *in vivo* and *in vitro* (Supplementary Figure 4.3C). Concordance in the expression of genes related to response to various hormones was illustrated in Supplementary Figure 4.4. While expression of genes associated with response to thyroid signaling (Supplementary Figure 4.4B) was

consistent *in vivo* and *in vitro*, genes associated with response to testosterone signaling (Supplementary Figure 4.4C) were less consistent, with expression of many genes much higher *in vitro* than *in vivo*. Overall gene expression patterns for genes associated with transporters (Supplementary Figure 4.5) and with microglia (Supplementary Figure 4.6) were generally similar *in vivo* and *in vitro*, though clear differences exist for specific genes.

DISCUSSION

Developmental neurotoxicology is an area where there is a need to develop and evaluate *in vitro* alternative methods (Aschner et al., 2010; Bal-Price et al., 2012; Coecke et al., 2007; Crofton et al., 2014; Crofton et al., 2012; Crofton et al., 2011; Lein et al., 2007). As we move forward in evaluating effects of toxicants on targeted pathways for neurodevelopment *in vitro*, understanding the relevance of *in vitro* pathways for *in vivo* biology will be critical. This current study offers a qualitative understanding of similarities and differences between *in vitro* and *in vivo* human gene expressions for targeted pathways of interest. This work highlights biological processes that are best captured in this model and define the most relevant applications of this model.

In the current study, we identified three clusters of temporal gene expression patterns in our *in vitro* hNPC culture system demonstrates a dynamic yet distinct gene expression phases (Figure 4.3A). Three clusters revealed that GO biological processes related to cell cycle and stem cell proliferation reached its maximum gene expression at day 3 and then decreased over time, suggesting that proliferation was prominent during the early days in culture. Gene expressions related to DNA replication were decreased over time, too. Over 21-days of the culture period, GO biological processes associated with differentiation including migration, axon guidance, and synapse formation were significantly enriched. Altogether, this suggested that *in vitro* hNPCs still have some proliferation signals upon initiation of differentiation; however, after day 3 in culture, these signals decrease over time, and the culture system mainly differentiated.

In vivo and *in vitro* genes involved in specific pathways from brain development were examined for comparison, and we found striking similarities between the two systems. From gene expression patterns, we concluded that our hNPCs were differentiating to have forebrain characteristics as increased concordance between *in vitro* and *in vivo* systems was observed for forebrain development compared to midbrain or hindbrain development. This finding is consistent with Gaspard and Vanderhaeghen (2010)

that Different morphogenic signals lead to different regional identification and specific fates in differentiating hNPCs, and that hNPCs with morphogen-free medium would differentiate into neurons with forebrain characteristics.

Moreover, expression of genes in targeted pathways of neuronal proliferation, differentiation, and epigenetic regulation is mostly consistent, suggesting that our *in vitro* hNPC model is able to capture these complex key processes of a developing brain. For example, epigenetic regulations are the intrinsic level of temporal and spatial regulation in neurodevelopment (MuhChyi et al., 2013). Genes involved in histone modification, DNA methylation, and chromatin remodeling all demonstrated strikingly similar concordance between *in vitro* and *in vivo*. For instance, methyltransferase EZH1 that catalyzes histone H3 lysine 27 trimethylation is associated with the proteins responsible for regulating the balance between self-renewal and differentiation of progenitor cells located in the cerebral cortex (Pereira et al., 2010).

Our gene expression results also indicated that genes associated with dopaminergic neuron differentiation in our *in vitro* hNPCs concorded well to the human *in vivo* neocortex samples. Dopamine plays an important role in brain development, especially in the development of forebrain differentiation and circuit formation (Money and Stanwood, 2013). Other subtypes of neuron differentiation such as GABAergic were less similar between the two systems.

Oxidative stress acts as an important regulator of developmental processes as well as a mediator of toxicity (Wells et al., 2010; Wells et al., 2009). Previously, Wells et al. (2009) reported that reactive oxygen species (ROS) and reactive nitrogen species (RNS) that are involved in signal transduction are tightly and temporally regulated. They also indicated that ROS and RNS are selective to cell types, organelles, and microenvironment within proteins and lipids and that this redox environment plays a role in regulating cellular proliferation, differentiation, apoptosis/necrosis, and epigenetics (Hansen, 2006; Hitchler and Domann, 2007; Wells et al., 2009). From our study, genes related to oxidative stress showed similar gene expression patterns between *in vitro* and *in vivo* over time, suggesting that our *in vitro* hNPCs differentiate with similar signal transduction and oxidative damage patterns with *in vivo* human neocortex.

Some pathways of interest including cortical neuron differentiation and synaptic transmission, however, illustrated less concordance when patterns of *in vitro* and *in vivo* gene expression were compared. Such inconsistency between human *in vitro* and *in vivo* models may be due to the fact that the human

neocortical samples used for this comparison are more complex tissues containing diverse cell types. Also, the extent of differentiation for *in vitro* hNPCs may not be reflective of *in vivo* samples used for the comparison. Together, these results suggested that our differentiating cultures would be an appropriate model to examine effects of neurotoxicants that affect forebrain region or dopaminergic neuron differentiation.

One of the limitations this study has included *in vivo* sample size. Microarray data from only 4 individuals (one per time point) were present from Kang et al. (2011) for *in vivo* human brain comparison. Ideally, one would demonstrate similarity and differences of response to toxicants in specific pathways *in vivo* and *in vitro*, but current analysis describes the baseline gene expression for multiple pathways of interest. Therefore, we found the interpretation difficult without concrete functional endpoints. When individual pathways are scrutinized, they would require in depth evaluation of specific genes.

In the future, further validation of *in vitro* developmental neurotoxicology models including hNPCs by comparing toxicogenomic signatures from *in vitro* and *in vivo* at early neurodevelopmental stages following toxicant exposures would be important. The current analysis stops short of quantitative comparisons between *in vivo* and *in vitro* gene expression across pathways to avoid discounting the vital role individual genes can play. This is because differences in single genes may have a large impact on pathway function while a whole pathway may be quite similar. Therefore, pathways should rather be evaluated in-depth gene by gene.

The aim of this analysis was to characterize the similarities and differences in *in vitro* and *in vivo* baseline expression patterns of pathways of interest to support in-depth explorations. With further validation of this system in the predictability of neurotoxicants, our hNPCs model may be used to identify perturbed pathways *in vitro* and anticipate adverse health outcomes by integrating obtained results into an AOP framework. This framework would allow us to link pathway perturbation measured *in vitro* to downstream adverse outcomes (Ankley et al., 2010; Bal-Price and Meek, 2017; EPA, 2013; Krewski et al., 2010; OECD, 2012). And furthermore, if AOPs can be organized into networks, they can serve to translate *in vitro* data for regulatory decisions and models such as hNPCs can facilitate this approach.

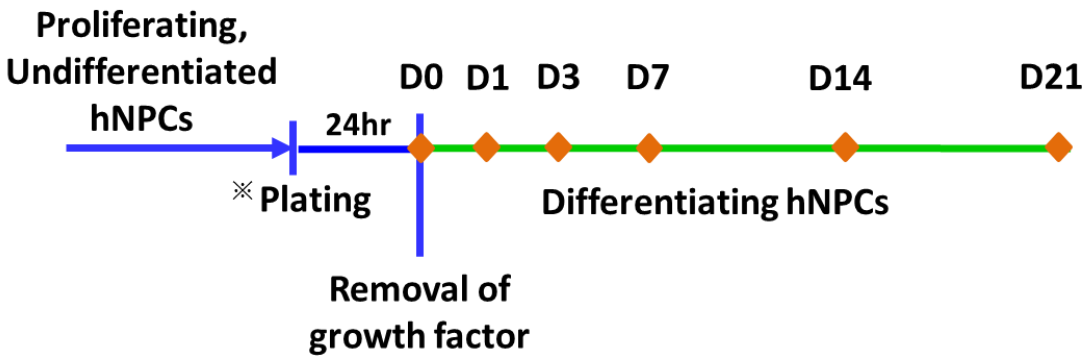

Figure 4.1. Human neural progenitor cells (hNPCs) study design. hNPCs were plated in proliferation media with a seeding density of 200,000 cells/mL. After 24 hours of plating, differentiation was initiated and maintained in differentiation media for 21 days. The media was changed every 2-3 days. The blue line represents hNPCs in proliferation media and green indicates those in differentiation media.

Table 4.1. Summary of *in vivo* human neocortical tissue sample data used to anchor our *in vitro* hNPCs. Period 1 included neocortical tissue samples from postcoital weeks 5.7 and 6, and Period 2 consisted of postcoital weeks 8 and 9. The letters 'L' and 'R' indicate the left and right side of the brain.

Human *In Vivo* Neocortex	Period 1		Period 2	
	HSB104 **PCW 5.7**	HSB185 **PCW 6**	HSB112 **PCW 8**	HSB148 **PCW 9**
FC, frontal cerebral wall	FC L; FC R	FC L; FC R		
OFC, orbital prefrontal cortex			OFC L; OFC R	OFC L; OFC R
DFC, dorsolateral prefrontal cortex			DFC L; DFC R	DFC L; DFC R
VFC, ventrolateral prefrontal cortex			VFC L; VFC R	
MFC, medial prefrontal cortex			MFC L; MFC R	MFC L; MFC R
MSC, motor sensory cortex			MSC L; MSC R	MSC L; MSC R
PC, parietal cerebral wall	PC L; PC R	PC L	PC L; PC R	PC L; PC R
TC, temporal cerebral wall	TC L; PC R	TC L; TC R		TC L; TC R
ITC, inferior temporal cortex			ITC L; ITC R	
STC, superior temporal cortex			STC L; STC R	
OC, occipital cerebral wall	OC L; OC R		OC L; OC R	OC L; OC R

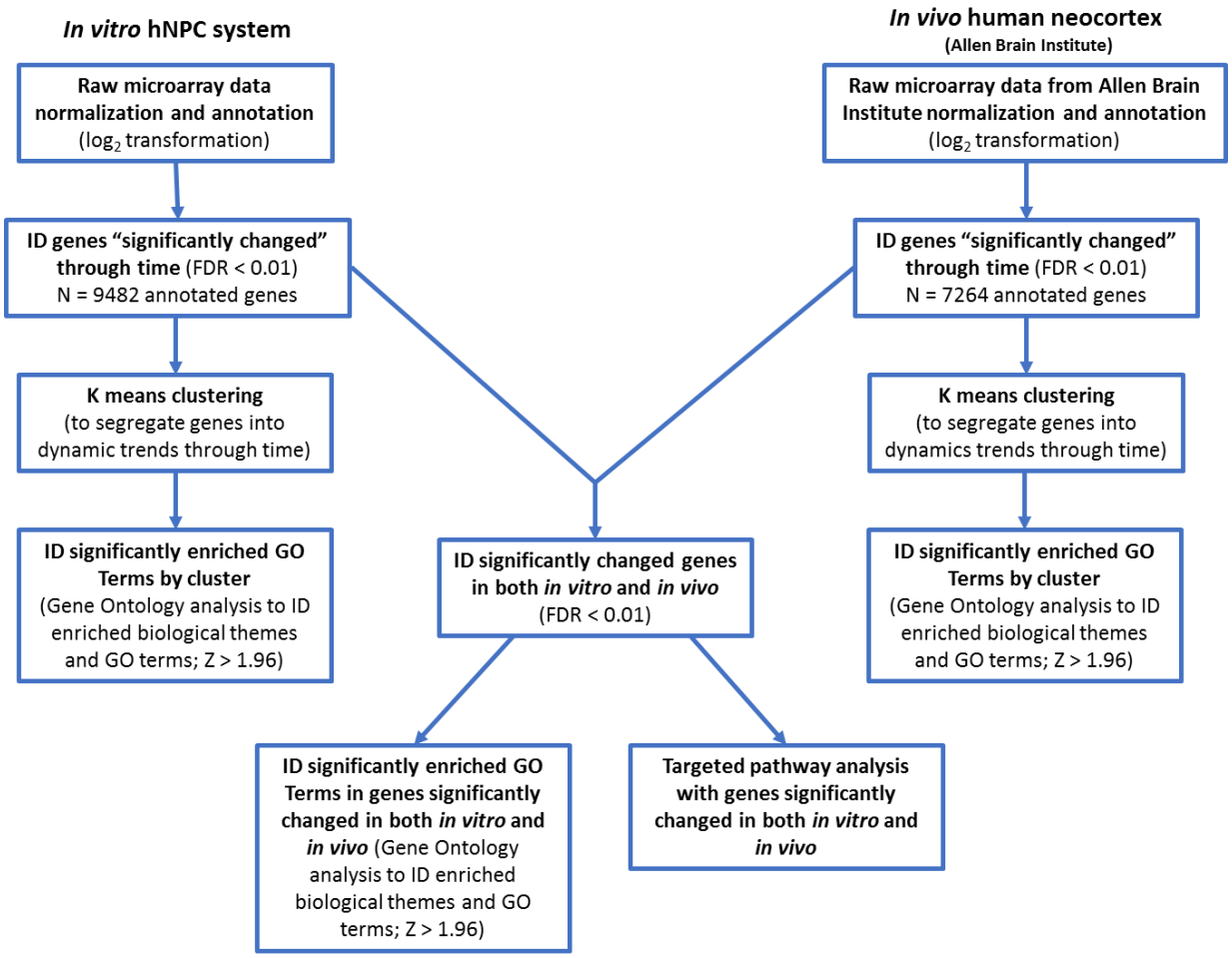

Figure 4.2. Flow diagram of *in vitro* and *in vivo* gene expression analysis. Once genes were normalized and annotated, genes that were significantly changed across time *in vitro* or *in vivo* were identified with the criteria of false discovery rate < 0.01 (FDR < 0.01). For genes that passed these criteria were used for clustering analysis, for identifying significantly enriched GO terms in each of *in vitro* or *in vivo* systems and both systems, and for targeted pathway analysis.

A

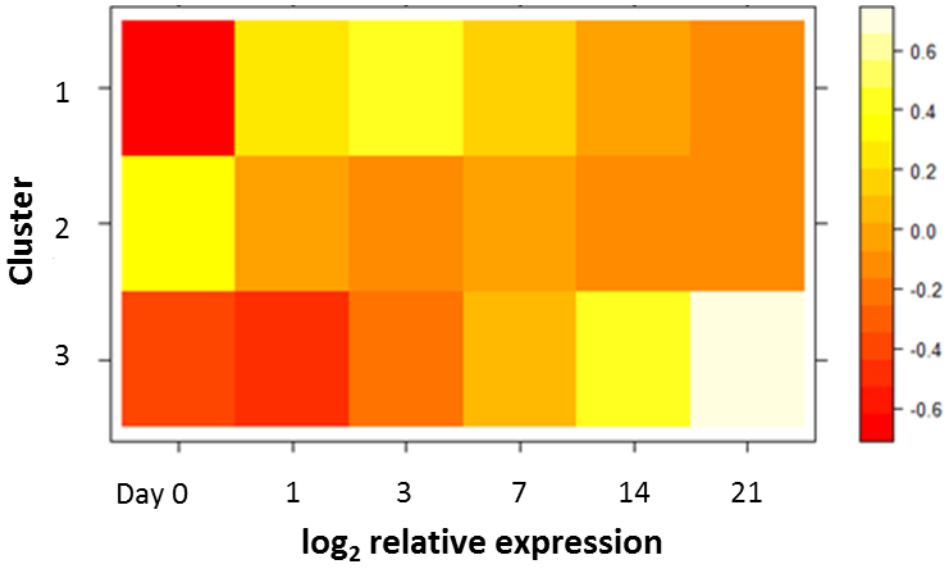

B

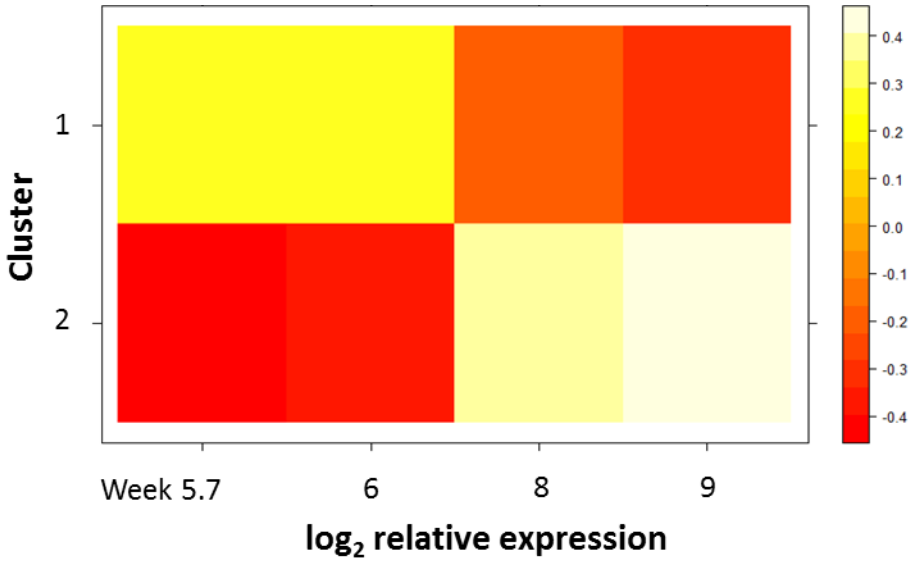

Figure 4.3. K-means clustering analysis for *in vitro* hNPCs and *in vivo* human neocortex. A total of 3 clusters was identified in our *in vitro* hNPC culture system while *in vivo* human neocortex samples illustrated 2 clusters when evaluated $\log_2$ relative expression to the mean gene expression across all time points for each gene. For this analysis, a criterion of FDR < 0.01 was applied to each of *in vitro* and *in vivo* dataset.

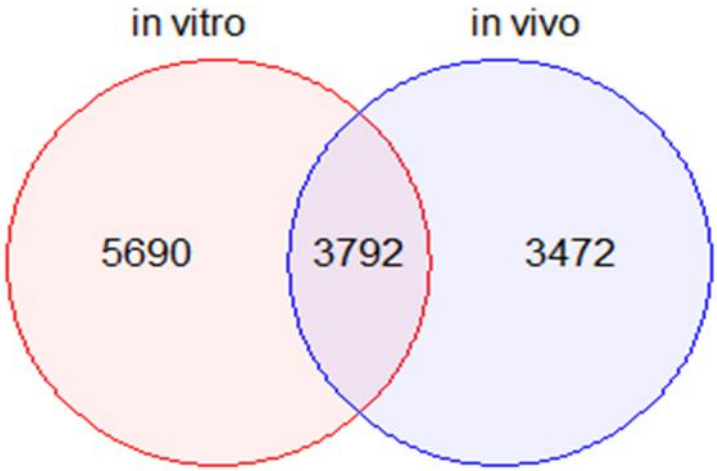

Figure 4.4. Van diagram of commonly or uniquely changed GO process terms. The number of genes that significantly changed its expression over time in both *in vitro* and *in vivo* was 2792 while 9482 and 7262 genes significantly changed its expression over time uniquely *in vitro* and *in vivo*, respectively.

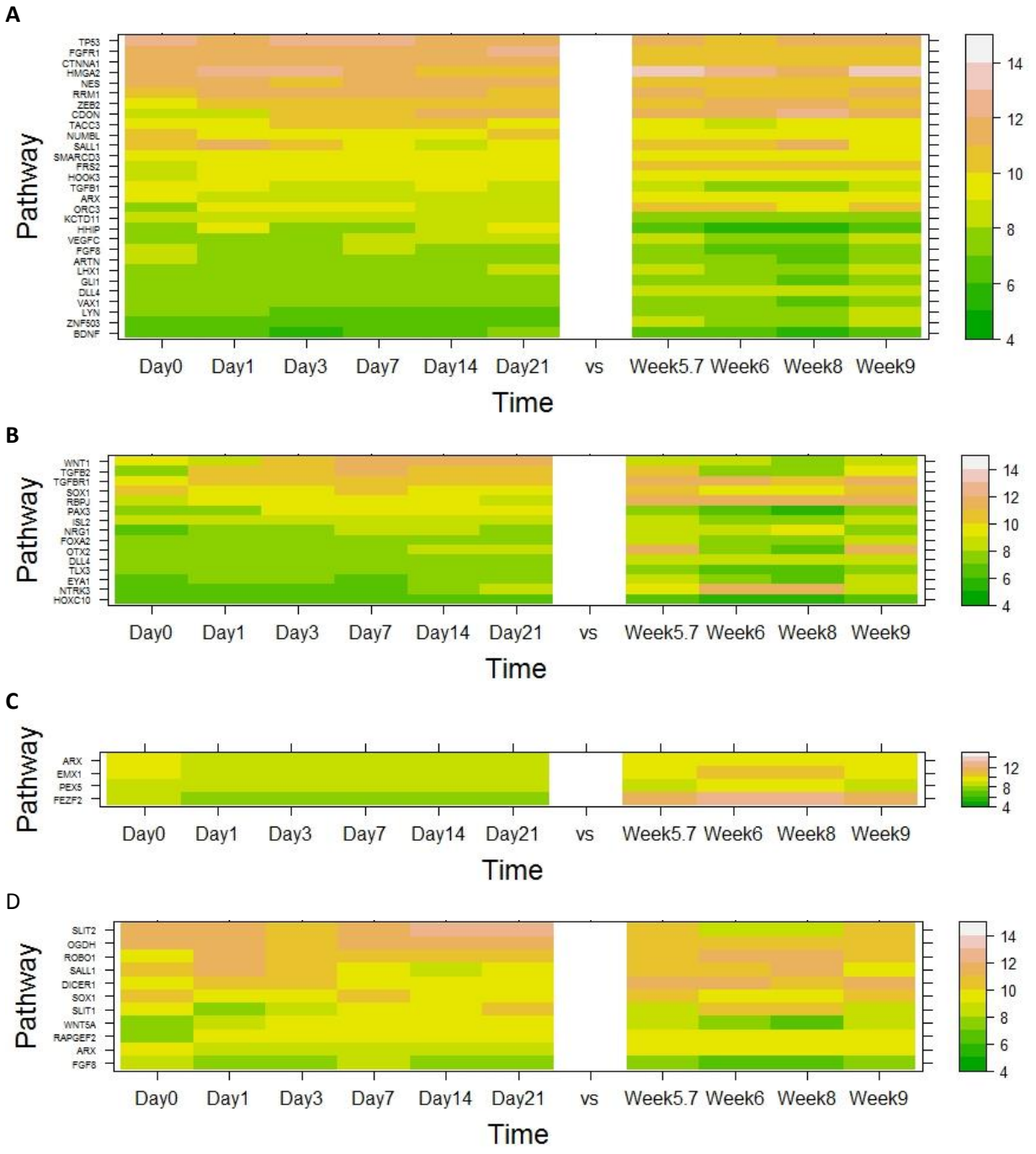

Figure 4.5. Example heatmaps comparing *in vitro* vs. *in vivo* gene expressions for genes involved in proliferation, differentiation, and fate commitment. *In vitro* and *in vivo* gene expressions for (A) hNPC proliferation, (B) neuronal fate commitment, (C) cortical neuron differentiation, and (D) forebrain neuron differentiation. Similarities and differences in gene expression patterns over time between *in vitro* and *in vivo* were observed. Left and right panels represent *in vitro* and *in vivo* data, respectively. The x-axis is time, and the y-axis is genes associated with a specific pathway of interest.

A

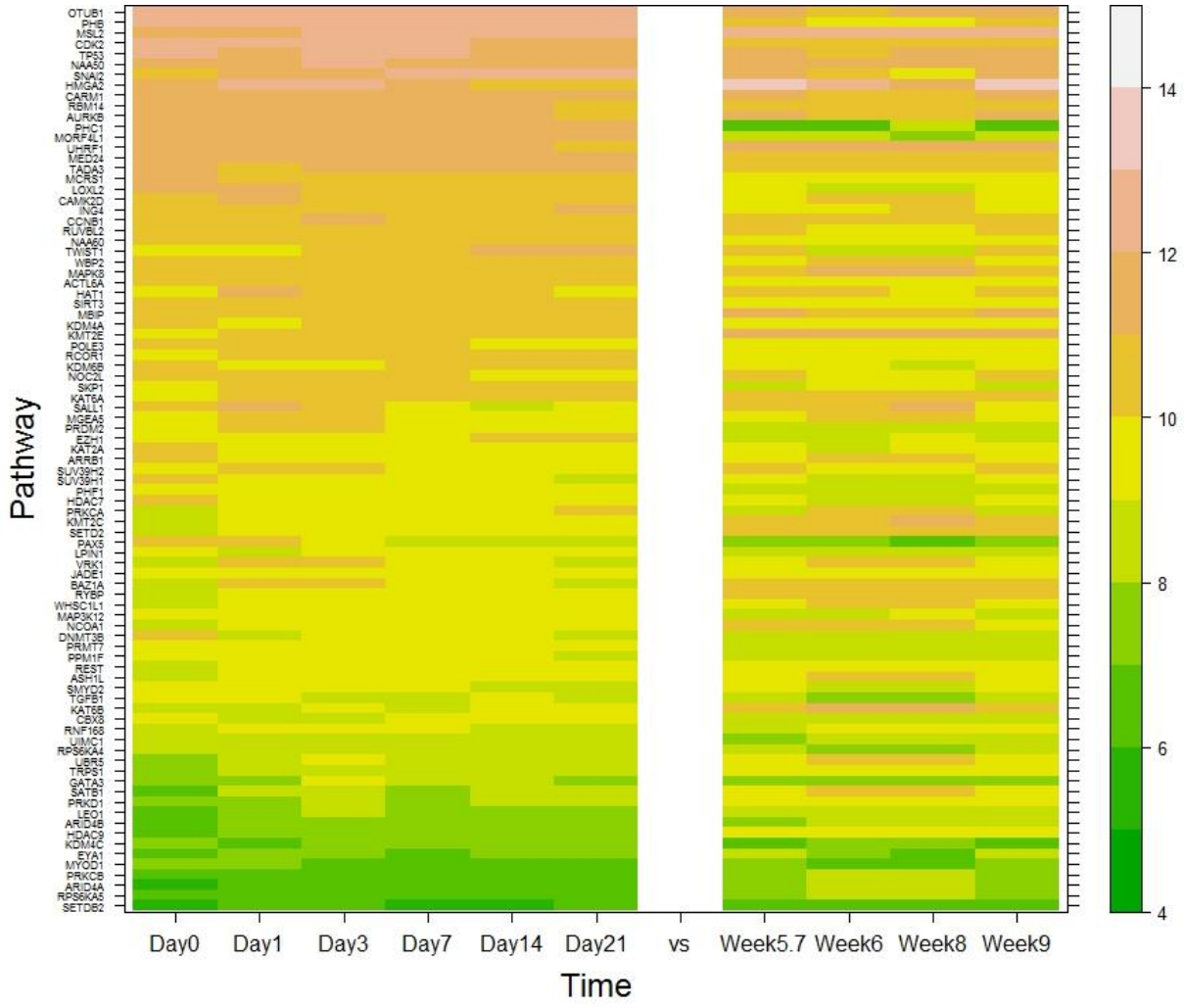
Pathway
OTUB1
PHB
MSL2
CDK2
TP53
NAA50
SNAI2
HMGA2
CARM1
RBM14
AURKB
PHC1
MORF4L1
UHRF1
MED24
TADA3
MCRS1
LOXL2
CAMK2D
ING4
CCNB1
RUVBL2
NAA60
TWIST1
WBP2
MAPK8
ACTL6A
HAT1
SIRT3
MBIP
KDM4A
KMT2E
POLE3
RCOR1
KDM6B
NOC2L
SKP1
KAT6A
SALL1
MGEA5
PRDM2
EZH1
KAT2A
ARRB1
SUV39H2
SUV39H1
PHF1
HDAC7
PRKCA
KMT2C
SETD2
PAX5
LPIN1
VRK1
JADE1
BAZ1A
RYBP
WHSC1L1
MAP3K12
NCOA1
DNMT3B
PRMT7
PPM1F
REST
ASH1L
SMYD2
TGFB1
KAT6B
CBX8
RNF168
UIMC1
RPS6KA4
LIN54
TRPS1
GATA3
SATB1
PRKD1
LEO1
ARID4B
HDAC9
KDM4C
EYA1
MYOD1
PRKCB
ARID4A
RPS6KA5
SETDB2
Day0
Day1
Day3
Day7
Day14
Day21
vs
Week5.7
Week6
Week8
Week9
Time
14
12
10
8
6
4

B

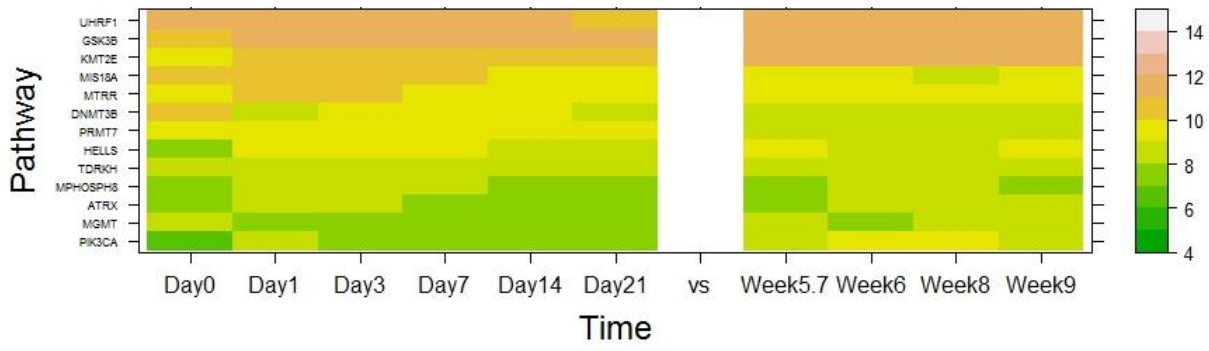
Pathway
UHRF1
GSK3B
KMT2E
MIS18A
MTRR
DNMT3B
PRMT7
HELLS
TDRKH
MPHOSPH8
ATRX
MGMT
PIK3CA
Day0
Day1
Day3
Day7
Day14
Day21
vs
Week5.7
Week6
Week8
Week9
Time
14
12
10
8
6
4

C

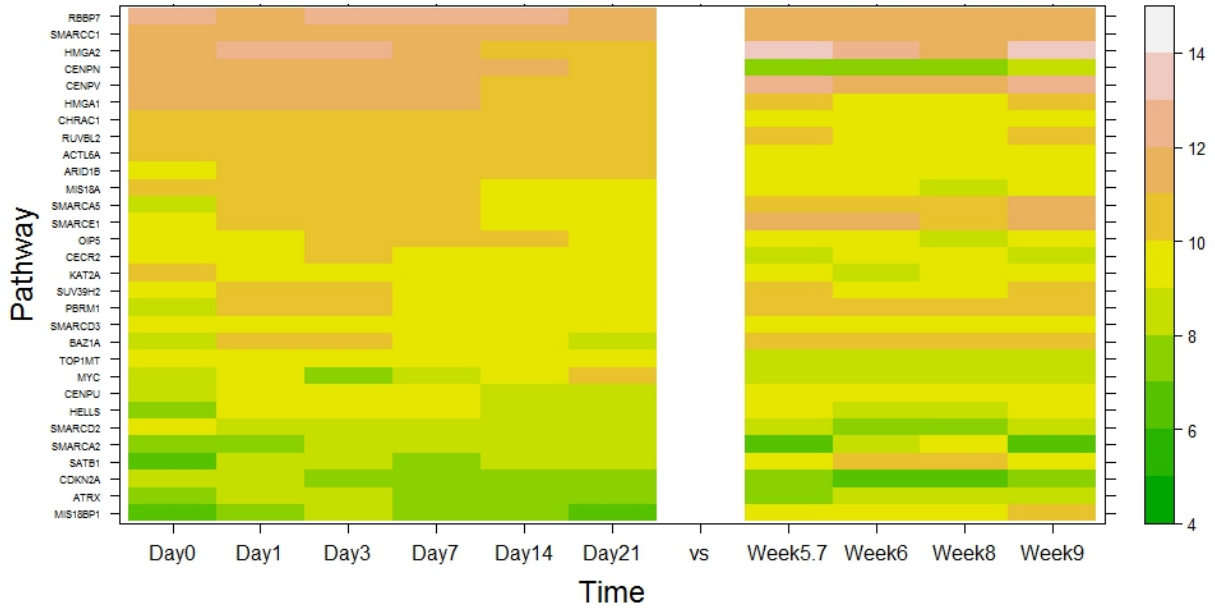

Figure 4.6. Heatmaps comparing *in vitro* vs. *in vivo* expressions of genes associated with epigenetic changes. Similar and different *in vitro* and *in vivo* gene expressions over time were illustrated for (A) histone modification, (B) DNA methylation, and (C) chromatin remodeling. The left panel represents *in vitro* and the right panel represents *in vivo* data. The x-axis is time, and the y-axis is genes associated with a specific pathway of interest.

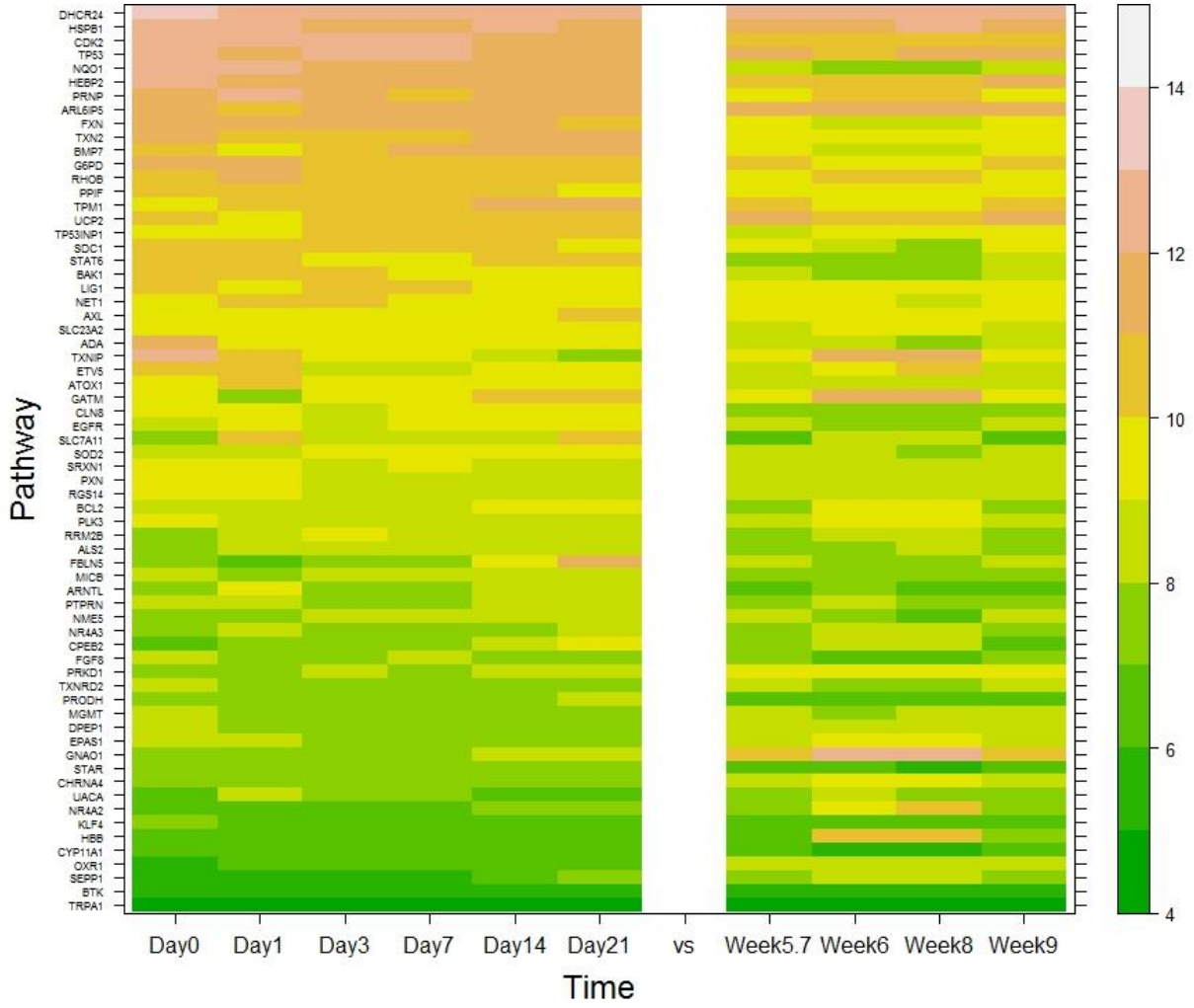

Figure 4.7. Heatmaps comparing *in vitro* vs. *in vivo* gene expressions for genes involved in oxidative stress. Similar and different gene expression patterns over time between *in vitro* and *in vivo* were demonstrated for oxidative stress. Left and right heatmaps represent *in vitro* and *in vivo* data, respectively. The x-axis is time, and the y-axis is genes associated with a specific pathway of interest.

CHAPTER 4 REFERENCES

Ankley, G. T., Bennett, R. S., Erickson, R. J. et al. (2010). Adverse outcome pathways: a conceptual framework to support ecotoxicology research and risk assessment. *Environ Toxicol Chem 29*, 730-741. http://dx.doi.org/10.1002/etc.34

Aschner, M., Crofton, K. M. and Levin, E. D. (2010). Introduction to the special issue on emerging high throughput and complementary model screens for neurotoxicology. *Neurotoxicol Teratol 32*, 1-3. http://dx.doi.org/10.1016/j.ntt.2009.08.006

Bailey, J., Knight, A. and Balcombe, J. (2005). The future of teratology research is in vitro. *Biogenic Amines 19*, 97-145.

Bal-Price, A. and Meek, M. E. (2017). Adverse outcome pathways: Application to enhance mechanistic understanding of neurotoxicity. *Pharmacol Ther* http://dx.doi.org/10.1016/j.pharmthera.2017.05.006

Bal-Price, A. K., Hogberg, H. T., Buzanska, L. et al. (2010). In vitro developmental neurotoxicity (DNT) testing: relevant models and endpoints. *Neurotoxicology 31*, 545-554. http://dx.doi.org/10.1016/j.neuro.2009.11.006

Bal-Price, A. K., Coecke, S., Costa, L. et al. (2012). Advancing the science of developmental neurotoxicity (DNT): testing for better safety evaluation. *ALTEX 29*, 202-215.

Barry, C., Schmitz, M. T., Jiang, P. et al. (2017). Species-specific developmental timing is maintained by pluripotent stem cells ex utero. *Dev Biol 423*, 101-110. http://dx.doi.org/10.1016/j.ydbio.2017.02.002

Buzanska, L., Zychowicz, M., Ruiz, A. et al. (2010). Neural stem cells from human cord blood on bioengineered surfaces--novel approach to multiparameter bio-tests. *Toxicology 270*, 35-42. http://dx.doi.org/10.1016/j.tox.2009.06.005

Carvalho, B. S. and Irizarry, R. A. (2010). A framework for oligonucleotide microarray preprocessing. *Bioinformatics 26*, 2363-2367. http://dx.doi.org/10.1093/bioinformatics/btq431

Carvalho, B. S. (2015). pd.hugene.1.0.st.v1: Platform Design Info for Affymetrix HuGene-1_0-st-v1. *R package version 3.14.1*

Charrad, M., Ghazzali, N., Boiteau, V. et al. (2014). NbClust: An R Package for Determining the Relevant Number of Clusters in a Data Set. *Journal of statistical software 61*, 1-36.

Coecke, S., Goldberg, A. M., Allen, S. et al. (2007). Workgroup report: incorporating in vitro alternative methods for developmental neurotoxicity into international hazard and risk assessment strategies. *Environ Health Perspect 115*, 924-931. http://dx.doi.org/10.1289/ehp.9427

Crofton, K., Fritsche, E., Ylikomi, T. et al. (2014). International STakeholder NETwork (ISTNET) for creating a developmental neurotoxicity testing (DNT) roadmap for regulatory purposes. *ALTEX 31*, 223-224. http://dx.doi.org/http://dx.doi.org/10.14573/altex.1402121

Crofton, K. M., Mundy, W. R., Lein, P. J. et al. (2011). Developmental neurotoxicity testing: recommendations for developing alternative methods for the screening and prioritization of chemicals. *ALTEX 28*, 9-15.

Crofton, K. M., Mundy, W. R. and Shafer, T. J. (2012). Developmental neurotoxicity testing: a path forward. *Congenit Anom (Kyoto) 52*, 140-146. http://dx.doi.org/10.1111/j.1741-4520.2012.00377.x

de Sanctis, L., Memo, L., Pichini, S. et al. (2011). Fetal alcohol syndrome: new perspectives for an ancient and underestimated problem. *J Matern Fetal Neonatal Med 24 Suppl 1*, 34-37. http://dx.doi.org/10.3109/14767058.2011.607576

EPA (2015). Use of High Throughput Assays and Computational Tools; Endocrine Disruptor Screening Program; Notice of Availability and Opportunity for Comment.

Faustman, E. M., Silbernagel, S. M., Fenske, R. A. et al. (2000). Mechanisms underlying Children's susceptibility to environmental toxicants. *Environ Health Perspect 108 Suppl 1*, 13-21.

Fritsche, E., Gassmann, K. and Schreiber, T. (2011). Neurospheres as a model for developmental neurotoxicity testing. *Methods Mol Biol 758*, 99-114. http://dx.doi.org/10.1007/978-1-61779-170-3_7

Gaspard, N. and Vanderhaeghen, P. (2010). Mechanisms of neural specification from embryonic stem cells. *Curr Opin Neurobiol 20*, 37-43. http://dx.doi.org/10.1016/j.conb.2009.12.001

Gautier, L., Cope, L., Bolstad, B. M. et al. (2004). affy—analysis of Affymetrix GeneChip data at the probe level. *Bioinformatics 20*, 307-315.

Gentleman, R. (2017). annotate: Annotation for microarrays. *R package version 1.54.0.*

Grandjean, P. and Landrigan, P. J. (2006). Developmental neurotoxicity of industrial chemicals. *Lancet 368*, 2167-2178. http://dx.doi.org/10.1016/S0140-6736(06)69665-7

Grandjean, P. and Herz, K. T. (2011). Methylmercury and brain development: imprecision and underestimation of developmental neurotoxicity in humans. *Mt Sinai J Med 78*, 107-118. http://dx.doi.org/10.1002/msj.20228

Grandjean, P. and Landrigan, P. J. (2014). Neurobehavioural effects of developmental toxicity. *Lancet Neurol 13*, 330-338. http://dx.doi.org/10.1016/S1474-4422(13)70278-3

Hansen, J. M. (2006). Oxidative stress as a mechanism of teratogenesis. *Birth Defects Res C Embryo Today 78*, 293-307. http://dx.doi.org/10.1002/bdrc.20085

Harrill, J. A., Freudenrich, T. M., Machacek, D. W. et al. (2010). Quantitative assessment of neurite outgrowth in human embryonic stem cell-derived hN2 cells using automated high-content image analysis. *Neurotoxicology 31*, 277-290. http://dx.doi.org/10.1016/j.neuro.2010.02.003

Hitchler, M. J. and Domann, F. E. (2007). An epigenetic perspective on the free radical theory of development. *Free Radic Biol Med 43*, 1023-1036. http://dx.doi.org/10.1016/j.freeradbiomed.2007.06.027

Judson, R., Richard, A., Dix, D. J. et al. (2009). The toxicity data landscape for environmental chemicals. *Environ Health Perspect 117*, 685-695. http://dx.doi.org/10.1289/ehp.0800168

Kang, H. J., Kawasawa, Y. I., Cheng, F. et al. (2011). Spatio-temporal transcriptome of the human brain. *Nature 478*, 483-489. http://dx.doi.org/10.1038/nature10523

Krewski, D., Acosta, D., Jr., Andersen, M. et al. (2010). Toxicity testing in the 21st century: a vision and a strategy. *J Toxicol Environ Health B Crit Rev 13*, 51-138. http://dx.doi.org/10.1080/10937404.2010.483176

Landrigan, P. J. (2010). What causes autism? Exploring the environmental contribution. *Current opinion in pediatrics 22*, 219-225. http://dx.doi.org/10.1097/MOP.0b013e328336eb9a

Lein, P., Locke, P. and Goldberg, A. (2007). Meeting report: alternatives for developmental neurotoxicity testing. *Environ Health Perspect 115*, 764-768. http://dx.doi.org/10.1289/ehp.9841

MacDonald, J. W. (2008). affycoretools: Functions useful for those doing repetitive analyses with Affymetrix GeneChips. *R package version 1.42.0.*

Money, K. M. and Stanwood, G. D. (2013). Developmental origins of brain disorders: roles for dopamine. *Front Cell Neurosci 7*, 260. http://dx.doi.org/10.3389/fncel.2013.00260

MuhChyi, C., Juliandi, B., Matsuda, T. et al. (2013). Epigenetic regulation of neural stem cell fate during corticogenesis. *Int J Dev Neurosci 31*, 424-433. http://dx.doi.org/10.1016/j.ijdevneu.2013.02.006

NRC (2000). In (eds.), *Scientific Frontiers in Developmental Toxicology and Risk Assessment*. Washington (DC): http://www.ncbi.nlm.nih.gov/pubmed/25077274

NRC (2007). *Toxicity Testing in the 21st Century: A Vision and a Strategy*. Vol. The National Academies Press. http://www.nap.edu/openbook.php?record_id=11970

Park, J. J., Weldon, B. A., Park, J. H. et al. (2017). Characterization of *in vitro* organotypic 3D embryonic mouse midbrain micromass cultures using C57BL/6 and A/J mice. *ALTEX* ***In submission***

Pereira, J. D., Sansom, S. N., Smith, J. et al. (2010). Ezh2, the histone methyltransferase of PRC2, regulates the balance between self-renewal and differentiation in the cerebral cortex. *Proc Natl Acad Sci U S A 107*, 15957-15962. http://dx.doi.org/10.1073/pnas.1002530107

Piersma, A. H. (2004). Validation of alternative methods for developmental toxicity testing. *Toxicol Lett 149*, 147-153. http://dx.doi.org/10.1016/j.toxlet.2003.12.029

Pratten, M., Ahir, B. K., Smith-Hurst, H. et al. (2012). Primary cell and micromass culture in assessing developmental toxicity. *Methods Mol Biol 889*, 115-146. http://dx.doi.org/10.1007/978-1-61779-867-2_9

Rice, D. and Barone, S. (2000a). Critical periods of vulnerability for the developing nervous system: Evidence from humans and animal models. *Environmental Health Perspectives 108*, 511-533. http://dx.doi.org/Doi 10.2307/3454543

Rice, D. and Barone, S., Jr. (2000b). Critical periods of vulnerability for the developing nervous system: evidence from humans and animal models. *Environ Health Perspect 108 Suppl 3*, 511-533.

Ritchie, M. E., Phipson, B., Wu, D. et al. (2015). limma powers differential expression analyses for RNA-sequencing and microarray studies. *Nucleic Acids Res 43*, e47. http://dx.doi.org/10.1093/nar/gkv007

Rodier, P. M. (1995a). Developing brain as a target of toxicity. *Environ Health Perspect 103 Suppl 6*, 73-76.

Rodier, P. M. (1995b). Developing Brain as a Target of Toxicity. *Environmental Health Perspectives 103*, 73-76. http://dx.doi.org/Doi 10.2307/3432351

Roque, P. J., Guizzetti, M. and Costa, L. G. (2014). Synaptic structure quantification in cultured neurons. *Curr Protoc Toxicol 60*, 12 22 11-12 22 32. http://dx.doi.org/10.1002/0471140856.tx1222s60

Shin, S., Mitalipova, M., Noggle, S. et al. (2006). Long-term proliferation of human embryonic stem cell-derived neuroepithelial cells using defined adherent culture conditions. *Stem Cells 24*, 125-138. http://dx.doi.org/10.1634/stemcells.2004-0150

Smirnova, L., Hogberg, H. T., Leist, M. et al. (2014). Developmental neurotoxicity - challenges in the 21st century and in vitro opportunities. *ALTEX 31*, 129-156. http://dx.doi.org/http://dx.doi.org/10.14573/altex.1403271

The R Core Team (2013). R: A language and environment for statistical computing. *R Foundation for Statistical Computing, Vienna, Austria*

Theunissen, P. T., Robinson, J. F., Pennings, J. L. et al. (2012). Compound-specific effects of diverse neurodevelopmental toxicants on global gene expression in the neural embryonic stem cell test (ESTn). *Toxicology and applied pharmacology 262*, 330-340. http://dx.doi.org/10.1016/j.taap.2012.05.011

Wegner, S. H., Stanaway, I. B., Kim, H. Y. et al. (2014). Anchoring a dynamic *in vitro* model of human neuronal differentiation to key processes of early brain development *in vivo*. Ph.D., University of Washington,

Wells, P. G., McCallum, G. P., Chen, C. S. et al. (2009). Oxidative stress in developmental origins of disease: teratogenesis, neurodevelopmental deficits, and cancer. *Toxicol Sci 108*, 4-18. http://dx.doi.org/10.1093/toxsci/kfn263

Wells, P. G., McCallum, G. P., Lam, K. C. et al. (2010). Oxidative DNA damage and repair in teratogenesis and neurodevelopmental deficits. *Birth Defects Res C Embryo Today 90*, 103-109. http://dx.doi.org/10.1002/bdrc.20177

Young, A., Machacek, D. W., Dhara, S. K. et al. (2011). Ion channels and ionotropic receptors in human embryonic stem cell derived neural progenitors. *Neuroscience 192*, 793-805. http://dx.doi.org/10.1016/j.neuroscience.2011.04.039

Zambon, A. C., Gaj, S., Ho, I. et al. (2012). GO-Elite: a flexible solution for pathway and ontology over-representation. *Bioinformatics 28*, 2209-2210. http://dx.doi.org/10.1093/bioinformatics/bts366

CHAPTER 4 SUPPLEMENTARY TABLES AND FIGURES

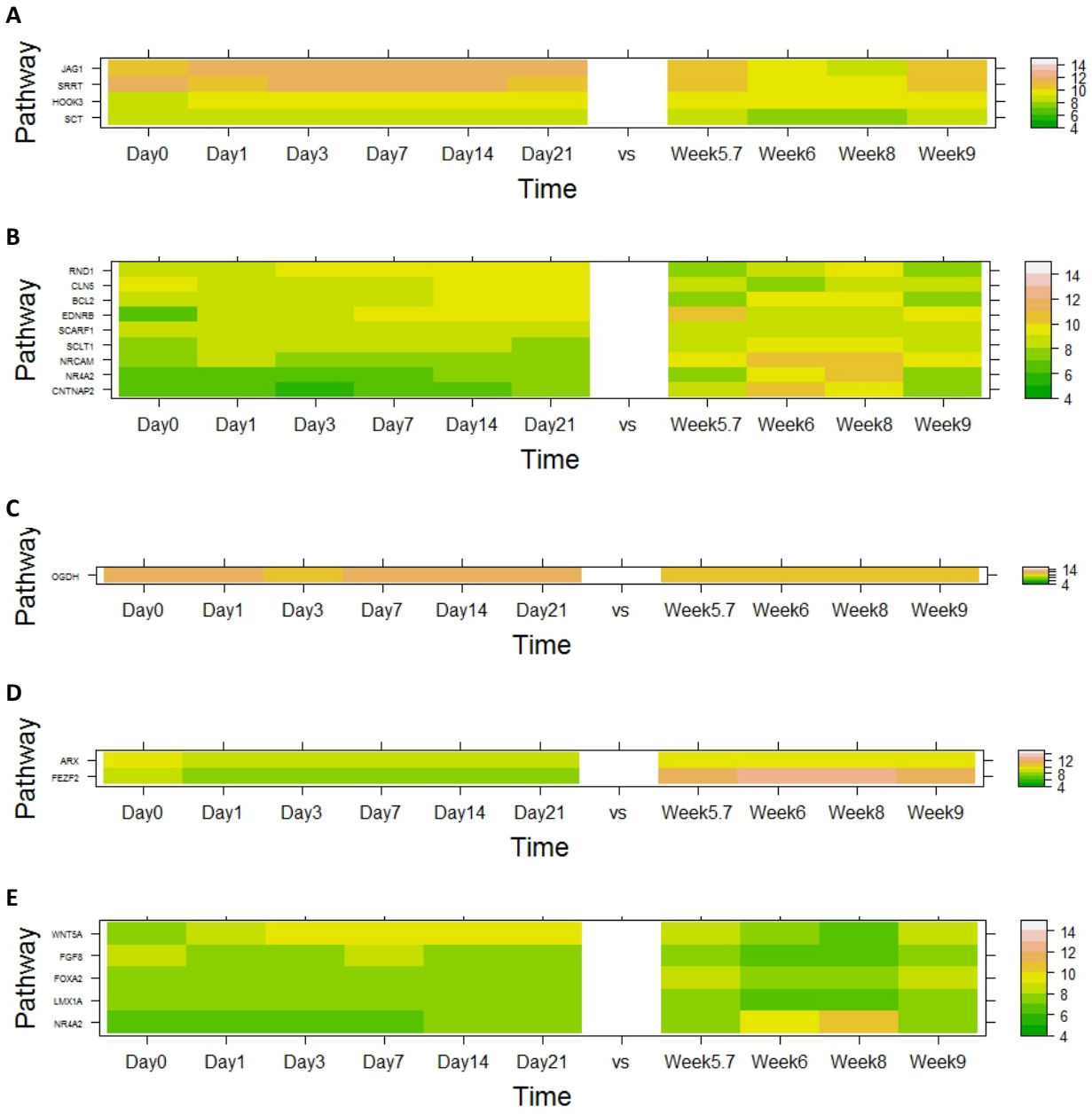

Supplementary Figure 4.1. *In vitro* hNPCs vs. *in vivo* human neocortical brain gene expressions for genes involved with proliferation and differentiation. These include (A) neural stem cell maintenance, (B) neuron maturation, (C) pyramidal neuron differentiation, (D) GABAergic neuron differentiation, and (E) dopaminergic neuron differentiation.

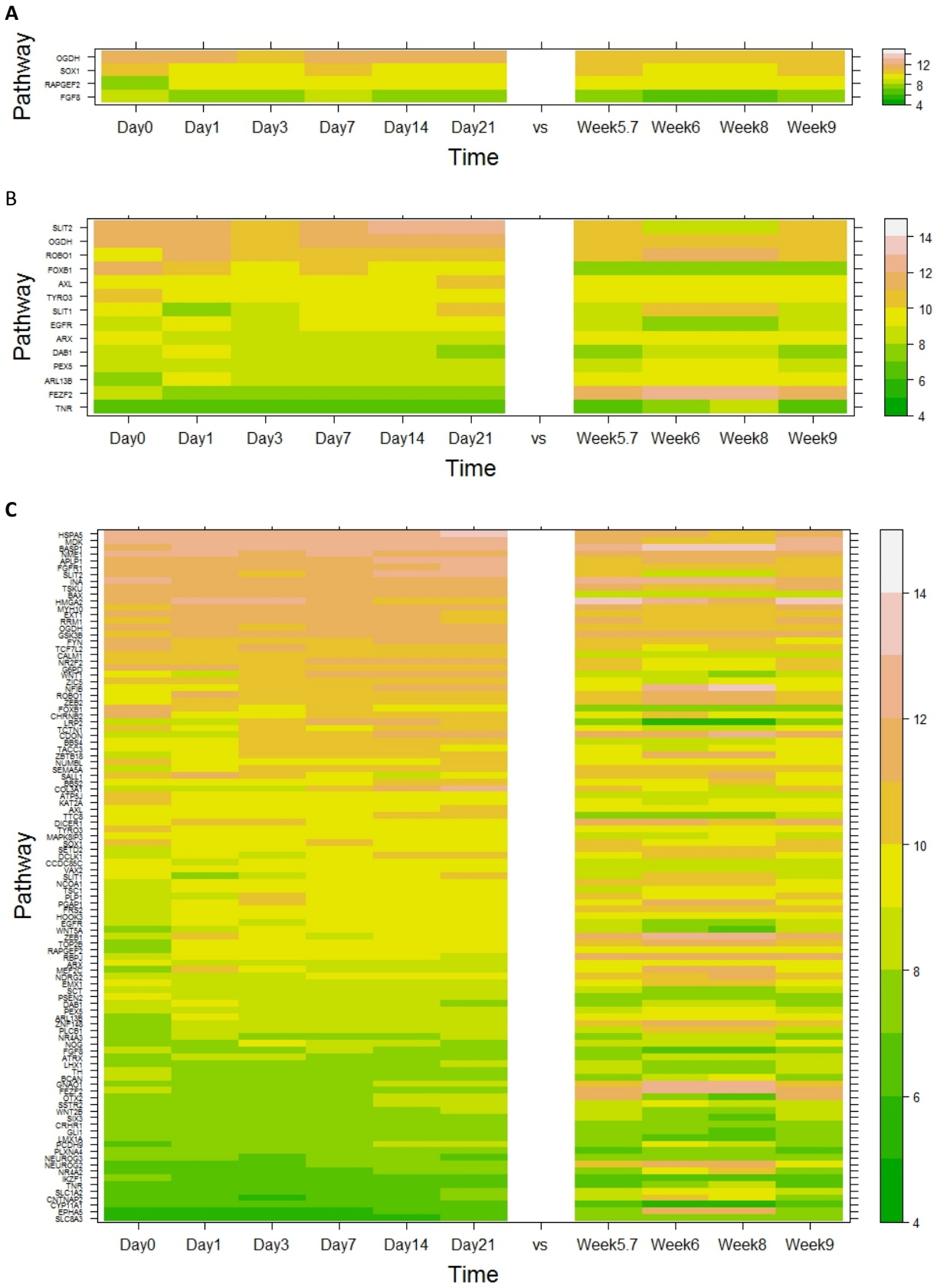
A
Pathway
OGDH
SOX1
RAPGEF2
FGF8
Day0
Day1
Day3
Day7
Day14
Day21
vs
Week5.7
Week6
Week8
Week9
Time
12
8
4
B
Pathway
SLIT2
OGDH
ROBO1
FOXB1
AXL
TYRO3
SLIT1
EGFR
ARX
DAB1
PEX5
ARL13B
FEZF2
TNR
Day0
Day1
Day3
Day7
Day14
Day21
vs
Week5.7
Week6
Week8
Week9
Time
14
12
10
8
6
4
C
Pathway
Day0
Day1
Day3
Day7
Day14
Day21
vs
Week5.7
Week6
Week8
Week9
Time
14
12
10
8
6
4

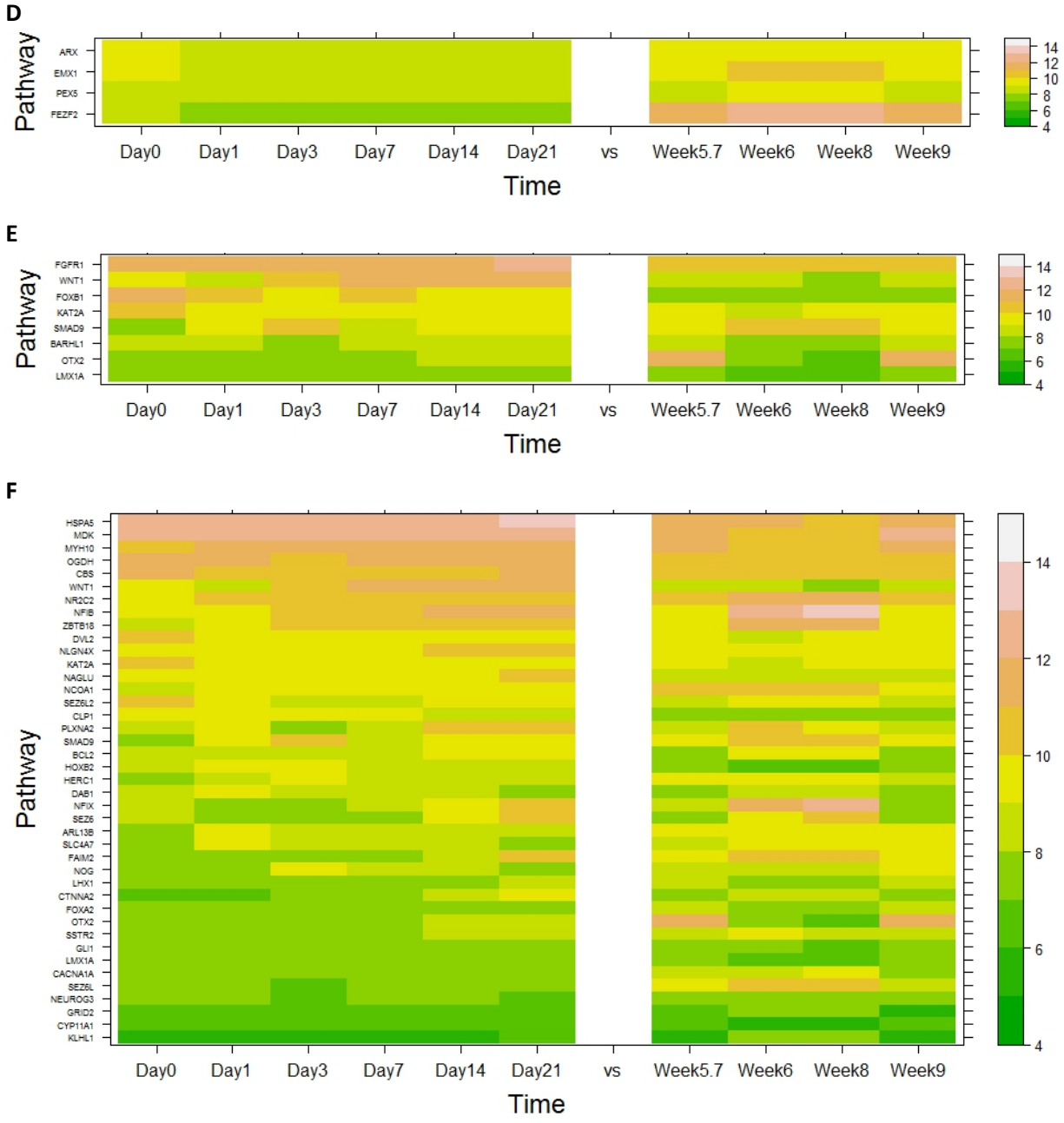

Supplementary Figure 4.2. *In vitro* hNPCs vs. *in vivo* human neocortical brain gene expressions for genes involved with brain regional identity including (A) forebrain neuron development, (B) forebrain cell migration, (C) forebrain development, (D) cortical neuron differentiation, (E) midbrain development, and (F) hindbrain development.

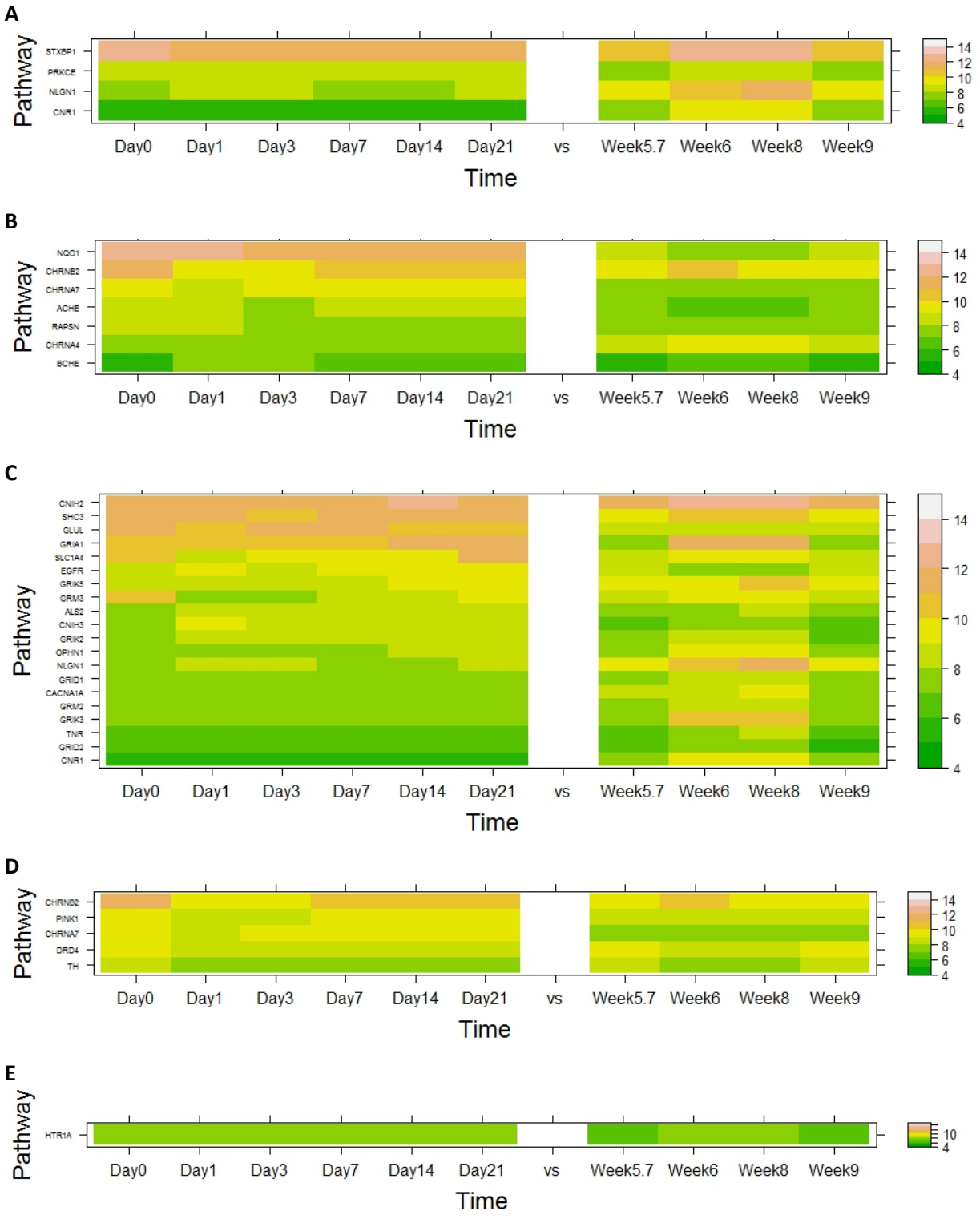

Supplementary Figure 4.3. *In vitro* hNPCs vs. *in vivo* human neocortical brain gene expressions for genes involved with synaptic activity including synaptic transmission of (A) GABA, (B) choline, (C) glutamate, (D) dopamine, and (E) serotonin.

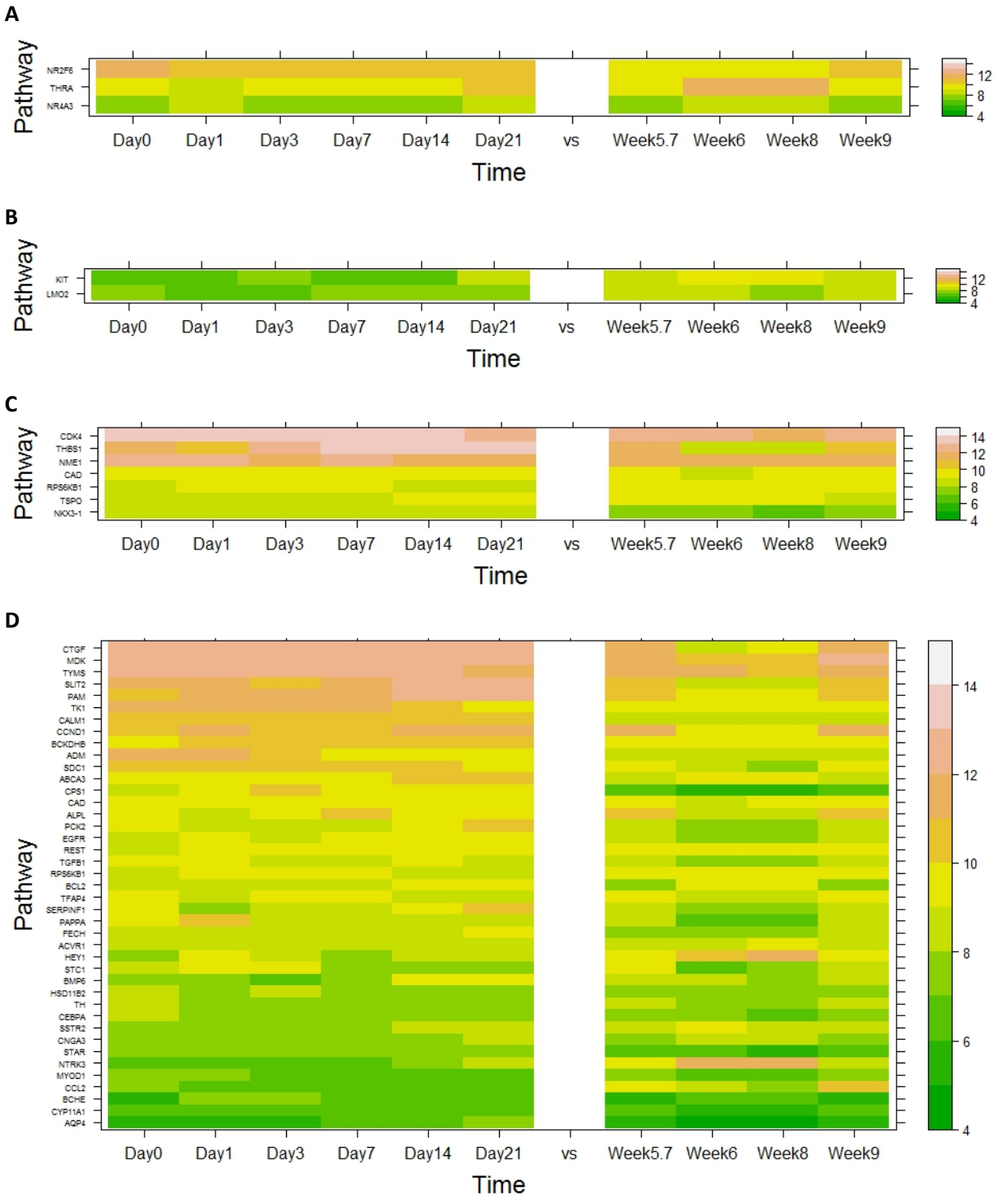

Supplementary Figure 4.4. *In vitro* vs. *in vivo* gene expressions for genes involved in response to hormones including (A) thyroid receptor activity, (B) thyroid, (C) testosterone, and (D) corticosteroid. No genes associated with estrogen responses were significantly changed *in vitro* hNPCs and *in vivo* human neocortex over time.

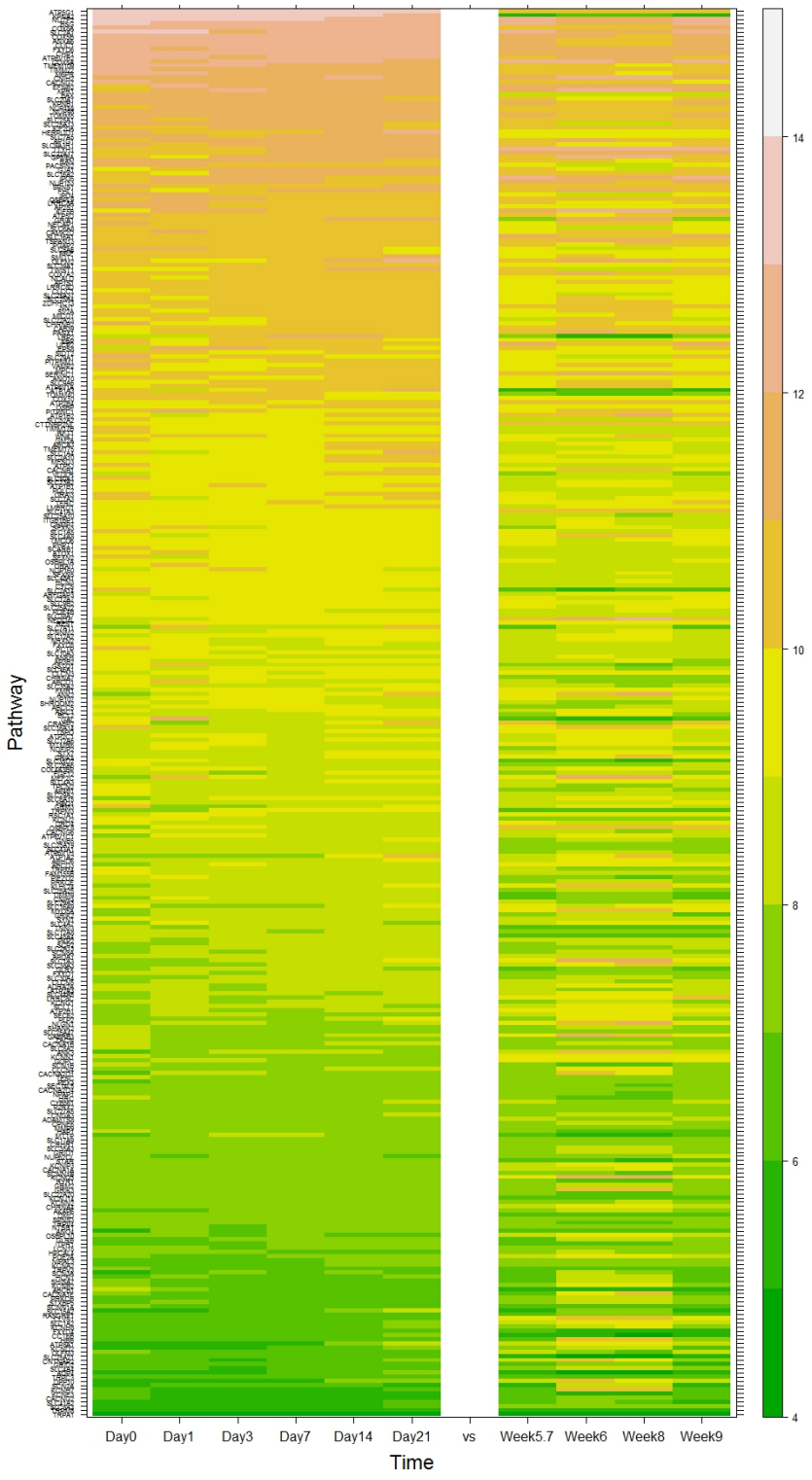

Supplementary Figure 4.5. *In vitro* hNPCs vs. *in vivo* human neocortex gene expressions for genes involved in transporters.

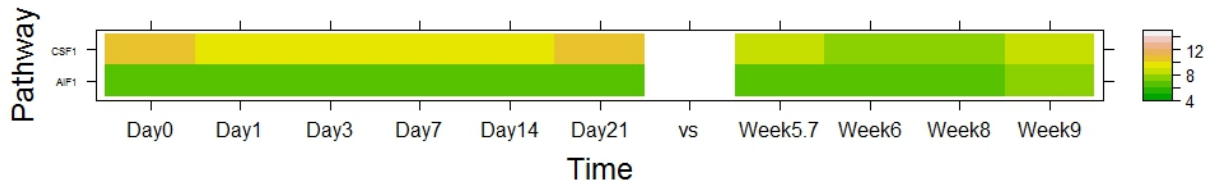

Supplementary Figure 4.6. *In vitro* hNPCs vs. *in vivo* human neocortex gene expressions for genes involved with microglia.

CHAPTER 5: Differential epigenetic effects of chlorpyrifos and arsenic in proliferating and differentiating human neural progenitor cells

Hee Yeon Kim[1, 2†], Susanna H. Wegner[1, 2†], Kirk P. Van Ness[2†], Julie Juyoung Park[1, 2†], Sara E. Pacheco[1†], Tomomi Workman[1], Sungwoo Hong[2], William Griffith[1], Elaine M. Faustman[1, 2*]

[1] Institute for Risk Analysis and Risk Communication, University of Washington, Seattle, WA, USA

[2] Department of Environmental and Occupational Health Sciences, University of Washington, Seattle, WA, USA

† These authors contributed equally to this manuscript

Reproductive Toxicology. 2016 Oct;65:212-23. (Epub 2016 Aug 11.)

* Corresponding author: Elaine M. Faustman

Institute for Risk Analysis and Risk Communication, Department of Environmental and Occupational Health Sciences, University of Washington, Seattle, WA, USA.

Email: faustman@uw.edu

ABSTRACT

Understanding the underlying temporal and mechanistic responses to neurotoxicant exposures during sensitive periods of neuronal development are critical for assessing the impact of these exposures on developmental processes. To investigate the importance of timing of neurotoxicant exposure for perturbation of epigenetic regulation, we exposed human neuronal progenitor cells (hNPCs) to chlorpyrifos (CP) and sodium arsenite (As; positive control) during proliferation and differentiation. CP or As treatment effects on hNPCs morphology, cell viability, and changes in protein expression levels of neural differentiation and cell stress markers, and histone H3 modifications were examined. Cell viability, proliferation/differentiation status, and epigenetic results suggest that hNPCs cultures respond to CP and As treatment with different degrees of sensitivity. Histone modifications, as measured by changes in histone H3 phosphorylation, acetylation and methylation, varied for each toxicant and growth condition, suggesting that differentiation status can influence the epigenetic effects of CP and As exposures.

INTRODUCTION

Neurogenesis is a precisely orchestrated process that occurs in specific structures at specific times during neurodevelopment. It requires temporally and regionally-specific developmental processes that include proliferation, differentiation, synaptogenesis, myelination, and apoptosis (Rice and Barone, 2000; Rodier, 1995). Maintaining the correct timing and regulation of neurogenesis is critical for nervous system development and function, as disruptions in the process can lead to altered function and disease (Gohlke et al., 2008; Hamby et al., 2008; Moreira et al., 2010; Robinson et al., 2011; Faustman et al., 2000; Daston et al., 2004). Chemical exposure during a key "window of susceptibility" can disrupt brain development and cause lifelong functional impairments (Rodier, 1994). For example, epidemiological evidence demonstrates that exposures to developmental neurotoxicants like chlorpyrifos (CP) and arsenic (As) are associated with cognitive effects (Grandjean and Landrigan, 2014). *In utero* exposure to CP in humans is associated with developmental delays in learning, impairments in mental and motor development, and attention problems (Horton et al., 2012; Rauh et al., 2006; Rauh et al., 2012; Eskenazi et al., 2010; Eskenazi et al., 2014; Eskenazi et al., 2007; Eskenazi et al., 2008; Engel et al., 2011). Similarly, prenatal and early postnatal exposures to inorganic arsenic from drinking water are associated with cognitive deficits that are apparent in pre-school children (Grandjean and Landrigan, 2014; Hamadani et al., 2011; Wasserman et al., 2007).

The extent of neurotoxicity during development is highly dependent on the timing of exposure and the differentiation status of the exposed tissues. Actively developing regions of the brain tend to be the most vulnerable to toxicant perturbations (Rice and Barone, 2000). Proliferating and differentiating neural stem cells have been shown to exhibit differential sensitivity to several toxicants, including the phthalate metabolite mono-(2-ethylhexyl) phthalate (Lim et al., 2009), methylmercury (Theunissen et al., 2010) and valproic acid (Debeb et al., 2010). Therefore, it is important to evaluate toxicant impacts on specific neural developmental processes within various stages of differentiation to evaluate life stage susceptibility.

Epigenetic gene regulation via DNA methylation, histone modification, and noncoding RNA-mediated processes plays an important role in directing the differentiation potential and fate specification of neuronal stem cells (Juliandi et al., 2010a; Sanosaka et al., 2009). Specifically, modulation of chromatin structure by histone tail modifications influences the accessibility of genes for transcription and is thought to be a key regulator of neuronal differentiation (Hsieh and Gage, 2004; Juliandi et al., 2010b; Ronan et al., 2013). These regulatory mechanisms are responsive to extracellular signals like cytokines, growth factors,

and environmental cues and epigenetic regulation of gene expression has been shown to be responsive to toxicant exposures such as CP and As (Arai et al., 2011; Cheng et al., 2012; Cronican et al., 2013; Hou et al., 2012; Juliandi et al., 2010a). Toxicant perturbation of chromatin remodeling during neuronal differentiation could mediate neurotoxicity by disrupting normal developmental gene expression patterns. Because chromatin structure changes throughout normal differentiation, toxicant effects on histone modifications are likely to be specific to differentiation state.

hNPCs cultures directed to undergo differentiation provide an opportunity to study early stages of neuronal differentiation processes and have become a valuable tool for neurodevelopmental toxicology (Radio and Mundy, 2008; Shin et al., 2006; Breier et al., 2008). ENStem-A™, a commercially available hNPCs line derived from human embryonic stem cell line WA09 (Thomson et al., 1998), provides a convenient and accessible model of human neuronal differentiation (Shin et al., 2006). Withdrawal of fibroblast growth factor (bFGF2) leads these multipotent hNPCs cells to undergo a dramatic morphological and functional transition to begin differentiation. Additional morphogenic factors can direct differentiation towards specific regional identities and neuronal subtypes (Young et al., 2011).

We used this model to explore differentiation stage-specific effects of CP exposures along with our positive control As exposures on hNPCs viability, histone modifications and protein expression of differentiation and cell stress markers.

METHODS

Human neural progenitor cell (hNPC) culture.

ENStem-A™ hNPCs (ArunA Biomedical, Athens, GA, USA) were expanded through passage eight and plated for experiments after reaching 90-100% confluence. Cells were counted by hemocytometer and seeded at 200,000 cells/mL in poly-L-ornithine (20 µg/mL) and laminin (5 µg/mL) double coated tissue culture treated polystyrene 35 x 10 mm dishes (2 mL) or 96-well black bottom microplates (100 µL) (Becton, Dickinson Co., Franklin Lakes, NJ, USA). Cells were cultured in neural proliferation media (EMD Millipore, Billerica, MA, USA) in a humidifying 37°C, 5% CO_2 incubator. Chemical treatments were administered at the same time as the initiation of differentiation (24 hours after plating). Media was replaced either with additional proliferation media containing fibroblast growth factor (FGF) or with HyClone differentiation

media without FGF (ThermoFisher Scientific, Waltham, MA, USA). All results are presented from 6 – 8 biological replicates and most biological replicates had triple technical replicates.

Chemical treatment.

Chlorpyrifos (CP; 99.5% purity, ChemService, West Chester, PA, USA) was dissolved in dimethyl sulfoxide (DMSO, Sigma St. Louis, MO, USA) for rapid and complete absorption (Whitney et al., 1995) and the DMSO concentration did not exceed a final volume concentration of 0.1%. The initial CP concentrations tested ranged from 0 – 570 µM (0, 7, 14, 29, 43, 57, 143, 285, and 570 µM) and working concentrations of 0, 14, 29, 57 µM in 0.1% DMSO were used based on Alamar Blue viability results. Sodium arsenite (As^{3+}), a positive control, was dissolved in DNase/RNase-free distilled water (Invitrogen, Waltham, MA, USA). Initial As concentrations in media ranged from 0 – 4 µM (0, 1, 2 and 4 µM) and 1 µM was chosen as the working concentration based on viability results.

Morphology.

All cell culture dishes and plates were monitored with a Nikon inverted microscope equipped with phase-contrast optics (Nikon, Tokyo, Japan) to assess general cellular morphology. Morphological images (not shown) were captured and digitized with a Coolsnap Camera (Roper Scientific, Inc. Duluth, GA, USA).

Alamar blue cell viability/proliferation assay.

After 24 or 72 hours of treatment, concentration-dependent cell viability was measured using the Alamar Blue Assay (Invitrogen, Waltham, MA, USA). Alamar Blue detects changes in the number of functional cells by measuring mitochondrial reductase activity of live cells by reducing non-fluorescent, blue resazurin dye to fluorescent, red resorufin (O'Brien et al., 2000). 10% Alamar Blue (v/v) was added directly in each well 3 hours in advance of the 24 and 72 hour time points and incubated at 37°C in a 5% CO_2 incubator for 3 hours. After incubation, the 96-well plates were read on a plate reader at 570 nm with reference wavelength 630 nm.

Alamar Blue assay results are presented as average percent of controls (total cells) ± 95% confidence interval. Wells containing media without cells were run to measure background fluorescence every time an assay was performed. The blank media fluorescence measurement was subtracted from fluorescence measurements of cells from the same assay. The percentage normalized by controls was calculated by dividing the adjusted fluorescence levels (FL) of tested cells to the adjusted level of control cells.

$$\%\ Cell\ viability = \frac{FL\ treated\ or\ control\ cells - FL\ blank}{FL\ control\ cells\ - FL\ blank} * 100$$

Live, dead, and apoptotic cell staining.

A three-color fluorescence assay was utilized to determine the number of live, dead and apoptotic cells. Non-fluorescent Calcein AM (Invitrogen, Carlsbad, CA, USA) dye permeates into live cells and is hydrolyzed to green fluorescent Calcein by intracellular esterase. Propidium iodide (PI, Invitrogen, Waltham, MA, USA) is not permeable to live cells, and selectively stains nuclei of damaged or dead cells with increased membrane permeability with red fluorescence. Hoechst 33342 was used to stain the total nuclei of both living and dead cells with UV fluorescence. The nuclei of live cells were evenly stained, whereas damaged or dead cells have intense and irregular staining. The live/dead assay was performed as previously described (Yu et al., 2005). A Nikon Labophot-2 (Nikon. Tokyo, Japan) was used to visualize the cells and images were captured and digitalized with a Spot Camera at 200x (Diagnostic Instruments, Sterling Heights, MI). MetaMorph software (Molecular Devices LLC. Sunnyvale, CA) was used to process the digitalized images.

Live/dead cell staining was analyzed quantitatively. The number of Hoechst 33342 stained nuclei were counted manually with the Cell Counting option in the Image J software (National Institute of Health, Maryland, USA). The live cells were Calcein AM positive and PI negative, whereas dead cells were PI positive and Calcein AM negative. Cells were categorized as apoptotic when they either expressed a mixture of Calcein AM and PI, had membrane vesicles and blebs, or Calcein AM was bright and condensed (Figure 5.1).

Total cell counts for each treatment were normalized to 24 hours control to assess concentration response. In addition to determining the effect of CP and As treatment on total cell counts, the proportion of live, dead, and apoptotic cells was determined in proliferating and differentiating conditions. Statistical analysis across doses was done comparing to corresponding control (i.e. 24 hour control data to 24 hour data and 72 hour control data to 72 hour data). The results of quantitative analysis of the live/dead cell staining assay were presented as the average percent relative to controls (total cells).

Western blot analysis of cellular neuronal markers.

hNPCs in both proliferation and differentiation conditions were harvested 72 hours after treatment and lysed in 40 µL cell lysis buffer containing 20 mM Tris-HCl (pH 7.5), 150 mM NaCl, 1 mM Na_2EDTA, 1 mM EGTA, 1% Triton, 2.5 mM sodium pyrophosphate, 1 mM β-glycerophosphate, 1 mM Na_3Vo_4, 1 µg/mL leupeptin (Cell Signaling, Danvers, MA, USA). The cell lysate was repeatedly frozen and thawed three times and insoluble materials were removed by centrifugation (13,000 rpm for 5 minutes at 4°C). Protein concentration was measured using the Bio-Rad protein assay kit (Bio-Rad. Hercules, CA, USA). Protein samples were prepared for western blotting by standardizing protein concentrations across samples (by addition of lysis buffer) and adding NuPage reducing agent and sample buffer (Life Technologies, Waltham, MA, USA). Samples were heated in boiling water for 5 minutes and 10 µg of protein was loaded in each lane of SDS-PAGE gels (Life Technologies, Waltham, MA, USA). Gels were transferred to polyvinylidene fluoride membrane (Millipore, Billerica, MA, USA) using a vertical transfer apparatus. Membranes were rinsed briefly in Tris-buffered saline (TBS, pH 7.6) and non-specific binding of the blotted membrane was blocked with 5% non-fat dried milk in TBS with 0.1% Tween-20 (TBBS) for 1 hour. The blocked membranes were incubated with primary antibody (1:1000 – 1:5000) overnight at 4°C. Following antibody incubation, the membrane was washed three times with TTBS and incubated 2 hours with a secondary antibody. After hybridization with secondary antibodies conjugated to horseradish peroxidase, the immunocomplex was detected with the ECL detection reagent (GE Healthcare, Little Chalfont, United Kingdom) and exposed to X-ray films. Band intensity was quantified by densitometry using Image J software (National Institute of Health, Maryland, USA). Expression intensity for each protein was first normalized to corresponding β -Actin, then to relevant controls. Statistical analysis was performed as described below. The results from the band densitometric quantification were presented as average fold change to concurrent gel controls ± 95% confidence interval.

The primary antibodies used were nestin (Proteintech Group, Chicago, IL, USA), β-tubulin III (Millipore, Billerica, MA, USA), microtubule-associated protein-2 (MAP-2; Proteintech Group, Chicago, IL, USA), p42/44 MAPK (Erk1/2) (Cell Signaling, Danvers, MA, USA), proliferating cell nuclear antigen (PCNA, Millipore, Billerica, MA, USA), SOX-2 (Proteintech Group, Chicago, IL, USA), and caspase 3 (Cell Signaling, Danvers, MA, USA). β-actin (Sigma-Aldrich, St. Louis, MO, USA) was used as a loading control. A description of the neuronal functional markers can be found in Table 5.1.

Western blot analysis for histone modifications.

The methods used for the western blot analysis for analyzing histone modifications were similar to those used above, except for the type of lysis buffer, antibodies, and internal control used. Cells were lysed with 120 µL of 1X SDS buffer (62.5 mM Tris-HCl (pH 6.8 at 25°C), 2% w/v SDS, 10% glycerol, 50 mM DTT, 0.01% w/v bromophenol blue). Primary antibodies (1:1000) that are specific to Histone H3 with epigenetic modifications at particular amino acid sites (DMH3Lys27, AH3Lys9, pAH3Ser10, DMH3Lys4, DMH3Lys9, DMH3Lys36, DMH3Lys79) and to HDAC4, an enzyme responsible for some epigenetic modifications, were examined. An antibody that detects all histone H3 regardless of site-specific modifications (1:1000- 1:3000) was used to normalize the data. All histone-related antibodies were purchased from Cell Signaling Technologies (Danvers, MA, USA).

Results from densitometric quantification of western bands are presented as average fold change to controls ± 95% confidence interval. Each protein was first normalized to corresponding H3, then to corresponding controls. Statistical analysis was performed as described below.

Statistical analysis.

Mixed effect model analysis was used to investigate significance differences between proliferation and differentiation cell culture conditions and dose response with CP or As exposures. Concentration was used as a continuous fixed effect in the analysis. Random effects for the protein markers and histone H3 were gels and experiment preparation dates.

For the neuronal protein and histone H3 marker endpoints, we used a linear mixed effects model of the change from controls, Y,

$$\log(Y(i)) = A + B^{*} X(i) + R(i) + E(i),$$

$$E(i) \sim N(0,s),\ R(i) \sim N(0,r)$$

$$\text{for } I = 1\ldots, i \text{ samples,}$$

where X(i) is the dose of CP or As, A is the intercept and B is the slope for the dose response to CP or As, R(i) is the random effect for gels and preparation date of the i^{th} sample, s is the residual variance after accounting for the fixed effect of dose and the random effects, r is the variance for the random effects.

For Alomar Blue assay, we used a linear model of Y

$$Y(i) = A + B^{*} X + R(i) + E(i),$$

$$E(i) \sim N(0,s), \quad R(i) \sim N(0,r)$$

for I = 1…, i samples.

Statistical analyses were performed using R statistical software (R Core Team, 2016) and the routine "lme4" for mixed effects models (Pinheiro and Bates, 2000; Bates el. Al, 2015).

RESULTS

Cell morphology under proliferation and differentiation conditions.

Phase-contrast microscopy demonstrated changes in morphology of untreated cells through time under proliferation and differentiation conditions. Under both culture conditions, cells become increasingly confluent through time. Under differentiation conditions we observed prominent neurite outgrowths after 24 hours. By 72 hours, cells under differentiation conditions reached full confluence and migrated to form increasingly dense neural networks. This morphology is consistent with what we have observed with our previous *in vitro* rat embryonic neuronal micromass cultures (Whittaker et al., 1993). CP and As treatments induced a concentration-dependent decrease in cell numbers. Morphological changes were also observed at both 24 and 72 hours (data not shown) after the exposure. Fluorescence microscopy images from the live, dead, and apoptotic cell staining assay support these observations and clearly show the changes in morphology in both proliferation and differentiation conditions following toxicant exposure. Under differentiation conditions, exposure to CP (57 µM) or As (1 µM) both resulted in reduced confluence, inhibited neurite outgrowth, and a failure to form clusters.

Cell viability as assessed by the Alamar Blue assay.

Alamar Blue cell viability data suggest that differentiating and proliferating hNPCs cultures respond to treatments with different degrees of sensitivity (Figure 5.2). Concentration-dependent decreases in cell viability of hNPCs are observed in proliferating (p-value < 0.01) cultures with IC_{10} value of 171 µM after 24 hours CP treatment, suggesting that proliferating cells were significantly more sensitive than differentiating cells following 24 hours CP exposure (Supplement Figure S5.1). By 72hours, CP treatment resulted in a significant concentration-dependent decrease in cell viability of hNPCs under both cell culture conditions (p-value < 0.01). hNPCs under differentiating conditions were significantly more sensitive to CP exposure than those in proliferating conditions (p-value < 0.01). When IC_{10} were calculated, IC_{10} in

proliferating hNPCs after 72 hours of CP exposure was 152 µM while that in differentiating hNPCs was 71 µM (Supplement Figure S5.1).

Differential susceptibility of cells in proliferating and differentiating conditions was also observed following As treatments. Concentration-dependent decreases in cell viability were observed under both proliferation and differentiation culture conditions following 24 and 72 hours of exposure to As. After 24 hours of As exposure, proliferating and differentiating hNPCs had IC_{10} of 1.4 µM and 1.0 µM, respectively (Supplement Figure S5.1). When hNPCs were exposed to As for 72 hours, IC_{10} value dropped to 0.5 µM in proliferation and 0.4 µM in differentiation conditions (Supplement Figure S5.1). These results demonstrate that concentration-dependent decreases in viability in response to As were significantly greater in cells under differentiation cell culture conditions at both time points.

Cytotoxicity as assessed by live, dead, and apoptotic cell staining.

Quantitative live/dead cell imaging using Calcein AM (green) and propidium iodide (red) supported our observations regarding differential susceptibility in proliferating and differentiating hNPCs.

CP exposure resulted in significant concentration-dependent decreases in total cell numbers after 24 hours of exposure under both proliferation and differentiation conditions (Figure 5.3; p-value < 0.01 for both). At CP concentrations of 57 – 285 µM, there were decreases in the percentage of live cells with concomitant increases in apoptotic and/or dead cells.

At 72 hours exposure of CP exposure, there was a concentration-dependent loss of cell count under both proliferating and differentiating conditions (Figures 5.3F and 5.3H) with proliferating cells having a greater proportion of dead cells than differentiating cells at 57 µM and above (Figure 5.3E and 5.3G).

Though exposure to As for 24 hours had minimal effect on total cell numbers as assessed by live, dead, and apoptotic cell staining assay in either culture condition (Figure 5.4B and 5.4D), the proportion of live and apoptotic cells were altered under both conditions. This effect was more prominent under proliferating conditions at 24 hours (Figure 5.4A and 5.4C). Exposure to As for 72 hours significantly reduced the total cell number, increased dead and apoptotic cells and decreased live cells in both proliferation (Figure 5.4E and 5.4F) and differentiation (Figure 5.4G) conditions (p-value < 0.01). This effect

was significantly larger at lower concentrations under differentiation conditions (p-value < 0.01) than in proliferating conditions.

Neuronal and developmental stage-specific protein marker expression.

Exposure to CP (0 – 57 μM) and As (1 μM) resulted in concentration-dependent effects on the protein expression of several differentiation stage-specific markers in hNPCs under both proliferating and differentiating conditions at 72 hours (Figure 5.5, Table 5.2, Supplement Figure S5.2 - S5.3). For example, CP exposure resulted in a significant concentration-dependent decrease in the expression of the neuronal marker -tubulin III (p – value < 0.01), the proliferation marker PCNA (p- value < 0.01), and the stem cell marker SOX-2 (p-value < 0.05) in both proliferating and differentiation conditions (Figure 5.5, Table 5.2, Supplement Figure S2) when compared to β-actin. CP exposure in each culture condition had differential effects on expression of p42/44MAPK (Erk1/2), a member of the Ras-Raf-MEK-ERK signal transduction cascade and a mediator of proliferation, differentiation, and stress response processes triggered by extracellular cues. There was a significant concentration-dependent decrease in the expression of p42/44 MAPK (Erk1/2) under proliferation conditions (p-value < 0.01), but no significant effect on cells under differentiating conditions.

Exposure to As also had differential effects on protein expression (Figure 5.5, Table 5.2, Supplement Figure S5.3). There was a significant decrease in SOX-2 expression unique to proliferation conditions (p-value < 0.05). Expression levels of MAP-2, caspase 3 and nestin were not significantly changed at any CP or As concentration in differentiating or proliferating cells.

Histone Modifications.

Exposure to CP (0 – 57 μM) and As (1 μM) differentially changed the relative amounts of several histone modifications in both differentiating and proliferating hNPCs after 72 hours (Figure 5.6, Table 5.3, Supplement Figure S5.4-S5.5). For example, CP induced a significant concentration-dependent increase in pAH3Ser10 in proliferating cells (p-value < 0.01) but not in differentiating cells (Figure 5.6, Table 5.3, Supplement Figure S5.4). Additionally, one of the enzymes responsible for histone modifications, HDAC4, was significantly decreased in a concentration-dependent manner under differentiation conditions (p-value < 0.05) following CP exposure but not under proliferation conditions. CP also induced a significant concentration dependent increase in DMH3Lys4 in both proliferation (p-value < 0.01) and differentiation conditions (p-value < 0.05).

Exposure to As significantly increased the expression of AH3Lys9 in both cell growth conditions (p-value < 0.05). However, DHM3Lys79 was decreased only under proliferation conditions (p-value < 0.05) and pAH3Ser10 was significantly increased (p-value < 0.05) only under differentiation conditions following As exposure (Figure 5.6, Table 5.3, Supplement Figure S5.5). These results suggest that differentiation status modifies the effects of CP and As exposure on histone modifications.

DISCUSSION

Early life exposures to As or CP can redirect neuronal developmental processes like differentiation (Visan et al., 2012; Ivanov and Hei, 2013), neurite outgrowth (Wang et al., 2010; Howard et al., 2005), neuronal subtype fate specification (Jameson et al., 2006), and apoptosis (Slotkin et al., 2007; Lu et al., 2014), and lead to neurological, behavioral and cognitive dysfunctions (Tyler and Allan, 2014). Transcriptional control is, in part, influenced by epigenetic gene regulation which has become an important emerging field for understanding the coordination of gene expression patterns during brain development, learning, and memory (Fagiolini et al., 2009; Juliandi et al., 2010a; Day and Sweatt, 2011; Rudenko and Tsai, 2014; Sanosaka et al., 2009) and is sensitive to perturbation by toxicants (Collotta et al., 2013; Wright and Baccarelli, 2007; Reichard and Puga, 2010). Previous research has demonstrated that differentiating cells have varying degrees of susceptibility to toxicants that is dependent on the stage of differentiation (Debeb et al., 2010; Lim et al., 2009; Theunissen et al., 2010); however, little work has been done to explore differential toxicant effects on epigenetic endpoints at different developmental stages. In the current research, we demonstrate that hNPCs differentiation state influences the type of histone modifications made in response to the toxicant in addition to modifying the effect of CP or As exposure on viability, apoptosis, morphology, and protein expression. These findings underscore the importance of developmental context and timing of exposure in neurodevelopmental toxicity, and further validate this *in vitro* hNPCs model as one capable of reflecting stage-specific developmental endpoints.

We characterized the dose-response of hNPCs to a range of concentrations of CP or As (positive control) under proliferating or differentiating conditions. These two toxicants were chosen as they are well-characterized developmental neurotoxicants with the capability of altering the epigenetic landscape in a variety of cell types (Cheng et al., 2012; Cronican et al., 2013; Hou et al., 2012; Salazar-Arredondo et al., 2008; Shin et al., 2014). Results from the Alamar Blue assay revealed no substantial changes in the abundance of functional cells within the working concentration ranges of CP (0 – 57 μM) after 24 hours.

We focused on concentrations that produced minimal changes in cell viability in the Alamar Blue assay at 24 hours to explore protein expression and histone modifications in this study. Results from the quantitative live/dead and apoptotic cell imaging assay for the same time points and concentrations indicated significant decreases in total cell number for proliferating and differentiating cells exposed to 57 μM CP for 72 hours. There were also concentration-dependent increases in the proportion of apoptotic cells after CP or As exposures. The image analysis results suggest that the proliferation phase had a more significant concentration-dependent increase in percentage of dead cells compared to the differentiation stage after CP exposures while percentages of apoptotic cells were greater in differentiating hNPCs compared to proliferating conditions. For As, the live/dead cell imaging at 72 hours suggests that differentiating cells are more susceptible than proliferating cells based on the results indicated by higher percentages of apoptotic/dead cells and greater reductions in cell numbers with the live, dead, apoptotic cell staining assay.

Protein markers were used to characterize the state of hNPCs differentiation and stress induced by the CP or As exposures. In our previous studies (unpublished), we have shown time dependent changes in markers of proliferation and differentiation where expression of PCNA peaks at day 10 in culture and then decrease while β-tubulin III and MAP-2 expressions increase over 21 days of culture. There were instances where changes in expression levels following treatment occurred for the same proteins in both the proliferation and differentiation conditions; however, the magnitude of this response for some markers was growth condition dependent. For example, CP exposure at 57 μM for 72 hours reduced SOX-2 expression, a transcription factor associated with maintaining cellular pluripotency, in differentiating cells approximately seven-fold more than proliferating cells. Expression levels of SOX-2 were also reduced after 72 hours of exposure to 1 μM As relative to controls but this effect was more pronounced in the proliferation phase than in differentiating cells. β-tubulin III, a component of microtubules found in the cytoskeleton and axons and a marker of differentiated neurons, was significantly reduced relative to controls following exposure to CP under both proliferation and differentiation conditions. These findings of stage-specific changes in protein expression following toxicant exposure are consistent with previous reports that CP exposure results in distinct transcriptional responses in proliferating and differentiating PC12 cells (Slotkin et al., 2007; Slotkin and Seidler, 2012) and that the effects of As on neurite outgrowth in PC12 cells are stage-specific (Frankel et al., 2009). Cell status imaging data suggesting concentration-dependent increases in apoptotic cells with CP and As exposure were not confirmed by concomitant increases of caspase-3, a marker of an activated apoptosis pathway. Indeed, chlorpyrifos (at 29 μM) has

been shown to target the genes that drive the apoptotic pathway and cell cycle in differentiated and undifferentiated PC12 neural cells with a higher number of apoptotic genes changed in differentiated cells and a reduction in cell cycle genes from proliferating cells (Slotkin and Seidler, 2012).

Histone modification profiles varied between proliferating and differentiating cells in response to exposure to either CP or As which have not been previously demonstrated *in vitro*. Our histone modification findings are consistent with our previous observation that CP exposure *in utero* altered the expression of genes associated with chromatin modifications in fetal mouse brains (Moreira et al. 2010). In our hNPC culture system, each toxicant altered the presence of at least one histone modification measured in a differentiation stage-specific manner. Specifically, we found that proliferating hNPCs treated with CP had increased expression of phosphorylated serine 10 in histone H3 (pAH3Ser10) which is functionally linked to apoptosis through PKCδ phosphorylation and Aurora B and VRK1-mediated chromatin condensation during mitosis (Crosio et al. 2002; Kang et al. 2007; Park and Kim 2012).We also found that the enzyme responsible for some of these histone modifications, histone deacetylase 4 (HDAC4), was significantly decreased relative to controls in differentiating but not in proliferating cells exposed to CP. HDAC4 is emerging as an important regulator of brain development (Majdzadeh et al., 2008), plasticity, and learning and memory (Sando et al., 2012).

Methylation of lysine 4 on histone H3 is associated with the activation of gene transcription, in particular, homeotic (HOX) genes which are integral in development and differentiation (Ruthenburg et al., 2007; Eissenberg and Shilatifard, 2010). Both proliferating and differentiating hNPCs exposed to CP had increased, relative to controls, di-methylated lysine 4 in histone H3 (DMH3Lys4), suggesting that CP exposure may affect the transcription of genes involved in neurodevelopment and differentiation.

Epigenetic effects associated with As exposure as measured by DNA methylation and histone methylation, acetylation and phosphorylation have been characterized by *in vivo* and epidemiological studies with a majority of studies reporting global hypomethylation patterns (Ray et al., 2014). Studies that specifically address the epigenetic effects of As exposure to developing neural tissue or in *in vitro* systems are limited. Moderate embryonic As exposure in mice resulted in decreased acetylation at lysine 9 in histone H3 (AH3Lys9) in brain tissue which was ultimately associated with behavioral and cognitive impairment in adult mice (Cronican et al., 2013). Changes in histone modification including acetylation of histone H3 lysine 9 were examined *in vitro* by Pournara et al. (2016), but the study was only done in T-lymphocytes

and kidney HEK293 cells. In our hNPCs model, we observed increased acetylation at this same site, relative to controls, in both proliferating and differentiating cells. AH3Lys9 has been found to decline during the first four days of neural differentiation of human embryonic stem cells (hESC) then levels gradually increase during days 4-8 as it is believed to play a dual role in hESC pluripotency maintenance and neural differentiation and is generally associated with an open chromatin state and increased transcriptional competency (Lee and Mahadevan, 2009; Peterson and Laniel, 2004; Qiao et al., 2015). Similar to proliferating hPNCs exposed to CP, differentiating cells exposed to As had an increase, relative to controls, of pAH3Ser10 that suggests a shift to active gene transcription and apoptosis (Lo et al., 2000; Koch et al., 2007; Park and Kim, 2012). Activation of the apoptosis pathway was confirmed with high proportions of apoptotic cells with cell status imaging but not with concomitant increases in caspase 3.

Global increases of di-methylated lysine 79 on histone H3 (DMH3Lys79) have been associated with genome integrity maintenance during mitosis (Fu et al., 2013; Guppy and McManus, 2015). Proliferating As-exposed hNPCs had decreased DMH3Lys79, relative to controls, suggesting that genomic stability may be becoming compromised. Indeed, gestational exposure to As in mice has been implicated in increased adult cancer risk and it appears that stem cells are targeted during the process (Tokar et al., 2011).

The consistency of histone modification sites targeted by As and CP across *in vivo* and *in vitro* systems demonstrates that our *in vitro* model is capable of reflecting molecular changes associated with functional outcomes *in vivo* during sensitive periods of neurodevelopment. It remains to be seen whether the changes in protein expression are a direct result of the histone modifications we observed. The concept of “developmental origins of adult disease” is a phenomenon that is thought to be, in part, mediated via perturbations of the epigenetic program during development (Skinner, 2007; Barker, 2007). These effects are particularly challenging to study given the long time period between developmental exposures and adult health outcomes. Our ability to detect epigenetic changes in a short-term *in vitro* assay suggests the exciting potential to rapidly screen for toxicants that have the potential to influence health many years after developmental exposures.

We believe our results of epigenetic changes in hNPCs as a result from As and CP exposure during proliferation and differentiation conditions not only contributes to the greater understanding of the epigenetic processes under the influence of environmental exposures, but also demonstrates the capacity of our *in vitro* system as a promising model for neurodevelopmental toxicity screening.

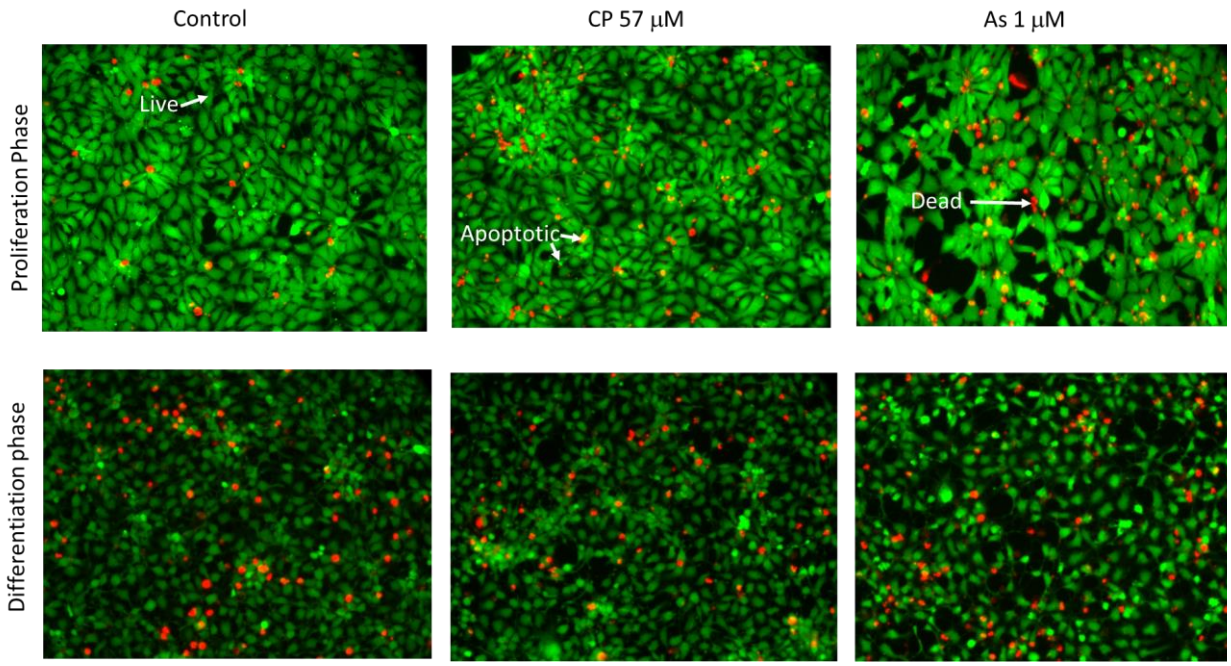

Figure 5.1. Reference staining for live, dead and apoptotic cell quantification. Examples (arrows) of staining for live, apoptotic, and dead cells stained with Calcein AM (green) and propidium iodide (red) used for cell status enumeration. Apoptotic cells tend to have a mixture of green and red and/or are light green with blebs or are brightly condensed green cells. The top row portrays examples of hNPCs at 72 hours under proliferation phase with controls, CP at 57 µM and As at 1 µM. In the row below, control cells under 72 hours of differentiation are shown with CP at 57 µM and As at 1 µM.

Table 5.1. Neuronal functional markers examined for *in vitro* human neural progenitor cells.

Marker	Biological Function	Cells Detected
determining region Y box-2 (SOX-2)	Transcription factor essential for maintaining self-renewal	Embryonic Stem Cells
Nestin	Intermediate filament protein involved in radial axon growth	Neural Progenitor Cells
β-tubulin III	Component of microtubules found in cytoskeleton and axons	Structural Neuron Specific Marker
Microtubule-associated protein 2 (MAP2)	Microtubule associated protein located primary in dendrites	Structural Neuron Specific Marker
p42/44 MAPK (Erk1/2)	Ras-Raf-MEK-ERK signal transduction cascade, stress marker	Ubiquitous
Proliferating Cell Nuclear Antigen (PCNA)	Proliferation	Proliferating Cells
Caspase 3	Role in apoptosis and in natural brain development	Ubiquitous

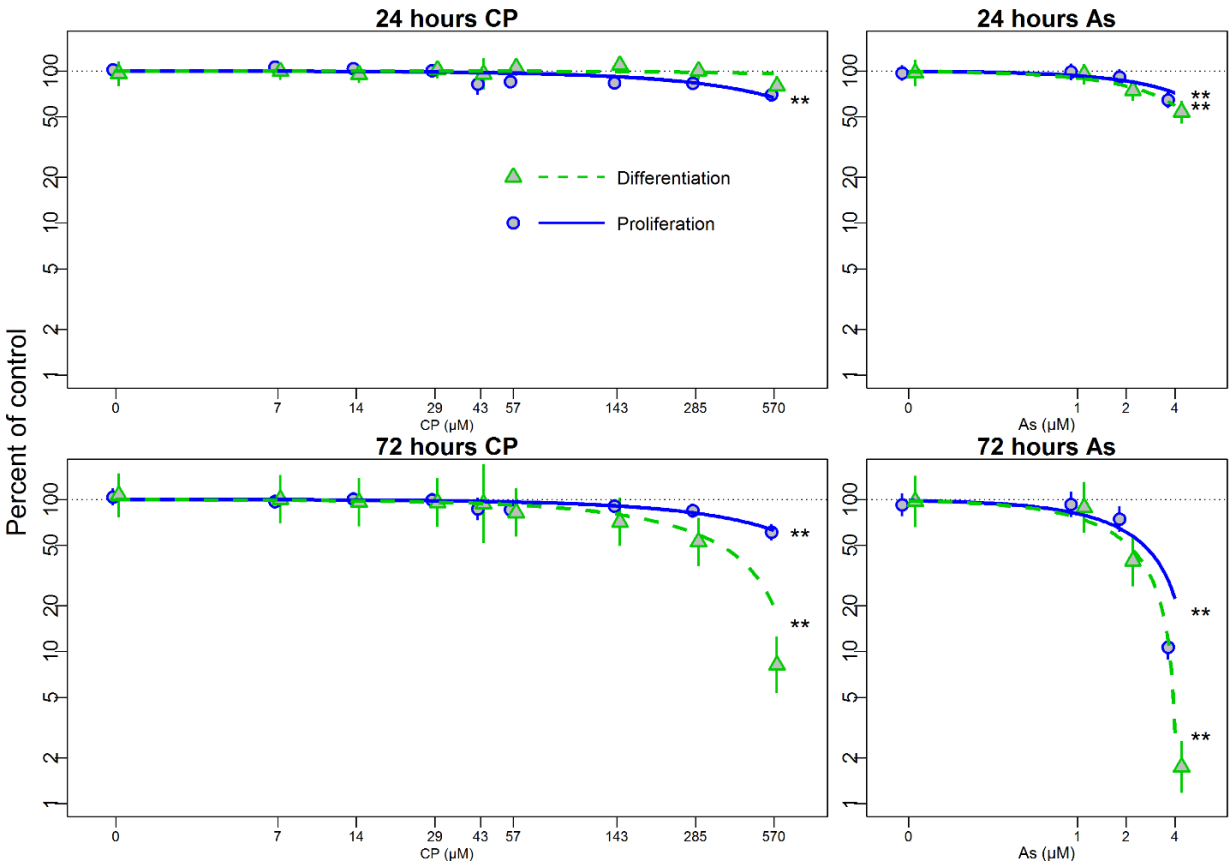

Figure 5.2. Alamar Blue cell viability assay with CP and As under proliferation or differentiation conditions. hNPCs were exposed to chlorpyrifos (CP 0-570 µM) or arsenic (As 0-4 µM) under proliferating (Blue) and differentiating (Green) conditions at 24h and 72h. Plots show means and 95% confidence intervals. Statistical significances, *: p-value < 0.05; **: p-value < 0.01; ***: p-value < 0.001, are based on a linear mixed effect model indicating significant dose response for each condition. In order to better illustrate the comparison of the data to regression line at low dose, we used a log scale for dose and percent of control, which led to curved trend lines.

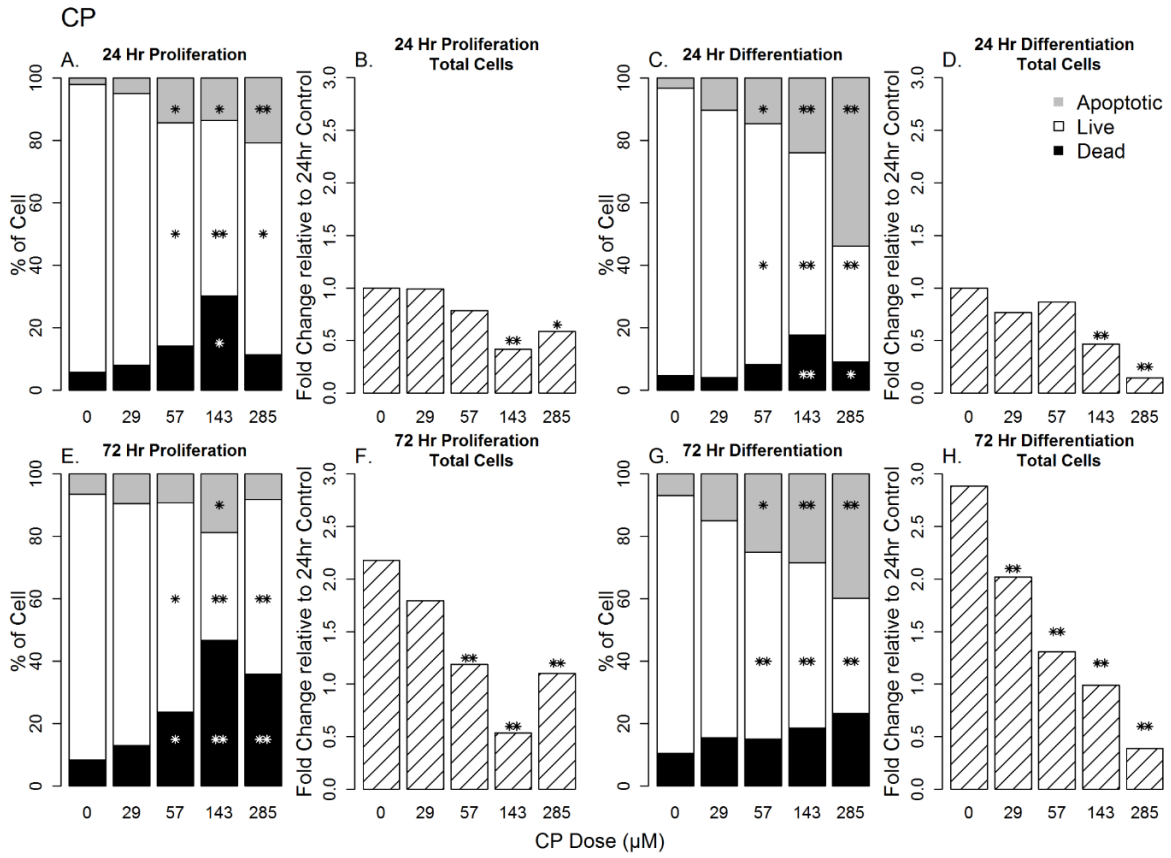

Figure 5.3. Concentration-dependent changes in cell number, cell death, apoptosis, and cell viability in CP-treated hNPCs under proliferation and differentiation conditions. Sections A, C, E and G represent the distribution of live, dead and apoptotic cells while Sections B, D, F and H represents fold changes in cell count relative to 24 h controls. *: p-value < 0.05; **: p-value < 0.01; ***: p-value < 0.001 compared to control.

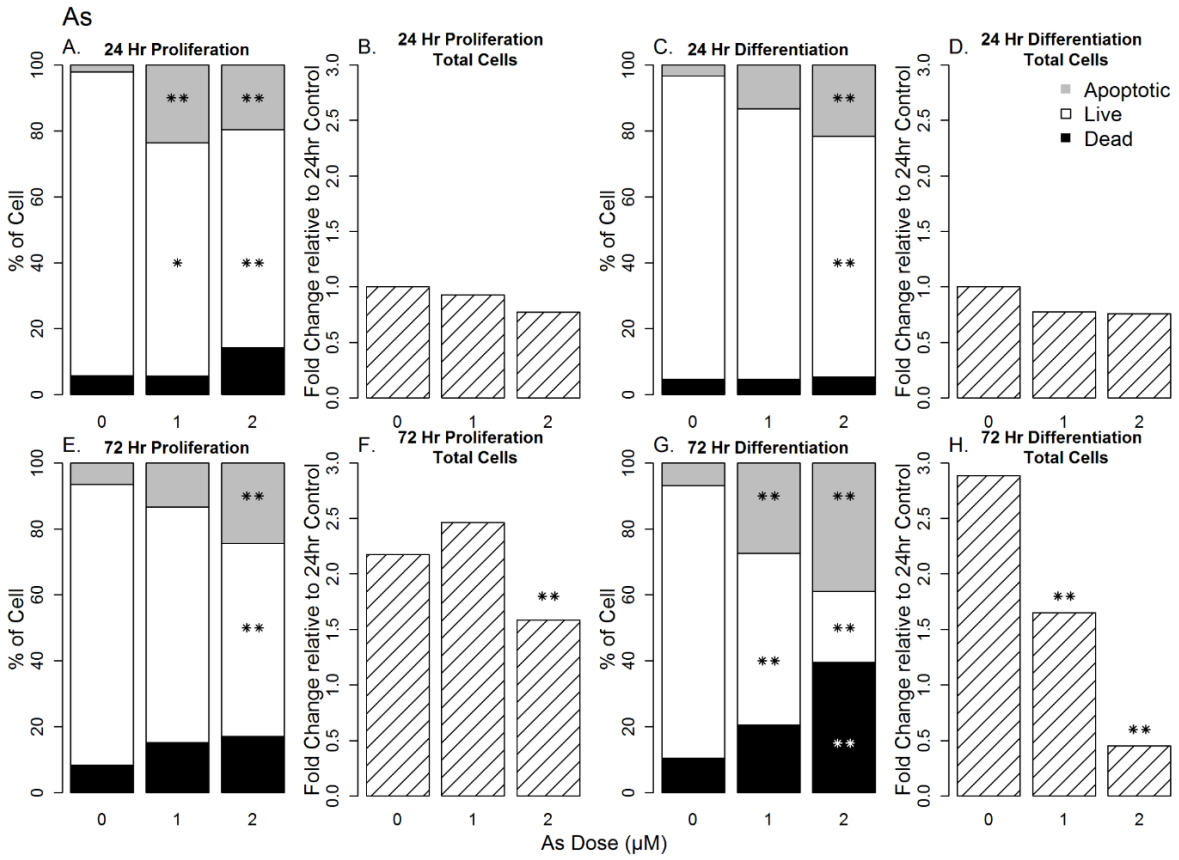

Figure 5.4. Concentration-dependent changes in cell number, cell death, apoptosis, and cell viability in As-treated hNPCs under proliferation and differentiation conditions. Sections A, C, E and G represent the distribution of live, dead and apoptotic cells within a culture at a given dose. Significance of the effect is presented relative to controls at the corresponding time point while Sections B, D, F and H represents changes in cell count relative to controls. Significance of the effect is presented relative to the 24 h controls to show the increase in cell number through time. *: p-value < 0.05; **: p-value < 0.01; ***: p-value < 0.001 compared to relative control.

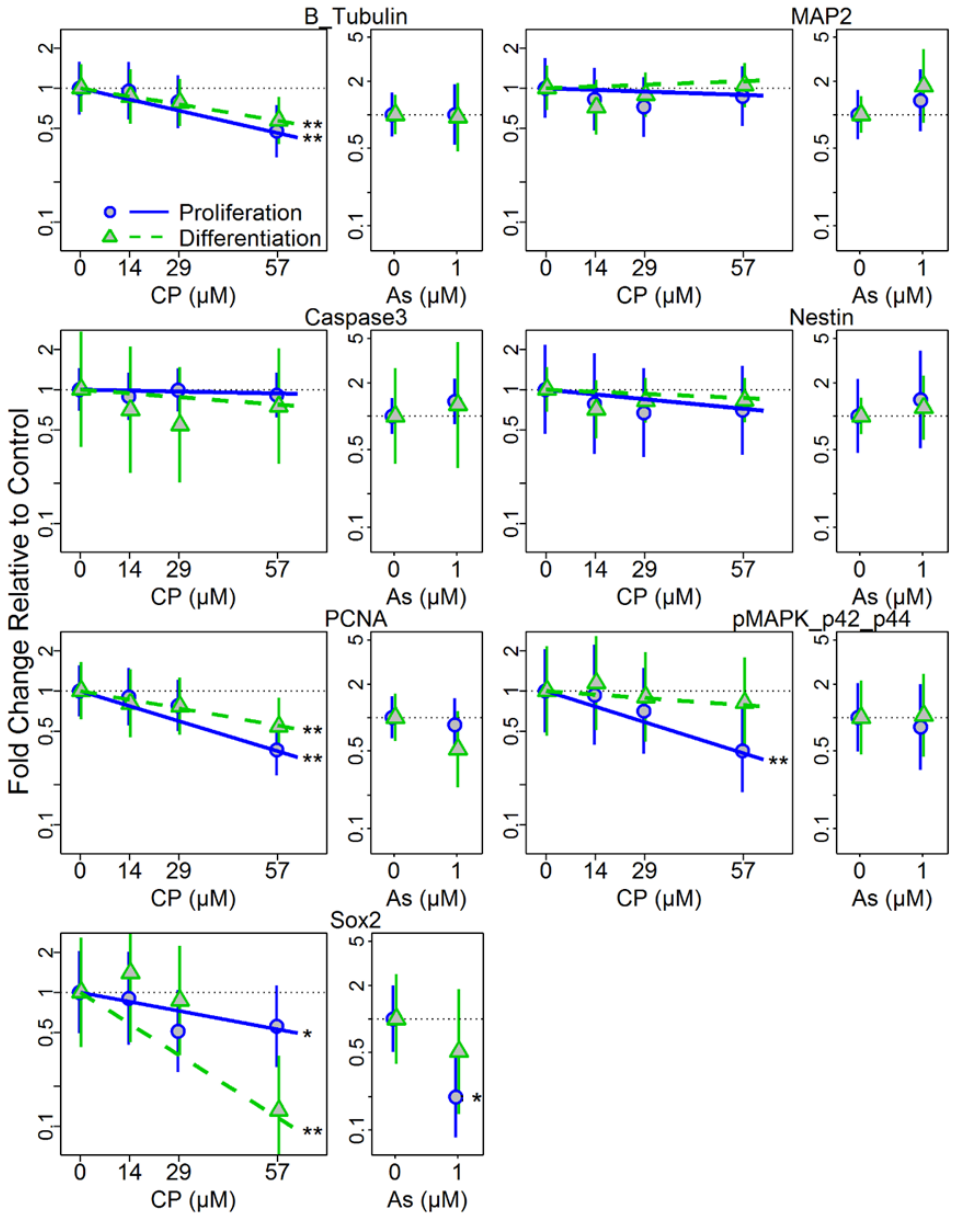

Figure 5.5. Changes in neuronal and stage specific protein marker expressions following treatment of hNPCs cultured under proliferation and differentiation conditions. Protein expression was quantified from western blotting following 72h treatment with CP or As (positive control) under proliferating or differentiating conditions. Plots show means and 95% confidence intervals. Statistical significances, *: p-value < 0.05; **: p-value < 0.01; ***: p-value < 0.001 compared to relative control, are based on a linear mixed effect model indicating significant dose response for each condition.

Table 5.2. Summary of toxicant effects on protein expression.

Marker	CP		AS	
	Proliferation	Differentiation	Proliferation	Differentiation
β-TUBULIN III	↓ **	↓ **	NS	NS
MAP-2	NS	NS	NS	NS
CASPASE 3	NS	NS	NS	NS
NESTIN	NS	NS	NS	NS
PCNA	↓ **	↓ **	NS	NS
MAPK	↓ **	NS	NS	NS
SOX-2	↓ *	↓ **	↓ *	NS

Note: *: p-value < 0.05; **: p-value < 0.01; NS = not significant; ↓ = decrease; ↑ = increase

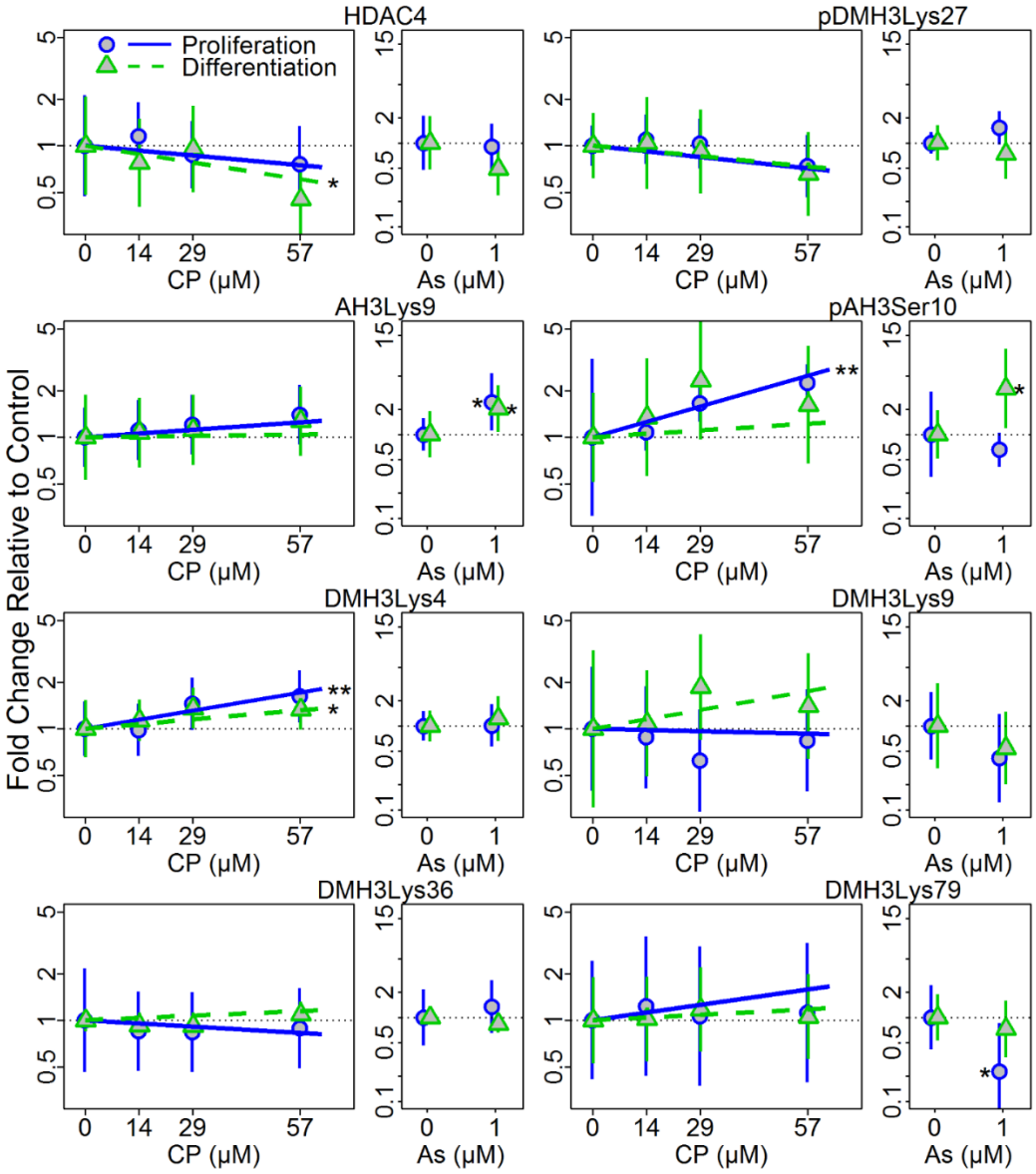

Figure 5.6. Changes of histone H3 acetylation and methylation following CP and As treatment of hNPCs cultured under proliferation and differentiation conditions at 72 h post treatment. Histone modifications at specific sites were quantified by western blotting following 72h treatment with CP or As (positive control) under proliferating or differentiating conditions. Plots show means and 95% confidence intervals. Statistical significances, *: p-value < 0.05; **: p-value < 0.01; ***: p-value < 0.001 compared to relative control, are based on a linear mixed effect model indicating significant dose response for each condition.

Table 5.3. Summary of toxicant effects on histone modifications.

Marker	CP		AS	
	Proliferation	Differentiation	Proliferation	Differentiation
HDAC4	NS	↓ *	NS	NS
DMH3Lys27	NS	NS	NS	NS
AH3Lys9	NS	NS	↑ *	↑ *
pAH3SeR10	↑ **	NS	NS	↑ *
DMH3Lys4	↑ **	↑ *	NS	NS
DMH3Lys9	NS	NS	NS	NS
DMH3Lys36	NS	NS	NS	NS
DMH3Lys79	NS	NS	↓ *	NS

Note: *: p-value < 0.05; **: p-value < 0.01; NS = not significant; ↓ = decrease; ↑ = increase

CHAPTER 5 REFERENCES

Arai, Y., Ohgane, J., Yagi, S. et al. (2011). Epigenetic Assessment of Environmental Chemicals Detected in Maternal Peripheral and Cord Blood Samples. *Journal of Reproduction and Development 57*, 507-517.

Barker, D. J. (2007). The origins of the developmental origins theory. *J Intern Med 261*, 412-417. http://dx.doi.org/10.1111/j.1365-2796.2007.01809.x

Breier, J. M., Radio, N. M., Mundy, W. R. et al. (2008). Development of a high-throughput screening assay for chemical effects on proliferation and viability of immortalized human neural progenitor cells. *Toxicological sciences : an official journal of the Society of Toxicology 105*, 119-133. http://dx.doi.org/10.1093/toxsci/kfn115

Cheng, T. F., Choudhuri, S. and Muldoon-Jacobs, K. (2012). Epigenetic targets of some toxicologically relevant metals: a review of the literature. *Journal of Applied Toxicology 32*, 643-653. http://dx.doi.org/Doi 10.1002/Jat.2717

Collotta, M., Bertazzi, P. A. and Bollati, V. (2013). Epigenetics and pesticides. *Toxicology 307*, 35-41. http://dx.doi.org/10.1016/j.tox.2013.01.017

Cronican, A. A., Fitz, N. F., Carter, A. et al. (2013). Genome-wide alteration of histone H3K9 acetylation pattern in mouse offspring prenatally exposed to arsenic. *PLoS One 8*, e53478. http://dx.doi.org/10.1371/journal.pone.0053478

Daston, G., Faustman, E., Ginsberg, G. et al. (2004). A framework for assessing risks to children from exposure to environmental agents. *Environ Health Perspect 112*, 238-256.

Day, J. J. and Sweatt, J. D. (2011). Epigenetic mechanisms in cognition. *Neuron 70*, 813-829. http://dx.doi.org/10.1016/j.neuron.2011.05.019

Debeb, B. G., Xu, W., Mok, H. et al. (2010). Differential radiosensitizing effect of valproic acid in differentiation versus self-renewal promoting culture conditions. *Int J Radiat Oncol Biol Phys 76*, 889-895. http://dx.doi.org/10.1016/j.ijrobp.2009.09.052

Eissenberg, J. C. and Shilatifard, A. (2010). Histone H3 lysine 4 (H3K4) methylation in development and differentiation. *Dev Biol 339*, 240-249. http://dx.doi.org/10.1016/j.ydbio.2009.08.017

Engel, S. M., Wetmur, J., Chen, J. et al. (2011). Prenatal exposure to organophosphates, paraoxonase 1, and cognitive development in childhood. *Environ Health Perspect 119*, 1182-1188. http://dx.doi.org/10.1289/ehp.1003183

Eskenazi, B., Marks, A. R., Bradman, A. et al. (2007). Organophosphate pesticide exposure and neurodevelopment in young Mexican-American children. *Environ Health Perspect 115*, 792-798. http://dx.doi.org/10.1289/ehp.9828

Eskenazi, B., Rosas, L. G., Marks, A. R. et al. (2008). Pesticide toxicity and the developing brain. *Basic Clin Pharmacol Toxicol 102*, 228-236. http://dx.doi.org/10.1111/j.1742-7843.2007.00171.x

Eskenazi, B., Huen, K., Marks, A. et al. (2010). PON1 and neurodevelopment in children from the CHAMACOS study exposed to organophosphate pesticides in utero. *Environ Health Perspect 118*, 1775-1781. http://dx.doi.org/10.1289/ehp.1002234

Eskenazi, B., Kogut, K., Huen, K. et al. (2014). Organophosphate pesticide exposure, PON1, and neurodevelopment in school-age children from the CHAMACOS study. *Environ Res 134*, 149-157. http://dx.doi.org/10.1016/j.envres.2014.07.001

Fagiolini, M., Jensen, C. L. and Champagne, F. A. (2009). Epigenetic influences on brain development and plasticity. *Curr Opin Neurobiol 19*, 207-212. http://dx.doi.org/10.1016/j.conb.2009.05.009

Faustman, E. M., Silbernagel, S. M., Fenske, R. A. et al. (2000). Mechanisms underlying Children's susceptibility to environmental toxicants. *Environ Health Perspect 108 Suppl 1*, 13-21.

Frankel, S., Concannon, J., Brusky, K. et al. (2009). Arsenic exposure disrupts neurite growth and complexity in vitro. *Neurotoxicology 30*, 529-537. http://dx.doi.org/10.1016/j.neuro.2009.02.015

Fu, H., Maunakea, A. K., Martin, M. M. et al. (2013). Methylation of histone H3 on lysine 79 associates with a group of replication origins and helps limit DNA replication once per cell cycle. *PLoS Genet 9*, e1003542. http://dx.doi.org/10.1371/journal.pgen.1003542

Gohlke, J. M., Hiller-Sturmhofel, S. and Faustman, E. M. (2008). A systems-based computational model of alcohol's toxic effects on brain development. *Alcohol Research & Health 31*, 76-83.

Grandjean, P. and Landrigan, P. J. (2014). Neurobehavioural effects of developmental toxicity. *Lancet Neurol 13*, 330-338. http://dx.doi.org/10.1016/S1474-4422(13)70278-3

Guppy, B. J. and McManus, K. J. (2015). Mitotic accumulation of dimethylated lysine 79 of histone H3 is important for maintaining genome integrity during mitosis in human cells. *Genetics 199*, 423-433. http://dx.doi.org/10.1534/genetics.114.172874

Hamadani, J. D., Tofail, F., Nermell, B. et al. (2011). Critical windows of exposure for arsenic-associated impairment of cognitive function in pre-school girls and boys: a population-based cohort study. *Int J Epidemiol 40*, 1593-1604. http://dx.doi.org/10.1093/ije/dyr176

Hamby, M. E., Coskun, V. and Sun, Y. E. (2008). Transcriptional regulation of neuronal differentiation: the epigenetic layer of complexity. *Biochim Biophys Acta 1779*, 432-437. http://dx.doi.org/10.1016/j.bbagrm.2008.07.006

Horton, M. K., Kahn, L. G., Perera, F. et al. (2012). Does the home environment and the sex of the child modify the adverse effects of prenatal exposure to chlorpyrifos on child working memory? *Neurotoxicol Teratol 34*, 534-541. http://dx.doi.org/10.1016/j.ntt.2012.07.004

Hou, L., Zhang, X., Wang, D. et al. (2012). Environmental chemical exposures and human epigenetics. *Int J Epidemiol 41*, 79-105. http://dx.doi.org/10.1093/ije/dyr154

Howard, A. S., Bucelli, R., Jett, D. A. et al. (2005). Chlorpyrifos exerts opposing effects on axonal and dendritic growth in primary neuronal cultures. *Toxicol Appl Pharmacol 207*, 112-124. http://dx.doi.org/10.1016/j.taap.2004.12.008

Hsieh, J. and Gage, F. H. (2004). Epigenetic control of neural stem cell fate. *Curr Opin Genet Dev 14*, 461-469. http://dx.doi.org/10.1016/j.gde.2004.07.006

Ivanov, V. N. and Hei, T. K. (2013). Induction of apoptotic death and retardation of neuronal differentiation of human neural stem cells by sodium arsenite treatment. *Exp Cell Res 319*, 875-887. http://dx.doi.org/10.1016/j.yexcr.2012.11.019

Jameson, R. R., Seidler, F. J., Qiao, D. et al. (2006). Chlorpyrifos affects phenotypic outcomes in a model of mammalian neurodevelopment: critical stages targeting differentiation in PC12 cells. *Environ Health Perspect 114*, 667-672.

Juliandi, B., Abematsu, M. and Nakashima, K. (2010a). Epigenetic regulation in neural stem cell differentiation. *Dev Growth Differ 52*, 493-504. http://dx.doi.org/10.1111/j.1440-169X.2010.01175.x

Juliandi, B., Abematsu, M. and Nakashima, K. (2010b). Chromatin remodeling in neural stem cell differentiation. *Curr Opin Neurobiol 20*, 408-415. http://dx.doi.org/10.1016/j.conb.2010.04.001

Koch, C. M., Andrews, R. M., Flicek, P. et al. (2007). The landscape of histone modifications across 1% of the human genome in five human cell lines. *Genome Res 17*, 691-707. http://dx.doi.org/10.1101/gr.5704207

Lee, B. M. and Mahadevan, L. C. (2009). Stability of histone modifications across mammalian genomes: implications for 'epigenetic' marking. *J Cell Biochem 108*, 22-34. http://dx.doi.org/10.1002/jcb.22250

Lim, C. K., Kim, S. K., Ko, D. S. et al. (2009). Differential cytotoxic effects of mono-(2-ethylhexyl) phthalate on blastomere-derived embryonic stem cells and differentiating neurons. *Toxicology 264*, 145-154. http://dx.doi.org/10.1016/j.tox.2009.08.015

Lo, W. S., Trievel, R. C., Rojas, J. R. et al. (2000). Phosphorylation of serine 10 in histone H3 is functionally linked in vitro and in vivo to Gcn5-mediated acetylation at lysine 14. *Mol Cell 5*, 917-926.

Lu, T. H., Tseng, T. J., Su, C. C. et al. (2014). Arsenic induces reactive oxygen species-caused neuronal cell apoptosis through JNK/ERK-mediated mitochondria-dependent and GRP 78/CHOP-regulated pathways. *Toxicol Lett 224*, 130-140. http://dx.doi.org/10.1016/j.toxlet.2013.10.013

Majdzadeh, N., Wang, L., Morrison, B. E. et al. (2008). HDAC4 inhibits cell-cycle progression and protects neurons from cell death. *Dev Neurobiol 68*, 1076-1092. http://dx.doi.org/10.1002/dneu.20637

Moreira, E. G., Yu, X., Robinson, J. F. et al. (2010). Toxicogenomic profiling in maternal and fetal rodent brains following gestational exposure to chlorpyrifos. *Toxicol Appl Pharmacol 245*, 310-325. http://dx.doi.org/10.1016/j.taap.2010.03.015

O'Brien, J., Wilson, I., Orton, T. et al. (2000). Investigation of the Alamar Blue (resazurin) fluorescent dye for the assessment of mammalian cell cytotoxicity. *Eur J Biochem 267*, 5421-5426.

Park, C. H. and Kim, K. T. (2012). Apoptotic phosphorylation of histone H3 on Ser-10 by protein kinase Cdelta. *PLoS One 7*, e44307. http://dx.doi.org/10.1371/journal.pone.0044307

Peterson, C. L. and Laniel, M. A. (2004). Histones and histone modifications. *Curr Biol 14*, R546-551. http://dx.doi.org/10.1016/j.cub.2004.07.007

Qiao, Y., Wang, R., Yang, X. et al. (2015). Dual roles of histone H3 lysine 9 acetylation in human embryonic stem cell pluripotency and neural differentiation. *J Biol Chem 290*, 2508-2520. http://dx.doi.org/10.1074/jbc.M114.603761

Radio, N. M. and Mundy, W. R. (2008). Developmental neurotoxicity testing in vitro: models for assessing chemical effects on neurite outgrowth. *Neurotoxicology 29*, 361-376. http://dx.doi.org/10.1016/j.neuro.2008.02.011

Rauh, V. A., Garfinkel, R., Perera, F. P. et al. (2006). Impact of prenatal chlorpyrifos exposure on neurodevelopment in the first 3 years of life among inner-city children. *Pediatrics 118*, e1845-1859. http://dx.doi.org/10.1542/peds.2006-0338

Rauh, V. A., Perera, F. P., Horton, M. K. et al. (2012). Brain anomalies in children exposed prenatally to a common organophosphate pesticide. *Proc Natl Acad Sci U S A 109*, 7871-7876. http://dx.doi.org/10.1073/pnas.1203396109

Ray, P. D., Yosim, A. and Fry, R. C. (2014). Incorporating epigenetic data into the risk assessment process for the toxic metals arsenic, cadmium, chromium, lead, and mercury: strategies and challenges. *Front Genet 5*, 201. http://dx.doi.org/10.3389/fgene.2014.00201

Reichard, J. F. and Puga, A. (2010). Effects of arsenic exposure on DNA methylation and epigenetic gene regulation. *Epigenomics 2*, 87-104. http://dx.doi.org/10.2217/epi.09.45

Rice, D. and Barone, S., Jr. (2000). Critical periods of vulnerability for the developing nervous system: evidence from humans and animal models. *Environ Health Perspect 108 Suppl 3*, 511-533.

Robinson, J. F., Yu, X., Moreira, E. G. et al. (2011). Arsenic- and cadmium-induced toxicogenomic response in mouse embryos undergoing neurulation. *Toxicol Appl Pharmacol 250*, 117-129. http://dx.doi.org/10.1016/j.taap.2010.09.018

Rodier, P. M. (1994). Vulnerable periods and processes during central nervous system development. *Environ Health Perspect 102 Suppl 2*, 121-124.

Rodier, P. M. (1995). Developing brain as a target of toxicity. *Environ Health Perspect 103 Suppl 6*, 73-76.

Ronan, J. L., Wu, W. and Crabtree, G. R. (2013). From neural development to cognition: unexpected roles for chromatin. *Nat Rev Genet 14*, 347-359. http://dx.doi.org/10.1038/nrg3413

Rudenko, A. and Tsai, L. H. (2014). Epigenetic regulation in memory and cognitive disorders. *Neuroscience 264*, 51-63. http://dx.doi.org/10.1016/j.neuroscience.2012.12.034

Ruthenburg, A. J., Allis, C. D. and Wysocka, J. (2007). Methylation of lysine 4 on histone H3: intricacy of writing and reading a single epigenetic mark. *Mol Cell 25*, 15-30. http://dx.doi.org/10.1016/j.molcel.2006.12.014

Salazar-Arredondo, E., de Jesus Solis-Heredia, M., Rojas-Garcia, E. et al. (2008). Sperm chromatin alteration and DNA damage by methyl-parathion, chlorpyrifos and diazinon and their oxon metabolites in human spermatozoa. *Reprod Toxicol 25*, 455-460. http://dx.doi.org/10.1016/j.reprotox.2008.05.055

Sando, R., 3rd, Gounko, N., Pieraut, S. et al. (2012). HDAC4 governs a transcriptional program essential for synaptic plasticity and memory. *Cell 151*, 821-834. http://dx.doi.org/10.1016/j.cell.2012.09.037

Sanosaka, T., Namihira, M. and Nakashima, K. (2009). Epigenetic mechanisms in sequential differentiation of neural stem cells. *Epigenetics 4*, 89-92.

Shin, H. S., Seo, J. H., Jeong, S. H. et al. (2014). Exposure of pregnant mice to chlorpyrifos-methyl alters embryonic H19 gene methylation patterns. *Environ Toxicol 29*, 926-935. http://dx.doi.org/10.1002/tox.21820

Shin, S., Mitalipova, M., Noggle, S. et al. (2006). Long-term proliferation of human embryonic stem cell-derived neuroepithelial cells using defined adherent culture conditions. *Stem Cells 24*, 125-138. http://dx.doi.org/10.1634/stemcells.2004-0150

Skinner, M. K. (2007). Endocrine disruptors and epigenetic transgenerational disease etiology. *Pediatr Res 61*, 48R-50R. http://dx.doi.org/10.1203/pdr.0b013e3180457671

Slotkin, T. A., MacKillop, E. A., Ryde, I. T. et al. (2007). Ameliorating the developmental neurotoxicity of chlorpyrifos: a mechanisms-based approach in PC12 cells. *Environ Health Perspect 115*, 1306-1313. http://dx.doi.org/10.1289/ehp.10194

Slotkin, T. A. and Seidler, F. J. (2012). Developmental neurotoxicity of organophosphates targets cell cycle and apoptosis, revealed by transcriptional profiles in vivo and in vitro. *Neurotoxicol Teratol 34*, 232-241. http://dx.doi.org/10.1016/j.ntt.2011.12.001

Theunissen, P. T., Schulpen, S. H., van Dartel, D. A. et al. (2010). An abbreviated protocol for multilineage neural differentiation of murine embryonic stem cells and its perturbation by methyl mercury. *Reprod Toxicol 29*, 383-392. http://dx.doi.org/10.1016/j.reprotox.2010.04.003

Thomson, J. A., Itskovitz-Eldor, J., Shapiro, S. S. et al. (1998). Embryonic stem cell lines derived from human blastocysts. *Science 282*, 1145-1147.

Tokar, E. J., Qu, W. and Waalkes, M. P. (2011). Arsenic, stem cells, and the developmental basis of adult cancer. *Toxicol Sci 120 Suppl 1*, S192-203. http://dx.doi.org/10.1093/toxsci/kfq342

Tyler, C. R. and Allan, A. M. (2014). The Effects of Arsenic Exposure on Neurological and Cognitive Dysfunction in Human and Rodent Studies: A Review. *Curr Environ Health Rep 1*, 132-147. http://dx.doi.org/10.1007/s40572-014-0012-1

Visan, A., Hayess, K., Sittner, D. et al. (2012). Neural differentiation of mouse embryonic stem cells as a tool to assess developmental neurotoxicity in vitro. *Neurotoxicology 33*, 1135-1146. http://dx.doi.org/10.1016/j.neuro.2012.06.006

Wang, X., Meng, D., Chang, Q. et al. (2010). Arsenic inhibits neurite outgrowth by inhibiting the LKB1-AMPK signaling pathway. *Environ Health Perspect 118*, 627-634. http://dx.doi.org/10.1289/ehp.0901510

Wasserman, G. A., Liu, X., Parvez, F. et al. (2007). Water arsenic exposure and intellectual function in 6-year-old children in Araihazar, Bangladesh. *Environ Health Perspect 115*, 285-289. http://dx.doi.org/10.1289/ehp.9501

Whitney, K. D., Seidler, F. J. and Slotkin, T. A. (1995). Developmental neurotoxicity of chlorpyrifos: cellular mechanisms. *Toxicol Appl Pharmacol 134*, 53-62. http://dx.doi.org/S0041-008X(85)71168-4 [pii]
10.1006/taap.1995.1168

Whittaker, S. G., Wroble, J. T., Silbernagel, S. M. et al. (1993). Characterization of cytoskeletal and neuronal markers in micromass cultures of rat embryonic midbrain cells. *Cell Biol Toxicol 9*, 359-375.

Wright, R. O. and Baccarelli, A. (2007). Metals and neurotoxicology. *J Nutr 137*, 2809-2813.

Young, A., Machacek, D. W., Dhara, S. K. et al. (2011). Ion channels and ionotropic receptors in human embryonic stem cell derived neural progenitors. *Neuroscience 192*, 793-805. http://dx.doi.org/10.1016/j.neuroscience.2011.04.039

Yu, X., Sidhu, J. S., Hong, S. et al. (2005). Essential role of extracellular matrix (ECM) overlay in establishing the functional integrity of primary neonatal rat Sertoli cell/gonocyte co-cultures: an improved in vitro model for assessment of male reproductive toxicity. *Toxicol Sci 84*, 378-393. http://dx.doi.org/10.1093/toxsci/kfi085

CHAPTER 5 SUPPLEMENTARY TABLES AND FIGURES

Supplementary Table 5.1. Alamar blue IC10 summary table: IC10 values for chlorpyrifos (CP) and arsenic (As) exposures

IC10 (μM)	24 h	72h
CP Proliferation	171	152
CP Differentiation	> 570	71
As Proliferation	1.4	0.5
As Differentiation	1.0	0.4

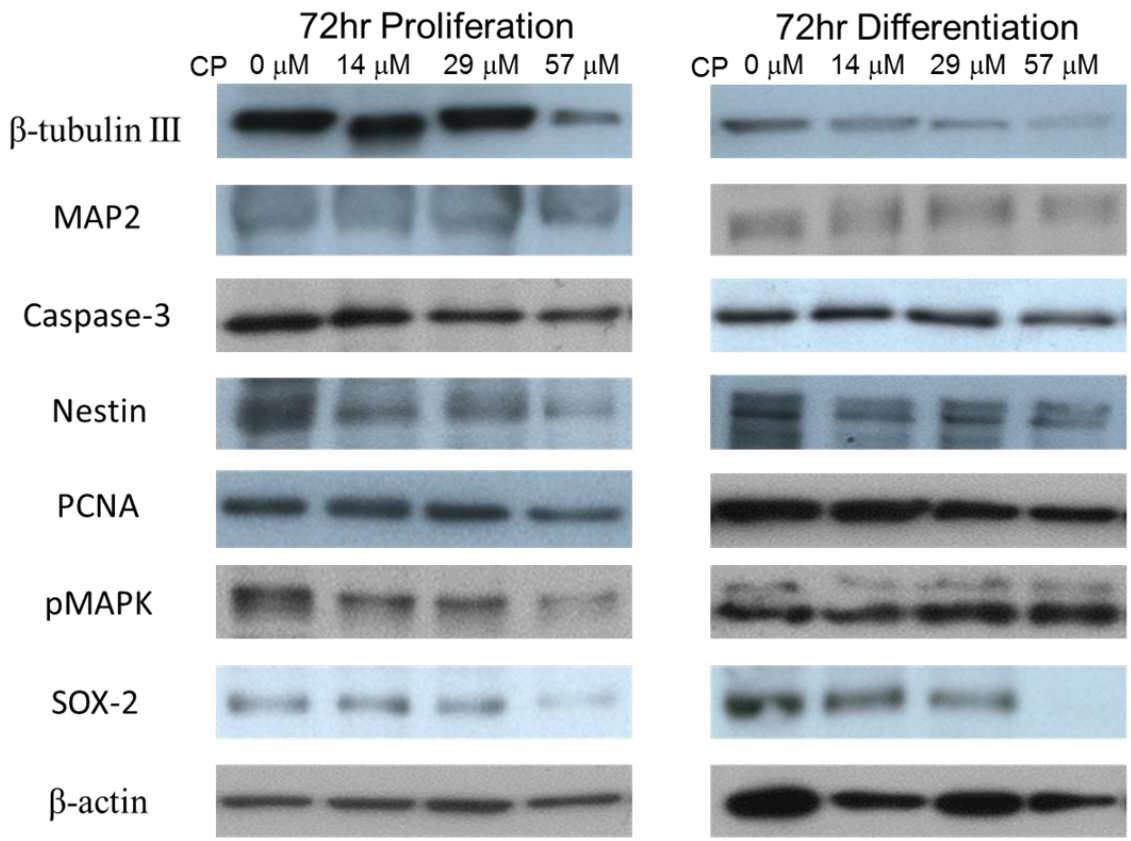

Supplementary Figure 5.2. Representative Western blots of neuronal markers for CP exposed hNPCs for 72 hours under proliferation and differentiating conditions. Representative β-actin are also shown.

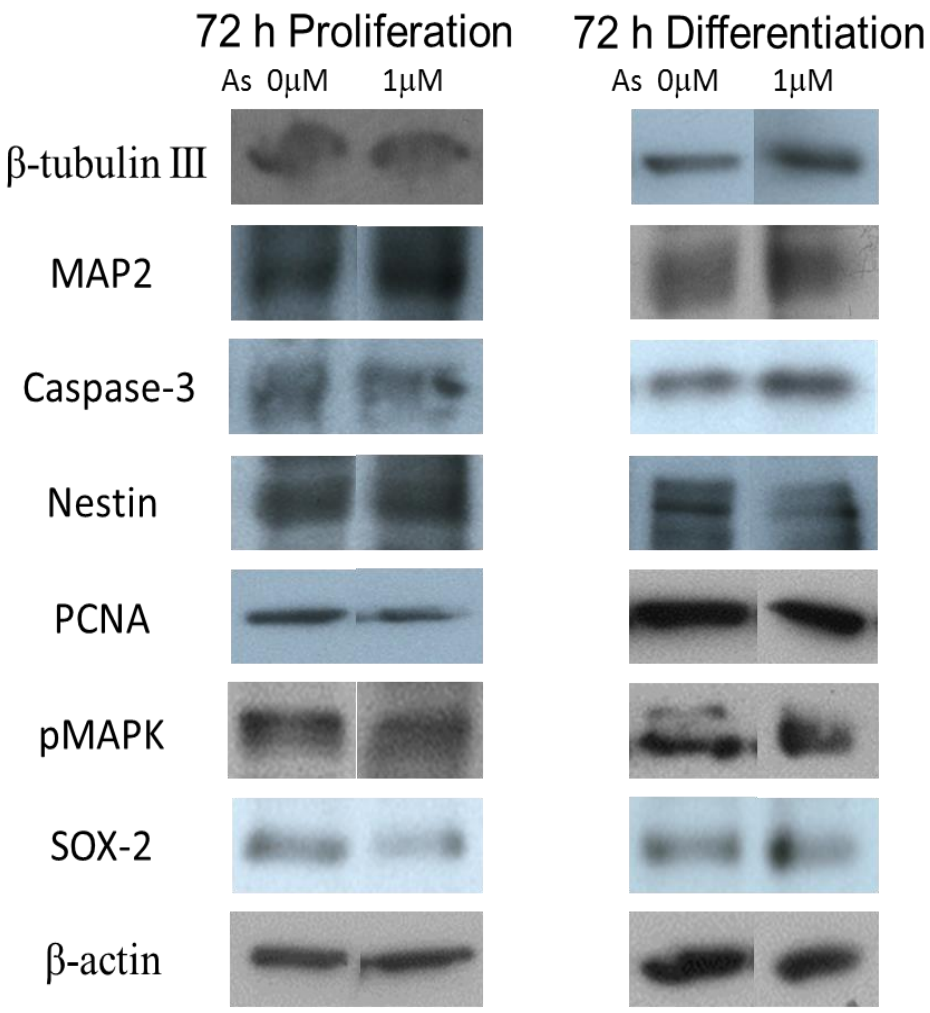

Supplementary Figure 5.3. Representative Western blots of neuronal markers for As (positive control) exposed hNPCs for 72 hours under proliferation and differentiating conditions.

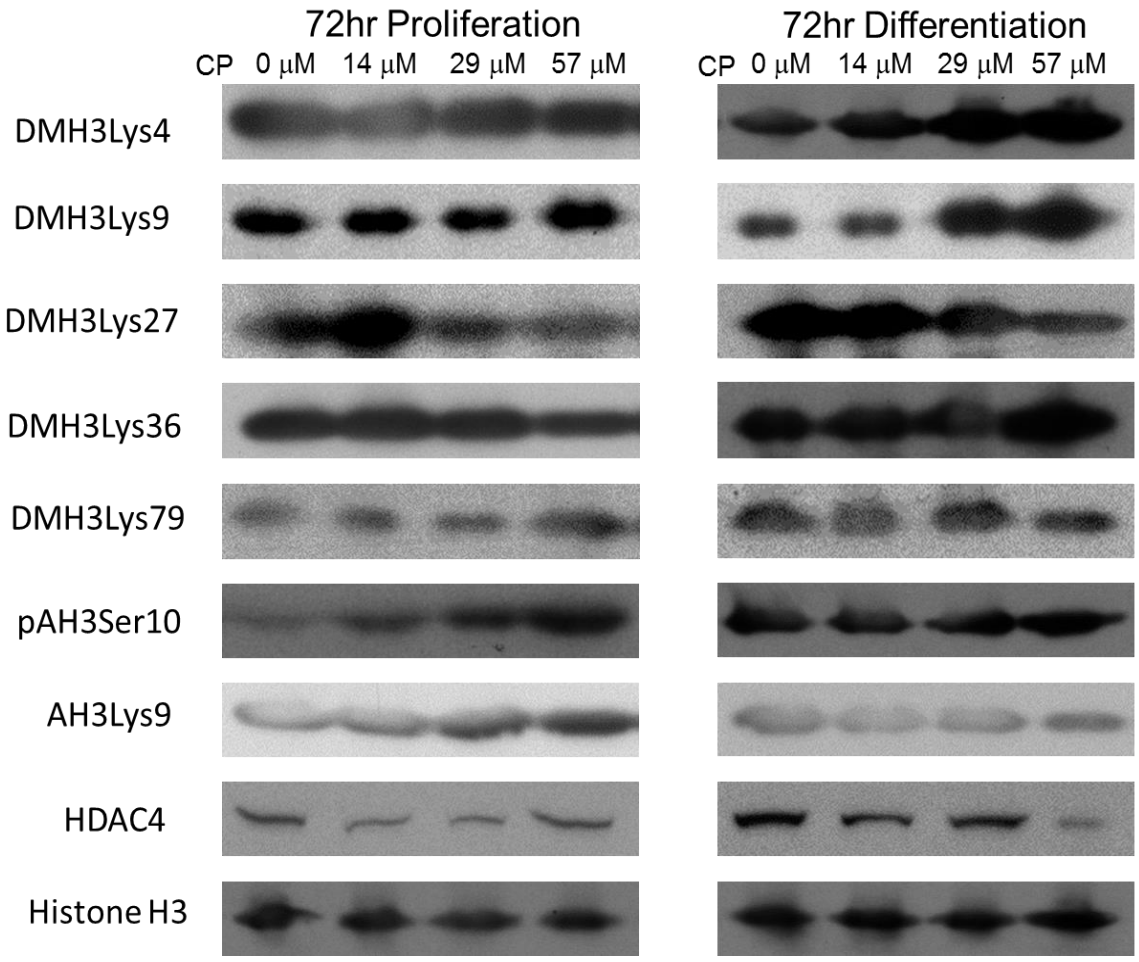

Supplementary Figure 5.4. Representative Western blots of epigenetic markers for CP exposed hNPCs for 72 hours under proliferation and differentiating conditions. Representative total Histone H3 are also shown.

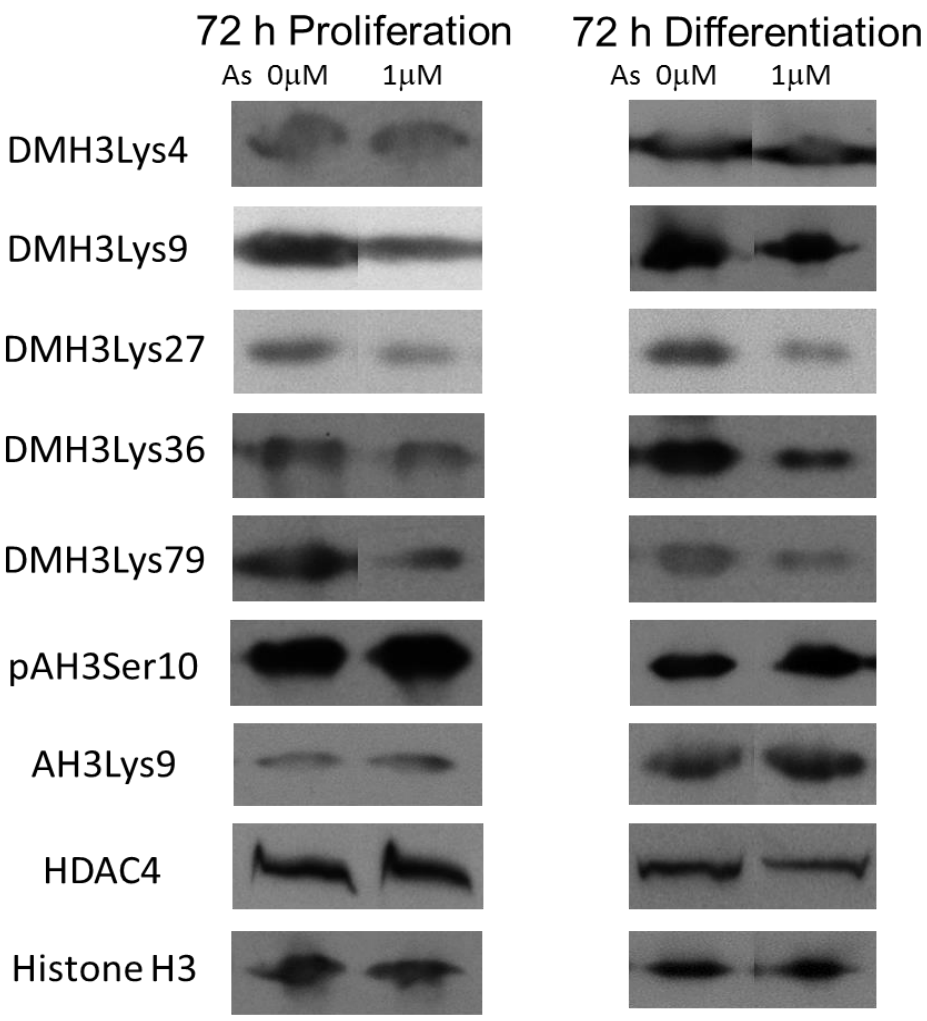

Supplementary Figure 5.5. Representative Western blots of epigenetic markers for As (positive control) exposed hNPCs for 72 hours under proliferation and differentiating conditions. Representative total Histone H3 are also shown.

CHAPTER 6: Effects of silver nanoparticles with various coatings and sizes on proliferating and differentiating human neural progenitor cell (hNPCs) *in vitro*

This Chapter is in preparation for submission. The authors of the manuscript are:

Julie Juyoung Park[1, 2], Sungwoo Hong[2], Tomomi Workman[1], William Griffith[1], Elaine M. Faustman[1, 2*]

[1] Institute for Risk Analysis and Risk Communication, University of Washington, Seattle, WA, USA

[2] Department of Environmental and Occupational Health Sciences, University of Washington, Seattle, WA, USA

* Corresponding author: Elaine M. Faustman

Institute for Risk Analysis and Risk Communication, Department of Environmental and Occupational Health Sciences, University of Washington, Seattle, WA, USA.

Email: faustman@uw.edu

ABSTRACT

Engineered nanomaterials (ENMs) are referred to materials with at least one dimension ranging from 1 to 100 nm. Silver nanoparticles (AgNPs) are ENMs that has been used increasingly in various consumer, medical, and commercial products for their unique antibacterial properties. Increasing number of studies, however, raised some concerns regarding exposures to AgNPs on their potential adverse impacts on human and environmental health. Research studies have shown that AgNPs cross the placenta and accumulate in the fetal brain, leading to concerns about effects on brain development and function. The objective of the current study is to examine the effects of gold-cored AgNPs on *in vitro* human neural progenitor cell (hNPC) cultures. Three types of AgNPs—20 nm AgCitrate, 110 nm AgCitrate, and 110 nm AgPVP—were used, and the effects of these particles were assessed on proliferating or differentiating hNPCs at day 1 or differentiating hNPCs at day 7. Exposures to AgNPs at four different doses (0 – 50 μg/mL) demonstrated significant dose-dependent decreases in cell viability. We discovered that the differentiating hNPCs at day 7 received the least impact compared to proliferating and differentiating hNPCs at day 1. For 20 nm AgCitrate, differentiating hNPCs at day 1 were the most susceptible to AgNPs; however, proliferating hNPCs at day 1 were most vulnerable to larger AgNPs (110 nm AgCitrate and 110 nm AgPVP). Significant effects of particle coatings, sizes, and neurodevelopmental stages were observed for all particles. Our results suggested that the "window of susceptibility" for AgNPs may depend on particle sizes; however, the impacts may be greater during the early developmental period than late. Together with other *in vitro* neurodevelopmental models, these offer approaches to assess both environmental and time-specific factors influencing neurodevelopmental susceptibility.

INTRODUCTION

Engineered nanomaterials (ENMs) include materials with at least one dimension ranging from 1 to 100 nm (Yokel and Macphail, 2011). With recent technological developments, ENMs have been employed in a wide array of fields from electronics to medical devices and children's product due to unique characteristics of ENMs. The ENMs have a large surface area with small size and are light-weighted. Silver nanoparticles (AgNPs) is one type of ENMs that are widely used in food storage, electronics, textile coatings, medical industry, and consumer products for their antimicrobial property (El-Nour et al., 2010; Woodrow Wilson International Center for Scholars, 2016). Particularly, AgNPs have been used in children's products (Quadros et al., 2013; Tulve et al., 2015). Although uses of AgNPs increase exponentially, very little is known about their potential impact on human and environmental health. For example, Reidy et al. (2013) demonstrated that AgNPs produce antibacterial effects by disrupting structural proteins, enzymes, and DNA, which then may lead to adverse health effects. Only a limited number of studies have been done investigating the potential negative effects of AgNPs on organ systems including developing central nervous system (CNS). Through *in vitro* and *in vivo* studies, Tang et al. (2009; 2010) discovered that AgNPs could cross the blood brain barrier. Other *in vivo* studies also revealed that translocated AgNPs throughout body organs including the brain upon oral or inhalational AgNP exposures resulted in inflammatory responses and decreased spatial cognition (Loeschner et al., 2011; Patchin et al., 2016; Tang et al., 2009; Wu et al., 2015; Yang et al., 2010). In addition to crossing blood brain barrier, silver was found to cross placenta regardless of its form, and that the amount of silver in developing fetuses increased after dams were exposed orally or intravenously (Fennell et al., 2017). Nanomaterials disintegrated from ENM-functionalized materials can enter our ecosystem (Levard et al., 2012) and increase the potential for environmental exposures in human and animals.

The central nervous system (CNS) plays a critical role in our everyday life including survival and prosperity. The CNS, however, is one of the sensitive target systems of toxicity, which can be damaged by various environmental and pharmacological toxicants. Rice and Barone (2000) reported that the developing nervous system has been shown to be more vulnerable to perturbations compared to a mature nervous system, and that disruption of the developing CNS may lead to lifelong consequences such as autism, attention deficit/hyperactivity disorder, cerebral palsy, and mental retardation (Grandjean and Landrigan, 2006). These disorders may, in turn, put burden not only on families but also the healthcare system and the society.

Currently, more than 80,000 compounds are registered in the U. S. Environmental Protection Agency (Miodovnik, 2011). Of these registered chemicals, less than 0.01% has been examined for potential neurodevelopmental toxicity (Miodovnik, 2011), suggesting data gap between the larger number of chemicals still in need to be tested and traditional *in vivo* models for developmental toxicity assessments. Traditional animal models require a large number of animals, labor-intensive, and time-consuming (Bailey et al., 2005; Piersma, 2004; Pratten et al., 2012), advocating for the development of high throughput and high content *in vitro* alternative methods that can capture key processes of brain development. Genschow et al. (2002) and Krewski et al. (2010) recommended developing such tools in order to screen and prioritize potential developmental neurotoxicants.

In this study, our *in vitro* human neural progenitor cell (hNPC) culture system was utilized for evaluating effects of AgNPs on neurodevelopment. Previously, we have successfully demonstrated that gene expressions of human *in vivo* from the Allen Brain Institute were comparable to our differentiating *in vitro* hNPCs over 21-days of the culture period (Wegner et al., 2014). Park et al. (2017) and Wegner et al. (2014) reported that this *in vitro* hNPCs culture can capture key processes of early brain development from proliferation and differentiation of neurons with forebrain characteristics to epigenetic changes and stress responses. In addition, hNPCs is of human origin, which means that *in vitro* effects that we see on hNPCs may be reflective of what we may observe in *in vivo* humans. This system also has advantages of being reproducible, high throughput, and high content as *in vitro* screening method (Park et al., 2017; Wegner et al., 2014). Moreover, current *in vitro* hNPCs model has enhanced our understanding of early brain development by reducing cost, time, and a number of animals sacrificed yet closely mimicking *in vivo* processes of neurodevelopment (Park et al., 2017; Wegner et al., 2014).

In addition to nanoparticles themselves exerting neurotoxicity, other factors such as particle coatings, sizes, and time of exposure may also contribute to susceptibility during early neurodevelopmental period. Based on the National Research Council Committee on Developmental Toxicology (2000), one in six children has a developmental disability. With such far-reaching implications, understanding how exposures to AgNPs adversely affect the developing nervous system would be important. For this study, we investigated adverse effects of AgNPs with various sizes and coatings and time of exposure using *in vitro* hNPCs model.

METHODS

Human neural progenitor cell culture system.

Commercially available hNP1™ human neural progenitor cells (hNPCs; ArunA Biomedical, Athens, GA, USA) were cultured expanded in proliferative conditions using AB2™ neural cell culture media (ArunA Biomedical, Athens, GA, USA) up to passage eight. Cells were plated onto Matrigel-coated 96-well black bottom microplates (Becton, Dickinson Co., Franklin Lakes, NJ, USA) or 24-well plates (Corning Life Science, Corning, NY, USA) at the density of 200,000 cells/mL. Cells were plated in proliferative AB2™ neural cell culture media (ArunA Biomedical, Athens, GA, USA) at 37°C with 5% CO_2 and then allowed to attach for 24 hours. Plated hNPCs were treated with various silver nanoparticles (AgNPs) either in proliferation or differentiation condition by replacing media with HyClone™ differentiation media (GE Healthcare Life Sciences, Little Chalfont, United Kingdom).

Treatment with silver nanoparticles (AgNPs).

Silver nanoparticles (AgNPs) with different sizes and coatings were obtained from NanoComposix (San Diego, CA, USA). AgNPs used in this experiment were 20nm AgCitrate, 110nm AgCitreate, and 110nm AgPVP, and all contained a 7 nm gold core. These AgNPs were chosen by the National Institute of Environmental Health Sciences (NIEHS) Centers for Nanotechnology and Health Implications Research (NCNHIR) Consortium laboratories, where their physiochemical properties were described by the manufacturer and are supplied in Fennell et al. (2017). AgNP stock solutions (1 mg/mL) were stored in 4°C in dark until treatment.

AgNPs (20 nm AgCitrate, 110 nm AgCitrate, and 110 nm AgPVP) were diluted either in proliferation or differentiation media to prepare exposure medium with 0, 6.25, 12.5, 25, and 50 µg/mL concentrations. For a positive and negative control, ZnO and TiO_2 at 50 µg/mL were used, respectively. As a coating controls for citrate- and PVP-coated particles, stabilizer coating controls sodium citrate (NaCitrate) at 100 µM and 40kD-sized PVP at 50 µg/mL, respectively, were used. Proliferating hNPCs at day 0 were treated with AgNPs for 24 hours by replacing cell culture medium with 500 µL of exposure medium and continuing incubation at 37°C with 5% CO_2. Differentiating hNPCs were treated with AgNPs 24 hours after (day 0) and 6 days after the initial plating in order to investigate effects at two different differentiation stages. Cell viability and dosimetry were measured by collecting cells 24 hours after the exposures, at day 1 and 7 as shown in Figure 6.1.

Morphology.

Microscopic images were captured using a Nikon inverted microscope equipped with phase-contrast optics (Nikon, Tokyo, Japan) to evaluate and monitor morphological changes of proliferating and differentiating hNPCs after AgNP exposures for 24 hours. 100X morphological images were captured and digitized using a Coolsnap Camera (Roper Scientific, Inc., Duluth, GA, USA) attached to the microscope.

Cell viability measured by Alamar Blue assay.

Dose-dependent cell viability 24 hours of AgNP treatment was quantified using Alamar Blue assay (Invitrogen, Waltham, MA, USA). Into each 96-well, 10% Alamar Blue (v/v) was added 3 hours prior to 24-hour time points and was incubated at 37°C with 5% CO_2. The 96-well plates with Alamar Blue reagent were then read on SpectraMax Gemini XS plate reader (Molecular Devices, Sunnyvale, CA, USA) at the emission wavelength of 570 nm and the reference wavelength of 630 nm. Live cells reduce non-fluorescent, blue resazurin dye into fluorescent, red resorufin via functional mitochondrial reductase activity unlike damaged or dead cells (O'Brien et al., 2000). These changes in cell's ability to reduce Alamar Blue reagent are detected, and the fluorescence intensities are reported.

To calculate percent viability relative to coating controls, a background fluorescence level (media without cells) was measured every time we performed the assay. This fluorescence was subtracted from those measured after AgNP treatments on hNPCs, then divided with appropriate coating control fluorescence levels in order to normalize values by coating controls as shown below.

$$\%\ \text{Cell Viability} = \frac{\text{Fluorescence}_{\text{treatment}} - \text{Fluorescence}_{\text{media background}}}{\text{Fluorescence}_{\text{coating control}} - \text{Fluorescence}_{\text{media background}}}\ \text{x}\ 100\ \%$$

The results were expressed as average percent of controls ± 95% confidence interval. All results were presented from 4 – 5 biological replicates.

Statistical analysis.

For 20 nm AgCitrate, 110 nm AgCitrate, or 110 nm AgPVP at each time points (DIV 8, 15, and 22), a linear mixed effects dose-response model was used to analyze significant differences among nominal treatment doses. Fixed and random effects included concentrations of AgNPs and experimental dates, respectively, in order to account for any variability between different experiment dates. The significance of dose-response curves, exposure timing, particle sizes, and particle coatings on cytotoxicity was investigated using analysis of variance (ANOVA). A posthoc analysis was then followed in order to compare between time points and particles for multi-parameter conditions.

All statistical analyses (dose-response and dosimetry adjusted cytotoxicity) were performed with "lme4" and "multcomp" packages (Bates et al., 2014) in R statistical software (https://www.R-project.org).

RESULTS

Morphology of proliferating and differentiating hNPCs after 24-hour exposures to AgNPs.

After 24 hours of exposures to 20 nm AgCitrate, 110 nm AgCitrate, and 110 nm AgPVP, changes in morphology were assessed by taking 100X phase-contrast microscopic images. A dose-dependent decrease in cell viability was observed for both proliferating and differentiating hNPCs upon 24-hour exposures to AgNPs at day 0 (Figure 6.2). At day 7, differentiating hNPCs exposed to AgNPs with various sizes and coatings illustrated dose-dependent cell viability (Figure 6.2). For all particles at all time points, reduced confluence was observed at the highest concentration of hNPCs treated with AgNPs in proliferation and differentiation condition.

Cell viability after AgNPs treatment.

An *in vitro* hNPCs culture system was used to assess the effects of various AgNPs on cell viability via Alamar blue assay. Cytotoxicity was measured 24 hours after AgNPs treatment at day 0 and day 6 as shown in Figure 6.1. At day 0, hNPCs were in two different conditions—either in proliferation or differentiation—while only differentiating hNPCs were exposed to AgNPs at day 6. Effects of dose, particle coatings and sizes, and exposure timing were examined.

Effects of particle coatings on cytotoxicity were investigated using proliferating and differentiating hNPCs. Comparing responses to 110 nm AgCitrate (Figure 6.3 purple) and 110 nm AgPVP (Figure 6.3 black) exposures revealed that particle coatings contribute to AgNP sensitivity on proliferating hNPCs at day 1 (p-value < 0.01) and differentiating hNPCs at day 7 (p-value < 0.01). For differentiating hNPCs exposed to 110 nm AgCitrate at day 1 and 7, larger slopes were found compared to 110 nm AgPVP. The slopes, however, were significantly different between 110 nm AgCirate and AgPVP only at day 7 (p-value < 0.01).

Differences in response due to particle sizes were observed when cytotoxicity after exposures to 20 nm (Figure 6.4 red) and 110 nm AgCitrate (Figure 6.4 purple) was compared. We found significant differences in cytotoxicity due to particle sizes in proliferating and differentiating hNPCs at day 1 and differentiating

hNPCs at day 7 (Figure 6.4). A posthoc test revealed a significant effect of size on cytotoxicity at day 1 proliferating hNPCs (p-value < 0.001), at day 1 differentiating hNPCs (p-value < 0.05), and at day 7 differentiating hNPCs (p-value < 0.05) as illustrated in Figure 7.4. This result suggested that particle size contributes to adverse effects on cytotoxicity.

Neurodevelopmental stages also affected responses of proliferating and differentiating hNPCs to AgNPs. Proliferating hNPCs at day 1 were sensitive to 20 nm AgCitrate than differentiating hNPCs at day 7 (Figure 6.5; p-value < 0.01) while differentiating hNPCs at day 1 were more vulnerable to 20 nm AgCitrate than those at day 7 (Figure 6.5; p-value < 0.05). For 110 nm AgCitrate, proliferating and differentiating hNPCs at day 1 were less viable compared to differentiating hNPCs at day 7 (Figure 6.5; p-value < 0.001 for both times). However, no significant differences in slopes were found for 110 nm AgPVP among three developmental stages.

Significant dose-response relationships were observed for all particles at all times (Figure 6.5; p-value < 0.001 except differentiating hNPCs exposed to 110 nm AgCitrate at day 7, which has p-value < 0.01).

DISCUSSION

Effects of various engineered nanomaterials (ENMs) are still an area that needs to be investigated for its potential adverse effects. Silver nanoparticles (AgNPs) are ENMs that are used in many consumer products from children's toys to clothes and cosmetics (Woodrow Wilson International Center for Scholars, 2016). The adverse effects of AgNPs have not been fully understood. With an increasing number of research studies reporting the potential of AgNPs as neurodevelopmental toxicants (Fennell et al., 2017; Loeschner et al., 2011; Morishita et al., 2016; Patchin et al., 2016; Tang et al., 2009; Tang et al., 2010; Yang et al., 2010), we focused on assessing the sensitivity of proliferating and differentiating human neural progenitor cells (hNPCs) *in vitro* to AgNPs with different sizes and coatings. We examined factors that can contribute to susceptibility of hNPCs including AgNP size, coating, and exposure timing.

Compared to *in vivo* developmental toxicology models that require a substantial number of animals, labor-intensive, and time-consuming, *in vitro* models offer several advantages. Multiple end points can be examined simultaneously at lower cost, allowing for high throughput and high content assessments. These characteristics of *in vitro* models become attractive and powerful especially when trying to keep pace with

assessing toxicity for newly developed chemicals that grow exponentially with time. Neurodevelopmental Toxicology is an area where there is a pressing need to develop and evaluate *in vitro* alternative methods (Aschner et al., 2010; Bal-Price et al., 2012; Coecke et al., 2007; Crofton et al., 2014; Crofton et al., 2012; Crofton et al., 2011; Lein et al., 2007) and anchor scientific findings back to *in vivo* biology to protect environmental and human health.

Additional advantages of using *in vitro* hNPCs model include its potential to recapitulate neural proliferation, migration, differentiation, and functional maturation *in vitro*. Moreover, hNPCs are a human-derived cell line, which may more closely represent human brain developmental processes and reflect potential effects of neurotoxicants than rodent-derived cell lines. Because different morphogenic signals lead to various regional identification and specific neuronal cell fates in differentiating hNPCs, use of hNPCs also offer potential to assess regional- and stage-specific effects of potential neurotoxicants.

Previously, we have developed our *in vitro* hNPCs culture system (Wegner et al., 2014) and discovered that gene expressions of our *in vitro* hNPCs were comparable to those of *in vivo* human neocortex provided by the Allen Brain Institute (Kang et al., 2011). We reported that differentiating hNPCs *in vitro* captured key brain developmental processes including NPC proliferation, forebrain neuron differentiation, epigenetic changes, transmission of glutamate, and oxidative stress (Park et al., 2017).

Using this system, we examined impacts of two particle coatings—citrate and polyvinylpyrrolidone (PVP) on proliferating and differentiating hNPCs. The particle coatings are used to stabilize AgNPs by moderating aggregation and agglomeration effects. We found that particle coatings significantly contribute to a decrease in cell viability for hNPCs at different neurodevelopmental stages. At day 1 and 7, larger slopes for differentiating hNPCs exposed to 110 nm AgCitrate than 110 nm AgPVP were observed (Figure 6.3). Weldon et al. (2017) discovered that coating had a significant effect on cytotoxicity at days *in vitro* (DIV) 22 using embryonic A/J midbrain micromass system; however, this effect disappeared after adjusting cytotoxicity using dosimetry. Upon adjusting to dosimetry, effects of particle coatings on our proliferating and differentiating hNPCs may also change, suggesting that dosimetry analysis would be critical in better understanding the impacts of coating on cell viability. Previous studies have been reporting mixed messages regarding the effects of nanoparticle coatings. Studies like Recordati et al. (2016) found that coating did not contribute to tissue distribution of AgNPs and hepatobiliary toxicity in male CD-1 mice after single intravenous exposures. However, Wang et al. (2014) and Wu et al. (2015) discovered that PVP

coating decreased pulmonary cytotoxicity and spatial cognition when compared to uncoated particles. However, these heterogeneous study reports may be due to examining different organ systems, cell types, and AgNPs.

Particle sizes were also shown to affect susceptibility to AgNPs on proliferating and differentiating hNPCs. Proliferating hNPCs were more vulnerable to larger particles while differentiating hNPCs were more sensitive to smaller particles (Figure 6.4). Our results regarding differentiating hNPCs are consistent with previous studies. Patchin et al. (2016) and Recordati et al. (2016) concluded that greater amount of smaller AgNPs deposit more in the rodent brain, which then leads to higher cytotoxicity. Moreover, Weldon et al. (2017) discovered that *in vitro* 3D mouse micromass culture system showed higher cytotoxicity after exposures to smaller particle (20 nm AgCitrate) at DIV 15 and 22; however, the culture was more sensitive to larger particle (110 nm AgCitrate) at DIV 8. However, with limited studies demonstrating adverse impacts of particle sizes on proliferating versus differentiating hNPCs, further validation studies to check if proliferating cells are more vulnerable to large particles needs to be assessed.

Effects of developmental status of hNPCS in response to AgNPs were also investigated. Proliferating and differentiating hNPCs revealed that developmental stages contributed to differences in response after 20 nm AgCitrate or 110 nm AgCitrate exposures, but not after 110 nm AgPVP exposures (Figure 6.5). This finding suggested that proliferation and early differentiation may be the "windows of susceptibility," which is consistent with conclusions drawn by Weldon et al. (2017). This is also the case for many other toxicants (Rodier, 1995, 1994) including manganese (Hernandez et al., 2011), lead (Bull et al., 1983; Deng et al., 2001; Silbergeld, 1992), and methylmercury (Barone et al., 1998). Exposures to these compounds during early neurodevelopmental stages lead to greater sensitivity compared to those exposed at late neural differentiation stages.

Our culture system has some limitations. First, we only investigated the effects of AgNPs on hNPCs derived from WA09 cells. These cells have normal 46 chromosomes with XX karyotype as described in WiCell (2014). It would be interesting to examine hNPCs with XY karyotypes to better understand potential gender differences in response to AgNP exposures as no such information exist to draw conclusions on gender-related differences (Llop et al., 2013). We also did not measure the extent of aggregation and agglomeration of AgNPs in media, which may result in decreased delivery rate to cells and affect AgNP uptakes and cell viability. Images of AgNP exposed cells were captured using phase microscope, but

visualization of cells via electron microscopy will be critical. Dosimetry also needs to be measured. This assessment will allow us to quantitate the amount of AgNPs associated with cells and provide a deeper insight on dose-response relationships. Microscopic images together with dosimetry will inform us if dissolution or intact particles are taken up by hNPCs. Elucidating mechanism of toxicity for AgNPs will also be important future study.

In this study, we have demonstrated that proliferating and differentiating hNPCs *in vitro* are sensitive to AgNPs. Particle coatings, sizes, and time of exposures were found to be contributory factors in response to AgNP exposures. Proliferating hNPCs were more sensitive to larger sized AgNPs while differentiating hNPCs were more vulnerable to smaller sized AgNPs. The model also illustrated that the cultures were more susceptible to AgNP exposures at early stages, at day 1, rather than at day 7. The current study adds to the information on AgNP-induced toxicity by examining potential impacts of particle coatings, sizes, and time of exposure using *in vitro* hNPCs model.

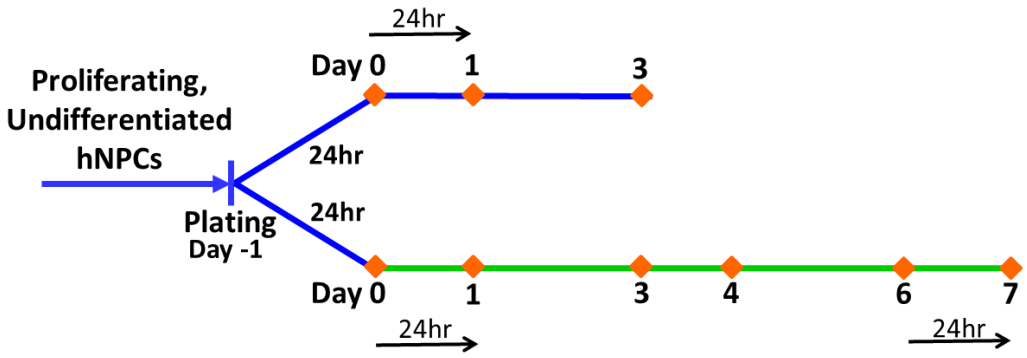

Figure 6.1. Study design for silver nanoparticle (AgNP) exposures on proliferating and differentiating human neural progenitor cells (hNPCs). Proliferating hNPCs were exposed to 20 nm AgCitrate, 110 nm AgCitrate, and 110 nm AgPVP for 24 hours at day 0, and differentiating hNPCs were treated at day 0 and 6 for 24 hours.

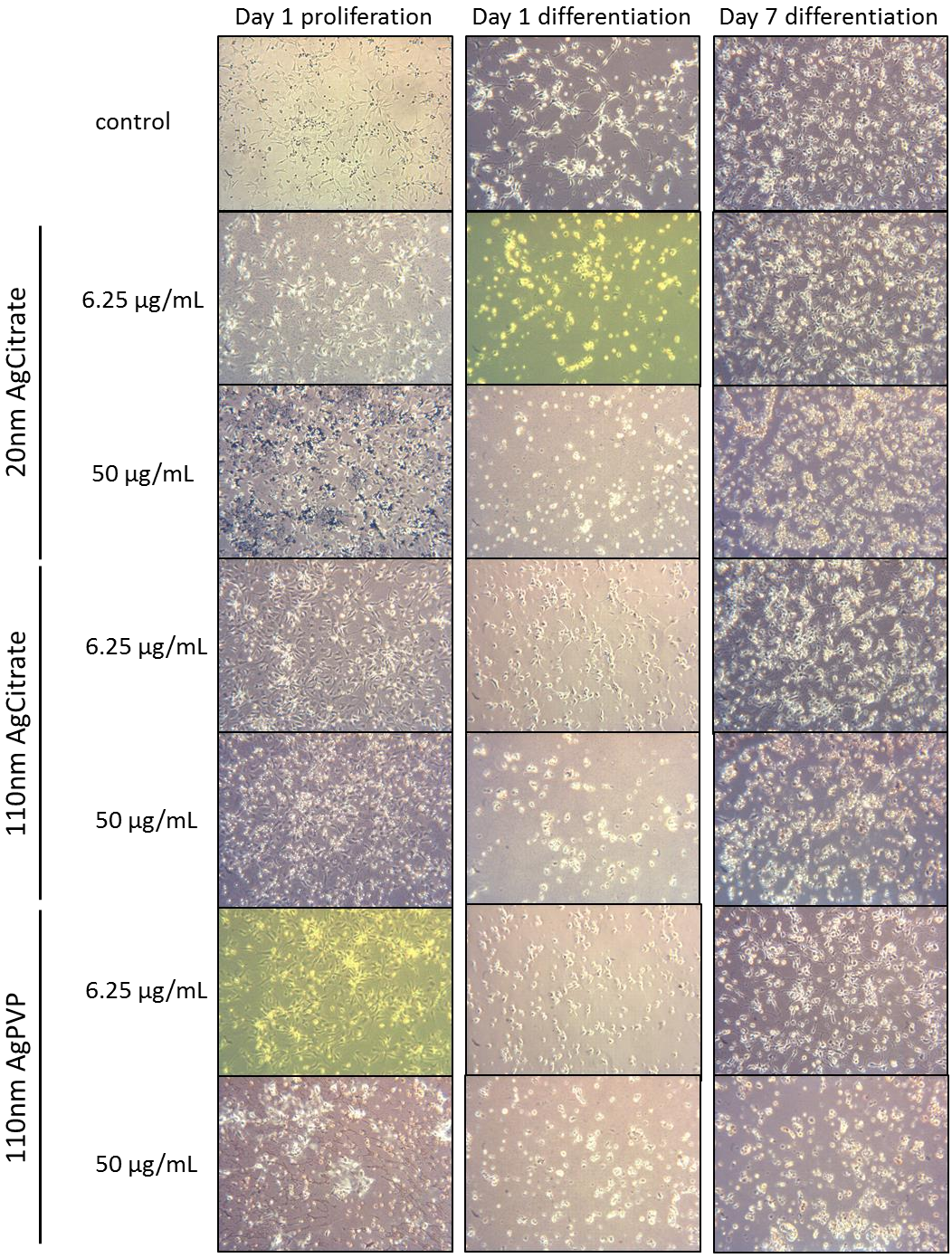

Figure 6.2. 100X phase microscope morphology of proliferating and differentiating hNPCs after 24 hours of AgNP exposures at day 1 and 7. The decrease in cell viability was observed for all particles at all time points (day 1 proliferation and differentiation and day 7 differentiation).

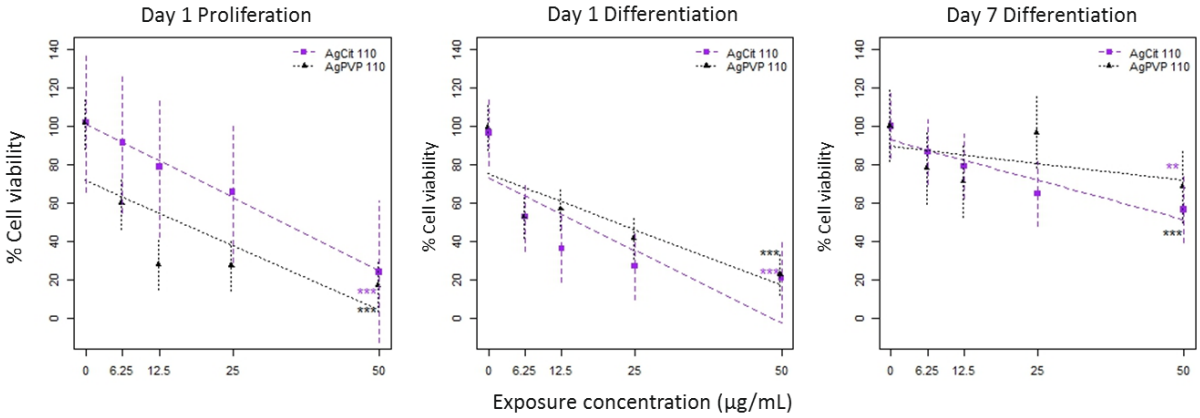

Figure 6.3. Dose-response curve for proliferating and differentiating hNPCs after 24 hours of 110 nm AgCirate and AgPVP exposures (coating comparison). Significant dose-response relationships were observed for both 110 nm particles (AgCitrate and AgPVP) at all times. At day 1 and 7, larger slopes were observed for differentiating hNPCs exposed to 110nm AgCitrate (purple) compared to 110 nm AgPVP (black). Plots show means ± 95% confidence intervals. Data points and lines were estimated from the mixed-effect model. **: p-value < 0.01 and ***: p-value < 0.001 represent significant dose response.

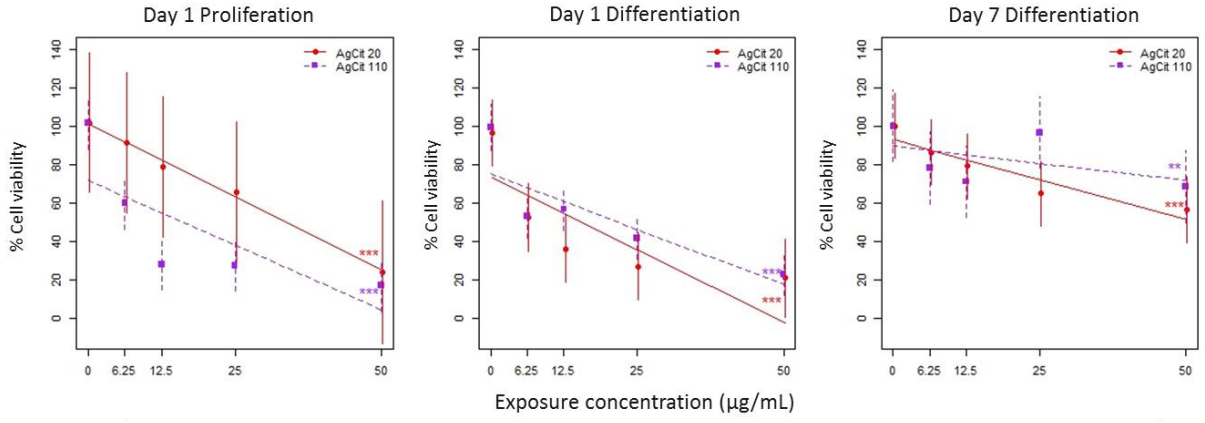

Figure 6.4. Dose-response curve for proliferating and differentiating hNPCs after 24 hours of 20 nm and 110 nm AgCirate exposures (size comparison). Significant dose-response relationships were found for 20 nm and 110 nm AgCitrate particles at all times. Proliferating and differentiating hNPCs at day 1 and differentiating hNPCs at day 7 demonstrated significant differences in response due to particle sizes. Plots show means ± 95% confidence intervals. Data points and lines were estimated from the mixed-effect model. **: p-value < 0.01 and ***: p-value < 0.001 represent significant dose response.

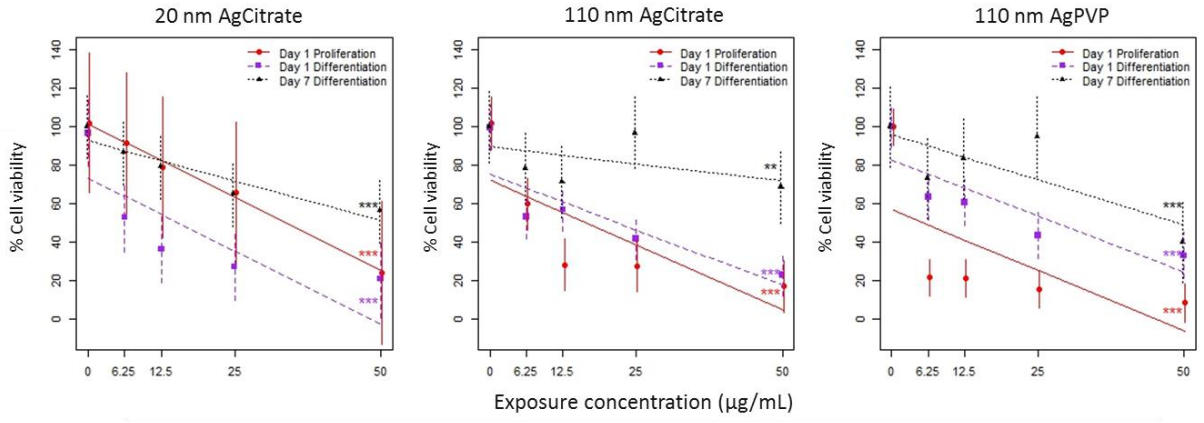

Figure 6.5. Dose-response curve for proliferating and differentiating hNPCs after 24 hours of various AgNP exposures (comparing the time of exposure). Significant dose-response relationships were found for all nanoparticles at all times. For 20 nm and 110 nm AgCitrate, proliferating (red) and differentiating (purple) hNPCs at day 1 were more vulnerable to AgNP exposures compared to differentiating hNPCs at day 7. No significant differences in slopes were observed for 110 nm AgPVP among developmental stages. Plots show means ± 95% confidence intervals. Data points and lines were estimated from the mixed-effect model. **: p-value < 0.01 and ***: p-value < 0.001 represent significant dose response.

CHAPTER 6 REFERENCES

Aschner, M., Crofton, K. M. and Levin, E. D. (2010). Introduction to the special issue on emerging high throughput and complementary model screens for neurotoxicology. *Neurotoxicol Teratol 32*, 1-3. http://dx.doi.org/10.1016/j.ntt.2009.08.006

Bailey, J., Knight, A. and Balcombe, J. (2005). The future of teratology research is in vitro. *Biogenic Amines 19*, 97-145.

Bal-Price, A. K., Coecke, S., Costa, L. et al. (2012). Advancing the science of developmental neurotoxicity (DNT): testing for better safety evaluation. *ALTEX 29*, 202-215.

Barone, S., Jr., Haykal-Coates, N., Parran, D. K. et al. (1998). Gestational exposure to methylmercury alters the developmental pattern of trk-like immunoreactivity in the rat brain and results in cortical dysmorphology. *Brain Res Dev Brain Res 109*, 13-31.

Bates, D., Machler, M., Bolker, B. M. et al. (2014). Fitting linear mixed-effects models using lme4. *Journal of Statistical Software 67*, 1-48.

Bull, R. J., McCauley, P. T., Taylor, D. H. et al. (1983). The effects of lead on the developing central nervous system of the rat. *Neurotoxicology 4*, 1-17.

Coecke, S., Goldberg, A. M., Allen, S. et al. (2007). Workgroup report: incorporating in vitro alternative methods for developmental neurotoxicity into international hazard and risk assessment strategies. *Environ Health Perspect 115*, 924-931. http://dx.doi.org/10.1289/ehp.9427

Crofton, K., Fritsche, E., Ylikomi, T. et al. (2014). International STakeholder NETwork (ISTNET) for creating a developmental neurotoxicity testing (DNT) roadmap for regulatory purposes. *ALTEX 31*, 223-224. http://dx.doi.org/http://dx.doi.org/10.14573/altex.1402121

Crofton, K. M., Mundy, W. R., Lein, P. J. et al. (2011). Developmental neurotoxicity testing: recommendations for developing alternative methods for the screening and prioritization of chemicals. *ALTEX 28*, 9-15.

Crofton, K. M., Mundy, W. R. and Shafer, T. J. (2012). Developmental neurotoxicity testing: a path forward. *Congenit Anom (Kyoto) 52*, 140-146. http://dx.doi.org/10.1111/j.1741-4520.2012.00377.x

Deng, W., McKinnon, R. D. and Poretz, R. D. (2001). Lead exposure delays the differentiation of oligodendroglial progenitors in vitro. *Toxicol Appl Pharmacol 174*, 235-244. http://dx.doi.org/10.1006/taap.2001.9219

El-Nour, K. M. M. A., Eftaiha, A., Al-Warthan, A. et al. (2010). Synthesis and applications of silver nanoparticles. *Arabian Journal of Chemistry 3*, 135-140.

Fennell, T. R., Mortensen, N. P., Black, S. R. et al. (2017). Disposition of intravenously or orally administered silver nanoparticles in pregnant rats and the effect on the biochemical profile in urine. *J Appl Toxicol 37*, 530-544. http://dx.doi.org/10.1002/jat.3387

Genschow, E., Spielmann, H., Scholz, G. et al. (2002). The ECVAM international validation study on in vitro embryotoxicity tests: results of the definitive phase and evaluation of prediction models. European Centre for the Validation of Alternative Methods. *Altern Lab Anim 30*, 151-176.

Grandjean, P. and Landrigan, P. J. (2006). Developmental neurotoxicity of industrial chemicals. *Lancet 368*, 2167-2178. http://dx.doi.org/10.1016/S0140-6736(06)69665-7

Hernandez, R. B., Farina, M., Esposito, B. P. et al. (2011). Mechanisms of manganese-induced neurotoxicity in primary neuronal cultures: the role of manganese speciation and cell type. *Toxicol Sci 124*, 414-423. http://dx.doi.org/10.1093/toxsci/kfr234

Kang, H. J., Kawasawa, Y. I., Cheng, F. et al. (2011). Spatio-temporal transcriptome of the human brain. *Nature 478*, 483-489. http://dx.doi.org/10.1038/nature10523

Krewski, D., Acosta, D., Jr., Andersen, M. et al. (2010). Toxicity testing in the 21st century: a vision and a strategy. *J Toxicol Environ Health B Crit Rev 13*, 51-138. http://dx.doi.org/10.1080/10937404.2010.483176

Lein, P., Locke, P. and Goldberg, A. (2007). Meeting report: alternatives for developmental neurotoxicity testing. *Environ Health Perspect 115*, 764-768. http://dx.doi.org/10.1289/ehp.9841

Levard, C., Hotze, E. M., Lowry, G. V. et al. (2012). Environmental transformations of silver nanoparticles: impact on stability and toxicity. *Environ Sci Technol 46*, 6900-6914. http://dx.doi.org/10.1021/es2037405

Llop, S., Lopez-Espinosa, M. J., Rebagliato, M. et al. (2013). Gender differences in the neurotoxicity of metals in children. *Toxicology 311*, 3-12. http://dx.doi.org/10.1016/j.tox.2013.04.015

Loeschner, K., Hadrup, N., Qvortrup, K. et al. (2011). Distribution of silver in rats following 28 days of repeated oral exposure to silver nanoparticles or silver acetate. *Part Fibre Toxicol 8*, 18. http://dx.doi.org/10.1186/1743-8977-8-18

Miodovnik, A. (2011). Environmental neurotoxicants and developing brain. *Mt Sinai J Med 78*, 58-77. http://dx.doi.org/10.1002/msj.20237

Morishita, Y., Yoshioka, Y., Takimura, Y. et al. (2016). Distribution of Silver Nanoparticles to Breast Milk and Their Biological Effects on Breast-Fed Offspring Mice. *ACS Nano 10*, 8180-8191. http://dx.doi.org/10.1021/acsnano.6b01782

National Research Council Committee on Developmental Toxicology (2000). In (eds.), *Scientific Frontiers in Developmental Toxicology and Risk Assessment*. Washington (DC): National Academies Press (US)

http://dx.doi.org/10.17226/9871

O'Brien, J., Wilson, I., Orton, T. et al. (2000). Investigation of the Alamar Blue (resazurin) fluorescent dye for the assessment of mammalian cell cytotoxicity. *Eur J Biochem 267*, 5421-5426.

Park, J. J., Wegner, S. H., Workman, T. et al. (2017). Concordance of in vitro and in vivo gene expression dynamics for specific pathways of interest for developmental neurotoxicity. PhD, University of Washington,

Patchin, E. S., Anderson, D. S., Silva, R. M. et al. (2016). Size-Dependent Deposition, Translocation, and Microglial Activation of Inhaled Silver Nanoparticles in the Rodent Nose and Brain. *Environ Health Perspect 124*, 1870-1875. http://dx.doi.org/10.1289/ehp234

Piersma, A. H. (2004). Validation of alternative methods for developmental toxicity testing. *Toxicol Lett 149*, 147-153. http://dx.doi.org/10.1016/j.toxlet.2003.12.029

Pratten, M., Ahir, B. K., Smith-Hurst, H. et al. (2012). Primary cell and micromass culture in assessing developmental toxicity. *Methods Mol Biol 889*, 115-146. http://dx.doi.org/10.1007/978-1-61779-867-2_9

Quadros, M. E., Pierson, R. t., Tulve, N. S. et al. (2013). Release of silver from nanotechnology-based consumer products for children. *Environ Sci Technol 47*, 8894-8901. http://dx.doi.org/10.1021/es4015844

Recordati, C., De Maglie, M., Bianchessi, S. et al. (2016). Tissue distribution and acute toxicity of silver after single intravenous administration in mice: nano-specific and size-dependent effects. *Part Fibre Toxicol 13*, 12. http://dx.doi.org/10.1186/s12989-016-0124-x

Reidy, B., Haase, A., Luch, A. et al. (2013). Mechanisms of Silver Nanoparticle Release, Transformation and Toxicity: A Critical Review of Current Knowledge and Recommendations for Future Studies and Applications. *Materials 6*, 2295.

Rice, D. and Barone, S. (2000). Critical periods of vulnerability for the developing nervous system: Evidence from humans and animal models. *Environmental Health Perspectives 108*, 511-533. http://dx.doi.org/Doi 10.2307/3454543

Rodier, P. M. (1994). Vulnerable periods and processes during central nervous system development. *Environ Health Perspect 102 Suppl 2*, 121-124.

Rodier, P. M. (1995). Developing Brain as a Target of Toxicity. *Environmental Health Perspectives 103*, 73-76. http://dx.doi.org/Doi 10.2307/3432351

Silbergeld, E. K. (1992). Mechanisms of lead neurotoxicity, or looking beyond the lamppost. *FASEB J 6*, 3201-3206.

Tang, J., Xiong, L., Wang, S. et al. (2009). Distribution, translocation and accumulation of silver nanoparticles in rats. *J Nanosci Nanotechnol 9*, 4924-4932.

Tang, J., Xiong, L., Zhou, G. et al. (2010). Silver nanoparticles crossing through and distribution in the blood-brain barrier in vitro. *J Nanosci Nanotechnol 10*, 6313-6317.

Tulve, N. S., Stefaniak, A. B., Vance, M. E. et al. (2015). Characterization of silver nanoparticles in selected consumer products and its relevance for predicting children's potential exposures. *Int J Hyg Environ Health 218*, 345-357. http://dx.doi.org/10.1016/j.ijheh.2015.02.002

Wang, X., Ji, Z., Chang, C. H. et al. (2014). Use of coated silver nanoparticles to understand the relationship of particle dissolution and bioavailability to cell and lung toxicological potential. *Small 10*, 385-398. http://dx.doi.org/10.1002/smll.201301597

Wegner, S. H., Stanaway, I. B., Kim, H. Y. et al. (2014). Anchoring a dynamic *in vitro* model of human neuronal differentiation to key processes of early brain development *in vivo*. Ph.D., University of Washington,

Weldon, B. A., Park, J. J., Hong, S. et al. (2017). Effects of developmental stage, particle size, and coating on dosimetry and toxicity of silver nanoparticles in developing primary organotypic mouse midbrain cultures. Ph.D., University of Washington,

Woodrow Wilson International Center for Scholars (2016). The project on emerging nanotechnologies.

Wu, J., Yu, C., Tan, Y. et al. (2015). Effects of prenatal exposure to silver nanoparticles on spatial cognition and hippocampal neurodevelopment in rats. *Environ Res 138*, 67-73. http://dx.doi.org/10.1016/j.envres.2015.01.022

Yang, Z., Liu, Z. W., Allaker, R. P. et al. (2010). A review of nanoparticle functionality and toxicity on the central nervous system. *J R Soc Interface 7 Suppl 4*, S411-422. http://dx.doi.org/10.1098/rsif.2010.0158.focus

Yokel, R. A. and Macphail, R. C. (2011). Engineered nanomaterials: exposures, hazards, and risk prevention. *J Occup Med Toxicol 6*, 7. http://dx.doi.org/10.1186/1745-6673-6-7

CHAPTER 7: Evaluation of cadmium effects on epigenetics using *in vitro* proliferating and differentiating human neural progenitor cell (hNPCs) cultures

This Chapter is in preparation for submission. The authors of the manuscript are:

Julie Juyoung Park[1, 2], Tomomi Workman[1], Sungwoo Hong[2], William Griffith[1], Elaine M. Faustman[1, 2*]

[1] Institute for Risk Analysis and Risk Communication, University of Washington, Seattle, WA, USA

[2] Department of Environmental and Occupational Health Sciences, University of Washington, Seattle, WA, USA

* Corresponding author: Elaine M. Faustman

Institute for Risk Analysis and Risk Communication, Department of Environmental and Occupational Health Sciences, University of Washington, Seattle, WA, USA.

Email: faustman@uw.edu

ABSTRACT

Cadmium (Cd), a naturally occurring heavy metal, is used in many industrial settings including electroplating, batteries, and pigments. Despite its usefulness, environmental and occupational exposures to Cd in humans are known to cause adverse effects such as “Itai-Itai” disease. Because the period of development is sensitive time frames, where exposures to toxicants can lead to long-lasting adverse health effects, it is important to examine the effects of Cd during development and define critical “windows of susceptibility.” Neurodevelopment is especially an important area to research because developing fetuses and young children do not have a fully developed blood-brain barrier. The objective of the study was to examine impacts of Cd on neurodevelopment *in vitro*. Proliferating hNPCs at day 0 and differentiating hNPCs at day 0 and 6 were treated with Cd (0 – 10 µM), and various end points including morphology, cell viability, protein expressions, and epigenetics were examined after 24 hours of exposure. Morphological images and Alamar blue assay revealed a significant decrease in cell viability for all hNPCs at different neurodevelopmental stages. Dosimetry analysis was also performed to predict neurotoxicity more accurately, but still found differentiating hNPCs at day 1 most susceptible to Cd exposures. Differential effects of protein expressions and histone modifications were found for hNPCs at various status. These suggested stage-specific effects of Cd. This study defines time as an important factor influencing sensitivity during neurodevelopment.

INTRODUCTION

Cadmium (Cd) is a heavy metal found in Earth's crust, but it also has many industrial uses including electroplating, pigments, batteries, electronic wastes, and plastics. Humans can also be exposed to Cd by cigarette smoking and by diet when consuming leafy vegetables, potatoes, grains and cereals (Agency for Toxic Substances and Disease Registry (ATSDR), 2008; Jarup and Akesson, 2009; Ray et al., 2014) because it occurs naturally in our environment. Despite its usefulness and abundance, Cd is one of the most toxic heavy metal in occupational and environmental settings. Upon exposures, Cd not only accumulates in our body over time but also have very slow excretion rate with the biological half-life of 15 to 30 years (Domingo, 1994; Godt et al., 2006; Ray et al., 2014). Chronic exposures to Cd is known to result in hepatotoxicity, nephrotoxicity, cancer, and reproductive and developmental toxicity. It is also known to be associated with "Itai-Itai" disease in Japan, which is toxicity exerted on bone including osteoporosis and osteomalacia (Ray et al., 2014). Unlike other toxic metals, Cd has been found to accumulate in placenta and may disrupt endocrine hormone synthesis and/or release (Henson and Chedrese, 2004; Lee et al., 2009). In addition, Flora et al. (2011) observed hydrocephaly when treated rats with Cd between gestational day 8 to 12 via intravenous (i.v.) injection. They hypothesized that vulnerability of the developing central nervous system (CNS) upon Cd exposures may be due to lack of functional blood-brain barrier in addition to disruption of the complex yet highly orchestrated cellular proliferation, differentiation, and synaptogenesis (Flora et al., 2011). Yet, limited information on the effects of Cd exposures during neurodevelopment is available.

Little is known about the mechanism of toxicity for Cd. Fotakis and Timbrell (2006) revealed that the mechanism of Cd toxicity in hepatoma cell lines involves affecting transporter pathways by competing with zinc and calcium. This may also be potential mechanisms for neurotoxicity as insufficient zinc concentrations during development may lead to growth retardation and changes in cognitive function (Flora et al., 2011). It is also suggested that exposures to Cd may result in generation of reactive oxygen species, which in turn cause necrosis. Moreover, Zhang et al. (2009) discovered that heavy metals including Cd decrease acetylcholine esterase activities leading to CNS function and structural impairment via oxidative stress. However, limited understandings of the mechanism of developmental neurotoxicity for Cd exist. Because neurodevelopment is one of the most sensitive time frames and perturbations during this period can lead to life-long effects, it is important to elucidate mechanisms of action for Cd toxicity during neurodevelopment.

In addition to the mechanism of toxicity, examining Cd-induced epigenetic changes is also important because of its potential to be inheritable. Previously, we illustrated that different compounds at various neurodevelopmental stages pose different effects on epigenetics. For example, exposures to an organophosphate pesticide, chlorpyrifos, significantly increased phosphorylation and di-methylation of histone H3 at serine 10 and lysine 4 in proliferating human neural progenitor cells (hNPCs), respectively (Kim et al., 2016). A significant decrease in HDAC4 and increase in di-methylation at histone H3 lysine 4, however, were observed in differentiating hNPCs as shown in Kim et al. (2016). We have also demonstrated that arsenic has differential effects on epigenetics compared to chlorpyrifos. Exposures to arsenic in proliferating and differentiating hNPCs significantly increased acetylation of histone H3 lysine 9 as well as a significant increase in phosphorylation of histone H3 in differentiating cells (Kim et al., 2016). For Cd, Gadhia et al. (2015) reported that mono-methylation of histone H3 lysine 27 was affected by acute Cd exposures on *in vitro* mouse embryonic stem cells. An increased tri-methylation at histone H3 sites lysine 4, 9, and 27 were also observed on transformed urothelial cells exposed to Cd (Somji et al., 2011). In addition to histone changes at specific sites, exposures to Cd have also been associated with upregulation of DNA methyltransferase (DMNT) 3B and 3L (Xu et al., 2016).

With a hope to enhance our understanding of the mechanism of action for Cd-induced neurotoxicity as well as epigenetic changes, this study utilized *in vitro* human neural progenitor cell (hNPCs) cultures discussed in Chapter 4 (Wegner et al., 2014). Previously, we have successfully anchored gene expressions of our *in vitro* differentiating hNPCs to those from the human *in vivo* data provided by the Allen Brain Institute (Wegner et al., 2014). This suggested that our *in vitro* hNPCs have the capacity to capture key processes of early neurodevelopment *in vivo* including proliferation, differentiation, and synapse formation. Another advantage of hNPCs culture system is its potential as a high throughput and high content yet reproducible *in vitro* neurodevelopmental toxicity screening model (Wegner et al., 2014). Moreover, the cell line is a human origin, which increases the likelihood that observed *in vitro* effects will be consistent with those seen in humans. The current study aims to investigate the effects of acute Cd exposures on cell viability, neuronal protein expressions, and epigenetics at various stages of neurodevelopment using *in vitro* hNPCs model.

METHODS

Human neural progenitor cell culture system.

Commercially available hNP1™ human neural progenitor cells (hNPCs; ArunA Biomedical, Athens, GA, USA) were expanded for eight passages in proliferative conditions using AB2™ neural cell culture media (ArunA Biomedical, Athens, GA, USA). Cells were plated onto Matrigel-coated 96-well black bottom microplates (Becton, Dickinson Co., Franklin Lakes, NJ, USA) or 35 x 10 mm dishes (Corning Life Science, Corning, NY, USA) at the density of 200,000 cells/mL. Cells were then allowed to attach in proliferative AB2™ neural cell culture media (ArunA Biomedical, Athens, GA, USA) at 37°C with 5% CO_2. After 24 hours of plating, hNPCs were treated with cadmium either in proliferation or differentiation condition by replacing media with HyClone™ differentiation media (GE Healthcare Life Sciences, Little Chalfont, United Kingdom).

Treatment with cadmium.

Cadmium chloride (Cd; Sigma-Aldrich, St. Louis, MO, USA) was dissolved in UltraPure™ distilled water (Invitrogen, Waltham, MA, USA) and filtered for sterilization. The initial study examined a range of Cd concentrations (0 – 50 µM) based on previous *in vitro* studies (Buzanska et al., 2009; Culbreth et al., 2012; Gartlon et al., 2006). Working concentrations of 0, 0.1, 1, and 10 µM were established from the pilot Alamar Blue viability assay results. Cd was diluted either in proliferation or differentiation media for treatments administered 24 hours after plating. Differentiating hNPCs were also treated with Cd 7 days after the initial plating to investigate effects at later differentiation stage. Cell viability, the amount of Cd associated with hNPCs, and western blot analysis looking at changes in protein expressions and epigenetics were examined 24 hours after treatment as shown in Figure 7.1.

Morphology.

A Nikon inverted microscope armed with phase-contrast optics (Nikon, Tokyo, Japan) was used to monitor morphological changes of hNPCs in proliferation and differentiation conditions. 100X morphological images were captured and digitized using a Coolsnap Camera (Roper Scientific, Inc., Duluth, GA, USA) attached to the microscope.

Cell viability using Alamar Blue assay.

The Alamar Blue assay from Invitrogen (Invitrogen, Waltham, MA, USA) was used to measure dose-dependent cell viability after 24 hours of Cd treatment. 10% Alamar Blue (v/v) was added into each well of 96-well plates 3 hours in advance of 24-hour time points and was incubated at 37°C with 5% CO_2. The

96-well plates were then read on SpectraMax Gemini XS plate reader (Molecular Devices, Sunnyvale, CA, USA) at the 570 nm emission wavelength and the reference wavelength of 630 nm. Unlike damaged or dead cells, live cells have functional mitochondrial reductase activity and thus, have an ability to reduce non-fluorescent, blue resazurin dye into fluorescent, red resorufin (O'Brien et al., 2000). Alamar Blue detects these changes and reports the fluorescence intensity.

The fluorescence of media without cells was measured as a background fluorescence level every time we performed the assay. Fluorescence from the blank media were subtracted from those measured after Cd treatments on hNPCs, then divided with control fluorescence levels to normalize values by controls as shown below.

$$\%\ \text{Cell Viability} = \frac{\text{Fluorescence}_{\text{treatment}} - \text{Fluorescence}_{\text{media background}}}{\text{Fluorescence}_{\text{control}} - \text{Fluorescence}_{\text{media background}}} \text{ x } 100\ \%$$

The results were expressed as average percent of controls ± 95% confidence interval.

Measuring the amount of Cd associated with hNPCs.

To quantify cadmium (Cd) metals taken up by or associated with hNPCs, inductively coupled plasma mass spectrometer (ICP-MS) method was utilized as described in Weldon et al. (2017). Free and loosely associated Cd were removed without disrupting pH or other cell culture conditions by washing samples with 450 µL of respective proliferation or differentiation media three times. 450 µL of fresh media was added for the fourth time to collect the cells, which were then transferred to 15 mL polystyrene tubes (Corning Life Science, Corning, NY, USA). The samples were stored at 4°C until the ICP-MS analysis. Samples included nontreated (controls) and Cd treated (1 and 10 µM) hNPCs in proliferation condition at day 1 and in differentiation condition at day 1 and 7.

Samples were prepared prior to ICP-MS analysis by adding nitric acid (TraceMetal Grade; Fisher Scientific, Hampton, NH, USA) and hydrochloric acid (TraceMetal Grade; Fisher Scientific, Hampton, NH, USA). After preparing samples, digestion with an open-vessel microwave was performed using MARS Xpress microwave (CEM Corporation, Mathews, NC, USA) with 800 W power. The microwave temperature was increased to 90°C in 10 minutes with a 20-minute hold. The final concentrations of a digestate were adjusted to have 7% nitric acid, 2% hydrochloric acid, and 10 ng/mL terbium (Tb) by adding deionized water (≥ 18 Mohm). Tb served as an standard internal recovery (EPA, 2007).

For detecting Cd, an Agilent 7900 ICP-MS machine (Agilent Technologies, Santa Clara, CA, USA) was used. The temperature of a spray chamber was held at 2°C, and a carrier and helium gas flow rate of 1.08 L/min and 4.3 mL/min, respectively, were used for acquisition. To remove isobaric polyatomic interferences, helium gas was used. Isotopes ^{110}Cd in conjunction with internal standards ^{193}Ir, ^{89}Y, and Tb were quantified. BDH® ARISTAR® Mulit-Element ICP and ICP-MS Certified Reference Standards (VWR International, Radnor, PA, USA) with independent check standard from second vendor, Ultra Scientific (North Kingstown, RI, USA) were used to make calibration standards. Calibration was done approximately every 30 samples, and data obtained from ICP-MS were adjusted with process blanks. Amount of Cd in each cell fractions were reported relative to mg of protein, measured by Bradford protein assay (Bio-Rad Laboratories, Hercules, California, USA).

Western blot analysis.

Changes in protein expression after 24 hours of Cd exposures were semi-quantitatively examined using western blotting. Total protein samples were harvested using 1X cell lysis buffer (Cell Signaling Technology, Danvers, MA, USA) and kept frozen in -80°C until use.

The amount of protein present in each sample was measured using Bradford protein assay (Bio-Rad Laboratories, Hercules, California, USA). Samples were repeatedly frozen and thawed for three times then centrifuged at the maximum speed for 5 minutes. After quantification, samples were diluted with 2X sample buffer (Life Technologies, Carlsbad, CA, USA) and reducing agent (Life Technologies, Carlsbad, CA, USA) so that samples have equal protein concentrations. Protein samples were run on 4-12% bis-tris SDS-PAGE gels (Life Technologies, Carlsbad, CA, USA). Proteins were then transferred onto poly-vinyl difluoride membrane (Merck Millipore, Billerica, MA, USA). After transfer, membranes were washed for 10 minutes in 1X Tris-buffered saline (TBS) followed by an hour incubation in 5% milk to avoid non-specific protein bindings. Membranes were then washed in 1X TBS with Tween (TTBS) three times for 5 minutes each, and incubated in primary antibody (1:1000 – 1:5000) overnight at 4°C. Primary antibodies examined in this study is summarized in Table 7.1. These include nestin (Proteintech, Rosemont, IL, USA), proliferating cell nuclear antigen (PCNA; Merck Millipore, Billerica, MA, USA), β-tubulin III (Merck Millipore, Billerica, MA, USA), microtubule-associated protein 2 (MAP-2; Proteintech, Rosemont, IL, USA), α-synuclein (BD Biosciences, Franklin Lakes, NJ, USA), and caspase-3 (Cell Signaling Technology, Danvers, MA, USA). β-actin (Sigma-Aldrich, St. Louis, MO, USA) served as a loading control.

The next morning, membranes were washed with 1X TTBS three times for 5 minutes before incubating them for 2 hours in 5% milk with the secondary antibody. Goat anti-mouse (BD Biosciences, San Jose, CA, USA) and goat anti-rabbit (BD Biosciences, San Jose, CA, USA) were used as secondary antibodies. After the incubation with secondary antibody, the membranes were washed three times with 1X TTBS for 5 minutes each. Each membrane was then incubated in Amersham ECL buffer (GE Healthcare Life Sciences, Little Chalfont, United Kingdom) for 2 minutes to detect the immunocomplex, and exposed to X-ray films. Developed films were analyzed using Image J software (National Institute of Health, Bethesda, Maryland, USA), and data were normalized to the corresponding β-actin. The results were expressed as mean fold change to concurrent gel control ± 95% confidence interval.

Western blot for epigenetic changes.

The method described in Kim et al. (2016) for examining histone modifications was modified to use 1X radioimmunoprecipitation assay (RIPA) buffer (ThermoFisher Scientific, Grand Island, NY, USA) for harvesting cells. After collecting samples, protein assay and western blotting protocols described in Kim et al. (2016) were followed. To examine histone modifications, acetyl histone H3 lysine 9 (AH3Lys9; Cell Signaling, Danvers, MA, USA), acetyl histone H3 lysine 18 (AH3Lys18; Cell Signaling, Danvers, MA, USA), acetyl histone H3 lysine 27 (AH3Lys27; Cell Signaling, Danvers, MA, USA), and histone deacetylase 6 (HDAC6; Cell Signaling, Danvers, MA, USA) were used. Primary antibodies were diluted in 1:1000, and a list of specific antibodies included in these sampler kits is summarized in Table 7.2. Histone H3 (Cell Signaling, Danvers, MA, USA) served as a loading control since it detects all histone H3 regardless of site-specific modifications.

Statistical analysis.

A linear mixed effects model analysis was performed to determine significant differences among different culture conditions—day 1 proliferation, day 1 differentiation, and day 7 differentiation—as well as dose-response relationship after 24 hours of Cd exposures. A continuous fixed effect was concentrations of Cd, and random effects included experimental dates and western gels. R statistical software with “lme4” package was used for statistical analyses and for modeling mixed effects (Bates et al., 2014).

RESULTS

hNPC morphology under proliferation and differentiation conditions after 24-hour exposures to Cd.

Changes in morphology after 24 hours of Cd exposures were examined by taking 100X phase-contrast microscopic images. A dose-dependent decrease in cell number was observed for proliferating and differentiating hNPCs exposed to Cd at day 0 for 24 hours (Figure 7.2). Unlike hNPCs at day 1, differentiating hNPCs treated with Cd at day 6 for 24 hours showed an increase in cell numbers at lower concentrations (Figure 7.2). The reduced confluence was observed at the highest concentration of hNPCs treated with Cd in proliferation and differentiation condition.

Cell viability after Cd treatment.

Alamar blue assay was used to examine the effects of Cd on cell viability. The cell viability assay suggested that hNPCs at various stages of neurodevelopment respond differently to acute Cd exposures. Dose-response relationship were observed for proliferating (p-value < 0.001) and differentiating hNPCs at day 1 (p-value < 0.001) as shown in Figure 7.3. Compared to proliferation, hNPCs in differentiation were more sensitive to Cd after 24 hours. When hNPCs were exposed to Cd at day 6 for 24 hours, a significantly increased cell viability was observed (Figure 7.3; p-value < 0.001). No significant difference in slopes was found among proliferating and differentiating hNPCs at day 1 and 7.

Dosimetry adjusted cell viability.

Dosimetry of hNPCs in proliferation and differentiation was measured using the ICP-MS method. A concentration-dependent dosimetry was observed (data not shown). Cell viability data adjusted by dosimetry revealed a significant dosimetry-response relationship for proliferating and differentiation hNPCs exposed to Cd at day 0 for 24 hours (Figure 7.4; p-value < 0.01 for both conditions). Similar to nominal dose-response lines, differentiating hNPCs were more vulnerable to Cd exposures than proliferating cells with the equivalent Cd associated with cells. hNPCs at day 7 showed an increasing trend of cell viability and were less sensitive to Cd than the differentiating cells at day 1.

Changes in neuronal markers after Cd exposures.

Changes in expressions of proteins involved in proliferation and differentiation were observed via western blot. hNPCs under both proliferation and differentiation at day 1 did not show any changes in proliferation marker expressions after adjusted to β-actin including proliferating cell nuclear antigen (PCNA; Figure 7.5A; Table 7.3) and nestin (Figure 7.5B; Table 7.3). Significant changes in PCNA and nestin were also not found

for differentiating hNPCs at day 7 (Figure 7.5A and 7.5B; Table 7.3). No significant changes in the structural protein, β-tubulin III, expressions were revealed for proliferating and differentiating hNPCs exposed to Cd at all time points (Figure 7.5C; Table 7.3). Another structural protein marker, microtubule-associated protein 2 (MAP-2), was also examined for early differentiation. Upon exposures to Cd for 24 hours, proliferating hNPCs at day 1 did not show any concentration dependent changes in MAP-2 expressions while a significant dose-related decrease in MAP-2 expression was observed (Figure 7.5D; Table 7.3; p-value < 0.01). hNPCs under differentiating conditions for 7 days were not affected by acute Cd exposures and thus, did not have a significant change in MAP-2 expressions (Figure 7.5D; Table 7.3). A dose-dependent increasing trend of caspase-3 was observed for hNPCs exposed to Cd under differentiation condition at day 1 and 7, but not for proliferating hNPCs at day 1 (Figur 7.5E; Table 7.3). Expression of a-synuclein was not observed for proliferating and differentiating hNPCs at all times, suggesting that hNPCs have not differentiated far enough to express proteins involved in presynaptic terminals of neurons (data not shown).

Histone modifications induced by Cd exposures on proliferating and differentiating hNPCs.

Changes in histone modifications were examined to understand if potentially inheritable changes in DNA is occurring after acute Cd exposures on *in vitro* hNPCs. We found stage-specific effects of histone modifications after acute Cd exposures. For example, Cd-induced a significant dose-dependent decrease in acetylated histone H3 at lysine 27 (AH3Lys27) in proliferating cells (p-value < 0.05), but not in differentiating cells at day 1 (Figure 7.6C; Table 7.4). No AH3Lys27 signal was detected for differentiating hNPCs at day 7 (Figure 7.6C; Table 7.4). However, a class II histone deacetylase called histone deacetylase 6 (HDAC6) illustrated was significantly increased in a concentration-dependent manner at day 7 under differentiation conditions following Cd exposures (p-value < 0.05), but not under proliferating and differentiating hNPCs at day 1. No signals were observed for hNPCs in proliferating or differentiating condition at day 1 (Figure 7.6D; Table 7.4). These suggested that specific histone modifications occur for Cd-exposed hNPCs at various developmental stages.

DISCUSSION

A heavy metal like cadmium (Cd) can lead to adverse human and environmental health effects including developmental neurotoxicity. Prenatal exposures to Cd in humans were linked to impact children's health including their general cognitive ability and cerebral palsy (Hong et al., 2016; Kippler et al., 2016). Studies

investigating the effects of *in utero* Cd exposures, however, are limited, and the mechanism of developmental neurotoxicity is not yet well-defined. In this research, Cd-induced toxicity and epigenetic changes were examined using proliferating and differentiating hNPCs in order to enhance our understanding on how Cd exerts developmental neurotoxicity.

From our study, a significant dose-response relationship was observed for hNPCs at various developmental stages, which was demonstrated via morphology and cell viability assay. Cell viability assay results with and without dosimetry analysis suggested that differentiating hNPCs at day 1 were impacted the most by acute Cd exposures followed by proliferating hNPCs at day 1 and differentiating hNPCs at day 7 (Figure 7.3 and 7.4). This finding is consistent with previous studies done by Buzanska et al. (2009) and Gartlon et al. (2006). They discovered that undifferentiated human neural stem cells (umbilical cord blood-derived) and PC12 cells were more sensitive to Cd exposures than cells in differentiation condition for 8 days to 4 weeks. Moreover, IC_{50} values for hNPCs in proliferation and differentiation conditions at day 1 fall between 10 to 50 µM, which concords with IC_{50} values from Cd-exposed human neural stem/progenitor cells and PC12 neuronal cells (Mori et al., 2015).

Given the same exposure doses, less amount of Cd was found to be associated with differentiating hNPCs at day 1 compared to hNPCs in proliferation at day 1 and differentiation at day 7. However, lower cell viability was observed for differentiating hNPCs at day 1, suggesting that early differentiation stages of neurodevelopment may be the critical “windows of susceptibility” for Cd exposures.

We also found that Cd-treated hNPCs at day 7 were not adversely affected at lower doses of Cd whether the cell viability was adjusted with and without dosimetry. Comparable results were observed in Gulisano et al. (2009). They found that primary human neuroblast cells showed a statistically significant increase in cell proliferation at lower Cd doses, and that cell viability measured via trypan blue increased in comparison with control cells (Gulisano et al., 2009).

Both results (with and without dosimetry adjustment) illustrated that early differentiation is the most and late differentiation is the least susceptible time frame to Cd exposures, but developmental stage-dependent cell viability became more evident when the results were adjusted by dosimetry. In case of nanoparticles, dosimetry is often assessed to incorporate particokinetics to better predict toxicity

(Teeguarden et al., 2007). The same may apply when evaluating metal-induced toxicity since dosimetry analysis provided more evident results.

Protein markers were utilized to characterize the developmental stages of hNPCs and Cd-induced stress. MAP-2, a microtubule-associated protein and a marker of differentiated neurons, was significantly reduced compared to controls following exposures to Cd under differentiation conditions on day 1. This finding of developmental stage-dependent changes in protein expression after exposures to toxicants is also observed with previous reports of other neurotoxicants such as chlorpyrifos and arsenic (Frankel et al., 2009; Kim et al., 2016; Slotkin et al., 2007; Slotkin and Seidler, 2012).

Impacts of acute Cd exposures on four epigenetic markers (acetylation of histone H3 at lysine 9, 18, and 27, and HDAC6) were examined in this study. A significant dose-dependent increase in the expressions of HDAC6 suggested that there may be increased cell cycle progression, microtubule formation, cell migration (Boyault et al., 2007; Iwata et al., 2005; Seigneurin-Berny et al., 2001). Increased cell viability and greater expressions for neuronal markers of proliferation and differentiation after may potentially be explained by significant changes in HDAC6, but further validation is needed. The biological functions of AH3Lys27 include being an enhancer, a substrate for a transcription co-factor for nuclear proteins such as p300/CBP, and a transcriptional antagonist of tri-methyl histone H3 at lysine 27, which has a role in repressing developmental genes (Calo and Wysocka, 2013; Jin et al., 2011; Rougeulle et al., 2004; Tie et al., 2009). A significantly decreased expression in AH3Lys27 after 24 hours of Cd treatment in proliferating hNPCs were observed, but more research is needed to understand potential implications of this change. No changes in AH3Lys9 was observed, but AH3Lys9 has been found to play a role in pluripotency maintenance and neural differentiation of human embryonic stem cells (hESC) (Qiao et al., 2015). We only observed AH3Lys9 signals during differentiation day 7, which can be explained by the previous finding that expression of AH3Lys9 decreases the first four days of hESC differentiation and then increase during days 4 – 8 (Lee and Mahadevan, 2009; Peterson and Laniel, 2004; Qiao et al., 2015).

This study has some limitations. We first would like to note that the linear mixed-effect model that we have used in our study did not fit well for differentiating hNPCs at day 7. We used it for consistency, but different a mixed-effect model may be used for future research. Moreover, our study focused on early neurodevelopmental effects of Cd using hNPCs characterized in Wegner et al. (2014) and Park et al. (2017), which is derived from WA09 and have normal 46 chromosomes with female (XX) karyotype (WiCell, 2014).

According to Llop et al. (2013), gender interaction between Cd exposures and neurodevelopmental disorders was observed previously; however, information is too scarce to draw any conclusion. Utilizing hNPCs with male karyotype will also be helpful to examine potential gender differences in response to Cd exposures. Moreover, exposures metal ions such as Cd at a developmental period or adult life are reported to alter DNA methylation, and therefore, increase susceptibility to disease including cancer (Baccarelli and Bollati, 2009; Calvanese et al., 2009; Feil and Fraga, 2012). We have examined histone acetylation and HDAC6, but future studies should investigate into effects of Cd on DNA methylation. Lastly, Rikans and Yamano (2000) found that Cd-induced acute hepatotoxicity involved two pathways, one from direct effects of Cd exposures and the other from inflammation. It would be interesting to examine if Cd induces neuroinflammation and causes subsequent injury.

In summary, we demonstrated cell viability with and without accounting for the amount of Cd associated with the cells, changes in neuronal markers of proliferation and differentiation, and alterations in epigenetics after acute exposures to Cd using *in vitro* hNPCs model. To the best of our knowledge, our study is the first to quantify the amount of Cd associated with neuronal cells at various developmental stages after exposures. We also believe our results not only demonstrate the ability of *in vitro* hNPCs system as a developmental neurotoxicity model but also enhance understanding of epigenetic changes under the influence of Cd.

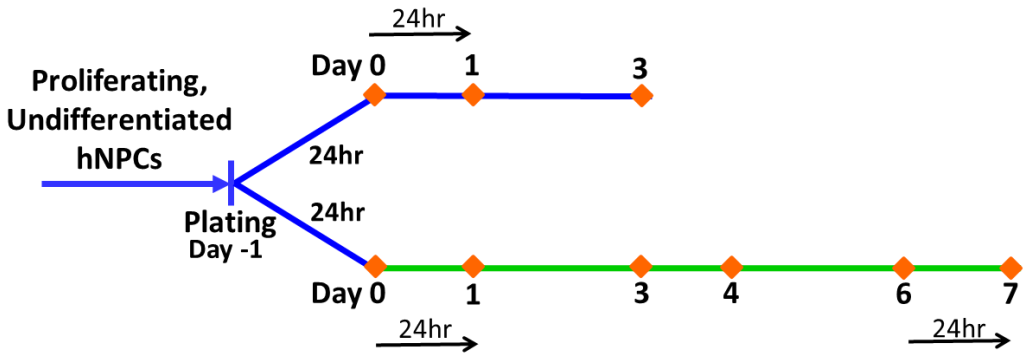

Figure 7.1. Study design for cadmium (Cd) exposures on proliferating and differentiating human neural progenitor cells (hNPCs). Proliferating hNPCs were exposed to Cd for 24 hours at day 0, and differentiating hNPCs were treated with Cd at day 0 and 6 for 24 hours.

Table 7.1. A list of neuronal markers used for *in vitro* human neural progenitor cell culture system (Modified from Kim et al. (2016))

Antibody	Biological Function	Cells Detected	References
Nestin	Intermediate filament protein involved in radial axon growth	Neural progenitor cells	Kim et al. (2016); Kuegler et al. (2010); Wilson and Stice (2006)
Proliferating cell nuclear antigen (PCNA)	Proliferation	Proliferating cells	Kim et al. (2016); Nguyen et al. (2014)
β-tubulin III	Component of microtubules found in cytoskeleton and axons	Structural neuron specific marker	Kuegler et al. (2010); von Bohlen Und Halbach (2007)
Microtubule-associated protein 2 (MAP-2)	Microtubule associated protein located primarily in dendrites	Structural neuron specific marker	Kuegler et al. (2010); Palaga et al. (2013)
α-synuclein	Neuronal vesicle trafficking in presynaptic terminals	Presynaptic terminals of neurons	Ettle et al. (2014)
Caspase-3	Role in apoptosis and in natural brain development	Ubiquitous	Ceccatelli et al. (2004)

Table 7.2. A list of histone modification antibodies used for *in vitro* human neural progenitor cell culture system (Modified from Kim et al. (2016))

Antibody	Specific Site Detected	Biological Function	References
Acetyl-Histone H3	Lysine 9	Histone deposition and chromatin assembly in some organisms	Hansen et al. (1998); Qiao et al. (2015); Strahl and Allis (2000)
Acetyl-Histone H3	Lysine 18	An enhancer; a substrate for p300/CBP	Calo and Wysocka (2013); Jin et al. (2011)
Acetyl-Histone H3	Lysine 27	An enhancer; a substrate for p300/CBP; transcriptional antagonist of tri-methyl histone H3 at lysine 27	Calo and Wysocka (2013); Jin et al. (2011); Rougeulle et al. (2004); Tie et al. (2009)
Histone deacetylase 6 (HDAC6)		Degradation of misfold proteins, cell cycle progression, migration, and developmental events including microtubule network	Boyault et al. (2007); Iwata et al. (2005); Seigneurin-Berny et al. (2001)

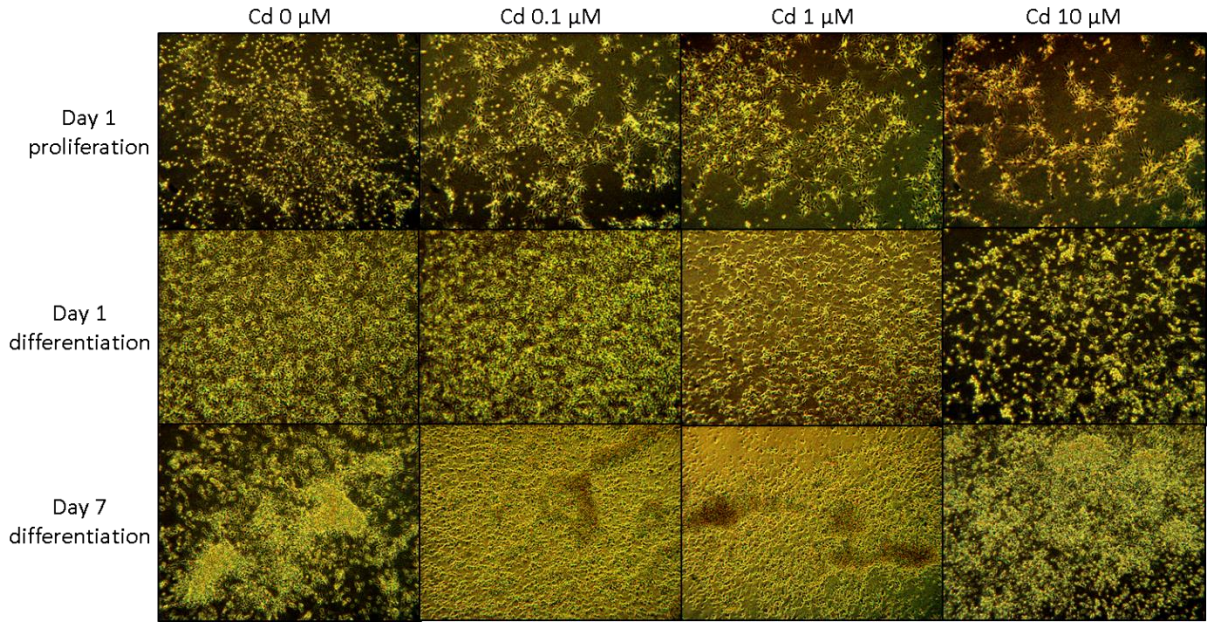

Figure 7.2. 100X phase microscope morphology of proliferating and differentiating hNPCs after 24 hours of cadmium exposures at day 1 and 7. The decrease in cell viability was observed in day 1 proliferation and differentiation while lower Cd exposures to differentiating hNPCs at day 6 increased.

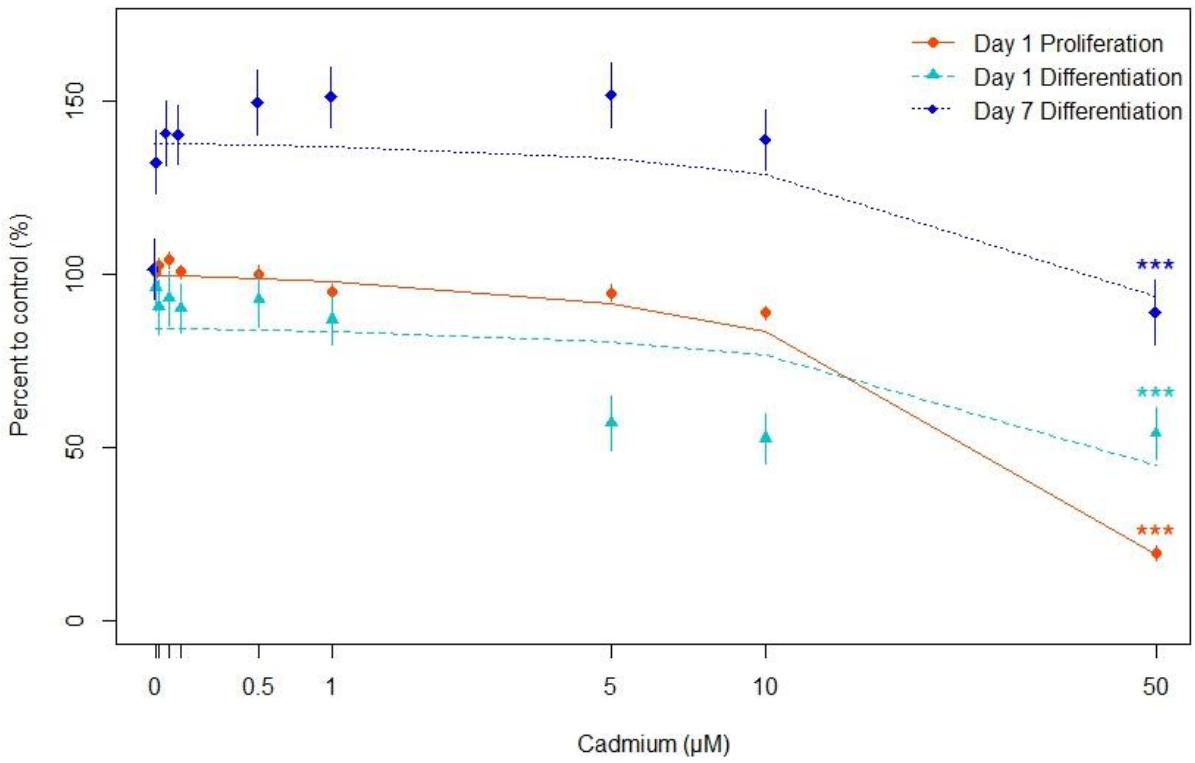

Figure 7.3. Dose-response curve for proliferating and differentiating hNPCs after 24 hours of Cd exposures. Proliferating (orange) or differentiating (day 1: turquoise; day 7: blue) hNPCs were exposed to cadmium (Cd 0-50 µM) for 24 hours. Plots show means ± 95% confidence intervals. Data points and lines were estimated from the mixed-effect model. ***: p-value < 0.001 represents significant dose response. Log-scaled x-axis resulted in curved linear regression lines.

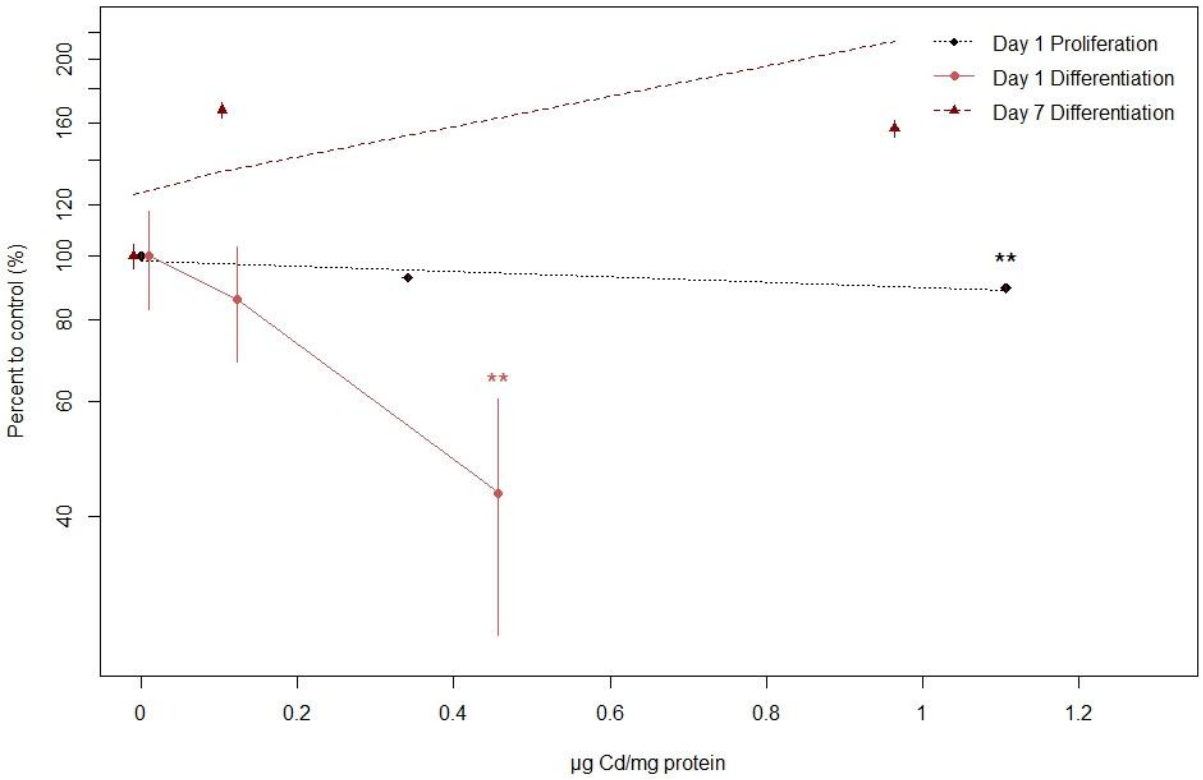

Figure 7.4. Dosimetry adjusted dose-response curve for proliferating and differentiating hNPCs after 24 hours of 0, 1, and 10 µM Cd exposure. Day 1 proliferation (black) and differentiation (indian red) hNPCs demonstrated significant dosimetry-response curves. Differentiating hNPCs at day 1 (indian red) was impacted greater compared to proliferating hNPCs at day 1 (black) and differentiating hNPCs at day 7 (dark red) at the equivalent amount of Cd associated with cells. Plots illustrate means ± 95% confidence intervals. Data points and lines were estimated from the mixed-effect model. **: p-value < 0.01 represents significant dosimetry response. Y-axis is log-scaled to better show impacts on cell viability for differentiating hNPCs at day 1.

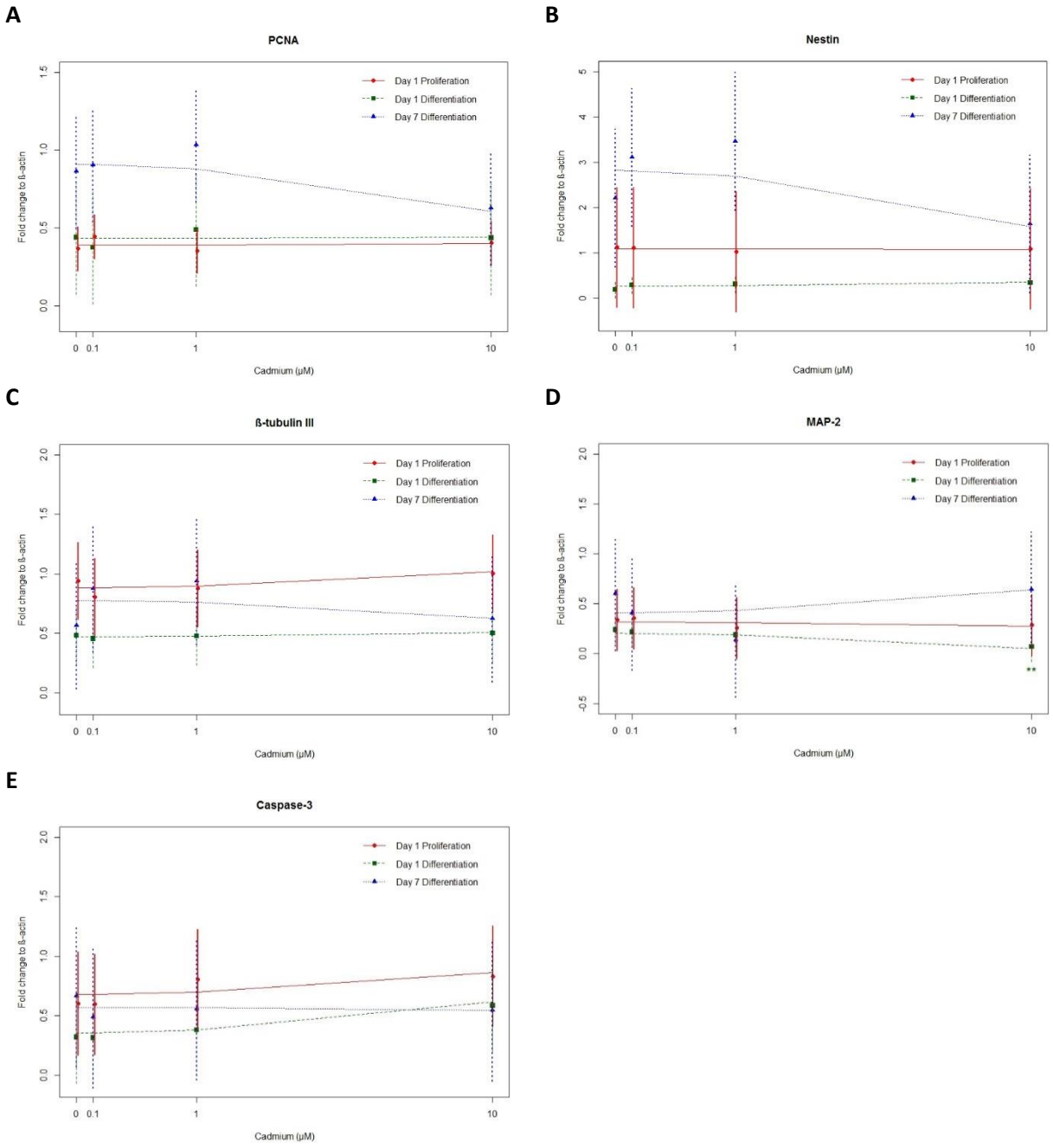

Figure 7.5. Neuronal protein expressions of proliferating and differentiating hNPCs Cd treatment. Changes in (A) PCNA, (B) nestin, (C) β-tubulin III, (D) MAP-2, and (E) caspase-3 expression levels in proliferating at day 1 (red) and differentiating hNPCs at day 1 (green) and day 7 (blue). A significant decrease in MAP-2 was observed for differentiating hNPCs at day 1 after 24-hour exposures to Cd. Plots illustrate means ± 95% confidence intervals, where points and lines were estimated from the mixed-effect model. **: p-value < 0.01 represents significant dose response. The x-axis is log-scaled to better show impacts on cell viability for differentiating hNPCs at day 1.

Table 7.3. Summary of changes in neuronal protein expressions for proliferating and differentiating hNPCs after Cd treatment. Protein expression changes for PCNA, nestin, β-tubulin III, MAP-2, and caspase-3 in proliferating at day 1 and differentiating hNPCs at day 1 and day 7 were summarized in this table. A significant decrease in MAP-2 was observed for differentiating hNPCs at day 1 after 24-hour exposures to Cd. N/A: no expression observed; NS: not significant; ↓: decrease in expression; **: p-value < 0.01 represents significant dose response.

	Day 1 Proliferation	Day 1 Differentiation	Day 7 Differentiation
PCNA	NS	NS	NS
Nestin	NS	NS	NS
β-tubulin III	NS	NS	NS
MAP-2	NS	↓ **	NS
α-synuclein	N/A	N/A	N/A
Caspase-3	NS	NS	NS

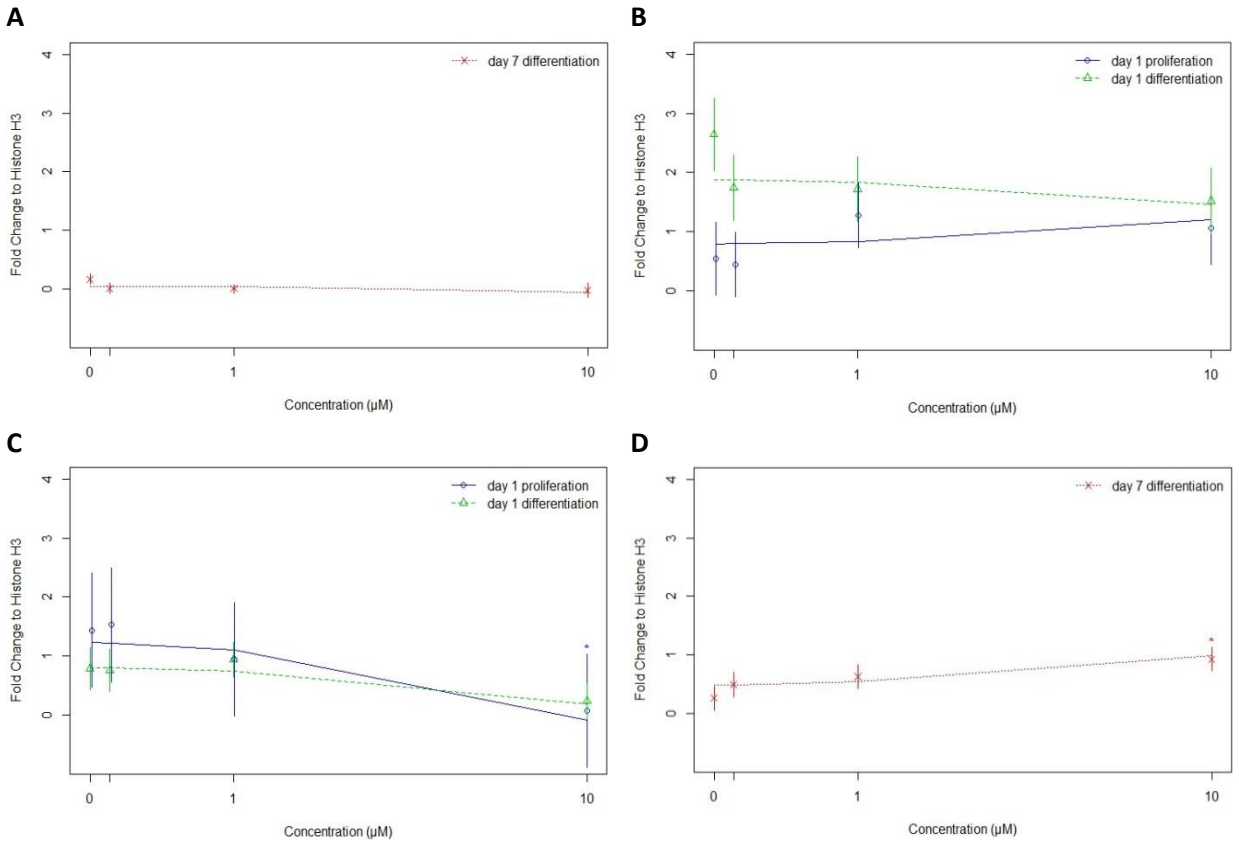

Figure 7.6. Epigenetic changes of proliferating and differentiating hNPCs after Cd treatment. Changes in (A) acetylation at lysine 9, (B) acetylation at lysine 18, (C) acetylation at lysine 27, and (D) HDAC6 in proliferating at day 1 (blue) and differentiating hNPCs at day 1 (green) and day 7 (red). hNPCs treated with Cd at different stages of neurodevelopment showed different trends for epigenetic changes. Data was not plotted if no signal was present throughout the doses for specific conditions. Plots illustrate means ± 95% confidence intervals, where points and lines were estimated from the mixed-effect model. *: p-value < 0.05 represents significant dose response. The x-axis is log-scaled to better show impacts on cell viability for differentiating hNPCs at day 1.

Table 7.4. Summary of epigenetic protein expression changes for proliferating and differentiating hNPCs after 24 hours of Cd exposures. Epigenetic protein expression changes in acetylation at lysine 9, 18, and 27 in addition to enzyme HDAC6 were summarized for proliferating hNPCs at day 1 and differentiating hNPCs at day 1 and day 7. ↓: decreasing trend in expression observed; ↑: increasing trend in expression observed; *: p-value < 0.05 represents significant dose response; N/A: no expression observed; NS = not significant.

	Day 1 Proliferation	Day 1 Differentiation	Day 7 Differentiation
Histone H3 acetyl lysine 9	N/A	N/A	NS
Histone H3 acetyl lysine 18	NS	NS	N/A
Histone H3 acetyl lysine 27	↓*	NS	N/A
HDAC6	N/A	N/A	↑*

CHAPTER 7 REFERENCES

Baccarelli, A. and Bollati, V. (2009). Epigenetics and environmental chemicals. *Curr Opin Pediatr 21*, 243-251.

Bates, D., Machler, M., Bolker, B. M. et al. (2014). Fitting linear mixed-effects models using lme4. *Journal of Statistical Software 67*, 1-48.

Boyault, C., Sadoul, K., Pabion, M. et al. (2007). HDAC6, at the crossroads between cytoskeleton and cell signaling by acetylation and ubiquitination. *Oncogene 26*, 5468-5476. http://dx.doi.org/10.1038/sj.onc.1210614

Buzanska, L., Sypecka, J., Nerini-Molteni, S. et al. (2009). A human stem cell-based model for identifying adverse effects of organic and inorganic chemicals on the developing nervous system. *Stem Cells 27*, 2591-2601. http://dx.doi.org/10.1002/stem.179

Calo, E. and Wysocka, J. (2013). Modification of enhancer chromatin: what, how, and why? *Mol Cell 49*, 825-837. http://dx.doi.org/10.1016/j.molcel.2013.01.038

Calvanese, V., Lara, E., Kahn, A. et al. (2009). The role of epigenetics in aging and age-related diseases. *Ageing Res Rev 8*, 268-276. http://dx.doi.org/10.1016/j.arr.2009.03.004

Ceccatelli, S., Tamm, C., Sleeper, E. et al. (2004). Neural stem cells and cell death. *Toxicol Lett 149*, 59-66. http://dx.doi.org/10.1016/j.toxlet.2003.12.060

Culbreth, M. E., Harrill, J. A., Freudenrich, T. M. et al. (2012). Comparison of chemical-induced changes in proliferation and apoptosis in human and mouse neuroprogenitor cells. *Neurotoxicology 33*, 1499-1510. http://dx.doi.org/10.1016/j.neuro.2012.05.012

Domingo, J. L. (1994). Metal-induced developmental toxicity in mammals: a review. *J Toxicol Environ Health 42*, 123-141. http://dx.doi.org/10.1080/15287399409531868

EPA (2007). Method 3051A: Microwave Assisted Acid Digestion Of Sediments, Sludges, Soils, and Oils.

Ettle, B., Reiprich, S., Deusser, J. et al. (2014). Intracellular alpha-synuclein affects early maturation of primary oligodendrocyte progenitor cells. *Mol Cell Neurosci 62*, 68-78. http://dx.doi.org/10.1016/j.mcn.2014.06.012

Feil, R. and Fraga, M. F. (2012). Epigenetics and the environment: emerging patterns and implications. *Nat Rev Genet 13*, 97-109. http://dx.doi.org/10.1038/nrg3142

Flora, S. J. S., Pachauri, V. and Saxena, G. (2011). Arsenic, cadmium, and lead. In R. C. Gupta (eds.), *Reproductive and developmental toxicology*. Oxford, UK: Elsevier Inc.

Fotakis, G. and Timbrell, J. A. (2006). Role of trace elements in cadmium chloride uptake in hepatoma cell lines. *Toxicol Lett 164*, 97-103. http://dx.doi.org/10.1016/j.toxlet.2005.11.016

Frankel, S., Concannon, J., Brusky, K. et al. (2009). Arsenic exposure disrupts neurite growth and complexity in vitro. *Neurotoxicology 30*, 529-537. http://dx.doi.org/10.1016/j.neuro.2009.02.015

Gadhia, S. R., O'Brien, D. and Barile, F. A. (2015). Cadmium affects mitotically inherited histone modification pathways in mouse embryonic stem cells. *Toxicol In Vitro 30*, 583-592. http://dx.doi.org/10.1016/j.tiv.2015.11.001

Gartlon, J., Kinsner, A., Bal-Price, A. et al. (2006). Evaluation of a proposed in vitro test strategy using neuronal and non-neuronal cell systems for detecting neurotoxicity. *Toxicol In Vitro 20*, 1569-1581. http://dx.doi.org/10.1016/j.tiv.2006.07.009

Godt, J., Scheidig, F., Grosse-Siestrup, C. et al. (2006). The toxicity of cadmium and resulting hazards for human health. *J Occup Med Toxicol 1*, 22. http://dx.doi.org/10.1186/1745-6673-1-22

Gulisano, M., Pacini, S., Punzi, T. et al. (2009). Cadmium modulates proliferation and differentiation of human neuroblasts. *J Neurosci Res 87*, 228-237. http://dx.doi.org/10.1002/jnr.21830

Hansen, J. C., Tse, C. and Wolffe, A. P. (1998). Structure and function of the core histone N-termini: more than meets the eye. *Biochemistry 37*, 17637-17641.

Henson, M. C. and Chedrese, P. J. (2004). Endocrine disruption by cadmium, a common environmental toxicant with paradoxical effects on reproduction. *Exp Biol Med (Maywood) 229*, 383-392.

Hong, J., Wang, Y., McDermott, S. et al. (2016). The use of a physiologically-based extraction test to assess relationships between bioaccessible metals in urban soil and neurodevelopmental conditions in children. *Environ Pollut 212*, 9-17. http://dx.doi.org/10.1016/j.envpol.2016.01.001

Iwata, A., Riley, B. E., Johnston, J. A. et al. (2005). HDAC6 and microtubules are required for autophagic degradation of aggregated huntingtin. *J Biol Chem 280*, 40282-40292. http://dx.doi.org/10.1074/jbc.M508786200

Jarup, L. and Akesson, A. (2009). Current status of cadmium as an environmental health problem. *Toxicol Appl Pharmacol 238*, 201-208. http://dx.doi.org/10.1016/j.taap.2009.04.020

Jin, Q., Yu, L. R., Wang, L. et al. (2011). Distinct roles of GCN5/PCAF-mediated H3K9ac and CBP/p300-mediated H3K18/27ac in nuclear receptor transactivation. *EMBO J 30*, 249-262. http://dx.doi.org/10.1038/emboj.2010.318

Kim, H. Y., Wegner, S. H., Van Ness, K. P. et al. (2016). Differential epigenetic effects of chlorpyrifos and arsenic in proliferating and differentiating human neural progenitor cells. *Reprod Toxicol 65*, 212-223. http://dx.doi.org/10.1016/j.reprotox.2016.08.005

Kippler, M., Bottai, M., Georgiou, V. et al. (2016). Impact of prenatal exposure to cadmium on cognitive development at preschool age and the importance of selenium and iodine. *Eur J Epidemiol 31*, 1123-1134. http://dx.doi.org/10.1007/s10654-016-0151-9

Kuegler, P. B., Zimmer, B., Waldmann, T. et al. (2010). Markers of murine embryonic and neural stem cells, neurons and astrocytes: reference points for developmental neurotoxicity testing. *ALTEX 27*, 17-42.

Lee, B. M. and Mahadevan, L. C. (2009). Stability of histone modifications across mammalian genomes: implications for 'epigenetic' marking. *J Cell Biochem 108*, 22-34. http://dx.doi.org/10.1002/jcb.22250

Lee, N. Y., Choi, H. M. and Kang, Y. S. (2009). Choline transport via choline transporter-like protein 1 in conditionally immortalized rat syncytiotrophoblast cell lines TR-TBT. *Placenta 30*, 368-374. http://dx.doi.org/10.1016/j.placenta.2009.01.011

Llop, S., Lopez-Espinosa, M. J., Rebagliato, M. et al. (2013). Gender differences in the neurotoxicity of metals in children. *Toxicology 311*, 3-12. http://dx.doi.org/10.1016/j.tox.2013.04.015

Mori, H., Sasaki, G., Nishikawa, M. et al. (2015). Effects of subcytotoxic cadmium on morphology of glial fibrillary acidic protein network in astrocytes derived from murine neural stem/progenitor cells. *Environ Toxicol Pharmacol 40*, 639-644. http://dx.doi.org/10.1016/j.etap.2015.08.018

Nguyen, H. X., Nekanti, U., Haus, D. L. et al. (2014). Induction of early neural precursors and derivation of tripotent neural stem cells from human pluripotent stem cells under xeno-free conditions. *J Comp Neurol 522*, 2767-2783. http://dx.doi.org/10.1002/cne.23604

O'Brien, J., Wilson, I., Orton, T. et al. (2000). Investigation of the Alamar Blue (resazurin) fluorescent dye for the assessment of mammalian cell cytotoxicity. *Eur J Biochem 267*, 5421-5426.

Palaga, T., Ratanabunyong, S., Pattarakankul, T. et al. (2013). Notch signaling regulates expression of Mcl-1 and apoptosis in PPD-treated macrophages. *Cell Mol Immunol 10*, 444-452. http://dx.doi.org/10.1038/cmi.2013.22

Park, J. J., Wegner, S. H., Workman, T. et al. (2017). Concordance of in vitro and in vivo gene expression dynamics for specific pathways of interest for developmental neurotoxicity. PhD, University of Washington,

Peterson, C. L. and Laniel, M. A. (2004). Histones and histone modifications. *Curr Biol 14*, R546-551. http://dx.doi.org/10.1016/j.cub.2004.07.007

Qiao, Y., Wang, R., Yang, X. et al. (2015). Dual roles of histone H3 lysine 9 acetylation in human embryonic stem cell pluripotency and neural differentiation. *J Biol Chem 290*, 9949. http://dx.doi.org/10.1074/jbc.A114.603761

Ray, P. D., Yosim, A. and Fry, R. C. (2014). Incorporating epigenetic data into the risk assessment process for the toxic metals arsenic, cadmium, chromium, lead, and mercury: strategies and challenges. *Front Genet 5*, 201. http://dx.doi.org/10.3389/fgene.2014.00201

Rikans, L. E. and Yamano, T. (2000). Mechanisms of cadmium-mediated acute hepatotoxicity. *J Biochem Mol Toxicol 14*, 110-117.

Rougeulle, C., Chaumeil, J., Sarma, K. et al. (2004). Differential histone H3 Lys-9 and Lys-27 methylation profiles on the X chromosome. *Mol Cell Biol 24*, 5475-5484. http://dx.doi.org/10.1128/MCB.24.12.5475-5484.2004

Seigneurin-Berny, D., Verdel, A., Curtet, S. et al. (2001). Identification of components of the murine histone deacetylase 6 complex: link between acetylation and ubiquitination signaling pathways. *Mol Cell Biol 21*, 8035-8044. http://dx.doi.org/10.1128/MCB.21.23.8035-8044.2001

Slotkin, T. A., MacKillop, E. A., Ryde, I. T. et al. (2007). Ameliorating the developmental neurotoxicity of chlorpyrifos: a mechanisms-based approach in PC12 cells. *Environ Health Perspect 115*, 1306-1313. http://dx.doi.org/10.1289/ehp.10194

Slotkin, T. A. and Seidler, F. J. (2012). Developmental neurotoxicity of organophosphates targets cell cycle and apoptosis, revealed by transcriptional profiles in vivo and in vitro. *Neurotoxicol Teratol 34*, 232-241. http://dx.doi.org/10.1016/j.ntt.2011.12.001

Somji, S., Garrett, S. H., Toni, C. et al. (2011). Differences in the epigenetic regulation of MT-3 gene expression between parental and Cd+2 or As+3 transformed human urothelial cells. *Cancer Cell Int 11*, 2. http://dx.doi.org/10.1186/1475-2867-11-2

Strahl, B. D. and Allis, C. D. (2000). The language of covalent histone modifications. *Nature 403*, 41-45. http://dx.doi.org/10.1038/47412

Teeguarden, J. G., Hinderliter, P. M., Orr, G. et al. (2007). Particokinetics in vitro: dosimetry considerations for in vitro nanoparticle toxicity assessments. *Toxicol Sci 95*, 300-312. http://dx.doi.org/10.1093/toxsci/kfl165

Tie, F., Banerjee, R., Stratton, C. A. et al. (2009). CBP-mediated acetylation of histone H3 lysine 27 antagonizes Drosophila Polycomb silencing. *Development 136*, 3131-3141. http://dx.doi.org/10.1242/dev.037127

von Bohlen Und Halbach, O. (2007). Immunohistological markers for staging neurogenesis in adult hippocampus. *Cell Tissue Res 329*, 409-420. http://dx.doi.org/10.1007/s00441-007-0432-4

Wegner, S. H., Stanaway, I. B., Kim, H. Y. et al. (2014). Anchoring a dynamic *in vitro* model of human neuronal differentiation to key processes of early brain development *in vivo*. Ph.D., University of Washington,

Weldon, B. A., Park, J. J., Hong, S. et al. (2017). Effects of developmental stage, particle size, and coating on dosimetry and toxicity of silver nanoparticles in developing primary organotypic mouse midbrain cultures. Ph.D., University of Washington,

Wilson, P. G. and Stice, S. S. (2006). Development and differentiation of neural rosettes derived from human embryonic stem cells. *Stem Cell Rev 2*, 67-77. http://dx.doi.org/10.1007/s12015-006-0011-1

Xu, P., Wu, Z., Xi, Y. et al. (2016). Epigenetic regulation of placental glucose transporters mediates maternal cadmium-induced fetal growth restriction. *Toxicology 372*, 34-41. http://dx.doi.org/10.1016/j.tox.2016.10.011

Zhang, Y. M., Liu, X. Z., Lu, H. et al. (2009). Lipid peroxidation and ultrastructural modifications in brain after perinatal exposure to lead and/or cadmium in rat pups. *Biomed Environ Sci 22*, 423-429. http://dx.doi.org/10.1016/s0895-3988(10)60021-9

CHAPTER 8: Significance of research findings and implications for risk assessment

Establishment of in vitro alternative methods for neurodevelopment.

With over 80,000 US EPA registered chemicals in commerce, we need a screening tool to prioritize these compounds for potential neurodevelopmental toxicity. However, creating robust *in vitro* models for brain development is challenging because neurodevelopment is a complex and highly regulated process. Therefore, established *in vitro* neurodevelopment models must be defined for its capability as well as advantages and limitations and must be validated to better understand the obtained results.

In this research, we have developed and characterized two *in vitro* alternative methods for midbrain development. The *in vitro* 3D organotypic mouse midbrain micromass systems with C57BL/6 and A/J mouse strains capture proliferation, migration, and differentiation processes of early midbrain development over 22 days *in vitro* (DIV). Basic characterization of micromass model illustrated that proliferation slows after DIV 6 as midbrain cells lose its capacity to proliferate and begin differentiation. The extent of differentiation in both C57BL/6 and A/J micromass systems increased linearly over 22-days of the culture period. Temporal dynamics of neurodevelopment was captured using stage-specific proteins, and similar expression patterns were found between C57BL/6 and A/J micromass systems.

The *in vitro* human neural progenitor cell (hNPC) culture in differentiation condition serves as a model for forebrain development. Transcriptomic analysis revealed that GO biological processes associated with proliferation prominently appeared during the early days in culture while GO biological processes related to differentiation enriched over 21-days of the culture period. Over time, we expected our *in vitro* hNPCs to have forebrain characteristics because no external morphogens were added to the system. This hypothesis was confirmed when gene expressions of *in vitro* hNPCs were compared with those of *in vivo* human neocortex, which was a publicly available dataset by Kang et al. (2011). Increased concordance was found for forebrain development compared to midbrain or hindbrain development. Targeted pathways of neuronal proliferation, differentiation, epigenetic regulation, dopaminergic neuron differentiation, and oxidative stress demonstrated concordance while pathways like GABAergic neuron differentiation and synaptic transmission were less similar.

In relation to the human *in vivo*, our two culture systems represent human development during the first trimester. Based on the characterization of each model, our *in vitro* 3D organotypic mouse midbrain

micromass cultures may roughly reflect human gestational week 4.6 to 8.6, while *in vitro* hNPCs may roughly represent human GW 4.7 to 6.1 (Figure 7.1).

Using both systems as neurodevelopmental toxicity screening tools, we would be able to capture regional- and stage-specific sensitivity of the brain to toxicant exposures. Further validation is needed, and characterized *in vitro* models here must be performed with additional assays in order to capture complex processes across cell types, brain regions, and developmental stages. However, this establishment of two medium-throughput, high-content *in vitro* neurodevelopmental models provide a framework for assessing chemical perturbation as a means to screening and prioritizing existing potential neurotoxicants.

Integration of gene x environment x time for developmental neurotoxicology.

Of children with developmental disabilities, only 3% is explained by environmental exposures (National Research Council Committee on Developmental Toxicology, 2000). On the other hand, 25% of children developmental disabilities are estimated to result from interactions between environmental factors and individual genetic sensitivity (National Research Council Committee on Developmental Toxicology, 2000). Likewise, exposures to various environmental factors do not explain all cases. Many factors contribute to the vulnerability of neurotoxic exposures including dose, gender, developmental stages, and genetic backgrounds (Barry et al., 2017; Faustman et al., 2000; Rice and Barone, 2000; Rodier, 1995).

In the current study, factors that may contribute to developmental neurotoxicity were examined using two established *in vitro* models. Embryonic C57BL/6 and A/J mouse midbrain cells were exposed to 20 nm or 110 nm silver nanoparticles (AgNPs) with citrate or polyvinylpyrrolidone (PVP) coatings. Dose-response relationships were found for all particles at all times in both mouse micromass systems except exposures to 20 nm AgCitrate at DIV8 on fetal C57BL/6 mouse midbrain cells. Particle coating, sizes, and neurodevelopmental stages demonstrated significant effects on response to AgNPs on both C57BL/6 and A/J mouse midbrain cells. Upon dosimetry analysis, particle coating and sizes affected responses of C57BL/6 or A/J midbrain cells at specific time points, and neurodevelopmental stages only contributed to AgNP sensitivity for 110 nm particles. At DIV 8, highest slopes for cytotoxicity were found in C57BL/6 cultures while A/J showed the highest slopes for cytotoxicity at DIV 15.

Proliferating and differentiating hNPCs *in vitro* were exposed to various compounds including chlorpyrifos, arsenic, silver nanoparticles, and cadmium. Differentiating hNPCs demonstrated increased susceptibility

to chlorpyrifos and arsenic after 72 hours of exposures while proliferating hNPCs were more vulnerable after 24 hours of chlorpyrifos exposures. Differentiating hNPCs showed a greater decrease in cell viability after 24 hours of arsenic exposures. For functional and structural protein expressions and epigenetics, differential effects of chlorpyrifos and arsenic on proliferating and differentiating hNPCs were revealed. These results suggested that compound- and stage-specific impacts are present, and factors such as toxicant and exposure timing contribute to developmental neurotoxicity as well as to alterations of epigenetics.

In vitro proliferating and differentiating hNPCs were also exposed to AgNPs with different coatings and sizes. Differentiating hNPCs at day 1 and 7 illustrated that particle coatings have significant effects on cell viability. hNPCs at various neurodevelopmental stages were affected by different particle sizes—proliferating cells were more sensitive to 110 nm particles while differentiating hNPCs were more vulnerable to 20 nm particles. Observations from this study suggested that proliferating and differentiating hNPCs at day 1 may be the critical "windows of susceptibility" and that many factors contribute to AgNP sensitivity.

Exposures to Cd on proliferation and differentiating hNPCs also demonstrated that differentiating hNPCs at day 1 were the most sensitive relative to other time points. Expression of a differentiation marker, MAP-2, was significantly decreased only for hNPCs in differentiation condition at day 1, suggesting stage-specific effects like CP, As, and AgNPs. Different epigenetic changes occurred depending on the status of hNPCs.

Generally, greater effects of environmental agents were observed during early brain development when both proliferation differentiation signals are present. However, we also found that multiple factors may impact susceptibility of neurodevelopment including genetics/epigenetics and time of exposures, resulting compound-, stage-, and regional-specific adverse effects. Thus, integrating these factors when evaluating developmental neurotoxicity will be important to better predict potential adverse health outcomes.

Translating in vitro data using risk assessment framework.

Characterized *in vitro* neurodevelopment models can be used to quantify various perturbed pathways *in vitro*, which can be anchored to *in vivo* development. To achieve this goal, risk assessors use tools like benchmark dose (BMD) to fit a mathematical model using available dose-response information and define

exposure levels corresponding to the specific level of changes in response (Edler, 2014; Kimmel et al., 1995). With a goal to assess impact levels of various compounds in midbrain and forebrain development, we translated and compared results from two *in vitro* alternative methods of neurodevelopment by calculating benchmark dose (BMD) with 10% response to controls after exposures to chlorpyrifos, arsenic, AgNPs, and cadmium. Summary of these results is tabulated in Table 7.1 and Table 7.2.

The EPA's Benchmark Dose Software was utilized to model and calculate BMDs and lower 95% confidence limit of BMDs (BMDLs) for each compound examined in two *in vitro* developmental neurotoxicity methods. Our obtained cytotoxicity or cell viability assay data were used, and data points with missing either dosimetry, cytotoxicity, and/or cell viability were excluded from the analysis. For all compounds, including ones with and without dosimetry data, a continuous linear dose-response function was used. Also, a default setting of one standard deviation away from the average control values was used as recommended by the EPA's report on benchmark modeling method (Davis et al., 2011). This shift of one standard deviation from the mean would correspond to approximately 10% change in response for a normal-distributed dataset, reflecting "adverse" level (Kavlock et al., 1995).

Within the *in vitro* micromass system prior to dosimetry analysis, embryonic C57BL/6 mouse midbrain cells showed the lowest BMD_{10} value at DIV 22 for all particles while the lowest BMD_{10} value was observed at DIV 15 for A/J (Table 7.1A). Dosimetry adjusted cytotoxicity, however, demonstrated the embryonic C57BL/6 and A/J mouse midbrain cells were most vulnerable to 20 nm particle exposures at DIV 22, but they were the most sensitive to 110 nm particles at DIV 8 (Table 7.1B). This result not only demonstrates the importance of dosimetry analysis but also demonstrates size-specific susceptibility of midbrain cells.

For *in vitro* hNPCs, a lower BMD_{10} value was observed for proliferating hNPCs after 24-hour exposures to chlorpyrifos or arsenic while differentiating hNPCs showed lower BMD_{10} value after exposures to chlorpyrifos or arsenic for 72 hours (Table 7.2A). This suggested stage-specific effects of chlorpyrifos. Exposures to 20nm AgCitrate showed the lowest BMD_{10} value for proliferating hNPCs at day 1 while the lowest BMD_{10} value was found for differentiating hNPCs exposed to 110nm particles at day 1 (Table 7.2B); however, this may change with dosimetry analysis. Cd-exposed hNPCs showed the lowest BMD_{10} for proliferating hNPCs, but dosimetry revealed that early differentiation (differentiating hNPCs at day 1) was the most vulnerable time frame for Cd exposures. Generally, BMDs from various compounds suggested that early differentiation stage may be the critical "windows of susceptibility."

Comparison of BMD between midbrain cells and hNPCs prior to dosimetry adjustment revealed potential regional- and/or cell type-specific responses to AgNPs in addition to developmental stage-specific effects. For example, 20 nm AgCitrate was more sensitive during proliferation of hNPCs while C57BL/6 and A/J midbrain cells showed that DIV 22 and 15, respectively, were the most vulnerable time frame. However, this needs further validation after performing AgNP dosimetry analysis for both systems.

In addition to calculating BMDs, findings from this study along with results from other developmental neurotoxicity assays can be used in the response-disease pathway and into adverse outcome pathway (AOP) framework in order to capture more in-depth analysis of perturbed neurodevelopmental pathways after exposures to toxicants. Defining molecular initiating events that lead to adverse cellular, organ, organism, and population responses will ultimately allow us to predict potential adverse neurodevelopmental impacts caused by exposures to environmental toxicants and to better inform risk assessors and policy makers.

Future directions.

Future work includes further validating *in vitro* systems described here or modifying the system to better reflect *in vivo* processes of neurodevelopment. For example, sensitivity and specificity of two *in vitro* models characterized will be important. Multiple mouse strains may be applied to the micromass system, which will provide us opportunities to perform gene x environment studies. Current systems may also be transferred to a microfluidic system, which may allow us to capture kinetics and dynamics of brain development.

For metals such as silver nanoparticles, the extent of dissolution or aggregation in media would be interesting to research. Moreover, quantifying the amount of metals associated with cells via dosimetry analysis is critical for understanding obtained results. Discussion on how we can incorporate factors that contribute to susceptibility into risk assessment framework and regulatory decisions will be interesting and important.

In conclusion, this research characterized two *in vitro* models of neurodevelopment using embryonic mouse midbrain cells and human neural progenitor cells. These methods were then used to examine impacts of various factors that contribute to susceptibility and their implications in developmental

neurotoxicity. We found that these factors including genetics/epigenetics, dose, gender, and developmental stages need to be integrated when assessing developmental neurotoxicity in addition to validating *in vitro* models for their sensitivity and specificity before using them as a screening tool. However, to protect public health and children from neurodevelopmental disorders, our environment needs to be preserved, and safe consumer products and drugs need to be developed before anticipating altered molecular pathways induced by toxicant exposures.

CHAPTER 8 REFERENCES

Barry, C., Schmitz, M. T., Jiang, P. et al. (2017). Species-specific developmental timing is maintained by pluripotent stem cells ex utero. *Dev Biol 423*, 101-110. http://dx.doi.org/10.1016/j.ydbio.2017.02.002

Davis, J. A., Gift, J. S. and Zhao, Q. J. (2011). Introduction to benchmark dose methods and U.S. EPA's benchmark dose software (BMDS) version 2.1.1. *Toxicol Appl Pharmacol 254*, 181-191. http://dx.doi.org/10.1016/j.taap.2010.10.016

Edler, L. (2014). Benchmark Dose in Regulatory Toxicology. In F.-X. Reichl and M. Schwenk (eds.), *Regulatory Toxicology*. Berlin, Heidelberg: Springer Berlin Heidelberg. http://dx.doi.org/10.1007/978-3-642-35374-1_93 http://dx.doi.org/10.1007/978-3-642-35374-1_93

Faustman, E. M., Silbernagel, S. M., Fenske, R. A. et al. (2000). Mechanisms underlying Children's susceptibility to environmental toxicants. *Environ Health Perspect 108 Suppl 1*, 13-21.

Kang, H. J., Kawasawa, Y. I., Cheng, F. et al. (2011). Spatio-temporal transcriptome of the human brain. *Nature 478*, 483-489. http://dx.doi.org/10.1038/nature10523

Kavlock, R. J., Allen, B. C., Faustman, E. M. et al. (1995). Dose-response assessments for developmental toxicity. IV. Benchmark doses for fetal weight changes. *Fundam Appl Toxicol 26*, 211-222.

Kimmel, C. A., Kavlock, R. J., Allen, B. C. et al. (1995). The application of benchmark dose methodology to data from prenatal developmental toxicity studies. *Toxicol Lett 82-83*, 549-554.

Knuesel, I., Chicha, L., Britschgi, M. et al. (2014). Maternal immune activation and abnormal brain development across CNS disorders. *Nat Rev Neurol 10*, 643-660. http://dx.doi.org/10.1038/nrneurol.2014.187

National Research Council Committee on Developmental Toxicology (2000). In (eds.), *Scientific Frontiers in Developmental Toxicology and Risk Assessment*. Washington (DC): National Academies Press (US)

http://dx.doi.org/10.17226/9871

Rice, D. and Barone, S., Jr. (2000). Critical periods of vulnerability for the developing nervous system: evidence from humans and animal models. *Environ Health Perspect 108 Suppl 3*, 511-533.

Rodier, P. M. (1995). Developing brain as a target of toxicity. *Environ Health Perspect 103 Suppl 6*, 73-76.

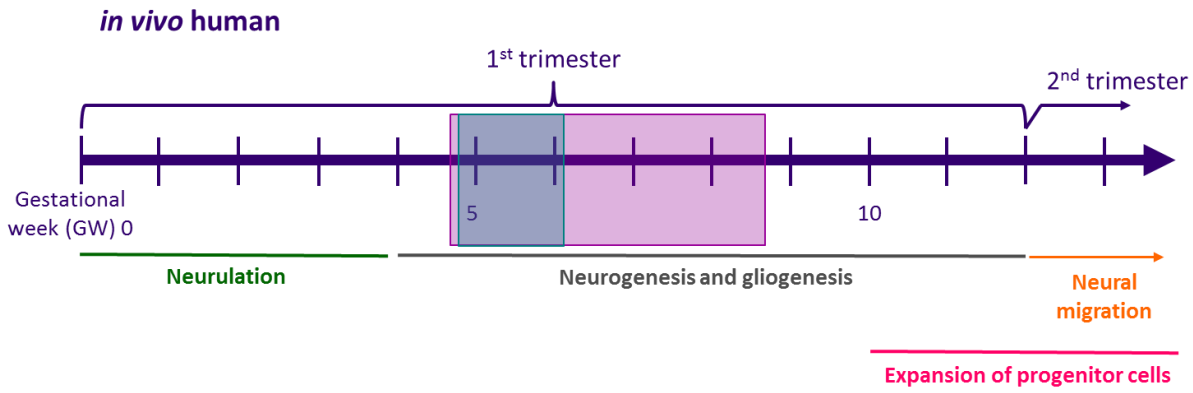

Figure 8.1. *In vitro* 3D organotypic mouse midbrain micromass system and *in vitro* human neural progenitor cell cultures were translated in terms of human *in vivo* based on our findings. Our 22-days of *in vitro* mouse micromass may reflect human gestational week 4.7 to 8.6 while 21-days of *in vitro* hNPCs may represent human gestational week 4.7 to 6.1. This plot was modified from (Knuesel et al., 2014)

Table 8.1. Benchmark dose 10% (BMD_{10}) for *in vitro* fetal mouse midbrain micromass system. BMD_{10} values for various AgNPs exposures on C57BL/6 and A/J micromass cultures in terms of (A) µg/mL and (B) ng Ag/mg protein. Lower 95% confidence interval values for BMD are in parenthesis.

A

	DIV 8		DIV 15		DIV 22	
Compound	**C57**	**AJ**	**C57**	**AJ**	**C57**	**AJ**
20nm AgCitrate	207 (53.4)	63.8 (37.2)	19.1 (14.5)	23.0 (18.4)	13.0 (10.3)	45.1 (29.5)
110nm AgCitrate	25.7 (18.4)	24.8 (19.6)	11.1 (8.98)	13.6 (11.5)	6.98 (5.80)	17.4 (14.0)
110nm AgPVP	26.7 (19.0)	35.9 (26.3)	11.3 (9.16)	11.5 (9.90)	9.02 (7.41)	37.8 (26.1)

Note: Lower 95% confidence interval values for BMD is in parenthesis

B

	DIV 8		DIV 15		DIV 22	
Compound	**C57**	**AJ**	**C57**	**AJ**	**C57**	**AJ**
20nm AgCitrate	3.76 (1.91)	19.5 (6.98)	2.06 (1.61)	17.2 (13.1)	1.95 (1.46)	12.2 (8.80)
110nm AgCitrate	6.57 (4.72)	8.71 (6.62)	12.8 (9.93)	12.0 (9.91)	10.5 (8.32)	24.3 (18.9)
110nm AgPVP	6.76 (4.96)	9.22 (6.64)	16.4 (12.7)	12.4 (10.4)	12.6 (10.0)	52.5 (34.1)

Note: Lower 95% confidence interval values for BMD is in parenthesis

Table 8.2. Benchmark dose 10% (BMD10) for *in vitro* human neural progenitor cell (hNPC) cultures. BMD_{10} values for (A) chlorpyrifos (µg/mL) and arsenic (µM), (B) silver nanoparticles (µg/mL), and (C) cadmium with (µM) and without (µg Cd/mg protein) dosimetry analysis for proliferating and differentiating hNPCs.

A

	Proliferation		Differentiation	
Compound	**24 hours**	**72 hours**	**24 hours**	**72 hours**
Chlorpyrifos	57.3 (42.5)	72.8 (48.9)	1080 (172)	32.4 (24.8)
Arsenic	1.52 (1.00)	0.55 (0.40)	1.53 (1.01)	0.46 (0.34)

Note: Lower 95% confidence interval values for BMD is in parenthesis

B

Compound	**Day 1 Proliferation**	**Day 1 Differentiation**	**Day 7 Differentiation**
20nm AgCitrate	16.8 (13.8)	18.3 (14.5)	26.4 (20.8)
110nm AgCitrate	16.9 (13.9)	12.7 (10.3)	50.3 (33.9)
110nm AgPVP	25.0 (19.5)	16.7 (13.1)	23.8 (19.1)

Note: Lower 95% confidence interval values for BMD is in parenthesis

C

Compound	**Day 1 Proliferation**	**Day 1 Differentiation**	**Day 7 Differentiation**
Cadmium without dosimetry analysis (µM)	3.86 (3.55)	26.9 (22.2)	28.2 (22.5)
Cadmium with dosimetry analysis (µg Cd/mg protein)	0.59 (0.48)	0.19 (0.16)	1.67 (1.00)

Note: Lower 95% confidence interval values for BMD is in parenthesis